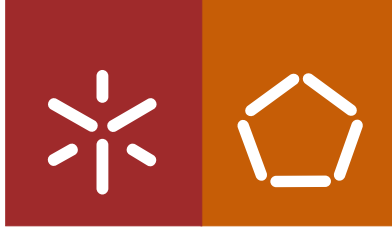


Universidade do Minho
Escola de Engenharia

David Campos Barbosa

**Combining Cycling and Biofeedback
as a Stroke Rehabilitation Therapy**



Universidade do Minho
Escola de Engenharia

David Campos Barbosa

Combining Cycling and Biofeedback as a Stroke Rehabilitation Therapy

Dissertação de mestrado
Mestrado Integrado em Engenharia Biomédica
Ramo de Eletrónica Médica

Trabalho efetuado sob a orientação da
Professora Doutora Cristina P. Santos

outubro de 2014

Declaração

Nome: David Campos Barbosa

Endereço eletrónico: david.campos.barbosa@gmail.com

Número de Cartão de Cidadão: 13893068

Título de Dissertação: Combining Cycling and Biofeedback as a Stroke Rehabilitation Therapy

Orientador: Professora Doutora Cristina P. Santos

Ano de conclusão: 2014

Designação do Mestrado: Mestrado Integrado em Engenharia Biomédica

Área de Especialização: Electrónica Médica

É AUTORIZADA A REPRODUÇÃO INTEGRAL DESTA DISSERTAÇÃO APENAS PARA EFEITOS DE INVESTIGAÇÃO, MEDIANTE DECLARAÇÃO ESCRITA DO INTERESSADO, QUE A TAL SE COMPROMETE.

Universidade do Minho, ___ / ___ / ___

Assinatura: _____

Acknowledgements

First of all, I want to thank my parents for all their love, absolute support and guidance, which have made me who I am now. The success throughout my life is the result of their advice and their persistence in that I always attempt to improve and to give the best in everything I do. I know that they are proud of me and I hope to never disappoint them.

I would like to express all my gratitude to my supervisor Cristina Santos for her unconditional support, experience, advice and for the encouragement to overcome all problems and challenges that came across during my work. I also want to thank professors Eurico Seabra, Lino Costa, Luís Gonçalves and Paulo Carvalhal for their assistance.

I want to show gratitude to Dr. Ana Matias and Dr. Fátima Pereira, from Hospital de Braga, for their professional advising and their role in the success of the clinical trials developed in the Department of Physical Medicine and Rehabilitation. I also wish to thank the therapists and the personnel of the Department of Physical Medicine and Rehabilitation for their help, in particular, the therapist Marília Canelas for her monitoring, help and advice during the clinical trials. To Eng. António Ribeiro, from Orthos XXI, for his logistic support.

To my colleagues from the ASBG, Ana Silva, Ana Tereso, Carlos Teixeira, César Ferreira, João Macedo, Jorge Barreira, Jorge Silva, Maria Martins, Miguel Oliveira, and Vítor Faria, for their friendship and support, always ready to help me when needed, and for providing moments of enjoyment. And to all volunteers, who performed the trials and contributed to this work.

And last but not least, I want to thank my brother Daniel, as well as, my friends for all support they have given during my life, and for believing in me. I wish to thank, in particular, Sofia Gomes for all the patience and encouragement that was given to me, during this work.

David Barbosa

Abstract

Stroke is a leading cause of long-term disabilities, such as hemiparesis, inability to walk without assistance and dependence of others in the activities of daily living. Motor function rehabilitation after stroke demands for therapies oriented to the recovery of the walking capacity. Due to the similarities with walking, cycling leg exercise may present a solution to this problem. In addition, the therapies should also promote the patient's motivation and active participation during the rehabilitation process, which may be obtained with the provision of biofeedback. The purpose of this study is to assess the application of cycling leg exercise together with force or EMG biofeedback in the rehabilitation of stroke patients.

A cycling device, *THERA-live*, was instrumented with sensors, in order to analyze the users' cycling performance (through training variables). A force biofeedback system was developed based on the data provided by load sensors. Healthy subjects were able to reduce the asymmetry of the force applied by each limb and change their pedaling strategy when force biofeedback was provided. Regarding EMG biofeedback, it was provided through a biofeedback device, *YSY EST EVOLUTION*. The tests of EMG biofeedback in the healthy subjects, showed that the users were able to increase their muscle activation pattern and to synchronize it with the target signal, when EMG biofeedback was provided.

A study was designed to assess the effects of an intervention of cycling with force or EMG biofeedback on stroke patients' pedaling strategy and cycling performance; on the evolution of the cycling performance (through training variables) throughout the intervention; and on the patient's motor function, especially on the locomotor abilities. Simpler versions of the designed study were implemented in three stroke patients. Single sessions in which force and/or EMG biofeedback was provided and/or interventions of 5 sessions (during 2 weeks) of cycling with EMG biofeedback were considered.

In overall, the tests performed in this preliminary study allowed to conclude that force and EMG biofeedback change the patients' pedaling strategy and improve their cycling performance. More tests are required to conclude which of these therapies may produce better results in stroke rehabilitation. The intervention of EMG biofeedback resulted in an improvement of the cycling performance throughout the intervention. Regarding the motor function, Patient 3 whose motor function was assessed at the beginning and end of the intervention, showed improvements. However, the number of patients to whom the intervention was implemented is insufficient to recommend or not cycling leg exercise together with force or EMG biofeedback as a stroke rehabilitation therapy. Therefore, the designed study should be implemented in more patients, in order to provide more information that allows to clarify the relevance of these therapies in the stroke rehabilitation.

Resumo

Os Acidentes Vasculares Cerebrais (AVC) são uma das principais causas de incapacidades a longo prazo, tais como hemiparesia, incapacidade de andar sem assistência e dependência de terceiros nas atividades do dia-a-dia. A reabilitação da função motora, após um AVC, requer terapias orientadas à recuperação da capacidade de marcha. Devido às suas semelhanças com a marcha, *cycling* nos membros inferiores, poderá representar uma solução para este problema. Além disso, as terapias devem promover a motivação dos pacientes e a sua participação ativa no processo de reabilitação, o que poderá ser obtido através do fornecimento de *biofeedback*. O objetivo deste estudo consiste na avaliação da aplicação de *cycling* em conjunto com *biofeedback* da força ou do sinal de EMG na reabilitação de pacientes vítimas de AVC.

Um dispositivo de *cycling*, *THERA-live*, foi equipado com sensores, de forma a analisar a performance dos utilizadores. Um sistema de *biofeedback* da força foi desenvolvido com base nos dados fornecidos por sensores de força. Utilizadores saudáveis conseguiram reduzir a assimetria da força aplicada por cada perna e mudar a sua estratégia de pedalar, quando *biofeedback* da força foi fornecido. O *biofeedback* do sinal de EMG foi fornecido através de um dispositivo de *biofeedback*, o *YSY EST EVOLUTION*. Testes em saudáveis demonstraram que os utilizadores são capazes de aumentar a ativação muscular e sincronizar o padrão de ativação com um sinal objetivo, quando *biofeedback* do sinal de EMG é fornecido.

Um estudo foi apresentado com o objetivo de avaliar os efeitos de uma intervenção de *cycling* com *biofeedback* da força ou do sinal EMG na estratégia de pedalar e na performance dos pacientes durante o exercício; na evolução da performance ao longo da intervenção; e na função motora dos pacientes, em especial, na capacidade de marcha. Versões simplificadas do estudo planeado foram implementadas em pacientes vítimas de AVC. Sessões únicas de *cycling* com *biofeedback* da força e/ou do sinal EMG; e/ou intervenções de 5 sessões (during 2 weeks) de *cycling* com *biofeedback* do sinal EMG, foram consideradas.

No geral, os testes efetuados neste estudo preliminar permitiram concluir que o *biofeedback* da força e do sinal EMG promove alterações na estratégia de pedalar dos pacientes e melhora a sua performance. É necessário realizar mais testes para inferir sobre qual das terapias poderá gerar melhores resultados na reabilitação de AVC. A intervenção de *biofeedback* do sinal EMG resultou numa melhoria da performance ao longo do período de reabilitação. No que concerne a função motora, o paciente cuja função motora foi avaliada no início e no fim da intervenção, apresentou melhorias. No entanto, o número de pacientes aos quais a intervenção foi implementada é insuficiente para recomendar ou não o uso das terapias estudadas na reabilitação de AVCs. Deste modo, o estudo planeado deverá ser aplicado a mais pacientes, de forma a fornecer mais informação que permita clarificar a relevância do uso de *cycling* em conjunto com *biofeedback* da força ou do sinal EMG como terapias de reabilitação de AVCs.

Contents

Acknowledgements	i
Abstract	iii
Resumo	v
Contents	vii
List of Figures	xi
List of Tables	xv
List of Acronyms	xvii
Nomenclature	xxi
1 Introduction	1
1.1 Motivation and Context	1
1.2 Research Questions	2
1.3 Objectives	3
1.4 Outline	4
1.5 Publications	5
2 State of the Art	7
2.1 Introduction	7
2.2 Stroke	8
2.3 Cycling Aims	9
2.3.1 Cycling Research	10
2.3.1.1 Cycling as a Motor Function Rehabilitation Method	11
2.3.1.2 Cycling as an Aerobic Training Method	12
2.3.1.3 Assessment Tools used in Cycling	13
2.3.2 Cycling-based Therapies	17
2.4 Feedback-research Questions	18
2.4.1 Intrinsic and Extrinsic Feedback	18
2.4.2 Knowledge of Results and Knowledge of Performance	19

2.4.3	Scheduling of Feedback	20
2.4.4	Types of Biofeedback	20
2.4.5	Biofeedback in Cycling	22
2.4.5.1	Protocols	23
2.4.5.2	Main Findings of Biofeedback combined with Cycling	25
2.5	Cycling Devices	26
2.6	Challenges and Future Work	29
2.7	Conclusions	29
3	Devices and Instrumentation	31
3.1	Introduction	31
3.2	<i>THERA-Live</i> Motorized Cycling Device	31
3.2.1	<i>THERA-Live</i> Operation	32
3.3	Cycling Device Instrumentation	33
3.3.1	Crank Angle	33
3.3.2	Pedal Angle	36
3.3.3	Force and Work	37
3.4	<i>YSY EST EVOLUTION</i>	40
3.5	Conclusions	41
4	Analysis of Cycling	43
4.1	Introduction	43
4.2	Lower Limbs Muscles	43
4.3	Biomechanical Model of Cycling	45
4.4	Muscle Abnormalities after Stroke	46
4.5	Influence on the EMG Patterns during Cycling	47
4.6	<i>Rectus Femoris, Tibialis Anterior and Gastrocnemius Medialis</i>	48
4.7	Joint Moments	49
4.8	User-Device Interaction	50
4.8.1	Procedure	50
4.8.2	Results	51
4.8.3	Discussion	55
4.9	Conclusions	60
5	Force and EMG Biofeedback	63
5.1	Introduction	63
5.2	Force Biofeedback	63
5.2.1	Force Biofeedback Experimental Setup	64
5.2.2	Procedure	66
5.2.3	Results	68
5.2.4	Discussion	70
5.3	EMG Biofeedback	72
5.3.1	EMG Biofeedback Experimental Setup	73
5.3.2	Procedure	75

5.3.3	Results	76
5.3.4	Discussion	78
5.4	Conclusions	80
6	Study Design and Case Studies	83
6.1	Introduction	83
6.2	Patient Selection – Inclusion and Exclusion Criteria	84
6.3	Sample Size	84
6.4	Protocol	85
6.4.1	Patients Assessment	85
6.4.1.1	Gait Assessment Test	86
6.4.1.2	Cycling Assessment Test	86
6.4.2	Procedure	87
6.4.3	Intervention	88
6.5	Case Studies	88
6.5.1	Patient 1	89
6.5.1.1	Assessment	90
6.5.1.2	Results and Discussion	91
6.5.2	Patient 2	98
6.5.2.1	Assessment	98
6.5.2.2	Results and Discussion	99
6.5.3	Patient 3	103
6.5.3.1	Assessment	105
6.5.3.2	Results and Discussion	106
6.6	Conclusions	114
7	7. Conclusions and Future Work	117
7.1	Conclusions	117
7.2	Future Work	119
	Bibliography	123
	Appendix A	135
A.1	<i>Thera-Live</i> Technical Data	135
A.2	<i>OPB763T</i> Optical Sensor	136
A.2.1	<i>OPB763T</i> Properties	136
A.2.2	Optical Sensors' Electronic Board	137
A.3	Sensors' Acquisition Board	138
A.4	<i>GY-521 – MPU6050</i> Accelerometer	139
A.4.1	<i>MPU6050</i> Accelerometer Features	139
A.4.2	<i>MPU6050</i> Accelerometer Specifications	139
A.5	<i>Flexiforce</i> Sensor	140
A.5.1	<i>Flexiforce</i> Properties	140
A.5.2	Sensors Calibration	140
A.6	Leg Supports	142

Appendix B	143
B.1 Biomechanical Analysis of Lower Limbs during Cycling	143
B.2 Body Segment Parameters	146
Appendix C	147
C.1 Procedures for Recording Muscle Activity	147
C.1.1 Recommendations for Electrodes Placement	147
C.1.2 Electrodes Position	147
Appendix D	149
D.1 Fugl-Meyer Assessment of Physical Performance	149
D.1.1 Balance	149
D.1.2 Lower Extremities	150

List of Figures

2.1	Balance platform and weight distribution visual biofeedback setup.	22
2.2	Visual biofeedback of the work produced by each leg, provided to the subjects in the study of Ferrante <i>et al.</i>	24
2.3	Visual biofeedback of the instantaneous mechanical effectiveness, provided to the subjects in the study of De Marchis <i>et al.</i>	25
2.4	Types of ergometers: (a) standard ergometer (Schwinn Bicycles Co, Illinois, USA) and recumbent ergometers (b) Ergys (Therapeutic Alliances Inc., Ohio, USA) and (c) Active Passive Trainer (Tzora Active Systems Ltd, Kibbutz Tzora, Israel).	27
2.5	Representation of the experimental setup used by Brown and Kautz.	27
2.6	Cycling wheelchair system developed by Seki <i>et al.</i> , (a) side view and (b) front view.	28
2.7	MOTOMed (RECK-Technik GmbH & Co. KG, Germany) (a) Viva and (b) Letto models, and (c) THERA-Trainer Tigo (Medica Medizintechnik GmbH, Germany) cycling device.	28
3.1	Cycling device views: (a) and (b) side view, (c) user view and (d) front view.	32
3.2	<i>THERA-Live</i> 's electronic control board.	32
3.3	<i>THERA-Live</i> 's control pad.	33
3.4	Representation of the two phases of one revolution: downstroke phase (solid green line) and upstroke phase (dashed red line), as well as, their equivalent angles.	34
3.5	System for measurement of the crank angle: (a) optical sensors and (b) optical encoder's disks.	34
3.6	Pinout configuration and connection between the electrical control board and the external optical sensor.	35
3.7	Electronic circuit to control the internal optical sensor.	35
3.8	Tilt angles measurement, using (a) a single axis accelerometer and (b) a 3-axis accelerometer.	37
3.9	<i>GY-521</i> board with a 3-axis accelerometer (<i>MPU-6050</i>).	37
3.10	Tridimensional model of the system to measure the applied force. Representation of (a) the mounted view and (b) the exploded view of the mechanical system.	38
3.11	Electronic circuit for the acquisition of the applied force on the force sensor (R_{fs}).	39
3.12	Right pedal with the mechanical system to measure the applied force.	39
3.13	Representation of the axes and angles to calculate the angle between the pedal and the crank axis.	39
3.14	EMG Biofeedback System: (a) <i>YSY EST EVOLUTION</i> and (b) display with the device software.	40
4.1	Muscles of lower limbs: (a) anterior and (b) posterior views.	44

4.2	Nine muscle sets of the model of Raasch <i>et al.</i> , formed by 15 individual muscles, which are described in Table 4.2.	45
4.3	Muscles activation pattern in (a) forward and (b) backward pedaling, according to the Raasch <i>et al.</i> 's computational biomechanical model.	46
4.4	EMG root mean square linear envelope of <i>rectus femoris</i> , <i>tibialis anterior</i> and <i>gastrocnemius medialis</i>	48
4.5	Five bar linkage model of the lower limb.	49
4.6	Mean logarithmic values of the magnitude between the maximum and the minimum value of the pedal angle, of all healthy subjects, for the 9 workload and cadence combinations workloads: 2, 8 and 15 Nm; cadences: 40, 50 and 60 rpm).	52
4.7	Mean values of the pedal angle for (a) three different workloads (2, 8 and 15 Nm) at 50 rpm; and (b) three different cadences (40, 50 and 60 rpm) at 8 Nm, for ten revolutions (11th to 20th revolution), for the left leg of the subject 4.	53
4.8	Mean values of the angle between the crank arm and the pedal, for (a) three different workloads (2, 8 and 15 Nm) at 50 rpm; and (b) three different cadences (40, 50 and 60 rpm) at 8Nm, for the left leg of the subject 4.	53
4.9	Mean logarithmic values of positive mechanical work, of all healthy subjects, for the 9 workload and cadence combinations workloads: 2, 8 and 15 Nm; cadences: 40, 50 and 60 rpm.	54
4.10	Mean logarithmic values of the positive mechanical work for the (a) 3 workload values (2, 8 and 15 Nm); and (b) 3 cadence values (40, 50 and 60 rpm), for each subject.	54
4.11	Mean of the square root of the absolute values of the negative mechanical work, of all healthy subjects, for the 9 workload and cadence combinations workloads: 2, 8 and 15 Nm; cadences: 40, 50 and 60 rpm.	55
4.12	Mean of the square root of the absolute values of the negative mechanical work for the (a) 3 workload values (2, 8 and 15 Nm); and (b) 3 cadence values (40, 50 and 60 rpm), for each subject.	55
4.13	Mean values of the effective force for (a) three different workloads (2, 8 and 15 Nm) at 50 rpm (subject 4); and for three different cadences (40, 50 and 60 rpm) at 8 Nm of (b) subject 4 and (c) subject 3.	56
4.14	Mean logarithmic values of the positive mechanical work (top) and mean square root values of the absolute negative mechanical work (bottom) for (a)(c) three different workloads and (b)(d) three different cadences, performed by the pushing and the coordination limbs.	57
4.15	Mean values of the effective force for the pushing and coordination limbs, at (a) 40 rpm and (b) 50 rpm, at 15 Nm, of the subject 4.	58
4.16	Mean values of the (a) ankle, (b) knee and (c) hip moments, for the pushing and coordination limbs, at 50 rpm and 15 Nm, of the subject 4.	59
5.1	Experimental setup used for the Force Biofeedback intervention.	64
5.2	Force biofeedback system: (a) green bars represent a symmetrical force pattern and (b) red bars represent an asymmetrical force pattern.	65
5.3	Mean of the cube root of the $ U $, of all healthy subjects, for each type of force biofeedback	68
5.4	Mean of the cube root of the $ U $ for each healthy subject and for each type of force biofeedback.	68
5.5	Number of revolutions where, for each trial of force biofeedback, (a) the $ U $ was less than or equal to 25%; and (b) the target band condition was fulfilled.	70

5.6	Mean values of the effective force for the pushing and coordination limbs, for cycling (a) without force biofeedback; and with force biofeedback (b) updated on each 32 degrees; (c) updated on each 64 degrees; and (d) of half a revolution, at 8 Nm, of the subject 5.	71
5.7	Experimental setup used for the EMG Biofeedback intervention.	73
5.8	Designed target signals: (a) triangular wave and (b) triangular 50% duty cycle wave.	74
5.9	<i>Rectus femoris</i> ' mean activation pattern (a) without EMG biofeedback and (b) with EMG biofeedback, at 43 rpm and 4 Nm, for subject 5.	77
5.10	<i>Gastrocnemius medialis</i> ' mean activation pattern (a) without EMG biofeedback and (b) with EMG biofeedback, at 43 rpm and 4 Nm, for subject 5.	77
5.11	<i>Tibialis anterior</i> ' mean activation pattern (a) without EMG biofeedback and (b) with EMG biofeedback, at 43 rpm and 4 Nm, for subject 5.	78
5.12	Mean values of the MAR of all healthy subjects, for the three workload values (0, 4 and 8 Nm) and for the three analyzed muscles.	79
5.13	Mean values of the net mechanical work, for the pushing and coordination limbs, of all healthy subjects, for the three workload values (0, 4 and 8 Nm) and for the three analyzed muscles.	80
5.14	Mean values of the effective for the pushing and coordination limbs, for the (a) <i>rectus femoris</i> , (b) <i>gastrocnemius medialis</i> and (c) <i>tibialis anterior</i> , at 43 rpm and 4 Nm, of the subject 5.	81
6.1	Schematic representation of the designed study.	86
6.2	Gait parameters: left stride length ($L1_L$), right stride length ($L1_R$), left step length ($L2_L$), right step length ($L2_R$), distance between heels ($L3$), distance between toes ($L4$), and paretic limb foot angle (γ).	87
6.3	Mean values of the effective force for both lower limbs, for cycling with (a) no biofeedback; (b) force biofeedback updated on each 32 degrees; and (c) force biofeedback of half a revolution, of Patient 1.	93
6.4	<i>Rectus femoris</i> ' mean activation pattern of Patient 1 with (a) no biofeedback; and (b) EMG biofeedback.	94
6.5	Mean values of the pedal angle for the paretic (solid red line) and healthy (dashed green line) limbs of Patient 1 with (a) no biofeedback; and (b) EMG biofeedback, of Patient 1.	95
6.6	Mean values of the effective force for both lower limbs, for cycling with (a) no biofeedback; and (b) EMG biofeedback, of Patient 1.	96
6.7	Mean values of the ankle (top), knee (middle) and hip (bottom) moments with (a) (c) (e) no biofeedback; and (b) (d) (f) EMG biofeedback, for both lower limbs of Patient 1.	97
6.8	Values of the MAR of the <i>rectus femoris</i> muscle of Patient 2, for the 5 sessions, without and with EMG biofeedback.	100
6.9	Mean values of the net mechanical work performed by the paretic and healthy limbs in the NF and EMGF trials, of Patient 2.	100
6.10	<i>Rectus femoris</i> ' mean activation pattern in the session 4 of Patient 2 with (a) no biofeedback; and (b) EMG biofeedback.	101
6.11	Mean values of the effective force for the paretic and healthy lower limbs, for cycling in session 4 (top) and in session 5 (bottom) with (a) (c) no biofeedback; (b) (d) EMG biofeedback, in the NF and EMGF trials, respectively) of Patient 2.	102
6.12	Mean values of the ankle (top), knee (middle) and hip (bottom) moments with (a) (c) (e) no biofeedback; and (b) (d) (f) EMG biofeedback, for both lower limbs of Patient 2.	104

6.13	Mean values of the pedal angle for both lower limbs, for cycling with (a) no biofeedback; (b) force biofeedback updated on each 32 degrees); and (c) force biofeedback of half a revolution, of Patient 3	107
6.14	Mean values of the effective force for both lower limbs, for cycling with (a) no biofeedback; (b) force biofeedback updated on each 32 degrees); and (c) force biofeedback of half a revolution, of Patient 3	108
6.15	Values of the MAR of the <i>rectus femoris</i> muscle of Patient 3, for the 5 sessions, without and with EMG biofeedback.	110
6.16	Mean values of the net mechanical work performed by the paretic and healthy limbs in the NF and EMGF trials, of Patient 3.	110
6.17	<i>Rectus femoris</i> ' mean activation pattern of Patient 3: (a) session 3 without biofeedback; (b) session 3 with EMG biofeedback; and (c) session 4 with EMG biofeedback.	111
6.18	Mean values of the pedal angle for both lower limbs, for cycling (a) without biofeedback (session 3); (b) with EMG biofeedback (session 3); and (c) with EMG biofeedback (session 4), of Patient 3. 112	
6.19	Mean values of the effective force for both lower limbs, for cycling (a) without biofeedback (session 3); (b) with EMG biofeedback (session 3); and (c) with EMG biofeedback (session 4), of Patient 3.	113
A.1	Technical data of the <i>THERA-Live</i> cycling device.	135
A.2	Absolute maximum ratings of the optical sensor <i>OPB763T</i>	136
A.3	Electrical characteristics of the optical sensor <i>OPB763T</i>	136
A.4	<i>Veroboard</i> for the connection of the external (<i>A</i>) and the internal (<i>B</i>) optical sensors with the electronic control board (<i>C</i>) and the sensors' acquisition board (<i>D</i>), respectively	137
A.5	Sensors' acquisition board. <i>A</i> – Voltage regulator circuit. <i>B</i> – External optical sensor connector. <i>C</i> – Internal optical sensor control circuit. <i>D</i> – I^2C protocol lines connector (accelerometers). <i>E</i> – Voltage divider circuits (<i>Flexiforce</i> sensors).	138
A.6	Voltage divider circuit.	138
A.7	Specifications of the <i>MPU6050</i> accelerometer.	139
A.8	Electrical tension (V) values as function of the applied force (N), for the left pedal (red) and right (green) pedals.	141
A.9	Accessory Leg Supports.	142
B.1	Free-body diagram.	145
C.1	Electrodes location in the three studied muscles: (a) <i>rectus femoris</i> , (b) <i>gastrocnemius medialis</i> (c) <i>tibialis anterior</i> , and (d) Reference electrode, which is placed on the wrist.	148

List of Tables

2.1	Major characteristics of the published cycling studies, applied in stroke patients	10
2.2	Assessment tools used in the reviewed studies to assess the patients': impairments, recovery, and the effect of different exercise characteristics and modes	14
2.3	Major characteristics of the published biofeedback cycling studies	22
2.4	Assessment tool of the biofeedback cycling studies	24
4.1	Region, group, antagonist and general function of the muscles of the biomechanical model developed by Raasch <i>et al.</i>	44
4.2	Muscle organization of the Raasch <i>et al.</i> 's model. Fifteen muscles are organized in nine muscles sets, which form six muscle groups that are arranged in three pairs	45
4.3	Mean and standard deviation values of the demographic and anatomical characteristics of the subjects	50
4.4	The F ratio values, degrees of freedom and the significance-values (p -value) resulted from an ANOVA with four factors (workload, cadence, subject and limb), on the magnitude of the pedal angle, positive mechanical work and negative mechanical work variables	52
5.1	Mean and standard deviation values of the demographic and anatomical characteristics of the subjects	66
5.2	The F ratio values, degrees of freedom (df) and the significance-values (p -value) resulted from a two-away ANOVA with replication of the factor trial and subject, and the interaction between these two factors, on the cube root of the $ U $	69
5.3	Cross tabulation table of the number of revolutions in which $ U $ less than or equal to 25% and that fulfill the target band condition, for each biofeedback trial	69
5.4	Results of the Pearson Chi-Square test for each for the tested conditions ($ U $ less than or equal to 25% and within the target band condition)	69
5.5	EMG biofeedback training cadences (rpm) for each complete passage time (s)	74
5.6	Mean and standard deviation values of the demographic and anatomical characteristics of the subjects	75
5.7	The F ratio values, degrees of freedom (df), the significance-values (p -value) resulted from two-away ANOVAs of the effects of the workload and subject, on the MAR and on the W performed by the pushing and coordination limbs variables, for each muscle	76
6.1	Inclusion and exclusion criteria of the designed study	84

6.2	Cycling tasks performed during a session of the study	88
6.3	Demographic, anatomical and medical characteristics of the studied patients	89
6.4	Patient 1 assessment tests' results	90
6.5	Mean (SD) values of the training parameters of the initial cycling assessment test of Patient 1	91
6.6	Mean (SD) values of cadence, absolute, negative and positive Unbalance Index values and number of revolutions that fulfill the conditions, in the different trials of the force biofeedback of Patient 1	91
6.7	MAR and work (mean (SD) values) performed by each limb, of Patient 1, during cycling without and with EMG biofeedback	94
6.8	Patient 2 assessment tests' scores	98
6.9	Mean (SD) values of the training parameters of the initial and final cycling assessment tests of Patient 2	99
6.10	Used workload and target cadence values; and mean (SD) cadence measure in the NF and EMGF trials, for each session, of Patient 2	99
6.11	Patient 3 assessment tests' scores	105
6.12	Mean (SD) values of the training parameters of the initial and final cycling assessment tests of Patient 3	106
6.13	Mean (SD) values of cadence, absolute, negative and positive Unbalance Index values and number of revolutions that fulfill the conditions, in the different trials of the force biofeedback of Patient 3	106
6.14	Used workload and target cadence values; and mean (SD) cadence measure in the NF and EMGF trials, for each session, of Patient 3	109
A.1	Physical properties and Typical performance of <i>Flexiforce</i> Sensor	140
A.2	Voltage readings (V) for different conditions of weight, in the left and right pedals	140
A.3	Coefficients values of the polynomial function, obtained through a polynomial curve fitting of the voltage readings	141
B.1	Body segments parameters estimated by Clauser <i>et al.</i>	146
C.1	Recommendations for the electrodes location of the <i>rectus femoris</i> , <i>gastrocnemius medialis</i> and <i>tibialis anterior</i> , according to SENIAM	148
D.1	Procedure and scoring criteria for assessment of the balance	149
D.2	Procedure and scoring criteria for assessment of the lower limbs	150

List of Acronyms

10MWT 10 Meters Walking Test. 2, 14, 24, 26, 83, 86, 90, 98, 105

6MWT 6 Minutes Walking Test. 14, 17, 24, 26

ADC Analog-to-Digital Converter. 38, 139

ADL Activity of Daily Living. 1, 7, 8, 13, 20, 21, 30, 46, 73

ANOVA Analysis of Variance. 51, 52, 67–69, 75, 76

ARC Aerobic. 10

AST Assessment. 10

BBS Berg Balance Scale. 14

BI Barthel Index. 14

BMI Body Mass Index. 89

C Control. 10, 22

CG Center of Gravity. 50, 144–146

CI Confidence Interval. 85

CMSA Chedoke-McMaster Stroke Assessment. 14

CNS Central Nervous System. 26, 84

CTG Control Group. 85, 114

E Experimental. 10, 22

ECG Electrocardiography. 14, 15, 24

EG1 Experimental Group 1. 84, 88, 114

EG2 Experimental Group 2. 84, 88, 114

EH Elderly healthy. 10, 22

EMG Electromyography. 2–4, 13, 14, 16, 17, 19–26, 30, 31, 40, 41, 46–49, 61, 63, 72–75, 78–84, 87–90, 93–96, 98–103, 105, 109–120, 147

EMGF EMG Biofeedback. 75–78, 90, 93–96, 98–103, 105, 109–113, 115

F32 Force Biofeedback Updated on each 32 degrees. 66, 68–72, 80, 81, 88, 90–93, 105–109, 112, 115–118, 120

F64 Force Biofeedback Updated on each 64 degrees. 66, 68–72, 80

FES Functional Electrical Stimulation. 7, 17, 18, 29

FHR Force Biofeedback of Half a Revolution. 67–72, 80, 81, 90–93, 105–109, 115, 116, 118, 120

FIM Functional Independence Measure. 14, 17

FMA Fugl-Meyer Assessment. 2, 14, 24, 83, 85, 90, 98, 105, 114, 115, 117, 119

H Healthy. 10, 22

HC Hemorrhagic. 10, 22

I²C Inter-Integrated Circuit. 37, 138

IC Ischemic. 10, 22

IEMG Integration of the EMG Activity. 14, 16, 23

KP Knowledge of Performance. 18–20

KR Knowledge of Results. 18–20

LED Light-Emitting Diode. 35, 36

MAS Modified Ashworth Scale. 14, 24, 84, 85, 89

min minutes. 10, 22

MOSFET Metal Oxide Semiconductor Field Effect Transistor. 36

N sample size. 10, 22

NF No Biofeedback. 66, 68–71, 75–78, 80, 90–96, 98–103, 105–113, 115, 116

NIHSS National Institutes of Health Stroke Scale. 14

NS not stated. 10, 22

PASS Postural Assessment Scale for Stroke. 14

PCB Printed Circuit Board. 137

PMC Premotor Cortex. 25

PRT Progressive Resistance Training. 13

PWM Pulse-Width Modulation. 36

r wheel revolutions. 10

RCT Randomized Controlled Trial. 10, 11

RMS Root Mean Square. 48

ROM Range of Motion. 2, 9, 12, 21, 46, 60, 72, 84, 85, 89, 90, 98, 105, 117

RPE Borg rate of Perceived Exertion. 13

RT Rehabilitation. 10

s/w sessions per week. 10, 22

SC Single Case. 10, 22

SCL Serial Clock Line. 138

SD Standard Deviation. 90–94, 99, 101, 102, 106, 107, 109, 112

SDA Serial Data Line. 138

SENIAM Surface Electromyography for the Non-Invasive Assessment of Muscles. 75, 88, 147

sg single session. 10, 22

SIAS Stroke Impairment Assessment Set. 14

SIS Stroke Impact Scale. 14

SSS Scandinavian Stroke Scale. 14

VR Virtual Reality. 21, 25

w weeks. 10, 22

Nomenclature

$m_{totalbody}$ Mass of the body. 146

ASI Area Symmetry Index. 14, 16, 17, 24, 25

F Effective Force. 38, 51, 54, 56–58, 67, 83, 88, 117, 145

F_p Normal Force. 37, 51, 64, 75, 88

GND Circuit Ground. 35, 137

I_{CG} Moment of inertia of a segment about its CG. 146

I_{fCG} Moment of inertia of the foot about CG. 145

I_{sCG} Moment of inertia of the shank about CG. 145

I_{tCG} Moment of inertia of the thigh about CG. 145

K_{CG} Length of the radius of gyration of the segment about its CG as a proportion of the segment's length.
146

$L1_L$ Left stride length. 87, 90

$L1_R$ Right stride length. 87, 90

$L2_L$ Left step length. 87, 90

$L2_R$ Right step length. 87, 90

$L3$ Distance between heels. 87, 90

$L4$ Distance between toes. 87, 90

L_2 Crank arm length. 49, 143

L_3 Horizontal seat distance. 49, 143

L_4 Vertical seat distance. 49, 143

P Mass proportion of a segment. 146

P_{av} Averaged Cycling Power. 14, 15, 25

RI Roughness Index. 14, 15, 24, 25

R_x Vertical component of the effective force. 145

R_y Horizontal component of the effective force. 145

$R_{proximal}$ Distance between the proximal end to the segment's CG as proportion of the segment's length. 146

SI Symmetry Index. 14, 17

SSI Shape Symmetry Index. 14, 16, 17, 24

U Unbalance Index. 14, 15, 24, 67, 83, 86–88, 90, 91, 98, 99, 105, 106, 109, 115–118

U^+ Positive Unbalance Index. 90–92, 105, 106, 115

U^- Negative Unbalance Index. 90–92, 105, 106, 115

VO_2 Maximal Aerobic Capacity. 12–14

V_{out} Output Voltage of the External Optical Sensor. 35, 137

W Net Mechanical Work. 40, 51, 64, 65, 72, 75, 76, 78–82, 86, 98, 100, 110, 114, 115, 118, 119

W^+ Positive mechanical work. 51–54, 57–59

W^- Negative mechanical work. 51–53, 55, 57–59

W_{HL} Net mechanical work performed by the healthy leg. 15, 87, 88, 91, 93, 94, 99, 100, 106, 110

W_L Net mechanical work performed by the left leg. 67

W_{PL} Net mechanical work performed by the paretic leg. 15, 87, 88, 91, 93, 94, 99, 100, 106, 110

W_R Net mechanical work performed by the right leg. 67

$\Delta\beta$ Magnitude between the maximum and the minimum values of the pedal angle. 51, 52, 55, 59

α Angle between the Crank Arm and the pedal. 38, 52, 53, 56

β Pedal Angle. 36–38, 41, 51, 53, 55, 56, 59, 61, 64, 67, 75, 83, 88, 95, 96, 101, 107, 111, 112, 115, 117, 143

$\ddot{\epsilon}_1$ Shank acceleration. 144

$\ddot{\epsilon}_2$ Foot angular acceleration. 143

$\ddot{\theta}$ Thigh angular acceleration. 144

$\dot{\epsilon}_1$ Shank angular velocity. 144

$\dot{\epsilon}_2$ Foot angular velocity. 143

$\dot{\epsilon}_3$ Angular velocity. 143

$\dot{\theta}$ Thigh angular velocity. 144
 ε_1 Shank angle. 143
 ε_2 Foot angle. 143
 ε_3 Crank angle. 143
 γ Paretic limb foot angle. 87, 90
 ϕ Crank Angle. 33, 34, 38, 41, 51, 52, 54–57, 64, 67, 75, 88, 115, 143, 145
 ϕ_{floor} Pedal Angle relative to the floor. 38
 τ Torque. 40
 θ Thigh angle. 143
 d Distance between the crank the pedal axes. 40
 d_1 Distance of thigh CG from proximal joint. 145
 d_2 Distance of shank CG from proximal joint. 145
 d_3 Distance of foot CG from ankle. 145
 l_1 Thigh length. 49, 143
 l_2 Shank length. 49, 143
 l_3 Foot length. 49, 143
 m_f Foot mass. 145
 m_s Shank mass. 145
 m_t Thigh mass. 145
 $r_{proximal}$ Distance from the CG to the proximal end of the segment. 146
 x Vertical (real) axis. 145
 y Horizontal (imaginary) axis. 145
 $|U|$ Absolute Unbalance Index. 67–72, 80, 91, 92, 99, 106, 107, 115
BFsh Biceps femoris short head muscle. 45, 46
GAS Gastrocnemius muscles. 45
GM Gastrocnemius medialis muscle. 48, 76, 78–82, 148
GMAX Set of Gluteus maximus and Adductor magnus muscles. 45
HAM Set of Medial hamstrings and Biceps femoris long head muscles. 45

IL Set of Iliacus and Psoas muscles. 45, 46

MAR Muscle Activation Rate. 75, 76, 78, 79, 87, 88, 91, 93, 94, 98–100, 106, 109, 110, 117

RF Rectus femoris muscle. 45, 48, 76, 78–82, 94, 95, 111, 113, 148

SOL Set of Soleus muscle and a muscle representing other uniarticular plantarflexors. 45

TA Tibialis anterior muscle. 45, 48, 76, 78–82, 148

VAS Set of Vastus intermedius Vastus medialis and Vastus lateralis muscles. 45

Introduction

1.1 Motivation and Context

Population aging is increasing the susceptibility to stroke and neurodegenerative diseases, being stroke the second main cause of death. Stroke patients generally exhibit sequels with consequences in their normal life, such as hemiparesis, incapacity to walk without assistance, aphasia and dependence in the Activities of Daily Living (ADLs) [1]. Lower limbs' impairments, in addition to the negative influence on the patient's independence, can induce other consequences that can, in severe cases, lead to death, such as musculoskeletal disturbances, cardiovascular problems and low aerobic endurance. The recovering of the walking ability is the major objective of lower limb rehabilitation after stroke, which requires continuous medical care and intensive rehabilitation, often one-on-one manual interaction with therapists [2]. However, due to time and budget restriction, this intensive rehabilitation program is difficult to administer.

The rehabilitation field lacks for solutions that promote a faster return to the normal daily activities, as well as, to increase the motivation and the actively participation of the patients in their own rehabilitation. To be more effective, these interventions should ensure early, intensive, task-specific and multisensory stimulation [3].

The use of robotic devices allows a continuous movement repetition by an unlimited period of time, requiring less therapists (reduce working costs), and with a lower physical load on them. In certain cases the patients could use the robotic devices without supervising for more repetitive tasks. These devices can provide for an autonomous measurement and storage of several exercise parameters. However, they, generally, are big (could require a dedicated room), expensive, are limited to a specific movement and/or exercise, and may require a long period of learning.

Cycling devices might be an alternative motor function's rehabilitation method. In addition to the advantages of the robotic devices, cycling devices are small, user-friendly and less expensive, allowing home-based rehabilitation. These devices allow lower and upper limbs exercise, requiring the involvement of several muscles, which may reduce the risk of immobility-related diseases. In addition, as cycling is cyclical and balance is not a factor in seated pedaling, the users may perform a task that has some similarities to walking, without submitting the patient to risky postural disturbances. Other therapies, such as biofeedback, can be used together with cycling to provide multisensory stimulation, increase the motivation and the participation of the patients in the rehabilitation process.

However, there is the need of more investigation to support the use of these cycling devices and

therapies in the stroke rehabilitation field. Current studies present high heterogeneity in the patients' characteristics, protocols and metrics. Therefore, new studies, addressing important aspects of this problematic, should be developed. This work will address the combined use of cycling leg exercise and biofeedback in the rehabilitation of the lower limbs of stroke patients.

1.2 Research Questions

A set of questions will be addressed in this study, regarding cycling leg exercise and biofeedback.

#RQ1 – Should cycling leg exercise combined with biofeedback be recommended as a stroke rehabilitation therapy?

The combined use of these two therapies requires more research before stating this approach ought to be recommended. Three key aspects have to be analyzed in different periods of the application of this therapy to clarify its relevance: its effects on the patient's motor ability; its effects in the training variables throughout the rehabilitation process; and its effects during the exercise performance.

#RQ2 – Does combining cycling leg exercise with either one of the two biofeedback types (force biofeedback and Electromyography (EMG) biofeedback) improve the patient's motor ability?

The recovering of the walking ability is the major objective of lower limbs rehabilitation after stroke [4]. Therefore, the effects of the therapy on the patient's motor ability should be one of the points to assess the effectiveness of the therapy. Patients' motor function will be assessed through the Fugl-Meyer Assessment (FMA) scale (lower limbs and balance domain). The Range of Motion (ROM) and the single support time, for each limb, will also be assessed to check if there were improvements in the lower limbs function. A walking assessment test (10 Meters Walking Test (10MWT)) will be performed, in order to explore the effects of the intervention on patient's walking ability (functional changes). The stroke patients will be assessed at the beginning and at the end of the intervention and, by comparing the scores of the described tests, will be possible to compare if the patient's motor ability improved after performing the suggested intervention. This work hypothesizes that an intervention of cycling leg exercise with force or EMG biofeedback can improve the patient motor ability. Regarding force biofeedback, as Ambrosini et al.'s study [5], this work also hypothesizes that training towards a symmetrical cycling pattern may induce motor changes and reduce muscle weakness and gait asymmetry. In addition, it is hypothesized that providing biofeedback related with the activity of the muscles (EMG) that have a major role in gait and in cycling exercise, may help the rehabilitation process, by stimulating the muscles that are related with the motor impairments, while performing a functional task.

#RQ3 – Does cycling together with either one of the two explored biofeedback types result in improvements throughout the intervention?

The evolution of a set of training variables, throughout the different therapy sessions, will be analyzed, in order to check for improvements on the patient's performance. The training variables include the training workload and cadence, the force applied in the pedals, the angle of the pedals, the net contribution of each limb to the movement, the symmetry of the force pattern and the muscle activation. The training variables' behavior will be analyzed, in order to assess if, over the course of the sessions, the parameters suggest an improvement of the performance of the patient, such as a more symmetrical force pattern or a higher contribution of the paretic limb to the movement. This work hypothesizes that some

of the training variables will improve throughout the rehabilitation process.

#RQ4 – Does this therapy have more effect on the cycling performance than cycling without biofeedback, when applied to stroke patients?

The comparison of cycling together with either of the two biofeedback types with cycling without biofeedback will allow verifying whether these therapies both alone or combined (cycling and biofeedback) improve the patient's performance. Performance will be assessed considering: (1) the achieved symmetry during cycling in terms of the force applied over the pedals; (2) the increase of the participation of the paretic limb in the exercise; and (3) the promotion of changes in the patient's pedaling strategy. More specifically, the assessment of which of the two biofeedback types (force or EMG biofeedback) has better results in the stroke rehabilitation is intended. All these aspects will be assessed through the training variables, described in the previous point. This work hypothesizes that providing force or EMG biofeedback leads to a more symmetrical cycling exercise. In addition, it also increases the contribution of the paretic limb. And lastly, this work hypothesizes that force or EMG biofeedback induces changings in the patient's pedaling strategy.

A set of biofeedback characteristics, for both types of biofeedback, should be analyzed and clarified, before applying the suggested therapies to stroke patients. Regarding force biofeedback, some aspects require further analysis, as follows. The best way to provide information of the force applied on the pedals by each limb, in order to achieve a more symmetrical force pattern. The frequency at which information should be provided, to achieve the best results. Whether an objective value should be defined for the user attempt to fulfil, and how this objective should be defined. The provision of EMG biofeedback, also requires the analysis of some issues, as follows. The appropriate selection of a muscle to provide EMG biofeedback. The best way to provide this type of biofeedback: providing only the muscle activation pattern or providing the muscle activation pattern and a target signal to be followed. The specification of the protocol is very relevant and involves the analysis of the parameters regarding the target population of these therapies, as well as, the most appropriate duration of the intervention (number of sessions per week) and of the session for target disease. These aspects will be explored by performing tests in healthy subjects, as well as, by analyzing the literature and the recommendations of the physicians that collaborate with this study.

1.3 Objectives

The purpose of this dissertation is the exploration of cycling exercise in combination with biofeedback as a feasibly method for stroke rehabilitation, especially in the rehabilitation of the motor abilities. In order to achieve the purpose of this dissertation, the following objectives were considered:

1. Summarize the functionalities, which a cycling device should possess for its application in the rehabilitation of patients with lower limbs motor impairments;
2. Implementation of data acquisition' systems in a cycling device, for assessment and characterization of patients, during the performance of different types of exercises;
3. Exploration of biofeedback mechanisms, in order to promote the recovery, increase the motivation and the participation of the patient on the rehabilitation process;

4. Exploration of the motor and functional characteristics to address, given the available human and material resources, and its rehabilitation importance;
5. Exploration and selection of the muscles more significant to the motor characteristics that are to be promoted;
6. Exploration and selection of the inclusion and exclusion criteria of patients, according to the healthcare practitioners' opinion;
7. Development of a biofeedback system for lower limbs motor recovery, in hemiparetic patients, using the EMG and the applied force;
8. Validation of the motor recovery and impact.

1.4 Outline

This thesis is organized as follows:

Chapter 1 describes the motivation, the research questions, the objectives and the structure of this thesis, as well as, the publications that resulted from this work.

In Chapter 2 is presented a critical review of the application of cycling leg exercise as a motor function rehabilitation method and as an aerobic training method, for stroke patients, as well as, the commonly used assessment tools. In addition, the potential benefits of use biofeedback combined with cycling are explored.

The cycling device used in this thesis (*THERA-Live*) is presented in Chapter 3, as well as, the sensors (optical sensors, force sensors and accelerometers) that were installed in the device, in order to obtain data about the user interaction with the device, such as the applied force and the angle of the pedals. In addition, the *YSY EST EVOLUTION*, a biofeedback and electrotherapy device, which was used in this thesis to provide EMG biofeedback, is also presented.

Chapter 4 includes the description of the lower limbs muscles, their general function and their function on cycling exercise. The muscle abnormalities observed in stroke patients, as well as, their possible causes, are also presented. The factors that influence the muscle activation patterns are addressed, followed by a further analysis of the muscles studied in this thesis. A biomechanical model of pedaling, used to compute the lower limbs' joints moments, is also introduced in this chapter. Finally, the influence of the workload and cadence in the force output, during training in a semi-recumbent cycling device, is analyzed.

The use of two types of biofeedback is address in Chapter 5. A system implemented to provide force biofeedback is described, as well as, the results of the application of this system in healthy subjects. The use of EMG biofeedback is also explored in this chapter. The biofeedback characteristics and the trials, conducted in healthy subjects, to test the systems, are presented.

In Chapter 6 are described all parameters of the protocol designed to test if the combination of EMG biofeedback or force biofeedback with cycling exercise may improve the motor function of stroke patients. This chapter includes the inclusion and exclusion criteria, the determination of the sample size and study groups, the assessment tests and the intervention, as well as, details about the procedure in each phase of the study. Lastly, the tests performed with three stroke patients are presented.

Chapter 7 presents the conclusions and major contributions of this thesis, indicating possible areas of interest for future research on this area and to continue this work.

1.5 Publications

From the work developed in this thesis resulted an International Conference article and a Journal paper:

D. Barbosa, M. Martins, C. P. Santos, et al., “Pedaling Parameters Behavior on Healthy Subjects: Towards a Rehabilitation Indication,” in EUSIPCO 2014 (22nd European Signal Processing Conference 2014), 2000-2004, 2014.

D. Barbosa, M. Martins, C. P. Santos, “The Application of Cycling and Cycling Combined with Feedback in the Rehabilitation of Stroke Patients: A Review” in Journal of Stroke and Cerebrovascular Diseases, 2014. (Published) .

State of the Art

2.1 Introduction

Population aging is increasing the susceptibility to stroke and neurodegenerative diseases, being stroke the second main cause of death. The patients which survive generally exhibit sequels with consequences in their normal life, such as hemiparesis, incapacity to walk without assistance, aphasia and dependence in the ADLs [1].

Rehabilitation's major objective in patients with motor impairments in the lower limbs is the recovery of the walking capacity [4]. This problem, besides the negative influence on the patient's independence, leads to immobility. Musculoskeletal disturbances (e.g. muscle atrophy, osteoporosis and contractures) and cardiovascular problems (e.g. minimized maximal oxygen consumption), as well as, low aerobic endurance, significantly affect the patient's ADLs performance and, in severe cases, may lead to death [2].

Some stroke patients are unable to perform exercises that are normally used in the rehabilitation of walking ability (e.g. walk with the support of parallel bars, Treadmill gait training), since the muscle force in the lower limbs is too weak to allow a secure body weight support [6]. Therefore, there is a demand for rehabilitation methods oriented to the recovery of the walking capacity of stroke patients. Due to the similarities with walking [7], cycling leg exercise may present a solution to this problem and might be an alternative motor function rehabilitation method. It allows a continuous repetition of movements, during an unlimited period of time, requiring less therapists, and with a lower physical load on them. As balance control is not required during cycling exercise, it can be used as a rehabilitation method in an early post-stroke phase, when gait training is not yet possible. Besides, in order to recover from motor impairments and to minimize the risk of secondary diseases that derive from immobility, stroke patients require an enduring therapy, like aerobic cycling exercise [2]. Assessment tools are needed to quantify the efficiency and efficacy of the applied cycling therapies. These tools assess the patient state and performance during different tasks, based in specific criteria.

Different therapies have been used together with cycling leg exercise to improve cycling's potential as a rehabilitation method, such as limb-load cycling [6, 8], Functional Electrical Stimulation (FES) [5, 9–14] and feedback [8, 15–19].

However, firstly, it is important to clarify several issues before the use of cycling as a rehabilitation method, such as the similarities and differences between cycling and walking, the advantages and limitations of cycling leg exercise when compared to walking on the rehabilitation of motor impairments,

and the type of stroke patients, which may benefit from cycling therapies. Moreover, information about the type of purposes where cycling leg exercise can be used, the applied protocols, as well as, the tools used to assess the state and the recovery of patients, are important to analyze the potential of cycling as a rehabilitation method. Finally, it is also important to verify if the use of other therapies together with cycling may lead to beneficial effects and, for instance, if it allows to overcome some cycling limitations.

In terms of therapies that can be used together with cycling, emphasis will be given to feedback based therapies in this chapter. Extrinsic feedback can be provided in cases where the patient's ability to evaluate their own movement is incapacitated [20]. This artificial information provided by an external source can be beneficial to motor recovery. It allows the assessment of the patient medical state and increases the performance and motivation of the patient on the execution of different cycling exercises [20]. Extrinsic feedback can also provide motivational mechanisms by displaying the performance metrics during the exercise, which promotes the participation of the patient during the rehabilitation process.

This chapter covers studies regarding the application of cycling therapies in stroke patients in order to identify the clinical evidence on the effectiveness of cycling therapies. Additionally, it tries to identify the main challenges which remain to be tackled. Considering health-care scenarios it is very important to assess if there is a robust evidence-based support to therapies before they become established in clinical settings. This thesis addresses lower limb cycling (leg exercise) and hereafter will be referred simply by cycling.

The chapter is organized as follows. In Section 2.2, a brief review of the stroke origin, consequences and associated rehabilitation processes is presented. Then, the cycling characteristics and applications are reviewed, especially its application as a rehabilitation and aerobic method, as well as, the assessment tools used to measure patient's impairments and recovery. In addition, some therapies combined with cycling are also introduced, presenting a more detailed review of the characteristics and applications of feedback. Finally, some of the existing cycling devices are explored.

2.2 Stroke

Stroke (or Cerebrovascular Accident) is the most common brain disorder and is characterized by sudden neurological symptoms, such as paralysis or loss of sensation, due to the destruction of brain tissue. Intracerebral hemorrhage (bleeding from a blood vessel in brain) – hemorrhage stroke – and, emboli (blood clots), or atherosclerosis (formation of plaques that block blood flow) of the cerebral arteries – ischemic stroke – are the common causes of stroke [21, 22]. Of all strokes, 87% are ischemic, 10% are intracerebral hemorrhage and 3% are subarachnoid hemorrhage strokes [1]. The risk factors of stroke include high blood pressure, high blood cholesterol, heart disease, diabetes, smoking, obesity, excessive alcohol intake, among others [21, 22].

In the USA, each year approximately 795 000 people are victims of a new or a recurrent stroke (data from 1999). About 610 000 of these are first attacks [1]. According to 2000 Census [23], the USA population was comprised of 281 421 906 people, therefore, the annual incidence (number of new cases of a disease that develop in a population per unit of time [1]) of first stroke per 1000 population was around 2.16. A study conducted [24], between 2004 and 2006, in 6 European countries, found an annual stroke incidence of first stroke per 1000 population of 1.41 in men and 0.94 in women.

Stroke is a leading cause of long-term disabilities, such as hemiparesis, inability to walk without assistance and dependence of others in the ADLs [1]. Motor impairments are characterized by paralysis

(hemiplegia) and weakness (hemiparesis), contralateral to the affected hemisphere of the brain [22]. Postural imbalance, muscle weakness (paresis), spasticity, asymmetrical movements between lower limbs, abnormal movement synergies, lack of mobility, loss of interjoint coordination and loss of sensation are generally observed in hemiparetic patients [3, 22]. Perform continuous and smooth reciprocal movements, such as walking, is a very difficult task for hemiparetic stroke patients [9].

The recovering of the walking ability is the major objective of lower limb rehabilitation after stroke [4]. The degree of recovery depends of several factors, such as lesion location and severity, and capacity for adaptation through training, and is higher in the first month after stroke [22]. The rehabilitation can begin in the acute phase of stroke (typically between 3 and 7 days), as soon as the patient is medically stabilized. Early mobilization prevents and reduces the effects of deconditioning and potential secondary impairments, by promoting functional reorganization through early stimulation and the use of the hemiparetic side. Patients with impairments continue the rehabilitation in the sub-acute (typically 7 days to 6 months) and in the chronic (more than 6 months post-stroke) phases. Currently, stroke rehabilitation approaches empathize task specific training with intense practice of functional tasks [22]. Treadmill gait training with or without suspension, supportive reciprocal stepping and muscle strength exercise have been used to overcome asymmetrical lower limbs' function and impaired postural control [25,26]. However, these interventions may not be suitable for some stroke patients due to, for instance, the degree of impairments. Typically, these interventions also have to be performed in a gym or clinical facilities.

The use of cycling together with feedback (work [18], symmetry, speed and workload [19]) also showed positive effects on walking ability in stroke patients. Given the similarities between walking and cycling, cycling may be used in stroke rehabilitation [27]. In the next sections this will be explored, as well as, the additional therapies which were used combined with cycling in the rehabilitation of stroke patients.

2.3 Cycling Aims

Cycling shares a similar kinematic pattern with walking, since both are cyclical; require reciprocal flexion and extension movements of hip, knee and ankle; and present an alternating and coordinated antagonist muscle activation [7]. Raasch *et al.* [7] suggested that cycling and walking share some sensorimotor control mechanisms. The ROM in cycling is superior than in walking, therefore pedaling helps maintaining the functional range of motion of the lower limbs required to walk [15]. Furthermore, cycling is safe, since balance is not a factor in seated pedaling. Thus, individuals do not experience too risky postural disturbances related to the initial stages of upright locomotor training [6]. When pedaling, the trajectory of feet is restricted to move in a circle, which limits abrupt changes in the direction of the movement and allows smooth phase transitions. Moreover, different intensities of training can be performed just by altering a few parameters (e.g. workload and speed) in the cycling device, without changing how the exercise is performed. These features, and the ability to exercise while seated, allow cycling to be accessible to patients in different disease phases (acute, sub-acute or chronic) [8]. However, walking involves the ability of force generation for body weight support and for coordinating weight shifting, while continuing on a cyclic trajectory. Hence, a limitation of cycling is the lack of body weight support and its shifting, when compared with walking [28].

Cycling can be used as a method to counter the consequences of immobility [2]. This type of training improves aerobic capacity, strength and cardiopulmonary function of subjects. Cycling devices can

perform a continuous and prolonged operation, whereas training capacity can be adjusted to patient's health status, physiologic response and rehabilitation evolution [29]. Cycling allows reversing muscular weakness in patients that only have one affected limb, since the healthy leg helps the affected one (through coupling of the pedals) during exercise performance. This encourages the use of the affected leg and the muscle control of the limbs, which may allow the affected leg to support more weight while standing [30].

There are two main modes of cycling exercise: active and passive. In the first, the subject does all the effort to move the legs and consequently the pedals, usually against a specific workload. This mode is similar to a normal cycling. In passive mode, the legs of the subject are driven by the pedals of the device, which are moved by a motor.

The positive effects of active cycling in stroke patients have been attributed to active contraction of the lower limbs muscles, although passive cycling exercise can trigger sensory inputs, which in turn can be beneficial to recovery. Passive cycling exercise can be used in people with ambulatory dysfunction in the acute rehabilitation setting, who are too weak or medically unstable to do motor active movements to regain motor function [16].

The effects of cycling have been studied in different diseases and conditions, such as Multiple Sclerosis [31], Parkinson (motor function [32–34], executive function [35], tremor and Bradykinesia [36]), in elderly patients [37], gait dysfunction (hip abductor weakness [38]), and stroke [2,6,39]. The application of cycling in stroke patients will be explored in the next sections, due to its high incidence and severe consequences, such as hemiparesis and hemiplegia.

2.3.1 Cycling Research

The major characteristics of the published cycling studies, applied in stroke patients, are summarized in Table 2.1.

Table 2.1: Major characteristics of the published cycling studies, applied in stroke patients. Acronyms: Aerobic (ARC), Assessment (AST), Control (C), Elderly healthy (EH), Experimental (E), Healthy (H), Hemorrhagic (HC), Ischemic (IC), minutes (min), not stated (NS), Randomized Controlled Trial (RCT), Rehabilitation (RT), sample size (N), sessions per week (s/w), Single Case (SC), single session (sg), weeks (w), wheel revolutions (r)

Study	Therapy		N	Population			Groups (E, C, H, EH)	RCT
	Aim	Length		Age (years (\pm SD))	Years after Stroke (\pm SD)	IC / HC Stroke		
Kamps <i>et al.</i> [2]	RT	16 w	31	C: 65.8 (10.7) E: 63.1 (8.1)	C: 1.28 (1) E: 1 (0.79)	31 / 0	E, C	
Katz-Leurer <i>et al.</i> [39]	RT	3 w (5 s/w)	24	63 (9)	NS	24 / 0	E, C	x
Seki <i>et al.</i> [40]	RT	8 r (sg)	10	69	0.19	6 / 4	E, H	
Fujiwara <i>et al.</i> [41]	RT	5 min (sg)	17	55.1 (10.9)	0.44 (0.16)	5 / 12	E	
Potempa <i>et al.</i> [29]	ARC	10 w (3 s/w, 30 min)	42	21 to 77	>0.5	NS	E, C	x
Tang <i>et al.</i> [42]	ARC	3 s/w (30 min)	23	64.7	0.05	17 / 5	E, C	
Holt <i>et al.</i> [43]	ARC	8 w (2/3 s/w, 30 min)	1	55	1.5	0 / 1	SC	
Quaney <i>et al.</i> [44]	ARC	8 w (3 s/w)	38	C: 58.96 (14.7) E: 64.10 (12.3)	4.9 (3.3)	NS	E, C	x
Lennon <i>et al.</i> [45]	ARC	10 w (2 s/w, 30 min)	48	C: 60.5 (10) E: 59 (10.3)	C: 4.72 (3.26) E: 4.56 (2.13)	48 / 0	E, C	x
Katz-Leurer <i>et al.</i> [46]	ARC	5 w (3/5 s/w, 30 min)	92	63 (11)	NS	80 / 12	E, C	x
Lee <i>et al.</i> [47]	ARC	10/12 w (3 s/w, 30 min)	52	63.2 (9)	4.75 (4.5)	33 / 9	E, C	x
Chen <i>et al.</i> [25]	AST	5 min (sg)	10	58.9 (13.5)	2.11 (1.61)	NS	E, EH	
Brown <i>et al.</i> [26]	AST	3 min (sg)	15	65.3 (5.8)	3.53 (3.59)	NS	E, EH	
Kautz <i>et al.</i> [30]	AST	3 min (sg)	15	65.3 (5.8)	3.53 (3.59)	NS	E, EH	
Brown <i>et al.</i> [28]	AST	3 min (sg)	15	65.3 (5.8)	3.53 (3.59)	NS	E, EH	
Rosecrance <i>et al.</i> [48]	AST	4.5 min (sg)	13	58.7 (8.9)	4.8 (3.5)	NS	E, EH	
Brown <i>et al.</i> [49]	AST	120 min (sg)	17	63.1 (5.0)	1.67 (0.43)	NS	E, EH	

Inclusion criteria varied throughout the studies. Regarding stroke phases, cycling exercise has been applied in sub-acute [5, 6, 39, 40, 42] and chronic [8, 17, 18, 25, 26, 28–30, 43–45, 48, 49] phase patients. The majority of the studies considered the time after stroke as an inclusion criterion, others [2, 39, 40, 46] did not. Although the sample size has been small in the different studies, in some, it was higher than twenty [2, 15, 29, 39, 42, 44–47]. Regarding the type of stroke, three studies [2, 39, 45] had ischemic stroke as inclusion criterion, the others considered the ischemic and hemorrhage types or did not provide information about the stroke type. Some studies divided the stroke patients into two groups, the experimental and the control groups [2, 8, 29, 39, 42, 44–47], which allowed a more reliable comparison of the applied cycling therapies. Some studies had a control group formed by healthy people [8, 18, 40], usually to compare the expected values for some variables used in the assessment of the cycling therapies. Elderly healthy subjects were also considered as a control group in some studies [25, 26, 28, 30, 48, 49] to determine the expected values in the same age group of the stroke patients (experimental group). Other studies, only had an experimental group [41] or were single case studies [17, 43]. Randomized Controlled Trial (RCT) was the study design implemented in the interventions of some other reviewed studies [29, 39, 44–47].

Through the analysis of the reviewed studies, it is possible to divide the application of cycling in two types of rehabilitation methods: motor function rehabilitation and aerobic training, which addresses the prevention of immobility-related secondary diseases, as well as, the rehabilitation of the motor functions. Assessments tools are used to assess the patient's medical conditions, as well as, the efficiency

2.3.1.1 Cycling as a Motor Function Rehabilitation Method

The major objective of the use of cycling in rehabilitation is the recovery of motor impairments. The improvement of motor abilities, balance and walking performance were some of the targets of the application of cycling in the rehabilitation of the motor function. This type of exercise was used in stroke patients both in sub-acute as in chronic phase.

In Katz-Leurer *et al.* [39] the purpose was to analyze the effect of early cycling, during 3 weeks, on balance and motor performance in 10 sub-acute stroke patients. At the end of the 3 weeks and in the follow-up (3 weeks later), the improvement in balance and motor abilities of the experimental group was higher than in the control group (14 sub-acute stroke patients, which performed only conventional therapy). These findings suggested that early cycling exercise at the sub-acute phase may improve balance and motor performance.

Kamps and colleagues [2] conducted a study to prove the effectiveness of cycling home training, during 4 months, in 16 stroke patients with hemiparesis. The results showed higher improvements in walking distance, comfortable gait speed and timed "UP&GO" test (time needed to stand up from a chair with armrest) in the experimental group when compared with the control group (15 stroke patients with hemiparesis that only performed conventional therapy). According to the authors, this study showed that it is possible to expand the capacity of mobility in post-stroke patients, even after six months since stroke.

Cycling induced muscle activity on stroke patients' paretic legs after only one session [40, 41]. Seki and colleagues [40] observed significant increases in the *rectus femoris*'s, the *tibialis anterior*'s, and the *soleus*' muscle activity of the affected leg, during cycling in comparison with a baseline isometric contraction. Fujiwara *et al.* [41] observed an increase in muscle activity, at the end of 5 minutes of cycling and 30 minutes later. According to the authors of these two latter studies, the results suggested

that cycling might be a useful method of muscle reeducation for paretic limbs.

2.3.1.2 Cycling as an Aerobic Training Method

Some diseases' sequels may cause reduced mobility, which may result in low endurance to exercise. This may contribute to poor rehabilitation outcomes, ambulatory function, social participation, quality of life and delays the return to normal life [29, 50]. After rehabilitation discharge, the low endurance might further decline, which may compound the energy cost of movements [29]. In Kelly *et al.* [51] the purpose was to assess the cardiorespiratory fitness of sub-acute stroke patients. The values of the maximal aerobic capacity (VO_2), maximal walking velocity and endurance were half of the reported values for a healthy age-matched group. Besides the application in the rehabilitation of motor function, cycling may be used as an instrument to prevent patient's immobility. Aerobic cycling exercise studies' aims include the prevention of immobility-related secondary diseases, such as cardiovascular and musculoskeletal complications, but also the rehabilitation of motor functions. Different studies investigated the effect of aerobic cycling exercise on walking ability [42–45, 47], independence and activity [46], maximal aerobic capacity [8, 29, 42, 45] and executive function [44]. In addition to the gait analysis metrics (walking speed, distance and number of climbed stairs), these type of studies also analyzed cardiorespiratory fitness indicators, such as maximal aerobic capacity, Cardiac risk score and endurance. The analysis of cardiorespiratory fitness indicators in aerobic cycling exercise studies is the differentiating factor from the use of cycling in motor function rehabilitation. The protocol of the aerobic cycling exercise studies, usually, includes a training workload defined through a percentage of the maximal training intensity that the patient can achieve.

Potempa and colleagues [29] investigated the effect of aerobic cycling exercise on cardiovascular and functional outcome measures in hemiparetic stroke patients. An experimental group performed a 10 weeks program of aerobic cycling exercise for 30 minutes, whereas the control group (23 hemiparetic stroke patients) executed passive ROM exercises. The 19 experimental subjects showed significant improvements in oxygen consumption, workload, and exercise time. The authors suggested that the improvements in maximal aerobic capacity were related to improvements in sensorimotor function, which indicates that this type of training is beneficial to subjects who are able to train at a high intensity. Tang *et al.* [42] also analyzed the effect of aerobic cycling exercise and observed greater improvements in VO_2 and 6-Minute Walk Test distance in the 23 sub-acute stroke patients aerobic group (30 minutes of cycling exercise, 3 days per week, in addition to the conventional therapy, until discharge) compared with the control group (22 sub-acute stroke patients), which only performed conventional therapy. A positive progression in walking speed, distance and muscle strength (Motricity index) with no adverse effects on spasticity in the upper or lower limbs was observed by Holt *et al.* [43] in a chronic stroke patient with hemiplegia, 19 days after 8 weeks of aerobic cycling exercise (2 or 3 sessions of 30 minutes per week).

Katz-Leurer *et al.* [46] investigated the effect of 8 weeks of early aerobic cycling exercise on independence in daily and social activities six months post-stroke. The authors observed significant improvements in the functional abilities (walking distance, gait speed and number of climbed stairs) of 46 stroke patients, after early aerobic cycling exercise, compared with the control group (46 stroke patients), which only performed conventional therapy. However, no significant differences were found on independence in daily and social activities between groups in a six months post-stroke follow-up.

Lennon *et al.* [45] evaluated the effect of 10 weeks of aerobic cycling exercise (upper and lower limbs cycling) on risk factor reduction and health-related quality of life of chronic stroke patients. Greater

improvements in maximal aerobic capacity, Cardiac risk score and Borg rate of Perceived Exertion (RPE) were observed the experimental group (24 patients) compared with the control group (24 patients that only performed conventional therapy).

In the study by Quaney *et al.* [44], the effects of 8 weeks of aerobic cycling exercise (45 minutes 3 sessions per week) in executive function, motor learning and mobility were analyzed. The experimental group (19 chronic stroke patients) improved significantly the VO_2 , information processing speed, predictive force accuracy, ambulation and sit-to-stand transfers compared with the stretching exercise group (19 chronic stroke patients) at the end of the intervention. However, in the follow-up only the balance control significantly improved. No significant difference was found in the executive function between the two groups.

Lee *et al.* [47] compared the effect of aerobic cycling exercise and Progressive Resistance Training (PRT) of lower limbs (training on a pneumatic resistance device with gradual increase of weight against which the muscle works) on walking ability in chronic stroke patients. Fifty-two stroke patients were divided in four groups: aerobic cycling exercise plus sham PRT, PRT plus sham aerobic cycling exercise, aerobic cycling exercise plus PRT and sham PRT plus sham aerobic cycling exercise (passive exercises). All patients performed 30 exercise sessions over 12 weeks. Neither of the two training modalities improved walking distance and gait velocity significantly more than passive exercise. However, progressive resistance training significantly improved stair climb power, muscle strength, power and endurance, whereas aerobic cycling exercise improved the cardiorespiratory fitness indicators. The large effects for mobility and impairment outcomes were observed in the group that performed the two modalities together.

Sibley *et al.* [8] analyzed the effect of aerobic cycling exercise combined with two therapies (limb-load cycling and EMG biofeedback), however, the responses of the aerobic variables varied in the three chronic stroke patients.

2.3.1.3 Assessment Tools used in Cycling

To assess patient's evolution during and at the follow-up of the rehabilitation program, assessment tools are necessary. These tools can be used also for assessing the effects of different exercise characteristics and modes.

The assessment tools used in the reviewed studies can be classified as qualitative or quantitative metrics, based on the type of information which is analyzed and on the way they are performed. The standard and stroke specific Functional Scales are qualitative metrics. The quantitative tools, include Gait Analysis Metrics, Cycling Exercise Metrics, Physiological Variables and EMG-based Variables. In Table 2.2, some assessment tools are presented, as well as, the studies they were used in.

The Functional Scales provide a standardized patient's assessment, indicating one's state, for example, based on one's ability to perform some tasks. Moreover, they are used to assess the patient's ambulation skills, determine the impact of impairments, monitor progress and check the efficacy of rehabilitation therapies. In specific, functional mobility skills (movement transitions, locomotion, transfers), basic ADL skills (feeding, hygiene, dressing), and instrumental ADL skills (communication, housekeeping tasks) are examined by Functional Scales [22], which can be or not specific for stroke.

The Functional Scales are used to assess the improvements of patients after the intervention. They are also used to perform an initial analysis of the impairments of the patients, for example as an inclusion criteria on the selection of the subjects. On the other hand, Functional Scales specific to stroke are used

Table 2.2: Assessment tools used in the reviewed studies to assess the patients’: impairments, recovery, and the effect of different exercise characteristics and modes

Qualitative Metrics	Functional Scales	FMA [15, 16, 19, 25, 26, 28–30, 39, 44, 49]; Functional Independence Measure (FIM) [6, 39, 42, 46]; Modified Ashworth Scale (MAS) [18, 19, 25, 39, 40, 43]; Berg Balance Scale (BBS) [2, 44]; Barthel Index (BI) [15, 19]; Motricity index [43].
	Functional Scales – Stroke	Postural Assessment Scale for Stroke (PASS) [39]; Chedoke-McMaster Stroke Assessment (CMSA) [8, 42]; Stroke Impairment Assessment Set (SIAS) [41]; Stroke Impact Scale (SIS) [42]; Scandinavian Stroke Scale (SSS) [46]; National Institutes of Health Stroke Scale (NIHSS) [42].
Quantitative Metrics	Gait Analysis Metrics	10 Meters Walking Test (10MWT) [2, 6, 18, 19, 43, 47]; 6 Minutes Walking Test (6MWT) [2, 6, 19, 42, 43, 47]; Stair climbing test [46, 47]; Timed "Up&Go" Test [2].
	Cycling Exercise Metrics	Cycling speed, Speed variability, Power, Workload, Distance and Duration; Roughness Index (<i>RI</i>) [25]; Averaged Cycling Power (<i>P_{av}</i>) [15]; Unbalance (<i>U</i>) [5, 18]; <i>BF_{perf}</i> [18];
Quantitative Metrics	Physiological Variables	Electrocardiography (ECG) signal, maximal aerobic capacity (<i>VO₂</i>), gas exchanges and blood pressure.
	EMG-based Variables	Integration of the EMG Activity (IEMG) [26, 28, 30, 41, 49]; Shape Symmetry Index (<i>SSI</i>) [15, 16, 25]; Area Symmetry Index (<i>ASI</i>) [15, 25]; Symmetry Index (<i>SI</i>) [16].

to assess stroke patients. Even though Functional Scales provide information about the motor function of the patients, they do not provide quantitative data about the effects induced by cycling on the affected lower limbs and on the performance of the exercise. Therefore, alternative assessments tools, for instance metrics based on cycling exercise, are necessary to perform different and quantitative analysis.

Some reviewed studies [2, 6, 18, 19, 43, 44, 46, 47] assessed the effects of the cycling therapies on the patients’ locomotion through Gait Analysis Metrics. In the 10MWT, variables like duration, mean velocity, stance and swing times and stride and step length, are usually analyzed. In the 6 Minutes Walking Test (6MWT), the covered distance and the speed are typically analyzed. Ferrante and colleagues [18] also analyzed the ratio between the stance time in percentage of stride time (*ST Ratio*) and the ratio between the swing velocity of the paretic and healthy leg (*SV Ratio*).

Other studies [2, 15, 16, 26, 29, 30, 43, 46] focused on Cycling Exercise Metrics (Table 2.2), which include cycling speed, speed variability, power, workload, distance and the duration of the exercise . In addition, specific measurements were performed to analyze the effects of the different training features on the patients’ performance. Chen *et al.* [25] introduced an index to represent the cycling smoothness, the Roughness Index (*RI*), which was also used by Lin *et al.* [15]. A stable instantaneous speed across the entire pedaling cycle, with a value close to the average cycling speed, is the ideal smooth cycling pattern. The roughness index (during one revolution) is given by (2.1):

$$RI = \frac{\sum_1^{360} \left| \frac{dR}{ds} \right|}{\bar{R}} \quad (2.1)$$

where *R* is the instantaneous cadence after polynomial curve fitting, and *s* is the crank position. The *RI* attempts to measure how the cycling speed is kept constant over the entire cycle: the higher the smoothness of the cycling pattern the higher is the *RI* value. When a steady instantaneous cadence is maintained

through the pedaling cycle, the RI will approach zero. Chen *et al.* [25] observed that hemiparetic patients showed a less smooth cycling than healthy elderly subjects. Moreover, they concluded that the use of a higher workload resulted in a decrease of cycling pattern smoothness, in the patients with hemiparesis.

To compute the cycling power across the pedaling cycle, Lin *et al.* [15], presented the Averaged Cycling Power (P_{av}), which is defined as the product of cadence ($S(n)$) and torque ($T(n)$) and represent the force output:

$$P_{av} = \frac{\sum_{n=1}^{n=360} S(n) \times T(n)}{360} \quad (2.2)$$

As one consequence of stroke is, generally, the lack of force on the affected limb, several studies compared the force output of both limbs. Therefore, the work applied on the pedals was analyzed in [5, 18, 26, 28, 30, 49], in pathological and healthy subjects. Brown *et al.* [26] studied the effects of speed in force output of the paretic limb of patients with post-stroke hemiparesis and observed that the reduction of this parameter was more significant at higher speeds. The main cause of this reduction was due to the increase of the negative work done, during the upstroke phase. The nonparetic limb increased the force output to compensate for the decreasing in pedal force by the unhealthy leg at higher speeds.

To analyze the unilateral motor deficit, it is important to compute unbalance in the mechanical work applied by the limbs during cycling exercise. Two studies [5, 18] used an Unbalance (U) that compares the work done by the paretic leg, in relation to the healthy one, which is given by (2.3):

$$U = \frac{|W_{HL} - W_{PL}|}{|W_{HL}| + |W_{PL}|} \quad (2.3)$$

where W_{HL} and W_{PL} are the work done by the healthy and paretic limb, respectively. The U could range from 0 (identical works) to 1 (W_{PL} negative or equal to zero). Others measurements were used to assess specific aspects of the studies, such as the BF_{perf} (ratio between the number of symmetrical revolutions and the total number of revolutions) and the *DynamicLoadIndex* (product between the load and the number of repetitions). The first one was used by Ferrante *et al.* [18] to analyze the cycling symmetry, whereas the second one was used by Brown *et al.* [6] to measure the success of the patients in performing the authors' limb-load cycling program.

According to Rosecrance and colleagues [48], the available assessment tools for evaluating patient's function may quantify the overall level of function, but cannot identify or precisely measure characteristics of the movement dysfunction. Therefore, the authors investigated stationary cycling as a method for measuring lower limb movement dysfunction, by comparing the kinematic characteristics of hemiplegic stroke patients with normal subjects. To accomplish that, angular displacements of the hip, knee and ankle were measured. The kinematic data were evaluated separately and regarding angular velocity versus angular displacement diagrams and angle-angle diagrams for hip-knee and knee-ankle displacements. The results showed that the average kinematic values were similar for normal and hemiplegic groups, however, displacements patterns and velocity were different. This demonstrates the importance of performing evaluations using isolated kinematic variables, as well as, dynamic analyses. The authors concluded that cycling might be used as a method to analyze motor control deficits in lower limbs movement dysfunction.

Physiological variables, such as heart rate, ECG signal, maximal aerobic capacity, gas exchanges and blood pressure have been measured in studies which address cycling as an aerobic exercise [8, 16, 29, 42–44, 46, 47]. The assessment of the physiological responses to aerobic exercise is important to evaluate

the therapy's effects on the patients. Furthermore, these variables could be used as safety measures to determine if the performed exercise is prejudicial to the patient's health [39].

Finally, EMG-based variables are used to study the muscles that contribute to the movement during cycling, in order to understand if and how motor impairments reflect in muscle activity, and if cycling improves the recovery of these impairments. In several studies [5, 8, 15–17, 25, 26, 28, 30, 40, 41, 49], the EMG signals or others measurements derived from them were used to assess the patients impairments or the different cycling therapies' effect. The Integration of the EMG Activity (IEMG) of different muscles, during different phases of the pedaling cycle, has been used to check for abnormalities in the timing of muscle excitation [26, 28, 30, 41, 49].

Brown and Kautz [26, 28, 30] used EMG signal and IEMG to analyze the effect of speed and workload on the muscle activity, and if the decreased ability to perform mechanical work by the paretic leg during pedaling was related to abnormalities in the timing of muscle excitation. In [8], the authors observed that paretic muscles are differently affected depending on their function, which influence the produced work in different ways. In [26], the authors did not observe an increase of inappropriate muscle activity at higher speeds, suggesting that the main contribution to the reduction in force output are the inherent mechanical demands of higher-speed pedaling. Concerning the workload [28], the authors verified an enhanced force output by the paretic leg at higher workloads, without the increase of inappropriate muscle activity. Furthermore, the nonparetic leg was able to respond to the increased demands, since no change was observed in the timing muscle activity patterns, and the same was observed in the control group. Fujiwara *et al.* [41] investigated muscle activities of the lower limbs in nonambulatory hemiparetic stroke patients, during cycling exercise. Although no significant difference was observed in the pattern of the affected side in comparison to the unaffected side, the IEMG values of the affected side were smaller.

The Shape Symmetry Index (*SSI*), introduced by Chen *et al.* [25], describes the similarity between the EMG linear envelopes of the two legs (after phase correction), and is given by (2.4):

$$SSI_j = \frac{|C_{xy}(j)|}{[\sum_{n=0}^{N-1} x^2(n) + \sum_{n=0}^{N-1} y^2(n)]^{\frac{1}{2}}}, j = 1, \dots, 360 \quad (2.4)$$

where x and y are N -point EMG linear envelopes and $C_{xy}(j)$ is the circular cross-correlation function with lag j between two linear envelopes. The comparison between the muscles activities of both legs, by measuring the cross-correlation between linear envelopes of EMG signals, may be used to analyze the cycling symmetry, regarding the muscle activation. A higher *SSI* value (maximum value of 1) implies a higher symmetry in EMG activities during cycling movement. Chen *et al.* [25] used the EMG signal of the quadriceps muscles to determine the cycling symmetry. The results showed that, while normal subjects maintained a high symmetry in muscle activities of both legs (meaning that both legs contributed equally to the pedaling exercise), stroke patients presented an asymmetric muscle activity (low *SSI*). Furthermore, the authors observed that the symmetry of muscle activity was not influenced by the increase of the workload. As *SSI* only compares the shape of the signal, Lin *et al.* [16] used Area Symmetry Index (*ASI*), which determines the overlapping area of two EMG linear envelopes, since this index uses information about the amplitude of the signals, as shown in (2.5):

$$ASI = 1 - \frac{\sum_{n=1}^N |x(n) - y(n)|}{\sum_{n=1}^N x(n) + \sum_{n=1}^N y(n)} \quad (2.5)$$

where $\sum x(n)$ and $\sum y(n)$ are the areas under the linear envelopes of the right and left sides and $\sum |x(n) - y(n)|$ is the non-overlapping area of the two linear envelopes. In Lin *et al.* [16], surface EMG of the

bilateral *rectus femoris* was recorded to compute the Symmetry Index (*SI*) of muscle activations (product between *ASI* and *SSI*). Lin and colleagues [15], analyzed the same variables as in [16], however, the EMG signal of the *biceps femoris* was recorded as well. The *ASI* and *SSI* allow a more detailed description of symmetry in EMG activity in terms of shape and magnitude in the assessment of neuromuscular control in stroke patients [15].

2.3.2 Cycling-based Therapies

Different therapies combined with conventional cycling have been proposed to maximize the rehabilitation effects, such as passive cycling, limb-load cycling, FES and feedback. The latter, in addition to the effects on the rehabilitation, may be a motivational tool, to increase the patient involvement in the rehabilitation process.

Passive cycling can be used in patients which are too weak or medically unstable to do motor active movements [16]. Furthermore, this cycling mode is also used to perform a warm-up and a cool-down period, before and after the active pedaling task [2, 5, 18, 19]. To study the potential effect of passive cycling exercise, Lin *et al.* [16] compared the activation of cortical regions in active and passive cycling modes in patients with subcortical stroke. The results showed that passive and active cycling activate similar cortical regions, although a lower intensity is evident in the sensorimotor cortex of the unaffected side. This lower activity may be due to the reduced demand of muscle contraction in passive exercise. The authors suggested that this finding supports the use of passive cycling in stroke rehabilitation as an adjunct or primary training program in an early intervention to facilitate motor recovery.

According to Brown *et al.* [6], limb-load cycling offers a task-oriented locomotor training to patients that are unable to support their entire body weight [6]. Furthermore, this technique allows overcoming the lack of weight bearing and shifting in conventional cycling exercise, since it requires coordinated transfer of the weight between the affected and the healthy limbs and demands force production by the lower-extremities. Brown and colleagues [6] tested an exercise protocol (limb-loaded cycling) in two sub-acute stroke patients with hemiparesis, using a modified cycling ergometer, which allows training with partial body weight support. During training, the patients increased the number of successful cycles and the percentage of the supported load. Furthermore, FIM score and the distance walked in 6 minutes increased during training. The authors suggested this protocol as a complement to conventional physical therapy, to more rapidly increase muscle performance. Sibley *et al.* [8] also used limb-loaded cycling as a modality to address aerobic training and increase the paretic limb's involvement, with the objective to improve the outcomes and productivity of therapy sessions. Three chronic stroke patients trained with 30% of body weight support, for 4 minutes at 50 rpm. The workload value of the training was 50% of the maximal workload achieved in a previous assessment test. Stroke patients were not able to pedal at the same load as healthy control patients. Even at a lower load they failed to increase the target muscle activation, as the healthy group did. The authors indicated the difficulty of establishing an exercise protocol in this area and suggested that this protocol may be more adequate for patients with higher function level, as an adjunct to walking exercise. Sullivan *et al.* [52] observed improvements in the walking speed and in the 6 Minutes Walking Test (6MWT) distance at the end and in the 6 months follow-up of a 6 weeks combined intervention (12 sessions of body-weight supported treadmill training and 12 sessions of limb-loaded cycling exercise), in a chronic stroke patient.

Functional Electrical Stimulation (FES) uses the electrical stimulation of a motor neuron to activate paralyzed or paretic muscles in a precise sequence and amplitude to accomplish functional tasks [53]. In

addition, FES exercise can increase strength and prevent muscle atrophy by using stimulation patterns that induce repetitive contractions in selected muscles [53]. Different studies have evaluated the efficacy of FES combined with cycling on motor recovery in sub-acute and chronic stroke patients. These studies showed positive benefits on muscle strength [9], cycling smoothness [10], maximal aerobic capacity [11, 12], locomotion performance [11, 13], postural control [14], spasticity [14], and motor coordination [5].

Feedback corresponds to the sensory information provided during or following task performance. Motor learning and the effectiveness of the training can be enhanced by providing feedback to healthy subjects. Feedback can be used to detect and correct errors in the performance, by comparing the movement with the expected goal, and can be categorized as either intrinsic or extrinsic [20]. Feedback will be explored in the following sections, due to its potential in the increasing of motor recovery, performance and motivation.

2.4 Feedback-research Questions

The next sections cover the main characteristics of feedback: the differences between intrinsic and extrinsic feedback; the differences between knowledge of results and knowledge of performance extrinsic feedback; the sources of feedback; and the scheduling problematic. Finally, studies of the application of extrinsic feedback combined with cycling, in stroke patients, will be presented. The characteristics of these studies will be presented and summarized in tables. A comparison among characteristics is presented focusing in protocols, statistics and assessment tools. Additionally, a summary of findings is presented and discussed.

2.4.1 Intrinsic and Extrinsic Feedback

Intrinsic feedback refers to a person's self-sensory perceptual information, available during performance of a task or movement. The sensory processes correspond to somatic information (such as vision, proprioception, touch, audition and pressure). Providing this information assists in formulating an internal representation of the desired movement [20, 54].

In some cases, intrinsic feedback mechanisms may be compromised due to impaired central sensory functions, for example, after peripheral or central nervous systems injuries, such as stroke [55]. Extrinsic feedback can be given in addition or in substitution of intrinsic feedback. This artificial feedback, provided from an outside source, may be beneficial in improving motor recovery. Extrinsic feedback can be characterized by its nature (Knowledge of Results (KR) or Knowledge of Performance (KP), timing (concurrent, terminal), and frequency of delivery to the subject (e.g. continuous, summary or faded), which will be explained on the following sections. Determining the feedback variables, that optimize motor recovery in different diseases, is important to increase the success of rehabilitation interventions [56], such as cycling.

Extrinsic feedback and instructions are different, since, in the first, information based on previous movement attempt is given [57]. Patients may use compensatory, but inefficient or ineffective movement patterns if extrinsic feedback is not provided [54]. Furthermore, the use of extrinsic feedback results in better retention of the learned skills [56]. The delivery of extrinsic feedback has been used and recommended to facilitate the relearning of movements and to increase the effectiveness of the rehabilitation programs, in stroke patients [20]. It improves patients' motivation, allows the assessment of the exercise

and may improve motor performance and enhance the motor relearning process, in different tasks such as balance, gait and cycling [20, 58–62].

Extrinsic feedback can be defined as biofeedback when biological performance quantities are delivered back to a biological system (human) [55]. Biofeedback corresponds to the use of instrumentation to provide information about physiological processes. Although this term has become widely accepted, some authors continue to refer it as extrinsic feedback.

The use of biofeedback provides the opportunity for patients with sensorimotor impairments to regain the ability to better evaluate and control the physiological responses [63]. Biofeedback is provided together with task-specific exercises to ensure that the exercise is performed with maximum efficiency, trying to lead to permanent changes in the capacity when performing the task [63, 64]. According to Wolf *et al.* [65], continued training with extrinsic feedback might establish new sensory engrams, by the activation of unused or underused synapses in executing motor commands, aiding patients to execute tasks later on without using extrinsic feedback. The involvement of auxiliary sensory inputs in biofeedback may enhance neural plasticity.

The effectiveness of biofeedback may be influenced by different variables such as the location or size of the brain lesion, the patient's motivation during therapy and/or the cognitive capacity of the patient [63]. Cycling has been used together with biofeedback, such as EMG biofeedback [8, 17], in the rehabilitation of stroke patients.

2.4.2 Knowledge of Results and Knowledge of Performance

Extrinsic feedback can be classified, in terms of its nature, as Knowledge of Results (KR) or Knowledge of Performance (KP) [15, 20, 54, 56].

KR (or terminal feedback) consists in information about the outcome of performing a task or achieving the goal of the performance. An example of KR consists of informing the patient that his symmetry level was 80%, during task performance. KP (or concurrent feedback) is extrinsic feedback about the movement characteristics that led to the task performance, in other words, feedback on the nature of movement pattern. For instance, informing the patient that he needs to apply more force with the left leg to improve the symmetry level. KP is mostly used in rehabilitation context [20, 54].

Some studies, such as [56, 66], examined the differences between KR and KP and concluded that the two types of extrinsic feedback, compared with no feedback, resulted in retention improvements in movement quality. For instance, Cirstea *et al.* [56] compared motor improvements in three different groups of chronic stroke patients with hemiparesis. Two groups practiced a pointing movement to a target without vision, with one group receiving 20% of terminal KR (information about movement precision) and the other group received faded concurrent KP about joint motion (shoulder flexion and elbow extension) during movement. The control group performed finger and hand exercise, but with the same intensity than the other groups. The results showed that motor improvements depended on the type of feedback provided. In comparison to the control group, subjects who received information about movement precision only improved that outcome, whereas the KP group improved more movement outcomes. Different feedback strategies produced different movement outcomes, since the KR group achieved more precise and faster movements. In contrast, a better movement time and variability was achieved by the KP group.

Providing KR feedback may produce no effects in certain cases where the task has inherent information about the movement outcome. For instance, Platz and colleagues [67], when providing KR feedback

did not achieve significant effect, on either immediate or long-term outcomes, comparing with the same tasks without feedback. This result may be due to the awareness of patients about their performance and progress regardless of feedback, for instance, a digital bar diagram regarding the placement of an object on the top of another did not result in better learning. Therefore, the authors suggested that, in certain cases, KR feedback may be redundant and will not result in additional improvements to the patient's abilities, except when it is a motivational factor and encourages patient's control of performance.

Ferrante *et al.* [18] and Yang *et al.* [19] provided KP feedback of work and symmetry, speed and workload, respectively, combined with cycling, for the rehabilitation of the walking abilities in stroke patients.

2.4.3 Scheduling of Feedback

The scheduling of feedback can be continuous (every trial), summary (after a fixed trial number) or faded (every trial at the beginning, then after several trials) [54]. Providing continuous feedback to the patient might be adverse to the learning process, despite improving the performance, since the reduction of the use of intrinsic feedback may lead to a potential dependency on extrinsic feedback to perform the task correctly [20]. There is no consensus about the most appropriate feedback schedule that should be used in order to achieve better results in rehabilitation. For instance, Van Vliet *et al.* [20] concluded that providing feedback on less than 100% of the trials (summary feedback) may enhance learning process in post-stroke patients. Winstein and colleagues [68] suggested that a faded feedback may be more beneficial for arm rehabilitation in stroke patients than a continuous feedback, although it is unknown if a reduced frequency is beneficial for all stroke patients. Although some authors indicate that a reduced feedback frequency is better for movement relearning and retention, the most suitable value is unknown. A reduced frequency of feedback is the cause indicated by Sibley *et al.* [8] for the unsuccessful of stroke patients in increasing the paretic limb involvement when EMG feedback was provided, whereas, in healthy subjects, muscle activation increased. The feedback frequency (updated every 30 seconds) was effective for the healthy group, while stroke participants could have benefited from an increased frequency. One possible solution may be the alteration of frequency of feedback according to the motor and cognitive impairment.

One way to limit the frequency of feedback is by providing bandwidth feedback, as done by Morris and colleagues [69]. They studied the effect of kinematic feedback using an electrogoniometer to limit knee hyperextension during standing and gait training. Auditory feedback only was provided if the knee extended more than the normal angle (bandwidth feedback) and the pitch was proportional to the hyperextension angle. At the end of the 4-week program, the experimental group reduced the knee hyperextension more significantly when compared with the control group (without feedback).

2.4.4 Types of Biofeedback

Huang and colleagues [63] classified biofeedback in two types: static and dynamic (or task-oriented) biofeedback. Learning to regulate a specific parameter through a quantified cue in a static position or doing a movement unrelated to the ADLs was defined as static feedback. Task-oriented biofeedback relies on the biofeedback provided during the performance of function-related task training to optimize motor function improvement. To increase effectiveness, the biofeedback cues of task-oriented biofeedback therapy should be multimodal to involve perceptive and cognitive functions; attractive and motivating, with

the purpose of retaining the subject's attention; and easy to understand, avoiding information overload. Nowadays technology makes this type of feedback simple to be implemented [63].

The type of biofeedback is an important factor in the motor relearning process [56]. The source and the way it is provided to patients are two key aspects of biofeedback. In the selection of the most appropriate biofeedback type, different aspects should be considered, for instance, the lesion type and location and patient medical condition. Different variables have been used as a biofeedback source, such as EMG signals [8, 17, 65, 70–73], kinematic quantities (range of motion of joints [56, 74], step length [60]) and kinetic measures (ground reaction forces [75], speed [15, 16], work [18]).

EMG biofeedback is used frequently as a biofeedback source, to represent neuromuscular control, since it typically results in an improvement of task performance [15]. The distinctive characteristics of it are the specificity of information about muscle activity and the speed at which information is provided to the subject. This type of biofeedback can be used, for instance, in stroke patients to help them learning to more effectively contract the flexor muscles of the paretic leg and in the inhibition of hypertonicity in the extensor muscles [65]. Several studies implemented EMG biofeedback showing that it results in an improvement of voluntary control of the activity of the trained muscles and in an increase in ROM of the joints that the trained muscles control [72, 73]. However, according to Huang *et al.* [63], the effect of this type of biofeedback on motor recovery is inconsistent.

Visual, auditory and haptic feedback are the most commonly delivery medium to provide feedback to the user. Visual feedback can be given by the therapist, by video or via visual displays as a demonstration [20]. This type of information can be presented by graphical elements, such as numbers, bars or graphs [8, 15–19, 74, 75]. Different studies have demonstrated that stroke patients can benefit from receiving visual feedback about different sources, such as weight distribution and weight shift [64, 75], training velocity [15], force output [18] and EMG activity [17, 71]. For instance, Sackley *et al.* [75] found significant improvements in stance symmetry and sway, motor function and ADLs compared with a control group, after a 4-weeks exercise program with visual feedback about weight distribution and shift, displayed on a computer screen (Figure 2.1), while performing balance tasks on a balance platform.

Auditory feedback is largely used by therapists (verbal feedback), although it is mainly motivational and reinforcing, with information feedback being rarely used, according to the study of Talvitie and colleagues [76]. In certain cases, an inaccurate verbal feedback can override the person's own correct visual feedback. Van Vliet's [20] review presents some studies in which the use of auditory of force production resulted in improvements in body weight distribution. Sound is a very effective feedback source for temporal information, whereas visual information is better for spatial feedback [63]. The authors suggested that melodies can be used instead simple tones or beeps, in order to make auditory feedback more pleasant and motivational. Auditory feedback of cadence was used by Chen *et al.* [25] to control the velocity of training, assisting the patients to maintain of a steady cadence.

Despite visual and auditory biofeedback being widely used in rehabilitation applications, haptic biofeedback solutions are less developed. This type includes gloves, pens, joysticks and exoskeletons, which provide a sense of touch and allow the user to feel a diversity of textures, as well as, texture changes [58]. The use of electronic systems (graphic monitors, loudspeakers or haptic displays) allows providing precise information on movement parameters more consistently than by individual therapists. The use of these technologies as adjunct therapies may enhance motor learning in stroke patients and increase patient's motivation [54]. Virtual Reality (VR) can be used as a method to integrate information of various senses, aiming to increase the patient's ability to process perceptual information in task-oriented

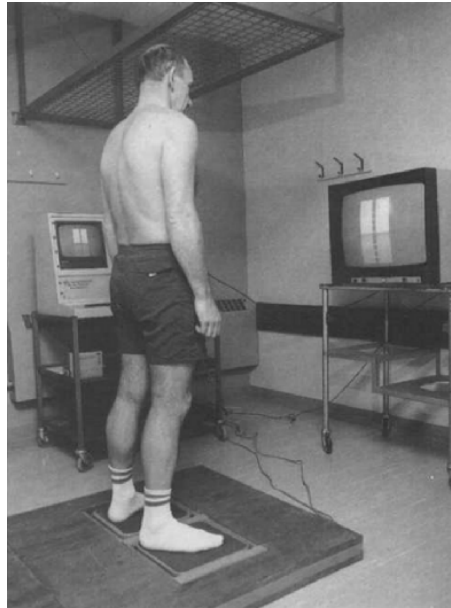


Figure 2.1: Balance platform and weight distribution visual biofeedback setup, used by Sackley *et al.* [75].

biofeedback exercises [20, 55, 58, 63]. Virtual environments that provide multimodal sensory cues can reproduce “real world” situations. This form of biofeedback can more easily be perceived by patients than multiple quantified presentations that use formulas and numbers [63]. Moreover, the information overloading problem can be overcome with the use of these multisensing biofeedback systems [63]. Virtual reality can make therapy sessions more motivating, by providing the sensation of presence in the virtual environment, while patient receives information about patient’s motor performance in an easy and intuitive way. Furthermore, virtual environments and training tasks are easily customized by computers [55].

2.4.5 Biofeedback in Cycling

Biofeedback has already been applied together with cycling in healthy subjects [77, 78], as well as, in stroke patients [8, 15–19]. Different sources of visual biofeedback were used, such as cycling speed [15, 16, 19], EMG activity [8, 17], work [18, 19], mechanical effectiveness [77] and weight shift [78]. The major characteristics of the biofeedback used in cycling of published studies are summarized in Table 2.3.

Table 2.3: Major characteristics of the published biofeedback cycling studies. Acronyms: Control (C), Elderly healthy (EH), Experimental (E), Healthy (H), Hemorrhagic (HC), Ischemic (IC), minutes (min), not stated (NS), sample size (N), sessions per week (s/w), Single Case (SC), single session (sg), weeks (w)

Study	Therapy		N	Population			Groups (E, C, H, EH)
	Feedback	Length		Age (years (±SD))	Years after stroke (±SD)	IC / HC Stroke	
Lin <i>et al.</i> [15]	Speed	8 min (sg)	43	59.95 (13.90)	2.6 (3.2)	27 / 16	E
Lin <i>et al.</i> [16]	Speed	8 min (sg)	17	55.53 (12.06)	1.6 (2.5)	8 / 9	E
Brown <i>et al.</i> [17]	EMG	10 min (3 s/w)	1	46	3	NS	SC
Sibley <i>et al.</i> [8]	EMG	4 min	3	51, 71, and 54	2, 4 and 5	2 / 1	E, H
Ferrante <i>et al.</i> [18]	Work	2 w (3 s/w)	3	23, 51, 27	1, 9 and 10	2 / 1	E, H
Yang <i>et al.</i> [19]	Symmetry, speed and workload	4 w	30	E1: 53.9 (10.5) E2: 54.5 (8.0)	E1: 0.93 (0.68) E2: 0.93 (0.81)	E1: 9 / 6 E2: 8 / 7	2 E
De Marchis <i>et al.</i> [77]	Mechanical Effectiveness	4 min (sg)	11	27.4 (2.5)	-	-	H
Song <i>et al.</i> [78]	Weight Shift	15 min (sg)	20	24	-	-	H

2.4.5.1 Protocols

Lin and colleagues [16] investigated cortical control, using near-infrared spectroscopy, during active cycling with and without extrinsic speed feedback in 17 chronic stroke patients with hemiparesis. The intervention included training with continuous feedback of the target and the actual speed of training and without any feedback, with a target speed of 50 rpm, in both modes. The feedback comprised visual bars indicating the target and the actual speed. In the session without feedback, the subjects started to pedal at a steady speed of 50 rpm with the cycling speed feedback, then, the feedback was removed and the test began. In the session with speed feedback, the subjects were asked to adjust their cycling speeds to match the target speed. The same protocol was applied by Lin *et al.* [15] in 43 stroke patients with hemiparesis to investigate if visual speed feedback could lead to improvements in task performance, such as cycling smoothness (low cadence variability during a revolution), muscle activation pattern and force output.

Brown *et al.* [17] suggested a protocol to maintain improved muscle balance after discharge, by means of EMG biofeedback. The protocol is comprised of two phases: muscle impairments analysis and training. Firstly, the extensor-flexor muscles patterns (raw EMG signal) of both legs should be analyzed with documentation of abnormalities in timing and output of the target muscles. Then, the patient should cycle with resistance while observing the biofeedback signal from the muscles of the normal leg and the affected side and be informed of the abnormalities by the therapist. The patient should attempt to duplicate the pattern from the healthy leg in the affected one. When the patient has learned to maintain the appropriate muscle activation pattern, the resistance should gradually decrease until the patient is able to maintain the correct pattern without resistance in the ergometer and, finally, the EMG biofeedback should be removed. This protocol was implemented in a stroke patient (2 years since onset) with spastic hemiparesis. The patient was able to walk independently with a cane and had marked spasticity in the right extension muscles. The EMG activity of the *rectus femoris* and the *hamstrings* muscles was provided to the patient during the training phase of the protocol.

In the study of Sibley *et al.* [8], 3 chronic stroke patients performed a training cycling program with EMG biofeedback to evaluate if visual feedback of muscle activity could be used to selectively increase the involvement of the target muscle without disturbing the overall movement. This study includes a healthy group (10 subjects) in order to compare and characterize the expected performance variations produced by the pedaling adaptations. Participants performed a control test at constant cadence (50 rpm for stroke and 70 rpm for healthy subjects), where the workload was increased every two minutes, until the participant indicated that he could not pedal any longer. Pedaling intensity was set at 50% of maximal workload from the control test for all conditions, and the stroke subjects pedaled at 50 rpm, during 4 minutes. Work rate and cadence were displayed continuously on the ergometer to verify appropriate pedaling intensity. The stroke patients were instructed to focus on the paretic limb while receiving visual information of the activity of *vastus lateralis* muscle from both legs. The EMG activity was presented in a bar graph format, for each limb (integration of the activity in the phase of higher activity of the muscle - IEMG), and updated every 30 seconds. The healthy group was instructed to pedal primarily with their self-selected dominant limb.

The effects of a biofeedback cycling program on cycling performance and in walking ability, in terms of gait speed and symmetry were investigated by Ferrante and colleagues [18]. Three chronic stroke patients were chosen after a cluster analysis of a categorization of gait pattern (gait mean velocity and symmetry) of a group of 153 chronic stroke patients, each one representative of the resulting clusters.

This study included a healthy group (12 subjects) in order to compute the normal values of the different performed tests. The patients trained 14 minutes, three days a week for two weeks. Each session included different modes of cycling (passive and active) with and without visual feedback. The biofeedback consisted in two bars with the work values produced by each leg and a band indicating the target values (Figure 2.2). The target values were computed based on a test to assess the maximal work done by the paretic leg. The target value ranged between 80 to 120% of the maximal paretic work.

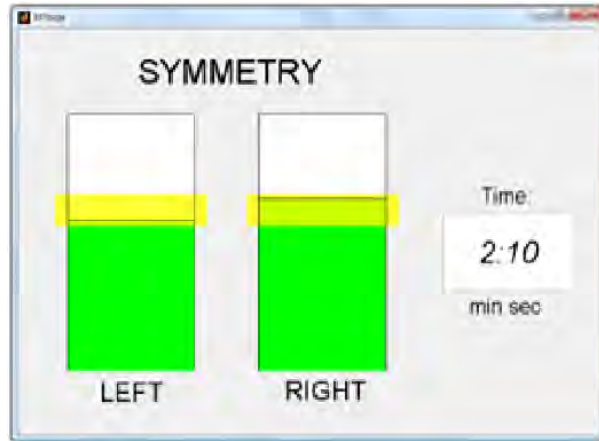


Figure 2.2: Visual biofeedback of the work produced by each leg, provided to the subjects in the study of Ferrante *et al.* [18]. The green bars represent the work produced and the yellow bands the target values.

Yang *et al.* [19] also studied the effect of a biofeedback cycling program on walking ability. Thirty hemiplegic stroke patients (between 3 months and 3 years since stroke) performed an 8 weeks crossover study, during which all patients received conventional rehabilitation. One group had additional 30 minutes of biofeedback cycling exercise during the first 4 weeks, whereas the other had it in the last 4 weeks. Information about cadence, cycling distance, performance, resistance and symmetry of bilateral lower limb exertion was provided to the patient, by the ergometer panel, during cycling exercise. The biofeedback period was comprised of 10 minutes of forward pedaling and another 10 minutes of backward pedaling. Both periods were preceded and succeeded, respectively, by a period of warm-up and cool-down of 2.5 minutes each.

The assessment tools used to analyze the outcomes of the reviewed biofeedback cycling studies are presented in Table 2.4.

Table 2.4: Assessment tool of the biofeedback cycling studies. Acronyms: 6 Minutes Walking Test (6MWT), 10 Meters Walking Test (10MWT), Area Symmetry Index (*ASI*), Electrocardiography (ECG), Electromyography (EMG), Fugl-Meyer Assessment (FMA), Modified Ashworth Scale (MAS), Roughness Index (*RI*), Shape Symmetry Index (*SSI*)

Study	Functional Scales	Gait Analysis Metrics	Outcomes		
			Cycling Exercise Metrics	Physiological Variables	EMG-based Variables
Lin <i>et al.</i> [15]	-	-	Speed, <i>RI</i> and Power	-	<i>SSI</i> and <i>ASI</i>
Lin <i>et al.</i> [16]	-	-	Speed and Speed Variation	-	-
Brown <i>et al.</i> [17]	-	-	-	-	EMG
Sibley <i>et al.</i> [8]	-	-	Power	ECG	EMG
Ferrante <i>et al.</i> [18]	-	Walking test	Cycling test, Work and Unbalance (<i>U</i>)	-	-
Yang <i>et al.</i> [19]	FMA and MAS	6MWT and 10MWT	-	-	-
De Marchis <i>et al.</i> [77]	-	-	Instantaneous mechanical effectiveness and Force	-	-
Song <i>et al.</i> [78]	-	-	Weight shift	-	-

2.4.5.2 Main Findings of Biofeedback combined with Cycling

De Marchis *et al.* [77] investigated the effect of visual feedback of the instantaneous mechanical effectiveness (Figure 2.3). The mechanical effectiveness is directly related to the ability to orient the pedal forces so that all of them contribute to the crank movement. The results showed that visual feedback improved significantly the mechanical effectiveness. Therefore, the feedback helped the subjects to orient the forces on the pedal more effectively.

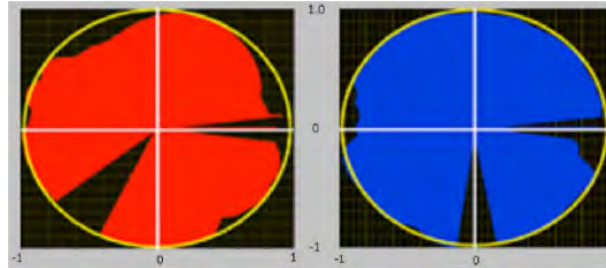


Figure 2.3: Visual biofeedback of the instantaneous mechanical effectiveness, provided to the subjects in the study of De Marchis *et al.* [77]. The circle represents one revolution, while the red and blue colors represent the instantaneous mechanical effectiveness of the left and right limbs, respectively.

Song and colleagues [78] developed a system, which combines a VR system with an unfixed bicycle to improve postural balance control. Healthy subjects performed cycling exercise with and without feedback of the weight shift condition. The results showed that weight shift lowered and was near 50% of balance condition, when feedback was provided. The authors suggested that this system was effective as a training device and that this technology might have a great potential in the rehabilitation field.

Cycling speed is a good indicator of cycling performance and can be easily understood by patients of different cognitive states [15]. Furthermore, this parameter is easily acquired, because the ergometers used in rehabilitation often provide this information. Lin and colleagues [16] concluded that visual feedback leads to a reduction in speed variation, an increasing in EMG symmetry and in cortical activation of the Premotor Cortex (PMC). The results also showed that visual feedback leads to a reduction in speed variation, an increase in EMG symmetry and in cortical activation of the PMC. Therefore, the use of speed feedback improves cycling performance with further cortical activation in stroke patients. The increase of EMG symmetry with speed feedback may be due to a greater attention to the control of the affected leg to achieve the targeted cycling speed. The authors suggested that the function of PMC activation might be to allow patients to utilize external feedback for online adjustment of the cycling movement. Moreover, the increased cortical activations were mainly found in the unaffected side, suggesting that part of the motor recovery of the affected leg might result of cortical reorganization in the unaffected hemisphere, instead of the affected one.

Lin *et al.* [15] observed that during cycling with visual feedback, the *ASI* increased in the *rectus femoris*, which indicates that the EMG amplitude of this muscle in the affected limb became more similar to that of the unaffected limb. The *RI* decreased and the *Pav* increased, indicating an improved speed control during a cycle and a higher power output, respectively. According to the authors, the results suggest that a smoother cycling movement (lower *RI*) may generate more power output due to better coordination of the limbs function. Hence, Lin *et al.* [15] also concluded that cycling with speed feedback aids to improve cycling performance. The authors suggested that visual speed feedback might be provided during cycling exercise to assist in the learning of more symmetrical muscle activation.

According to Brown *et al.* [17], to maintain improved muscle balance after discharge, a task should

be similar to gait by requiring reciprocal use of both lower limbs, with active involvement of flexor and extensor muscles. The task ought to tend to promote the symmetry of the movement and have a rate similar to normal walking. Moreover, it should also be something the patient knew how to exercise before the Central Nervous System (CNS) lesion and should provide proprioceptive and timing cues to help the patient performing the exercise properly. The training equipment should provide facilitative resistance and be simple to use. Cycling may fulfil all these characteristics, if the patient learns to use the affected limb effectively. This can be performed with EMG feedback, firstly, to assess muscle imbalance or improperly muscle activity and, then, to train appropriate pedaling. Afterwards, when the patient has learned to pedal properly, the feedback is removed and the patient should continue to train independently, to maintain what has been learned. After the implementation of the protocol suggested by the authors, the patient presented improvements, such as the absence of previously observed hip circumduction, a decrease in trunk flexion during swing-through, and an increase in hip extension toward the end of stance. The authors suggested that cycling with EMG feedback can be used to assist in the correction of muscle imbalance and to help patients with hemiparesis to perform reciprocal lower limbs exercise with a higher degree of symmetry and speed.

The exercise program implemented by Sibley *et al.* [8] was more tolerated than the limb-load cycling exercise. Healthy participants were able to use EMG feedback to increase the target muscle activity, with minimal compensations in other muscles. However, stroke patients failed in increasing the paretic limb involvement. Nevertheless, the nonparetic muscle activation was reduced, which indicates that patients were attempting to perform the task. As previously mentioned, the authors support these results with the reduced frequency of feedback.

The main goal of post-stroke lower limb rehabilitation is the restoration of the walking ability. Different studies have suggested that cycling might improve the lower limbs function, with a positive effect on walking ability [6, 28, 29]. Therefore, Ferrante and colleagues [18] investigated the effects of a biofeedback cycling program on cycling performance and in walking ability, in terms of gait speed and symmetry indices. The patients improved cycling performance during the training with biofeedback of the work done by each leg. The treatment significantly improved symmetry and gait speed in a patient with a very asymmetrical and inefficient gait, and was beneficial to a patient who overused the healthy leg in order to compensate the asymmetry. This study suggests that a treatment of only 6 days can produce improvements in terms of pedaling symmetry and, in some cases, in walking capacity.

Yang *et al.* [19] observed that the improvements in the lower extremity subscale of Fugl-Meyer Assessment, 6MWT, 10MWT and Modified Ashworth Scale were significantly superior in the cycling exercise period than in the non-cycling period. The authors suggested that their biofeedback cycling exercise can improve functional recovering and walking ability in patients with chronic stroke, and recommend it as a clinical protocol in rehabilitation or as home exercise.

2.5 Cycling Devices

Different devices developed by different entities with different objectives were used in the reviewed studies. Two different types of devices were used in the reviewed studies. Standard ergometers (Figure 2.4 (a)), which are similar to normal bicycles, and the exercise is done in an upright, seated position; and recumbent ergometers (Figure 2.4 (b) and (c)), where the subject pedals with the legs stretched forward. In recumbent bicycles, the subject performs the exercise while his back is resting on a backrest.

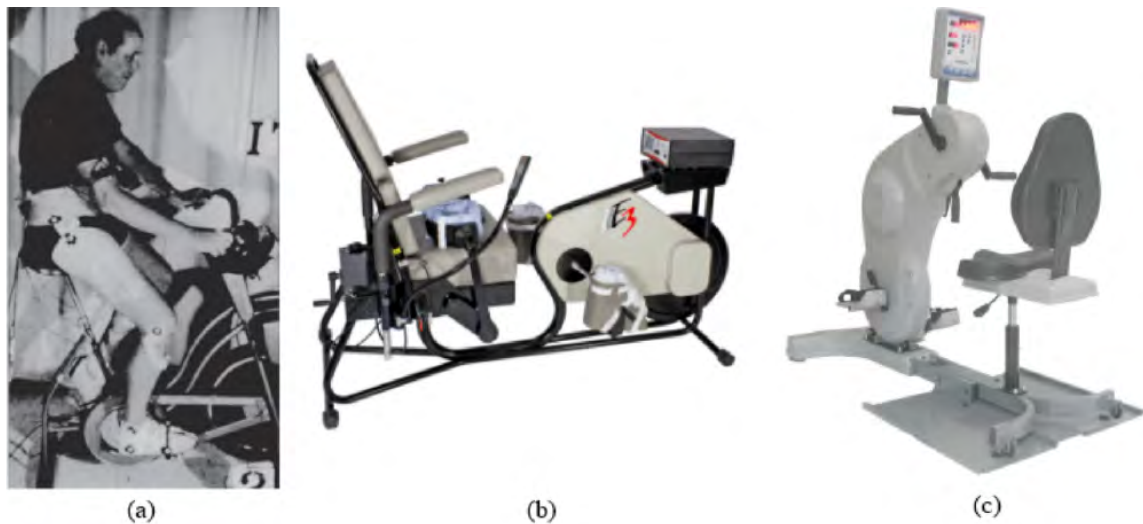


Figure 2.4: Types of ergometers: (a) standard ergometer (Schwinn Bicycles Co, Illinois, USA – used by Rosecrance *et al.* [48]) and recumbent ergometers (b) Ergys (Therapeutic Alliances Inc., Ohio, USA) [79] and (c) Active Passive Trainer (Tzora Active Systems Ltd, Kibbutz Tzora, Israel – used by Katz-Leurer *et al.* [39]) [80].

Brown and Kautz [26, 28, 30, 49] modified a standard ergometer with a frictionally loaded flywheel to include a backboard seating mechanism with shoulder and lap harnesses to stabilize the subject and remove the need to control balance, as shown in Figure 2.5.

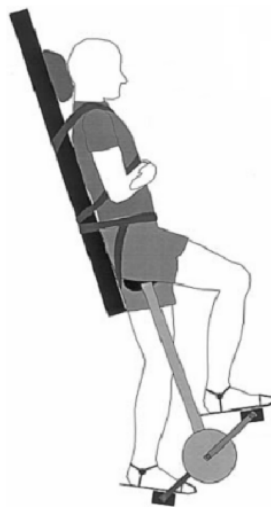


Figure 2.5: Representation of the experimental setup used by Brown and Kautz [28].

To allow the limb-load cycling intervention, Brown *et al.* [6] modified a recumbent ergometer (Biodex Medical Systems Inc., New York, USA). To provide support and safety, the device was equipped with a waist belt, upper-body seat belt, and straps on the pedals. The device included a seat that could slide along a linear track and, to prevent the seat from sliding forward, the patients were required to maintain a loading force on the sliding seat mechanism. The system allowed the selection of the percentage of the body weight, which the patient would have to support. A metal safety block on the track prevented excessive forward displacement of the seat and provided auditory feedback to the patients, indicating that they were unable to maintain the load and were in an unloaded position.

Seki and colleagues [40] developed a cycling wheelchair device, as shown in Figure 2.6. A pedaling

system is installed at the position of the footrest of a standard wheelchair. The pedal system is connected to the rear wheels, which allow the control of the movement of the wheelchair by pedaling, or only static pedaling.

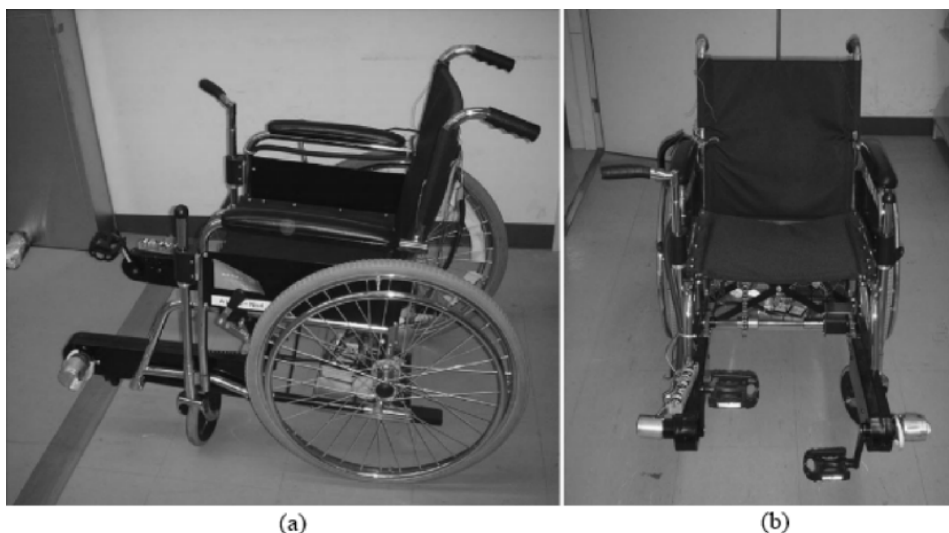


Figure 2.6: Cycling wheelchair system developed by Seki *et al.* [40], (a) side view and (b) front view.

Some companies have developed commercial ergometers specifically to rehabilitation applications, such as the THERA-Trainer (Medica Medizintechnik GmbH, Germany) and the MOTomed (RECK-Technik GmbH & Co. KG, Germany), as shown in Figure 2.7. These devices have already been used in studies, for instance, Ferrante *et al.* [18] used a THERA-Live device, whereas MOTomed models were used in [2, 16, 47]. MOTomed Viva (Figure 2.7 (a)) and THERA-Trainer Tigo (Figure 2.7 (c)) allow cycling exercises while the user is sitting in a chair or wheelchair, whereas the MOTomed Letto was designed for bedridden patients, which cannot perform upright exercises, thus this type of models can be applied in early stages of the recovery [81–83].



Figure 2.7: MOTomed (RECK-Technik GmbH & Co. KG, Germany) (a) Viva and (b) Letto models [82,83], and (c) THERA-Trainer Tigo (Medica Medizintechnik GmbH, Germany) cycling device [81].

These ergometers allow active and passive modes of cycling, forward and backward movement, and allow training of the upper and lower extremities. It is possible to control several training variables, such as cadence (passive mode), exercise time and workload, and to provide information to the users about the covered distance, actual cadence, power and time performed in each mode. Both brands have a spams

detection system, which stops the exercise and performs a chosen action (forward or backward movement) [81–83]. MOTOMed models allow data training storage, which enables a periodic monitoring of training characteristics by doctors and therapists [2]. These models are also prepared to be coupled with a FES system. THERA-Trainer models have specific programs to different impairments and mini-games to motivate the users during cycling exercise [81–83]. Both models have accessories for specific cases, such as calf supports, fixed to the pedals, to keep especially the paretic leg in the right position and avert an abnormal movement. In addition, both devices can provide information about cycling symmetry, however, the biofeedback information is based on the motor torque instead of the torque produced independently by each limb. Using motor torque to provide information about cycling symmetry can be misleading, since, if the patient only uses the healthy leg to propel the crank (push and pull) without performing any effort with the unhealthy leg, the biofeedback will indicate a symmetrical pedaling. Therefore, improved torque measuring systems, such as the ones implemented in [84–87], are required.

2.6 Challenges and Future Work

Despite the positive results of the application of cycling alone and combined with feedback, in stroke patients, more studies are needed. There is a high heterogeneity among these studies, such as the patients' characteristics, protocols and metrics. The influence of cycling should be addressed in different phases of stroke, especially in acute and sub-acute phases, once the highest rate of functional recovery can be obtained during the first months after stroke [22]. Large-scale studies should be performed in health-care scenarios with the cooperation of the medical community. These studies should be preferably randomized controlled trials, with a large sample size, in order to allow generalizing the results. The existing interventions present great variability of task characteristics, which complicates the assessment of the potential and efficacy of cycling as a rehabilitation tool. Therefore, there is a need to develop guidelines, which allow higher efficiency and efficacy of cycling therapy. To accomplish that, the interventions should also be implemented during more time and with more prolonged follow-ups, since it may result in a higher progress in the locomotor ability and to investigate the long-term effects of cycling.

The effects of combining cycling with other therapies, such as FES and biofeedback, should be more investigated, since the literature already shows some positive effects with the use of therapies alone and in combination with cycling. Regarding feedback, more investigation is needed in the selection of the most effective source of feedback and in its display, emphasizing the scheduling issue.

Finally, the selection of the appropriate metrics or the development of new ones to assess the efficacy of cycling therapies is crucial, since it will facilitate the comparison of the different interventions and cycling-based therapies. As the main goal of lower limb rehabilitation, after stroke, is the recovering of the walking ability, future studies should verify the effects of the implemented interventions on the patient's locomotion.

The outcomes of these normalized studies and assessments will enable to identify the required technological advances which have to be included in current cycling devices

2.7 Conclusions

The application of cycling in stroke rehabilitation approaches has shown promising results. Cycling exercise is simple and repeatable; can be applied to a wide range of patients, combined with different

therapies and external measurements devices; and is a low cost and portable technology. This makes it suitable for clinical and home-based settings. Positive effects on motor abilities were found with the application of cycling as a motor function rehabilitation method in sub-acute and chronic patients. In addition to the rehabilitation of the motor function, it can be used as an aerobic training method, to minimize the risk of secondary diseases caused by immobility, and as an assessment tool, to characterize the impairments and assess the patients' recovery evolution. The application of cycling in aerobic programs also resulted in improvements in walking ability, as well as, in independence and maximal aerobic capacity.

Different tools were used to assess the patients and training, such as Functional Scales (standard or stroke specific), Gait Analysis Metrics, Cycling Exercise Metrics, Physiological variables and EMG-based variables. The Functional Scales were used to assess the patient's ADLs capacity, with emphasis on the stroke specific Functional Scales, usually to perform an initial assessment of the patient. As the major goal is the recovery of the walking capacity, some studies also performed walking tests, to assess the gait parameters of the patients (Gait Analysis Metrics). Patient-device interaction was evaluated through Cycling Exercise Metrics, whereas the effects of the cycling on the biological parameters were supervised by physiological variables, especially the muscle activity (EMG-based variables). Extrinsic feedback was used with positive results in stroke patients. The patient's performance and motivation on the execution of different exercises increased, as well as, the walking capacity, when feedback was provided.

Devices and Instrumentation

3.1 Introduction

As stated in the review of the application of cycling and feedback in the rehabilitation of the lower limbs of stroke patients, held in Chapter 2, in order to assess the effects and the major characteristics of cycling and feedback, several analysis should be taken into account.

A semi-recumbent cycling device (*THERA-Live* motorized cycling device) was instrumented with several sensors (optical sensors, force sensors and accelerometers), in order to obtain data regarding the interaction between the user and the device during cycling, as well as, the derived metrics.

The knowledge of the lower limbs' muscle activation pattern, during cycling at different conditions, may provide relevant information about the role of each muscle. This knowledge might be used in rehabilitation approaches in order to train and recover specific muscles, which are impaired due to disease. A biofeedback and electrotherapy device, *YSY EST EVOLUTION*, which allows the analysis of the muscle activation pattern, in real-time, was also used in this dissertation. The data of this device was used as EMG biofeedback in order to study its potential in the stroke rehabilitation field.

The next sections present the major characteristics of the cycling device, the instrumentation added to the device, as well as, the equations to obtain some target metrics, which were not addressed in Chapter 2. Furthermore, the major characteristics of the *YSY EST EVOLUTION* are presented.

3.2 *THERA-Live* Motorized Cycling Device

The *THERA-Live* motorized cycling device (Medica Medizintechnik GmbH, Germany – Figure 3.1) allows upper and lower limbs exercise in active and passive modes of training. During the training, the user can control the resistance (workload) of the exercise (up to a maximum of 22 Nm), the training time, and the direction of rotation; while information about cadence (rpm), power (watt), energy consumption (kcal), distance (km) and remaining training time (min) are provided to the user. In passive mode, the user can also control the cadence of the motor. The electronic specifications of the device are presented in Appendix A.1.

The ergometer has a system to help patients place their feet on the footrests, which lower to the nearest point relative to the floor, helping patients with severe impairments to start the exercise. During training, if the rotary movement is stopped, for instance by a spasm, the pedals of the ergometer will move freely, to decrease the spasm, and the device restarts the training 3 seconds later.

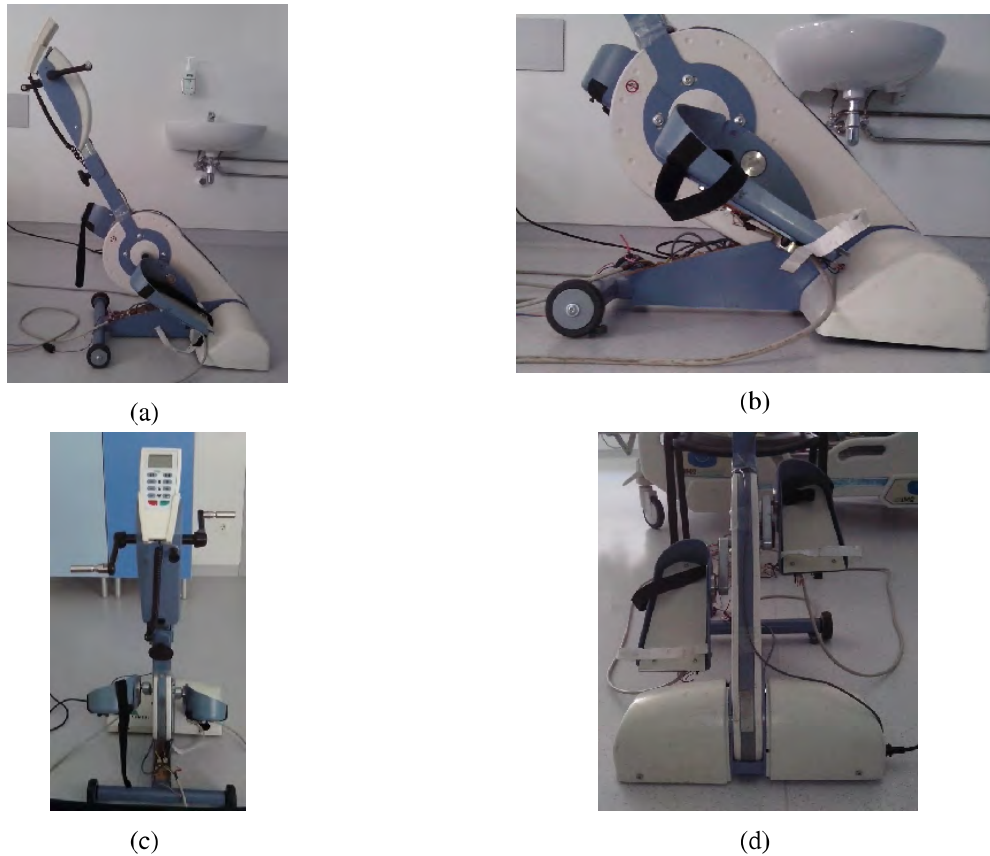


Figure 3.1: Cycling device views: (a) and (b) side view, (c) user view and (d) front view.

3.2.1 THERA-Live Operation

The device can be divided in four major components, which are responsible for powering and controlling the cycling device: the electronic control board, the motors, the control pad and the optical sensor.

The electronic control board, shown in Figure 3.2, connects all the others components. It receives instructions and data from the control pad and the optical sensor, powers and controls the motors, and sends operational data to the control pad.

The device contains two motors, one for the lower limbs pedals and other for the upper limbs pedals. The motors are responsible for providing the movement of the pedals during passive mode operation,



Figure 3.2: THERA-Live's electronic control board.



Figure 3.3: *THERA-Live*'s control pad.

and to induce mechanical resistance (workload) and movement aid during active mode operation.

The control pad (Figure 3.3) controls the operation of the device. The users can select the buttons to activate the device; change the type of training (lower or upper limbs); change the direction of rotation; and control cadence, workload and training time. The control pad also has a display, where training status data is showed.

3.3 Cycling Device Instrumentation

In order to acquire important signals to characterize and assess the cycling exercise, the cycling device was instrumented with different sensors, which will be described in detail in the following sections. The analysis of the applied force during cycling allows the computation of several metrics that can be used to assess motor impairments in stroke patients, such as the difference between the motor ability of the lower limbs.

The data from the sensors was acquired using a microcontroller board *Arduino Mega 2560*. A sensors' acquisition board was developed in order to control the sensors, connect them to the microcontroller board and to acquire the data from them. The components and the configuration of the sensors' acquisition board are presented in Appendix A.3. The microcontroller board was powered through a PC, whereas the sensors were powered through a 12 V battery. However, as the recommended supply voltage of the sensors is 5 V, a voltage regulator circuit was installed in order to convert the 12 V of the battery into 5 V. Further information about the voltage regulator circuit is presented in Appendix A.3.

3.3.1 Crank Angle

For better understanding, when referring to the upstroke phase, it will correspond to the area between 0 and 180 degrees of one revolution (indicated by a dashed red line in Figure 3.4), while the downstroke phase will correspond to the area between 180 and 360 degrees (indicated by a solid green line in Figure 3.4). The zero degree of the crank angle (ϕ) was defined as when the crank arm is perpendicular to the ground surface and the right pedal is on bottom, as shown in Figure 3.4.

The commercial ergometer includes one optical sensor (*OPB763T* – Optek Technology, Inc., USA – Figure 3.5 (a)) and two optical encoder disks, as shown in Figure 3.5 (b) that provide information to the device about the pedals position, which allows the device to compute training status information, such as the training cadence and covered distance. The disks are comprised of white and black sectors and are attached to the crank axis. The external disk has six sectors with unequal size (one black sector of 120 degrees; two white of the 60; and two black and one white of 40 degrees), which give information about the absolute angle and motion direction, although with low resolution. The internal disk has a higher resolution, since it is composed of ninety sectors of equal size (4 degrees).

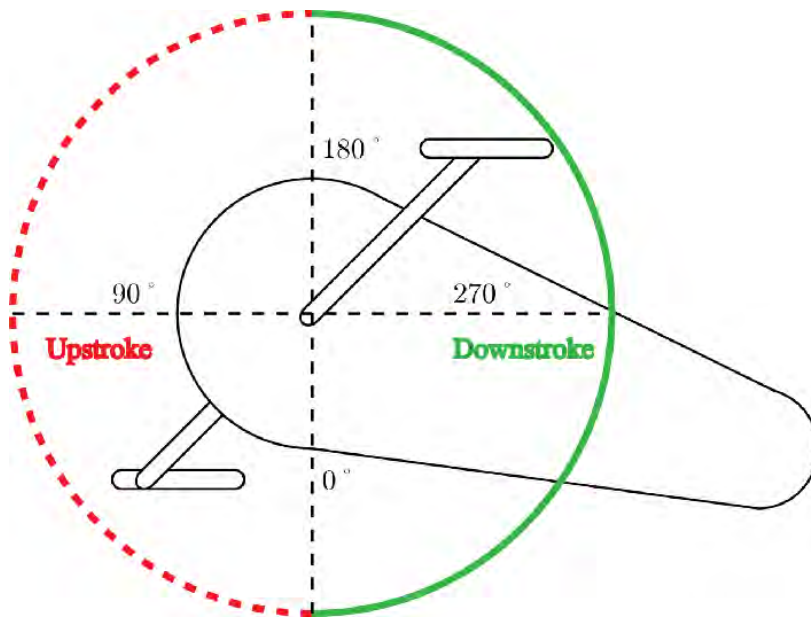


Figure 3.4: Representation of the two phases of one revolution: downstroke phase (solid green line) and upstroke phase (dashed red line), as well as, their equivalent angles.



(a)



(b)

Figure 3.5: System for measurement of the crank angle (ϕ): (a) optical sensors and (b) optical encoder's disks. External disk with 6 unequal size sectors and the Internal disk with 90 equal size black and white sectors.

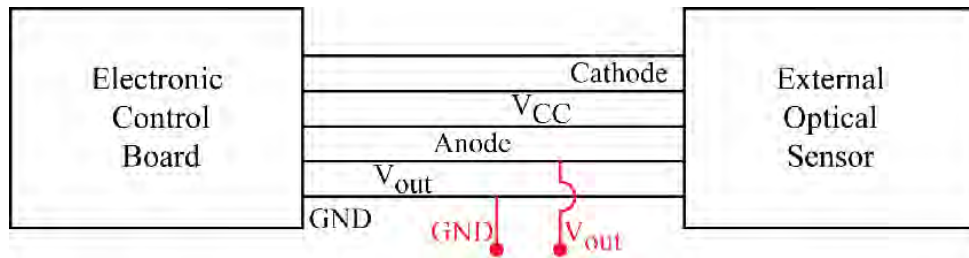


Figure 3.6: Pinout configuration and connection between the electrical control board and the external optical sensor.

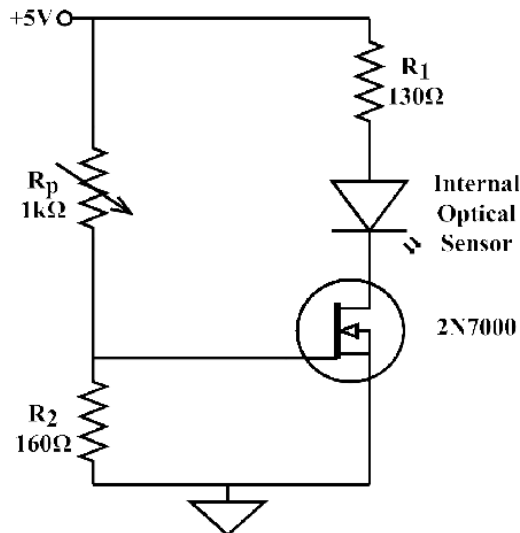


Figure 3.7: Electronic circuit to control the internal optical sensor.

The optical sensor of the device is placed on the external encoder's disk region. The connection between the optical sensor and the electronic control board, as well as, the pinout configuration of the optical sensor are presented in Figure 3.6.

In order to acquire the data from this optical encoder, the signals of the pins (V_{out}) and (GND) were wired to a new circuit, as shown in Figure 3.6. As the resolution of the installed sensor is too low for a more complex analysis of cycling training, an additional sensor was installed in the internal encoder's disk region. An equal optical sensor (*OPB763T*) was chosen, due to its dimensions being suitable to the device's mechanical system. The electronic specifications of the optical sensor are presented in Appendix A.2. As *THERA-Live* is not equipped to control two optical sensors at the same time, an electronic circuit had to be built to control the new sensor. The schematic of the electronic circuit, is presented in Figure 3.7.

The *OPB763T* is comprised of a photodiode and a photoelectric receiver. The sensor's operation is based on the amount of infrared light, emitted by the photodiode, which is reflected by the different surfaces, and detected by the receiver. A black surface does not reflect the infrared light, and the sensor's output will be in the logic state 1; whereas a white surface reflects the light, and the sensor's output changes to the logic state 0.

Based on the brightness of the Light-Emitting Diode (LED), which is controlled by the current flowing on its terminals (the higher the current, the higher the brightness), the amount of the reflected light changes. If the LED is too bright, the black sectors could start to reflect or the neighboring white sectors could reflect part of the light, which might result in the loss of a commutation or in an unequal time in

each state. The developed circuit, presented in the Figure 3.7, allows to control the LED's brightness, so that the signal's duty cycle is 50%. As *OPB763T* can be powered with a maximum of 10 V (during 3 seconds), the chosen value was 5 V, which allows a continuous power supply. The maximum current that the LED supports is 40 mA, therefore, a resistance of 130 Ω (R_1) was placed in series with the optical sensor to limit the current (Figure 3.7). To control the amount of the current flowing in the LED, an n-channel signal Metal Oxide Semiconductor Field Effect Transistor (MOSFET) (*2N7000*) was used (Figure 3.7). In the cutoff region the current flowing on the LED is null, therefore, the LED will be OFF. In the saturation region, the value of the current will be, practically, defined by the resistance. The interest zone is the triode region, where the value of the current flowing in the sensor will be dependent on the gate voltage. To control the gate voltage, a voltage divider (precision potentiometer of 1 k Ω in series with a resistance of 160 Ω (R_2)) was implemented. When the resistance of the potentiometer is zero, the voltage on the gate is approximately 5 V; whereas, when the potentiometer's resistance value is maximum, the voltage on the gate is approximately 0.7 V (threshold voltage). The use of a MOSFET will allow, in the future, an automatic control of the current flowing on the sensor, using a microcontroller and Pulse-Width Modulation (PWM) instead of the voltage divider. An electronic board was developed to connect the optical sensors to the sensors' acquisition board, in order to power the internal optical sensor and to obtain the signal from the two optical sensors. Further information about this board is presented in Appendix A.2. By combining the information of the two sensors, it is possible to obtain a maximum resolution of 4 degrees. However, this resolution requires a higher computational cost than the microcontroller board capacity (*Arduino Mega 2560*). Therefore, a resolution of 8 degrees was used to acquire the data of all sensors.

3.3.2 Pedal Angle

As a pedal moves freely around the crank axis, the angle of the two pedals might provide relevant information about the pedaling strategy of the user, and this angle is also necessary for the calculation of the effective force component applied on the pedals.

For the calculation of the pedals angles, three solutions were idealized: the use of precision potentiometers, optical sensors or accelerometers. The first option was abandoned, since the axis configuration and the space between the crank arm and the pedal does not allow the installation of the potentiometer. For the optical sensors solution, in addition to the space limitation, it would be required a quadrature encoder to know the direction of the rotation (two optical sensors for each pedal), making this solution the most expensive. Therefore, two accelerometers were installed in the pedals to obtain the pedals angles.

An accelerometer measures the projection of the gravity vector on the sensing axis. The amplitude of the sensed acceleration changes according to the sine of the angle between the sensing axis and the horizontal plane, as shown in Figure 3.8 (a).

The data from a 3-axis accelerometer can be used in order to improve tilt sensitivity and accuracy [88]. The value of the pedal angle (β), as shown in Figure 3.8 (b), is given by (3.1):

$$\beta = \arctan \left(\frac{A_{x1}}{\sqrt{(A_{y1})^2 + (A_{z1})^2}} \right) \quad (3.1)$$

where A_{x1} , A_{y1} and A_{z1} are the normalized accelerometer raw measurements in the x , y and z axes, respectively.

A *GY-521* board (Figure 3.9), equipped with a 3-axis accelerometer (*MPU-6050* – electronic speci-

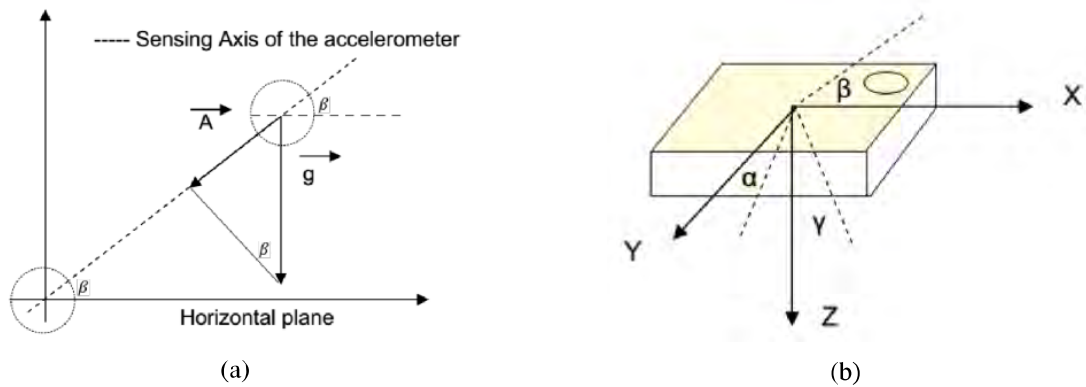


Figure 3.8: Tilt angles measurement, using (a) a single axis accelerometer and (b) a 3-axis accelerometer. Adapted from [88].

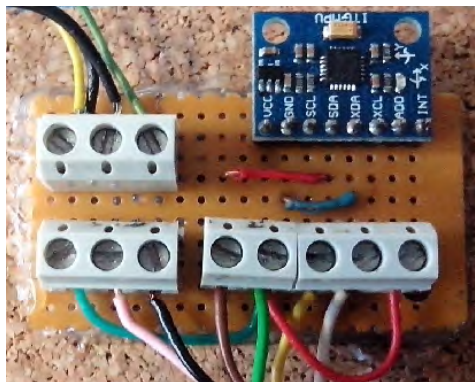


Figure 3.9: GY-521 board with a 3-axis accelerometer (MPU-6050).

fications in Appendix A.4), was placed under the pedal, in the line where the crank arm connects to the pedal, in order to measure its angle (β) relative to the floor. The communication between the accelerometers and the microcontroller board is done using the Inter-Integrated Circuit (I²C) protocol.

3.3.3 Force and Work

The force applied in the pedals has been studied for numerous purposes, such as the analysis of the pedaling technique in professional cyclists [89], in order to achieve an optimization of the performance during cycling; and in patients with lower limbs impairments, as quantitative assessment [26, 28, 90] and rehabilitation (force biofeedback) [18, 19] tools.

Studies have analyzed a maximum of three force components (normal, anterior-posterior and/or medio-lateral) and the related moments, using strain gauges [84–87, 89], load cells [89] or piezoresistive force sensors [89]. Strain gauges were installed in the crank arm [84, 87] or in the pedals [85, 86]. These two options could not be implemented in the available *THERA-Live* since, the crank arm of the cycling device is a steel bar, which prevents its deformation, and the second option will require the construction of a new pedal. Therefore a new mechanical system with two piezoresistive force sensors (*Flexiforce* sensor – electronic specifications in Appendix A.5), placed on the surface of the pedal, on the line where the crank arm connects to the pedal, was developed in order to measure the normal force (F_p), applied in the pedals by the lower limbs.

The system, as shown in Figure 3.10, is comprised of one metal plate and one acrylic plate with the shape of the pedal, together with two rubber cubes, smaller than the sensing area. These cubes were

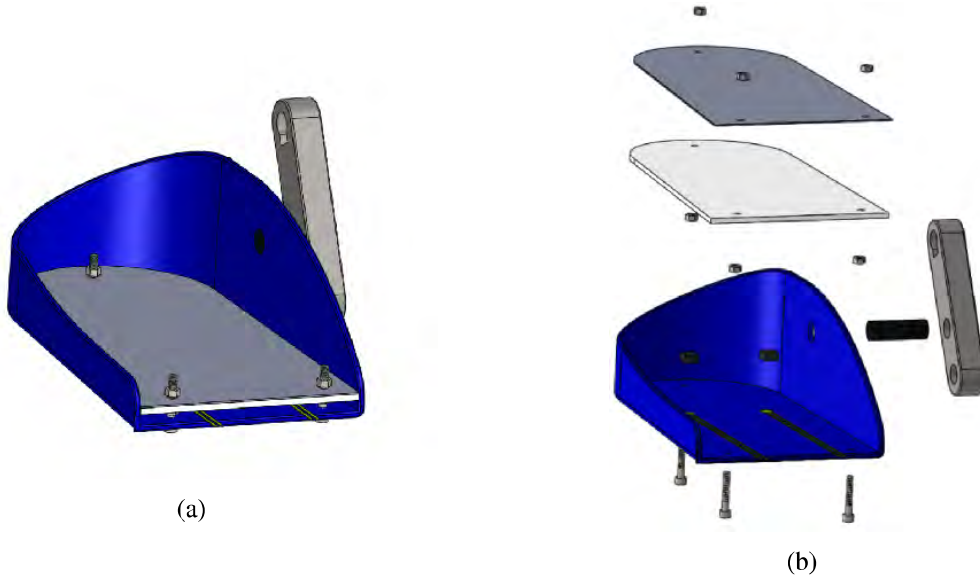


Figure 3.10: Tridimensional model of the system to measure the applied force. Representation of (a) the mounted view and (b) the exploded view of the mechanical system.

placed above the sensing area (9.5 mm of diameter) of the force sensors, to ensure that the load applied by the foot on the plates is transferred to the sensing area through the rubber cubes. To avoid force detection when the pedal is unloaded, and to allow the down movement and the stability of the mechanical system, three metal springs and screws were placed between the plates and pedal.

Initially, the system had only one force sensor, centered on the line where the crank arm connects to the pedal. However, this system was unstable and the force applied in the pedals did not transfer totally to the sensing area of the force sensors. Therefore, a new force sensor was installed, and the sensors were placed spaced from each other in order to provide stability.

Each force sensor acts as a variable resistor (R_{fs}) in a voltage divider circuit (Figure 3.11). Each sensor is in series with a parallel between a resistance of 100 k Ω (R_1) and a capacitor of 10 nF (C_1 – to stabilize the voltage on the microcontroller’s Analog-to-Digital Converter (ADC) port). When the sensor is unloaded, its resistance is very high (greater than 5 M Ω); when force is applied to the sensor, the resistance decreases. The force sensors were powered with 5 V.

Different known weights were used to calibrate the force sensors. The calibration values are presented in Appendix A.5. The right pedal with the installed mechanical system is shown in Figure 3.12.

In order to calculate the effective force, the angle between the crank arm and the pedal, α , has to be measured (Figure 3.13). This angle was obtained through the crank and pedal angles relative to the floor (ϕ_{floor} and β , respectively).

The angle of the crank arm relative to the floor (ϕ_{floor}) was calculated as given by (3.2)

$$\phi_{floor} = -\frac{\pi}{2} - \phi \quad (3.2)$$

where ϕ is the angle of the crank arm, which is known from the information given by the optical encoders. Finally, the angle between the two components (α) was calculated as follows:

$$\alpha = \phi_{floor} - \beta \quad (3.3)$$

The effective force (F – force applied at the end of the crank arm), which contributes to the movement

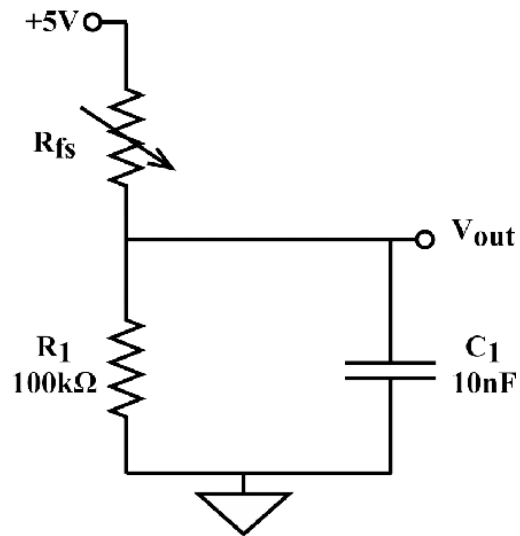


Figure 3.11: Electronic circuit for the acquisition of the applied force on the force sensor (R_{fs}).



Figure 3.12: Right pedal with the mechanical system to measure the applied force.

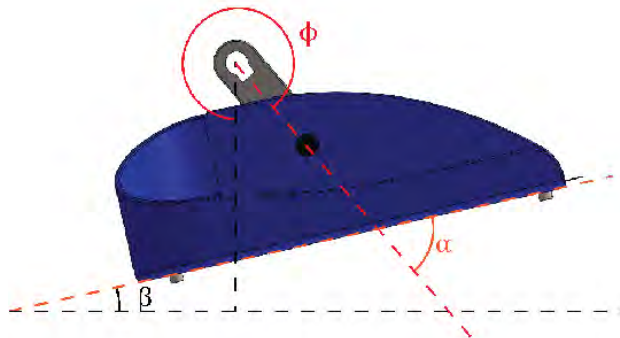


Figure 3.13: Representation of the axes and angles to calculate the angle between the pedal and the crank axis.



Figure 3.14: EMG Biofeedback System: (a) *YSY EST EVOLUTION* and (b) display with the device software.

of the crank axis, was obtained from equation (3.4)

$$F = F_p \times \cos \alpha \quad (3.4)$$

The value of the torque (τ) was calculated by the product of the effective force and distance (d), in meters, between the crank axis and the pedal axis (where the crank arm connects to the pedal) according to equation (3.5)

$$\tau = F \times d \quad (3.5)$$

Finally, the net mechanical work (W) applied by the leg can be computed as follows:

$$W = \int \tau d\phi \quad (3.6)$$

The net mechanical work done by each leg represents the leg contribution to the movement, during a complete revolution. It can be positive, meaning that the leg assists crank propulsion, negative, if the leg resists crank propulsion, or zero if the contribution and the resistance to the movement are equal.

These metrics were computed for each pedal, allowing an individual analysis of the contribution to the movement of each limb, as well as, the comparison of the two lower limbs. The data of these metrics, for different cycling conditions in healthy and stroke subjects is presented in Chapter 4 and 5 and Chapter 6, respectively.

3.4 *YSY EST EVOLUTION*

YSY EST EVOLUTION (YSY Medical, France – Figure 3.14) is a device that can perform real-time EMG Biofeedback or Electrotherapy. The EMG biofeedback function can be used in muscle rehabilitation. This device includes several biofeedback protocols, automatic calibration, and can provide visual and auditory feedback [91]. It is used, for instance, in the Hospital de Braga, for strengthening the pelvic muscle, in the treatment of urinary incontinence.

The device has two biofeedback modes: biofeedback scrolling and biofeedback long scrolling. The main difference between the two modes is the velocity of the signal. In the first, the signal can do a complete passage, from the beginning to the end of the display, in 1 second, whereas in the biofeedback

long scrolling mode the minimum time is 10 seconds. As the exercise in the cycling device is performed at high velocities, requiring a fast signal update, the biofeedback scrolling mode was used. In this mode, the resting time (period of rest between two passages) and the working time (period of muscle activity reading) can be defined. Furthermore, the device allows displaying a target signal shape (working model), in addition to the muscle activity signal. This target signal could be one of the several predefined signals, or can be personalized to optimize the muscle training to the specific problem and type of training. Two active electrodes and one reference electrode are required to provide biofeedback of one muscle. The reference electrode should be placed on an osseous point of the user. After connecting the electrodes to the device, the zero value of the muscle activation signal has to be defined. The user cannot make any contraction during this period and should relax the target muscle to remove the base tonus. Then, the calibration is performed through several muscle contractions, during one passage, to define the sensibility of the EMG channel according to the maximum activity value of the contractions. The higher line in the signal display corresponds to the sensibility value, whereas the lower line corresponds to the zero value. The average signal of all passages, as well as, the maximum, average, minimum and the base tonus values, are presented at the end of the training time.

This device was used in healthy (Chapter 5) and stroke (Chapter 6) subjects to provide EMG Biofeedback.

3.5 Conclusions

In this chapter, the major characteristics of the *THERA-Live* cycling device and the *YSY EST EVOLUTION*, two devices that were explored in this work, are presented. The instrumentation added to the device, as well as, the equations to obtain some target metrics are also described.

Two optical sensors and two optical encoder's disks were used to measure the crank angle (ϕ). The values of the pedals angle (β) were measured using accelerometers. These two angle values are important to the calculation of the effective force value. A mechanical system was developed to measure the normal force, applied on each pedal, by the lower limbs. The force value was acquired through two piezoresistive sensors placed on each pedal. Using the normal force and the angle values was possible to measure the work applied on the pedals.

The data of the instrumented sensors allowed the computation of several metrics, some held in Chapter 2, in order to assess the effects and the major characteristics of cycling and biofeedback, in healthy and stroke subjects.

Analysis of Cycling

4.1 Introduction

A complete knowledge of the lower limbs' muscle activation pattern, during pedaling, is important to improve rehabilitation protocols and cycling performance. The identification of the activated lower limbs' muscles and their level and timing of activation is required to understand the pedaling movement. The analysis of the most relevant muscles for pedaling will allow to infer about the pedaling performance. Then, the abnormalities in the muscle activation patterns can be identified. Through the understanding of muscle activation patterns, it is possible to focus on a particular phase of pedaling action to train a particular muscle group. Cardiovascular, plasma metabolite and endocrine responses can be influenced by specific patterns of muscle activation during pedaling exercise [92].

The first step to analyze the relations between walking and cycling is to identify the role of each muscle during the two activities. Lower limbs' muscles and their general function are presented in this chapter, as well as, a biomechanical model of the cycling that identifies the role and the moment of activation of the major muscles during pedaling.

The abnormalities generally observed after stroke are also addressed. The analysis of the muscle activation pattern also requires the identification of the influence of training parameters, such as workload, cadence and body position, on the muscle activation level and timing. Finally, based on these factors, the muscles, which will be addressed in this study, can be selected.

The analysis of the force patterns and joints' moments of the lower limbs is required in order to relate the causes of the motor impairments with their output. Therefore, a model for biomechanical analysis of the lower limbs during cycling will be implemented, in order to compute the moments of the lower limbs' joints (hip, knee and ankle). The influence of workload and cadence on the force output have already been studied [26, 28, 90, 93, 94], but the studied devices were standard cycling devices. Thus, an analysis of the influence of workload and cadence on the force output during cycling in a semi-recumbent device, in healthy subjects, is also presented.

4.2 Lower Limbs Muscles

The stabilization of the body position, the production of movement, and the transportation of substances within the body, are the main functions of the muscular system. Movements, generally, result from the action of several skeletal muscles as a group. Most skeletal muscles are arranged in antagonist

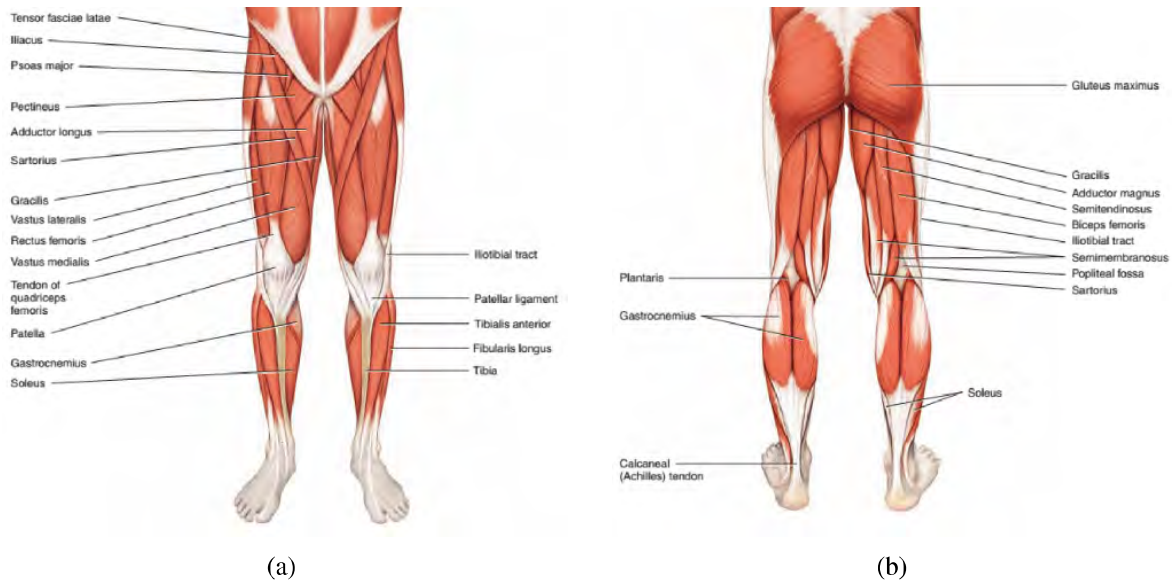


Figure 4.1: Muscles of lower limbs: (a) anterior and (b) posterior views. Adapted from [21].

(opposing) pairs, such as flexors-extensors and abductors-adductors. The pair is comprised of the agonist, which contracts to cause an action, and the antagonist that stretches to the effects of the agonist. This pair is usually located in opposite sides of the bone and joint and, for different movements, the role of each muscle can switch [21].

Regarding the lower limbs, three different regions, with different functions, may be considered: the muscles of gluteal region that move the femur; the thigh muscles that move the femur, tibia and fibula; and the leg muscles, which move the foot and toe [21]. The major muscles of the lower limbs are shown in Figure 4.1.

Raasch *et al.* [7] developed a computational biomechanical model of the muscle function during pedaling. The model includes nine muscles sets that are comprised of 15 muscles. The region, group, antagonist and general function of these muscles are shown in Table 4.1.

Table 4.1: Region, group, antagonist and general function [21, 95] of the muscles of the biomechanical model developed by Raasch *et al.* [7]

Region	Group	Muscle	Antagonist	Action / Function
Gluteal Region	<i>Iliopsoas</i>	<i>Iliacus</i> <i>Psoas major</i>	<i>Gluteus Maximus</i>	Thigh flexion at hip joint; Thigh lateral rotation;
	<i>Gluteal</i>	<i>Gluteus Maximus</i>	<i>Iliacus and Psoas</i>	Thigh extension at hip joint; Thigh adduction and at hip joint and thigh rotation;
Gluteal Region and Thigh	<i>Adductor</i>	<i>Adductor Magnus</i>		Tight flexion (anterior part) and extension (posterior parte) at hip joint;
Thigh	<i>Quadriceps femoris</i>	<i>Rectus femoris</i> <i>Vastus (lateralis, medialis and intermedius)</i>	<i>Hamstrings</i>	Leg extension at kneejoint; Thigh flexion at hip joint;
	<i>Hamstrings</i>	<i>Biceps Femoris (long-head and short-head)</i> <i>Semimembranosus</i> <i>Tibialis Anterior</i>	<i>Quadriceps femoris</i> <i>Tibialis Posterior, Soleus and Gastrocnemius</i>	Leg flexion at kneejoint; Thigh extension at hip joint;
Leg	<i>Triceps Surae</i>	<i>Gastrocnemius (lateralis and medialis)</i> <i>Soleus</i>	<i>Tibialis Anterior</i>	Foot dorsiflexion at anklejoint; Foot inversion at intertarsal joint; Foot plantar flexion at ankle joint; Leg flexion at knee joint; Foot plantar flexion at ankle joint;

4.3 Biomechanical Model of Cycling

The four major functions of muscular activity during normal pedaling [96] are to produce external power during extension, aid limb recovery during flexion, assist in the transition between extension and flexion, and assist in the transition between flexion and extension.

The Raasch *et al.*'s [7] computational biomechanical model is formed by nine muscle sets that are shown in Figure 4.2 and described in Table 4.2.

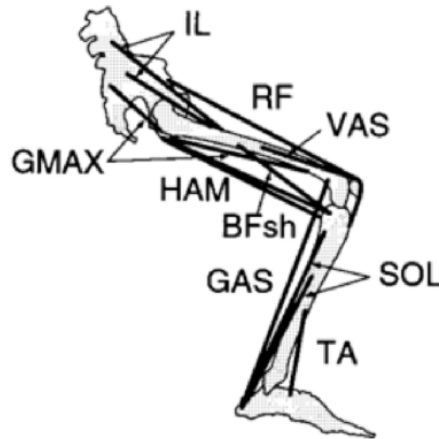


Figure 4.2: Nine muscle sets of the model of Raasch *et al.* [7], formed by 15 individual muscles, which are described in Table 4.2.

Table 4.2: Muscle organization of the Raasch *et al.*'s [7] model. Fifteen muscles are organized in nine muscles sets, which form six muscle groups that are arranged in three pairs

Pair	Group	Set	Muscles
1	Limb extensors	GMAX	<i>Gluteus maximus</i> and <i>Adductor magnus</i>
		VAS	<i>Vastus intermedius</i> , <i>Vastus medialis</i> and <i>Vastus lateralis</i>
	Limb flexors	IL	<i>Iliacus</i> and <i>Psoas</i>
2	Ankle plantarflexors	BFsh	<i>Biceps femoris short head</i>
		SOL	<i>Soleus</i> and a muscle representing other uniarticular plantarflexors
	Ankle dorsiflexors	GAS	<i>Gastrocnemius</i>
3	Ankle dorsiflexors	TA	<i>Tibialis anterior</i>
	Hamstring muscles	HAM	Medial hamstrings and <i>Biceps femoris long head</i>
		<i>Rectus femoris</i>	RF

In this model, six muscle groups, organized in three pairs, participate in forward and backward pedaling exercise. The phase (angle) of activation of two pairs (pairs 1 and 2) does not change with pedaling direction. The first pair of alternating muscles groups produces the energy needed to propel the crank during limb extension (GMAX and VAS, respectively – Table 4.2) and flexion (IL and BFsh, respectively). The second pair is formed by the ankle plantarflexors (SOL and GAS, respectively – Table 4.2) and the ankle dorsiflexors (TA). The ankle plantarflexors transfer the energy from the limbs inertia near the end of limb extension and during the transition between the extension and flexion, whereas the ankle dorsiflexors transfer the energy near the end of flexion and during the transition between flexion and extension. The phasing (moment of activation) of the third pair reverses with the pedaling direction. In forward pedaling, the hamstring muscles (IL – Table 4.2) are excited during the transition between the extension and flexion, while in backward pedaling, the activation occurs during the opposite transition (flexion to extension). The *rectus femoris* (RF – Table 4.2) alternates the moment of activation with the hamstrings. It also propels prior to the transition, whilst the hamstrings propel the crank subsequent to the transition [7]. The region of activity of the different muscle sets in forward and backward, according

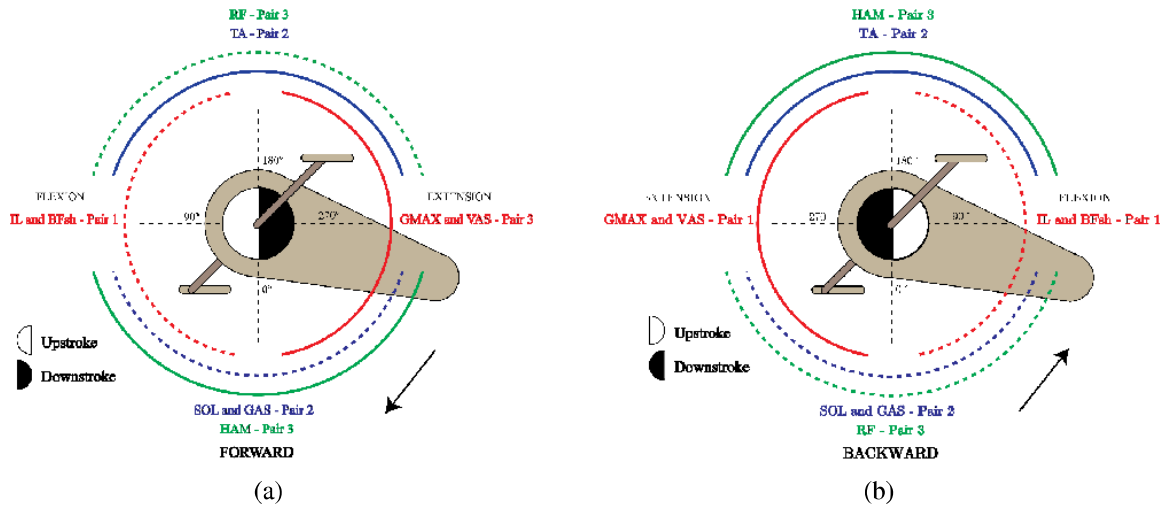


Figure 4.3: Muscles activation pattern in (a) forward and (b) backward pedaling, according to the Raasch *et al.*'s [7] computational biomechanical model.

to the Raasch *et al.*'s [7] computational biomechanical model, is represented in Figure 4.3.

Hug and colleagues analyzed the EMG activity pattern of several muscles, in 9 trained cyclists [97] and 11 healthy subjects [98], and found similarities with the model of Raasch *et al.* [7]. However, the authors did not record EMG activity in IL and BFsh group, since these muscles are difficult to record using surface EMG, for instance, the *psaos major* is a deep muscle and can only be recorded with intramuscular electrodes.

4.4 Muscle Abnormalities after Stroke

Inappropriate muscle contraction between the agonists and antagonists, muscle spasticity, limited ranges of motion (ROM), and abnormal synergistic muscle activity patterns are some of the causes of the asymmetrical limbs function [22].

A decrease in the number of functioning motor units, a reduction in the motor unit firing frequencies, an impaired motor unit recruitment and changes in the morphology of motor fibers are some changes at motor unit level that occur after stroke, which are associated with muscle weakness [22].

An increased muscle tone (spasticity) is frequently observed in stroke patients. In the lower limbs, spasticity is often strong in the hip adductors and internal rotators, hip and knee extensors, plantarflexors, supinators and toe flexors. A spastic posture can lead to the development of painful spasms, degenerative changes and fixed contractures [22]. Foot drop is frequently observed in stroke patients, consisting of a loss of angular dorsiflexion motion (weakness in dorsiflexors muscles). Very strong spasticity of *gastrocnemius* and *soleus* muscles, counteracting activity of the *tibialis anterior*, may cause foot-drop [99].

Due to abnormal obligatory synergies (abnormal patterns of co-activation of muscles), which emerge with spasticity, stroke patients may be unable to perform an isolated movement of a limb segment without moving others segments of the limb. The execution of ADLs is often affected by these synergies, for instance, a patient with a strong lower limb's extensor synergy will have difficulty in walking, due to plantarflexion and inversion of the foot, when the hip and knee are extended [22].

Inefficient muscle activation patterns, such as the co-activation of agonist and antagonist, limits force production during voluntary movements and increases patients' effort and fatigue [13, 22]. The assess-

ment of the functional consequences of inappropriate excitation has been difficult due to the complexity of multi-joint movements in gait. The analysis of the EMG patterns and kinematic data (joint angles and muscle lengths) allows the description of several types of disturbed motor control in hemiplegic gait [30].

Based on the model of Raasch *et al.* [7], Brown and Kautz [26, 28, 30] analyzed the muscle activation pattern of some muscles of the model, during cycling exercise, in stroke patients with residual hemiplegia. The authors identified two abnormalities associated with the abnormal net mechanical work done by the plegic limb: prolonged excitation of power-producing muscles (*vastus medialis* and *soleus*) and phase-advanced excitation (early initiation and early termination) of transition muscles (*semimembranosus*, *biceps femoris*, *gastrocnemius* and *tibialis anterior*). *Rectus femoris* exhibited prolonged excitation or early initiation and early termination. The prolonged excitation of power-producing muscles, when the muscles are lengthening (muscle extension), produce negative work (resistance of the limb to pedaling propulsion). Phased advanced excitation of transition muscles can also affect motor performance. An early initiation, while the muscle is lengthening can result in negative work, whereas an early termination, while the muscle is shortening (muscle flexion), can reduce the amount of positive work (contribution of the limb to pedaling propulsion).

Rosecrance and colleagues [48] identified three abnormal ankle patterns in hemiplegic stroke patients, during cycling: an alternating plantar-flexion-extension response; a prolonged plantarflexion response during the upstroke phase; and limited ankle joint excursion.

4.5 Influence on the EMG Patterns during Cycling

The lower limbs muscles' activity can be influenced by numerous factors such as workload, pedaling rate, body position, shoe-pedal interface and fatigue [92]. Changes in muscle activity level and activation timing may be induced by different cycling conditions.

Hug *et al.* [92] reported several studies that assessed the effects of different cycling conditions in the EMG patterns. Some studies have shown an increase of EMG activity level in some muscles as the workload increased, such as *vastus medialis* and *rectus femoris*. Regarding muscle activation timing, few studies have analyzed the influence of the workload, and one suggested that the EMG activity patterns are not significantly influenced by workload [92].

The influence of the pedaling rate in muscle activity level is not consensual, since different studies reported contradictory results (an increasing or a decreasing) due to the different workload conditions that were used. Some authors observed a trend of the EMG activity peak to occur earlier, in the pedaling cycle, for several muscles, as the pedaling rate increases [92].

The body posture also influences the EMG pattern, for instance, the change from seated to standing position induced changes in intensity and timing of EMG activity [92].

Two different types of shoe-pedal interface have been analyzed, the platform pedals (standard pedals) and the toe-clip or clipless pedals. The first type allows the application of positive effective force only during the downstroke phase, whereas the toe-clip and clipless pedals also permit the application of positive effective force during the upstroke phase. Changes in the activity level of different muscles were reported by two studies.

According to Hug *et al.* [92], direct EMG measurements may be useful, as biofeedback for clinicians and coaches, for improving the activation pattern of lower limbs' muscles, during rehabilitation and training programs.

As the cycling device used in this thesis, *THERA-Live*, is a semi-recumbent cycling device, the muscles' activity level and activation timing may differ from these studies, which were performed in standard ergometers.

4.6 *Rectus Femoris, Tibialis Anterior and Gastrocnemius Medialis*

Rectus femoris plays an important role in the cycling biomechanics. It is one of the major power muscles and is responsible for the maintenance of the crank progression during phase transitions [28]. Moreover, it is a large muscle and easy to assess. This muscle also plays an important role in the lower limbs' movement combinations, which emerge during the motor recovery process following stroke, when the obligatory synergies start to decline [22, 100]. The activation region of *rectus femoris*, during forward pedaling, includes the end of the upstroke and the start of the downstroke phases, as shown in Figure 4.4 (RF), in the transference of energy between joints and in the control of the direction of the produced force [92]. This muscle was chosen as the target muscle for this study, due to the mentioned reasons and by recommendation of the physicians that collaborate in this thesis. Two other muscles, *tibialis anterior* and *gastrocnemius medialis*, were also studied in this thesis, due to their characteristics and functions during cycling.

The *tibialis anterior* transfers energy from the limbs at the end of the upstroke phase and during the transition between upstroke and downstroke phases (Figure 4.4 – TA) [7]. Ankle dorsiflexion and inversion obligatory synergy patterns are related with this muscle [22].

Gastrocnemius medialis is activated, at the end of downstroke phase and in the transition between downstroke and upstroke phases (Figure 4.4 – GM) [7]. This muscle is associated with the ankle plantarflexion obligatory synergy pattern [22].

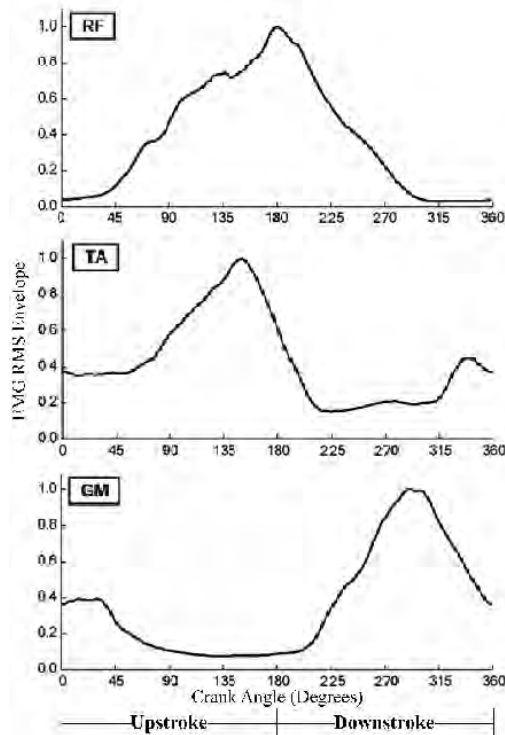


Figure 4.4: EMG root mean square (Root Mean Square (RMS)) linear envelope of *rectus femoris* (RF), *tibialis anterior* (TA) and *gastrocnemius medialis* (GM). Adapted from [92].

4.7 Joint Moments

In order to understand the pedaling process, different information is needed, such as the lower limbs' muscles that contribute to the pedaling action, the applied forces and the kinematics of the lower limbs' segments [101]. A model for biomechanical analysis of the lower limbs during cycling, developed and studied by Hull *et al.* [101] and Mimmi *et al.* [102], was implemented in order to obtain information about the internal muscular actions (without EMG measurements) and the moments acting on the lower limbs' joints. This data may be used to provide complementary quantitative indicators about the lower limbs' functionality and to assess the rehabilitation degree [90].

The model, represented in Figure 4.5, is formed by a close loop five-bar linkage with two fixed links (L_3 and L_4) and four moving links (thigh, shank, foot and crank arm – l_1 , l_2 , l_3 and L_2 , respectively).

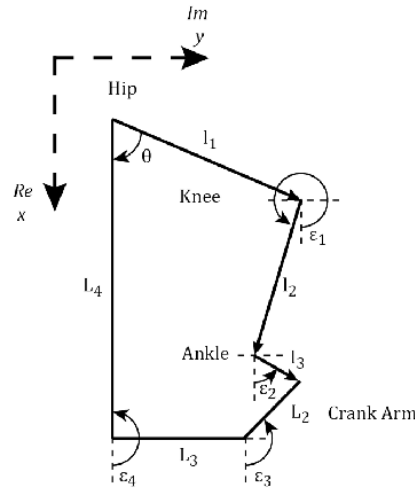


Figure 4.5: Five bar linkage model of the lower limb.

The internal actions and the moments acting on each joint can be determined as follows:

$$\sum_{foot} F_x^* = 0 \Rightarrow H_B = R_x - m_f(a_{fx} + g) \quad (4.1)$$

$$\sum_{foot} F_y^* = 0 \Rightarrow V_B = -m_f a_{fy} - R_y \quad (4.2)$$

$$\sum_{foot} M_{(B)}^* = 0 \Rightarrow M_{mf} = I_{fCG} \ddot{\epsilon}_2 + l_3 R_x \sin \epsilon_2 + l_3 R_y \cos \epsilon_2 + d_3 m_f a_{fy} \cos \epsilon_2 - d_3 m_f (a_{fx} + g) \sin \epsilon_2 \quad (4.3)$$

$$\sum_{shank} F_x^* = 0 \Rightarrow H_A = H_B - m_s(a_{sx} + g) \quad (4.4)$$

$$\sum_{shank} F_y^* = 0 \Rightarrow V_A = V_B - m_s a_{sy} \quad (4.5)$$

$$\sum_{shank} M_{(A)}^* = 0 \Rightarrow M_{ms} = I_{sCG} \ddot{\epsilon}_1 - l_2 V_B \cos \epsilon_1 - l_2 H_B \sin \epsilon_1 + d_2 m_s a_{sy} \cos \epsilon_1 + d_2 m_s (a_{sx} + g) \sin \epsilon_1 \quad (4.6)$$

$$\sum_{thigh} M_{(O)}^* = 0 \Rightarrow M_{mt} = I_{tCG}\ddot{\theta} - l_1 V_A \cos \theta + l_1 H_A \sin \theta + d_1 m_t a_{ty} \cos \theta - d_1 m_t (a_{tx} + g) \sin \theta \quad (4.7)$$

This model requires the computation of the angular accelerations of the segments, pedal forces, center of gravity (Center of Gravity (CG)) accelerations, free-body diagram, masses of the segments and the moments of inertia of the segments about their CG. Further details of the model can be found in Appendix B and in [101, 102]. The masses, the moments of inertia and the CG locations were determined using parameters outlined by Clauser *et al.* [103]. Further information about the determination of the body segment parameters can be found in Appendix B.

The results of the application of this model in healthy and in stroke subjects are presented in this chapter and in Chapter 6, respectively.

4.8 User-Device Interaction

The influence of cadence and workload on force output during pedaling was studied in this thesis. Similar studies have been performed in [26, 28, 90, 93, 94], but the cycling device was different (standard ergometer), and thus this study is needed. The device used in this thesis (semi-recumbent ergometer) is the type normally used in hospital facilities and rehabilitation clinics. Therefore, these trials were performed in order to compare the user-device interactions on the different types of cycling devices. Furthermore, this study might allow the identification of effective quantitative indicators of the rehabilitation degree and qualitative indicators of the quality of the movement, which may be employed in the characterization of the lower limbs in stroke patients.

4.8.1 Procedure

Six healthy subjects (Table 4.3) were recruited to test the developed system.

Table 4.3: Mean and standard deviation values of the demographic and anatomical characteristics of the subjects

Age (years)	23.50 (1.61)
Sex (Male / Female)	3 / 3
Height (m)	1.73 (0.04)
Weight (Kg)	65.33 (6.39)
Preferred Foot (Left / Right)	2 / 4
Thigh Length (cm) – trochanter to tibiale	53.17 (2.27)
Shank Length (cm) – tibiale to sphyrion	42.83 (3.39)
Foot Length – heel to tip longest toe	26.17 (1.07)
Distance of the chair to the crank axis (cm)	45.83 (6.12)

All subjects were asked to perform 9 workload and cadence combinations (workloads: 2, 8 and 15 Nm; cadences: 40, 50 and 60 rpm). During pedaling trials, a metronome was used to provide auditory feedback of the target cadence, allowing the user to synchronize the cadence.

The subjects seated in a chair with 43 cm of height. To standardize the condition under which the cycling test was conducted, the distance from the seat edge to the crank axis was adjusted so that the knee extension angle was 10 degrees less from full extension when the subjects extended their knees maximally, as used by Fujiwara *et al.* in [41]. As stated in Chapter 3, the zero degree of the crank angle

(ϕ) was defined as when the crank arm is perpendicular to the ground surface and the right pedal is at the bottom. To reduce the influence of the weight and inertial forces on the force results, a constant value, computed through a passive exercise of 10 revolutions at 40 rpm and 8 Nm, was subtracted from the force values, for each pedal.

The angles values (ϕ and β) and the force applied in the force sensors (F_p) were used to obtain the effective force values (F), which allow the calculation of the positive, negative and net mechanical work done by each leg (W^+ , W^- , W , respectively). The results were obtained in steady conditions, during 30 seconds for each combination, to ensure a lower deviation on the results. A rest period of 1 minute was respected between each trial. The angles values (ϕ and β), the applied force (F_p) and net mechanical work (W), the cadence, as well as, the moments of the lower limbs joints (hip, knee and ankle), during 10 revolutions (11th to 20th), were analyzed for each trial and subject. The first 10 revolutions were not considered in order to ensure a lower deviation on the results.

Statistical analysis was performed using the *SPSS* software (IBM Corporation, USA). The magnitude of the pedal angle ($\Delta\beta$), the positive mechanical work (W^+) and the negative mechanical work (W^-) underwent descriptive analysis first to determine if they were normally distributed and their variances homogeneous. The results show the variables were skewed and thus the logarithmic transformation of the magnitude of the pedal angle ($\Delta\beta$) and of the positive mechanical work (W^+), as well as, the square root transformation of the negative mechanical work (W^-) were used in the statistical tests. An analysis of variance (Analysis of Variance (ANOVA)) with four factors (workload, cadence, subject and limb) was used to identify the differences of each factor on the magnitude of the pedal angle ($\Delta\beta$), positive mechanical work (W^+) and negative mechanical work (W^-). The effects of the factors and interactions were considered statistically significant when the *p-value* was < 0.05 .

4.8.2 Results

Although data was recorded for six subjects, to better describe the observed results, a detailed analysis of the variables of subject 4 is presented. The variables' variation for the others subjects was largely similar to this subject. The cases where a different pattern was observed are detailed in next section.

The results of an analysis of variance (ANOVA) with four factors (workload, cadence, subject and limb), on the magnitude of the pedal angle ($\Delta\beta$), positive mechanical work (W^+) and negative mechanical work (W^-) variables, are represented in Table 4.4. Although the full model was used, only the main effects and the interaction between the workload and cadence are presented.

The effects of workload, cadence, interaction between the workload and the cadence, subject and limb are all statistically significant, for the three variables, with the exception of the effect of the limb in the magnitude of the pedal angle ($\Delta\beta$).

The mean logarithmic values of the magnitude between the maximum and the minimum values of the pedal angle ($\Delta\beta$), of all healthy subjects, for the 9 workload and cadence combinations, are represented in Figure 4.6. The 40, 50 and 60 rpm curves are represented by the solid red, dotted green and dashed blue lines, respectively.

The plots of Figure 4.7 (a) and (b) display the mean values of the pedal angle (β) for three different workloads (2, 8 and 15 Nm – solid red, dotted green and dashed blue lines, respectively) at 50 rpm, and for three different cadences (40, 50 and 60 rpm – solid red, dotted green and dashed blue lines, respectively) at 8 Nm, for the left leg of subject 4, with respect to crank angle (ϕ), respectively. In the plots where a variable is analyzed with respect to crank angle (ϕ), the grey area represents the upstroke

Table 4.4: The F ratio values, degrees of freedom (df) and the significance-values (p -value) resulted from an ANOVA with four factors (workload, cadence, subject and limb), on the magnitude of the pedal angle ($\Delta\beta$), positive mechanical work (W^+) and negative mechanical work (W^-) variables. Only the main effects and the interaction between the workload and cadence are presented

Variable	Factor	df	F	p -value
$\Delta\beta$	Cadence	2	3859.44	<0.01
	Workload	2	119.31	<0.01
	Cadence \times Workload	4	37.68	<0.01
	Subject	5	52.29	<0.01
	Limb	1	0.00	0.95
W^+	Cadence	2	255.53	<0.01
	Workload	2	2655.85	<0.01
	Cadence \times Workload	4	14.09	<0.01
	Subject	5	154.51	<0.01
	Limb	1	1071.60	<0.01
W^-	Cadence	2	6.82	<0.01
	Workload	2	30.31	<0.01
	Cadence \times Workload	4	72.58	<0.01
	Subject	5	181.03	<0.01
	Limb	1	169.55	<0.01

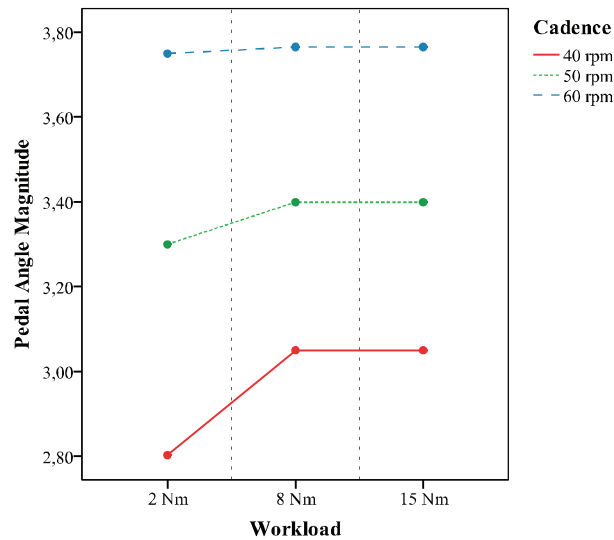


Figure 4.6: Mean logarithmic values of the magnitude between the maximum and the minimum value of the pedal angle ($\Delta\beta$), of all healthy subjects, for the 9 workload and cadence combinations workloads: 2, 8 and 15 Nm; cadences: 40, 50 and 60 rpm). The 40, 50 and 60 rpm curves are represented by the solid red, dotted green and dashed blue lines, respectively.

phase of the left limb and the shaded area along the curves represents the standard deviation values. In addition, the data of the curves correspond to the average values of 10 revolutions (11th to 20th revolution).

The mean values of the angle between the crank arm and the pedal (α) for three different workloads (2, 8 and 15 Nm – solid red, dotted green and dashed blue lines, respectively) at 50 rpm, and for three different cadences (40, 50 and 60 rpm – solid red, dotted green and dashed blue lines, respectively) at 8Nm, for the left leg of subject 4, with respect to crank angle (ϕ), are presented in Figure 4.8 (a) and (b), respectively.

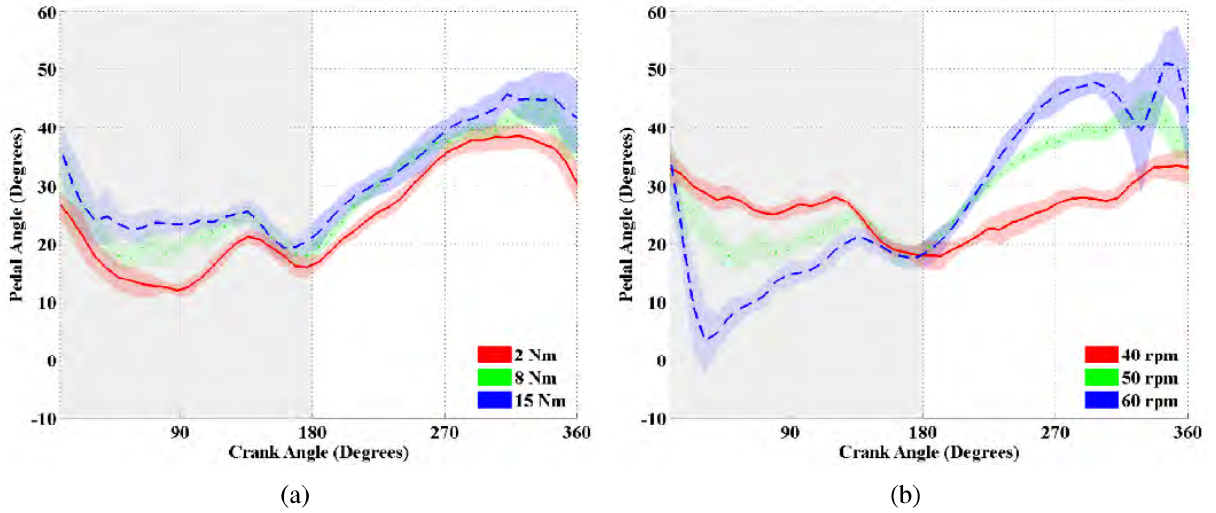


Figure 4.7: Mean values of the pedal angle (β) for (a) three different workloads (2, 8 and 15 Nm – solid red, dotted green and dashed blue lines, respectively) at 50 rpm; and (b) three different cadences (40, 50 and 60 rpm – solid red, dotted green and dashed blue lines, respectively) at 8 Nm, for ten revolutions (11th to 20th revolution), for the left leg of the subject 4. The grey area represents the upstroke phase of the left limb and the shaded area along the curves represents the standard deviation values.

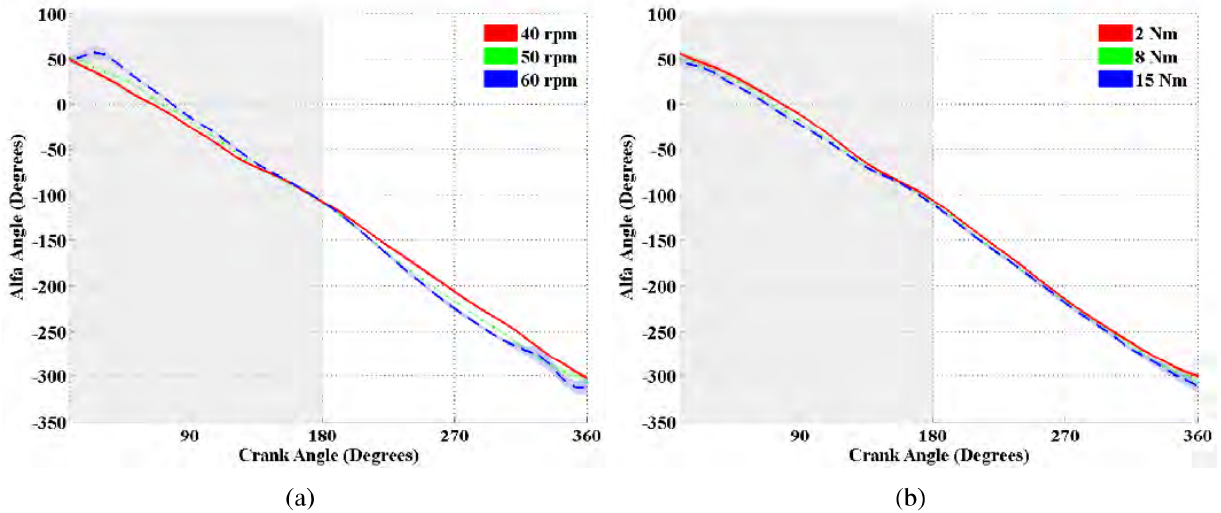


Figure 4.8: Mean values of the angle between the crank arm and the pedal (α), for (a) three different workloads (2, 8 and 15 Nm – solid red, dotted green and dashed blue lines, respectively) at 50 rpm; and (b) three different cadences (40, 50 and 60 rpm – solid red, dotted green and dashed blue lines, respectively) at 8Nm, for the left leg of the subject 4.

Figure 4.9 presents the mean logarithmic values of the positive mechanical work (W^+), of all healthy subjects, for the 9 workload and cadence combinations. The 2, 8 and 15 Nm curves are represented by the solid red, dotted green and dashed blue lines, respectively.

The mean logarithmic values of the positive mechanical work (W^+) for the 3 workload values and for the 3 cadence values, for each subject, are represented in Figure 4.10 (a) and (b).

The plots of Figure 4.11 present the mean of the square root of the absolute value of the negative mechanical work (W^-), of all healthy subjects, for the 9 workload and cadence combinations. The 2, 8 and 15 Nm curves are represented the solid red, dotted green and dashed blue lines, respectively.

The mean of the square root of the absolute values of the negative mechanical (W^-) work for the 3 workload values and for the 3 cadence values, for each subject, are displayed in Figure 4.12 (a) and (b),

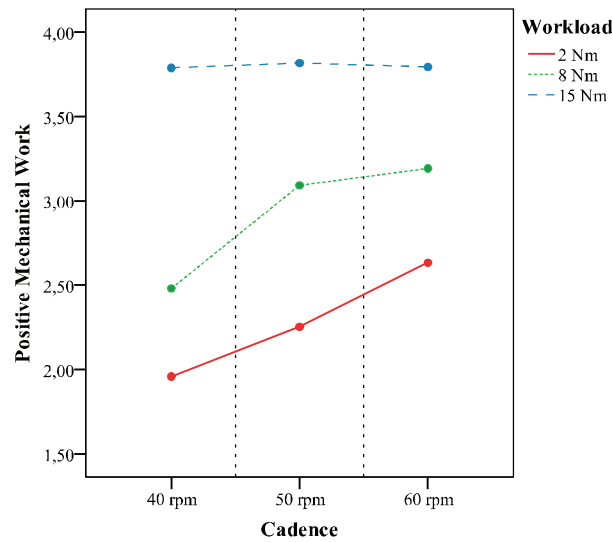


Figure 4.9: Mean logarithmic values of positive mechanical work (W^+), of all healthy subjects, for the 9 workload and cadence combinations workloads: 2, 8 and 15 Nm; cadences: 40, 50 and 60 rpm. The 2, 8 and 15 Nm curves are represented by the solid red, dotted green and dashed blue lines, respectively.

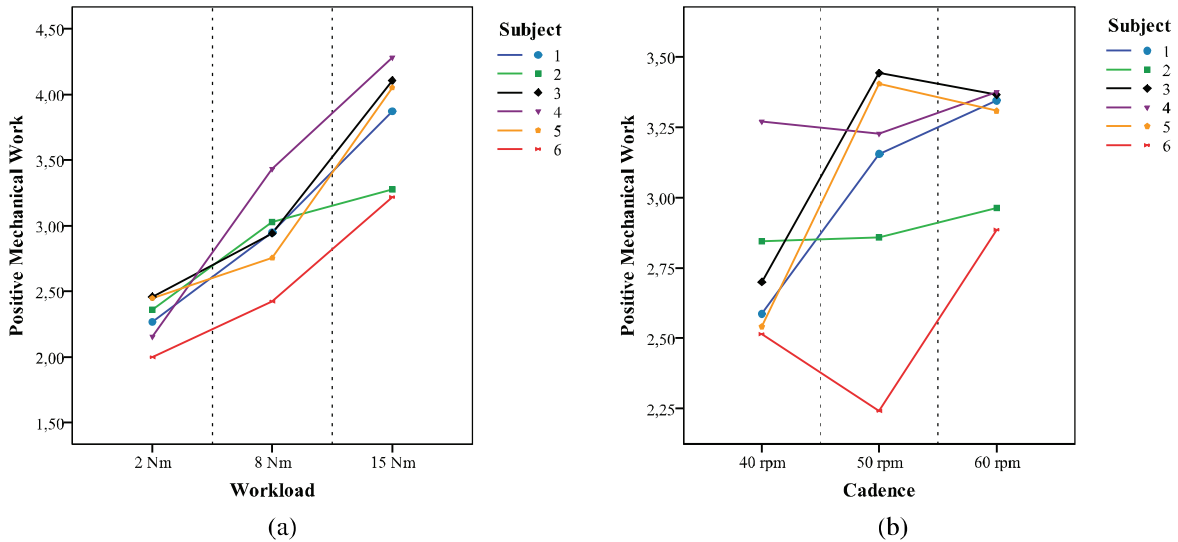


Figure 4.10: Mean logarithmic values of the positive mechanical work (W^+) for the (a) 3 workload values (2, 8 and 15 Nm); and (b) 3 cadence values (40, 50 and 60 rpm), for each subject.

respectively.

The plots of Figure 4.13 present the mean values of the effective force (F) for three different workloads (2, 8 and 15 Nm – solid red, dotted green and dashed blue lines, respectively) at 50 rpm for the left leg of subject 4 (a), and for three different cadences (40, 50 and 60 rpm – solid red, dotted green and dashed blue lines, respectively) at 8Nm, for the left leg of subjects 4 (b) and 3 (c), with respect to crank angle (ϕ).

The mean logarithmic values of the positive mechanical work (W^+ – (a) and (b)) and the mean square root values of the absolute negative mechanical work (W^- – (c) and (d)), performed by the pushing (solid red line) and the coordination (dashed green line) limbs, for the different workload and cadence conditions, are represented in Figure 4.14.

The plots of Figure 4.15 (a) and (b) show the mean values of the effective force (F) for both lower limbs (pushing and coordination limbs – solid red and dashed green line, respectively) at 40 and 50 rpm, at 15 Nm, of the subject 4, with respect to crank angle (ϕ), respectively. In the plots where the behavior of

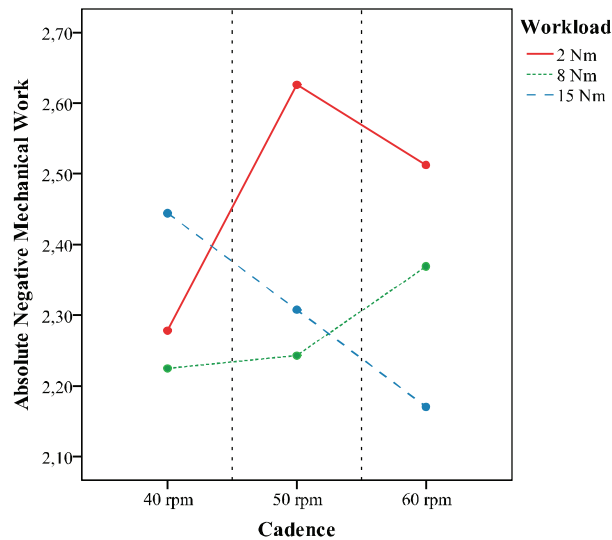


Figure 4.11: Mean of the square root of the absolute values of the negative mechanical work (W^-), of all healthy subjects, for the 9 workload and cadence combinations workloads: 2, 8 and 15 Nm; cadences: 40, 50 and 60 rpm. The 2, 8 and 15 Nm curves are represented by the solid red, dotted green and dashed blue lines, respectively.

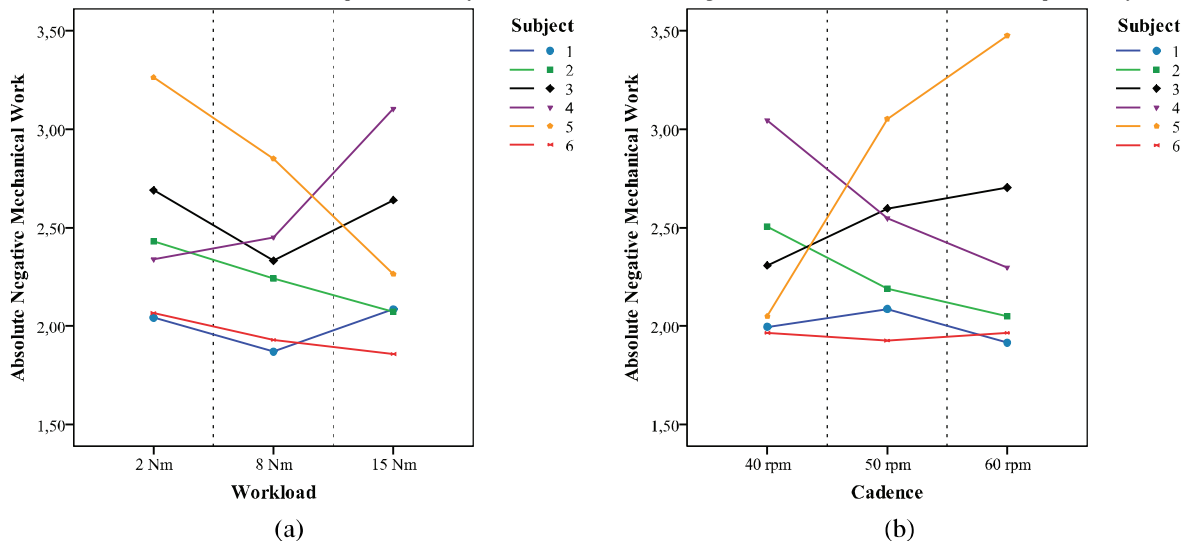


Figure 4.12: Mean of the square root of the absolute values of the negative mechanical work (W^-) for the (a) 3 workload values (2, 8 and 15 Nm); and (b) 3 cadence values (40, 50 and 60 rpm), for each subject.

the pushing and coordination limbs is analyzed with respect to crank angle (ϕ), the grey area represents the upstroke phase of the pushing limb.

The mean values of the ankle, knee and hip moments for the pushing (solid red line) and coordination (dashed green line) limbs, at 50 rpm and 15 Nm, of the subject 4, with respect to crank angle (ϕ), are presented in Figure 4.16 (a), Figure 4.16 (b) and Figure 4.16 (c), respectively.

4.8.3 Discussion

The pedal angle amplitude ($\Delta\beta$) increased with workload and cadence, as shown in Figure 4.6. The variation of the pedal angle (β) as the workload increases is lower, when comparing to the results of the increased cadence. The cadence increase involves a faster pedal movement, which results in a faster feet dorsiflexion and plantarflexion, to perform the transitions between the cycling phases. At lower cadence the user has a higher control of the feet orientation in the pedals. The increase of β results in a higher

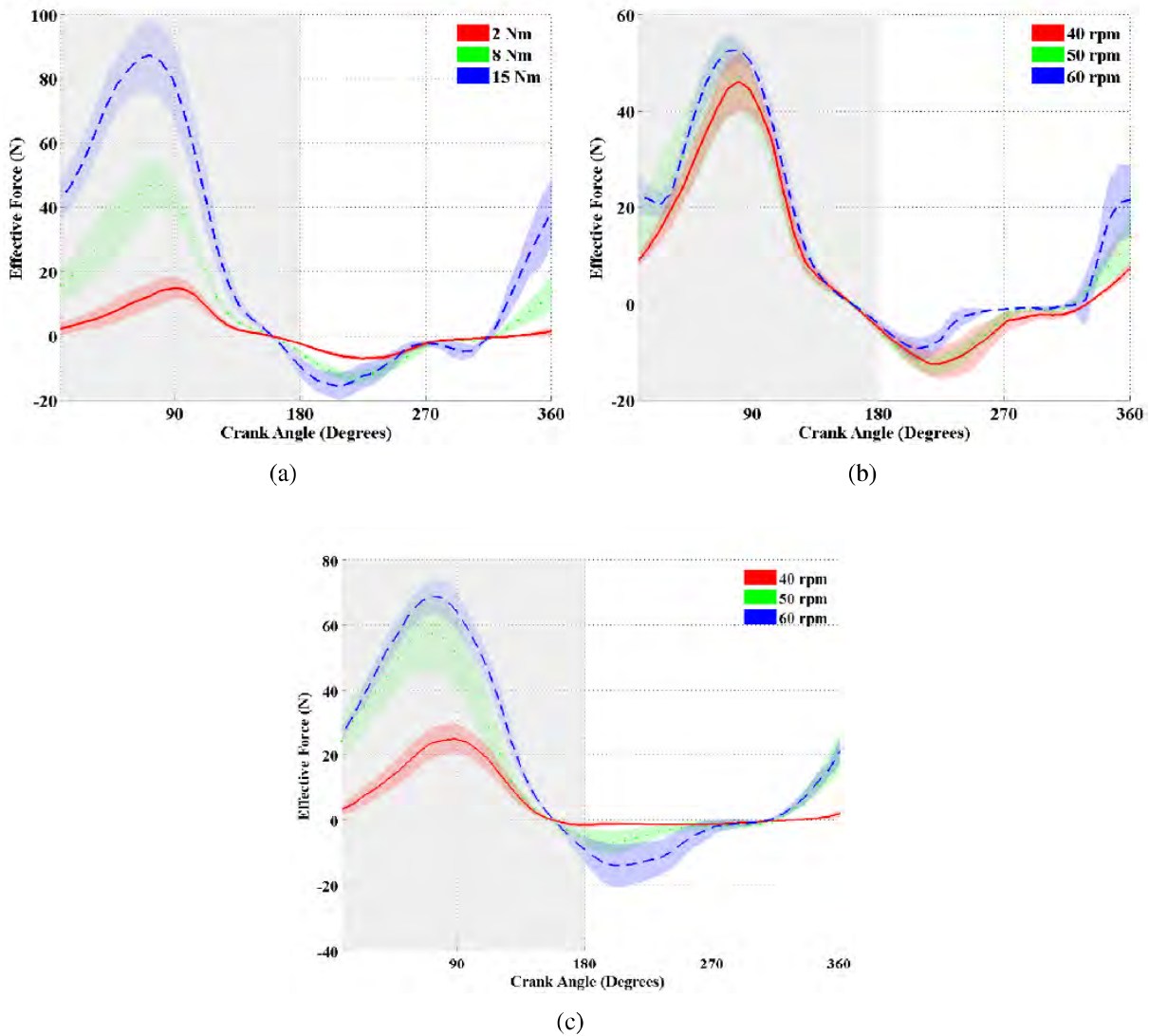


Figure 4.13: Mean values of the effective force (F) for (a) three different workloads (2, 8 and 15 Nm) at 50 rpm (subject 4); and for three different cadences (40, 50 and 60 rpm) at 8 Nm of (b) subject 4 and (c) subject 3. The 2, 8 and 15 Nm curves and the 40, 50 and 60 rpm curves are represented by the solid red, dotted green and dashed blue lines, respectively.

angle between the pedal and the crank arm (α), during the downstroke phase, which reduces the effective force (F) component of the applied force.

The plots of Figure 4.7 show the pedal angle (β) follows approximately a sinusoidal behavior, where the points of inflexion occur in the transition between cycling phases (at 0 and 180 degrees). As β is never zero, the crank angles (ϕ), for which the F is maximal, will not occur precisely at 90 and 270 degrees. In addition, the angles, where the F is null, will not occur precisely at 180 and 360 degrees. The pedal angle reduces, during the first half of the downstroke phase (0 to 90 degrees for the left leg). This behavior maximizes the effective component of the applied force. The higher pedal angle value occurs when the foot is closer to the body, during the second half of upstroke phase (between 270 and 360 degrees – left leg).

The α angle (Figure 4.8) shows a linear trend, which indicates that the variability of the pedal angle does not influence significantly the α angle values. The change of the workload does not have much impact on the α angle, since the values are almost equal. Otherwise, the cadence has a higher effect on

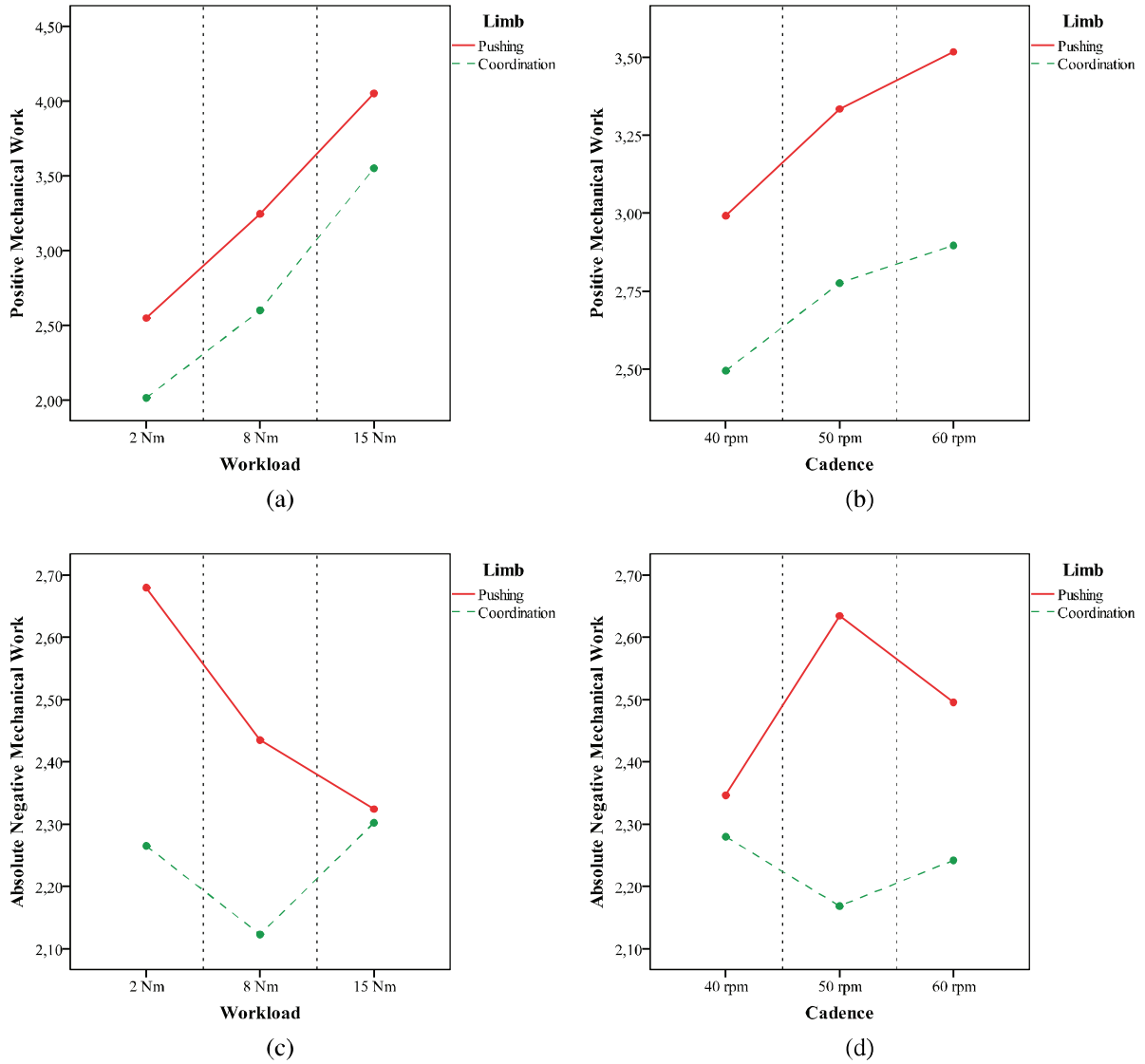


Figure 4.14: Mean logarithmic values of the positive mechanical work (W^+ – top) and mean square root values of the absolute negative mechanical work (W^- – bottom) for (a)(c) three different workloads and (b)(d) three different cadences, performed by the pushing (solid red line) and the coordination (dashed green line) limbs.

the angle between the pedal and the crank arm, which influences the effective component of the applied force. These plots confirm that the crank angle (ϕ) where the F is equal to the applied force and where the forces are opposed did not occur at 90 and 270 degrees, respectively, as usual in a standard cycling device [90].

As the workload increased, the subjects showed an increased positive mechanical work (W^+) done by each leg. This is shown in Figure 4.9 and Figure 4.10 (a) where, the value of the W^+ increased for higher workloads. These results are consistent with previous studies of Sanderson *et al.* [93]. At higher workloads, it is required to apply more force during downstroke phase to overcome resistance and to move the crank, which results in a higher positive effective force. The negative mechanical work (W^-) presented two different behaviors with the increase of the workload (Figure 4.12 (a)). Some subjects reduced the W^- , as previously observed in [93], which suggests that the subjects adopted a strategy to improve the effective application of force by reducing the retarding force during the upstroke phase and, consequently, reducing the need of a higher demand on the propulsive leg, which is in the downstroke phase, to overcome the recovery leg. This pedaling strategy, shown in Figure 4.13 (a), increases the pedal

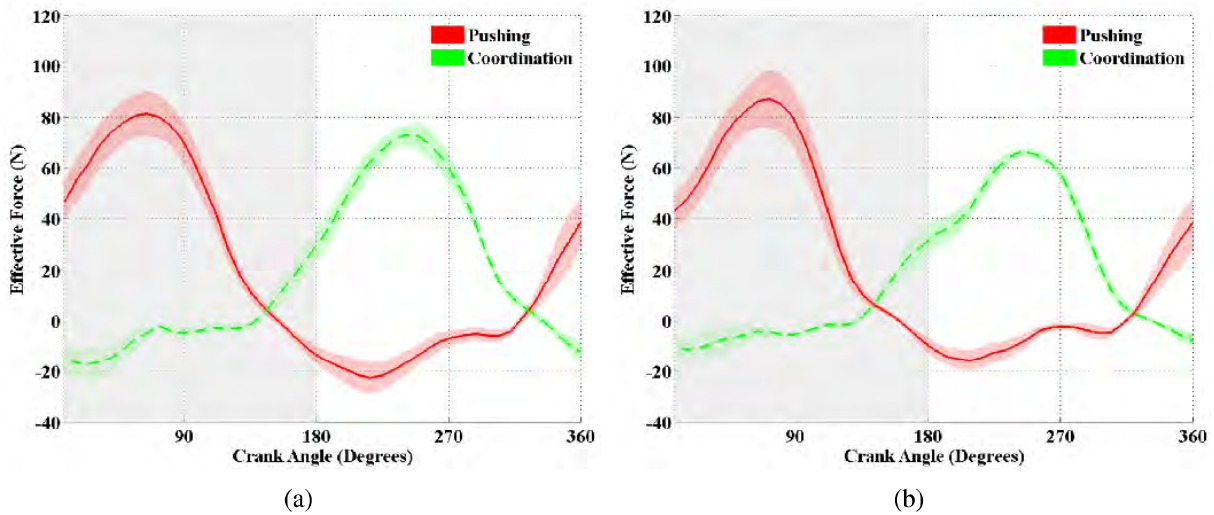


Figure 4.15: Mean values of the effective force (F) for the pushing (solid red line) and coordination (dashed green line) limbs, at (a) 40 rpm and (b) 50 rpm, at 15 Nm, of the subject 4. The grey area represents the upstroke phase of the pushing limb.

force effectiveness [89], but it was not adopted by all subjects.

The cadence results show a trend for an increased positive mechanical work (W^+), with the increase of cadence (Figure 4.9 and Figure 4.10 (b)). However, these results are inconsistent with the study of Sanderson *et al.* [93], where higher cadences resulted in a lowered W^+ . Conversely, in Mimmi *et al.*'s [104] study, an increased normal force was measured with the increase of cadence. In [93], a reduction of the negative force with the cadence increase is reported, which is observed in four of six subjects of this study Figure 4.12 (b). The distinct behavior may result from the effects of the non-muscular components of the applied force, reported by Kautz and colleagues [94]. The authors decomposed the force applied during cycling in two different types: the muscular and the non-muscular force components. The first is the force applied due to the net intersegmental moments (activity of leg muscles), whereas the non-muscular force component is comprised of the weight and inertial forces. A higher cadence resulted on the same trend for muscular and non-muscular force components, although the last one is predominantly responsible for the changes in the applied pedal force. The authors observed that the weight had a lower variance with the cadence, since gravity is a static force. However, the amplitude of the inertial force component increased with the raise of the cadence (higher positive and negative forces) [94]. This behavior is consistent with the results observed in some subjects, for instance, as shown in Figure 4.13 (c). The effects of weight and the inertial components can be reduced through the subtraction of the measured forces during passive exercise [94], which was done through a passive trial of 10 revolutions at 40 rpm and 8 Nm. Therefore, the weight component may not have considerable impact on the force applied on the pedals. Regarding the inertial component, as the passive test was performed at 40 rpm, it may influence the obtained force values, since two trials were performed at higher cadences (50 and 60 rpm).

Regarding the contribution performed by each limb, the results showed an asymmetrical cycling. The subjects performed more force with one of the two limbs, which is evidenced by statistical significance of the limb factor, for the W^+ and W^- variables. Mimmi *et al.* [90] described a specific function for each lower limb: the pushing function for one limb and the coordination function for the other. One limb applies more propulsive and resistive force ("pushing" limb) and the other coordinates the movements

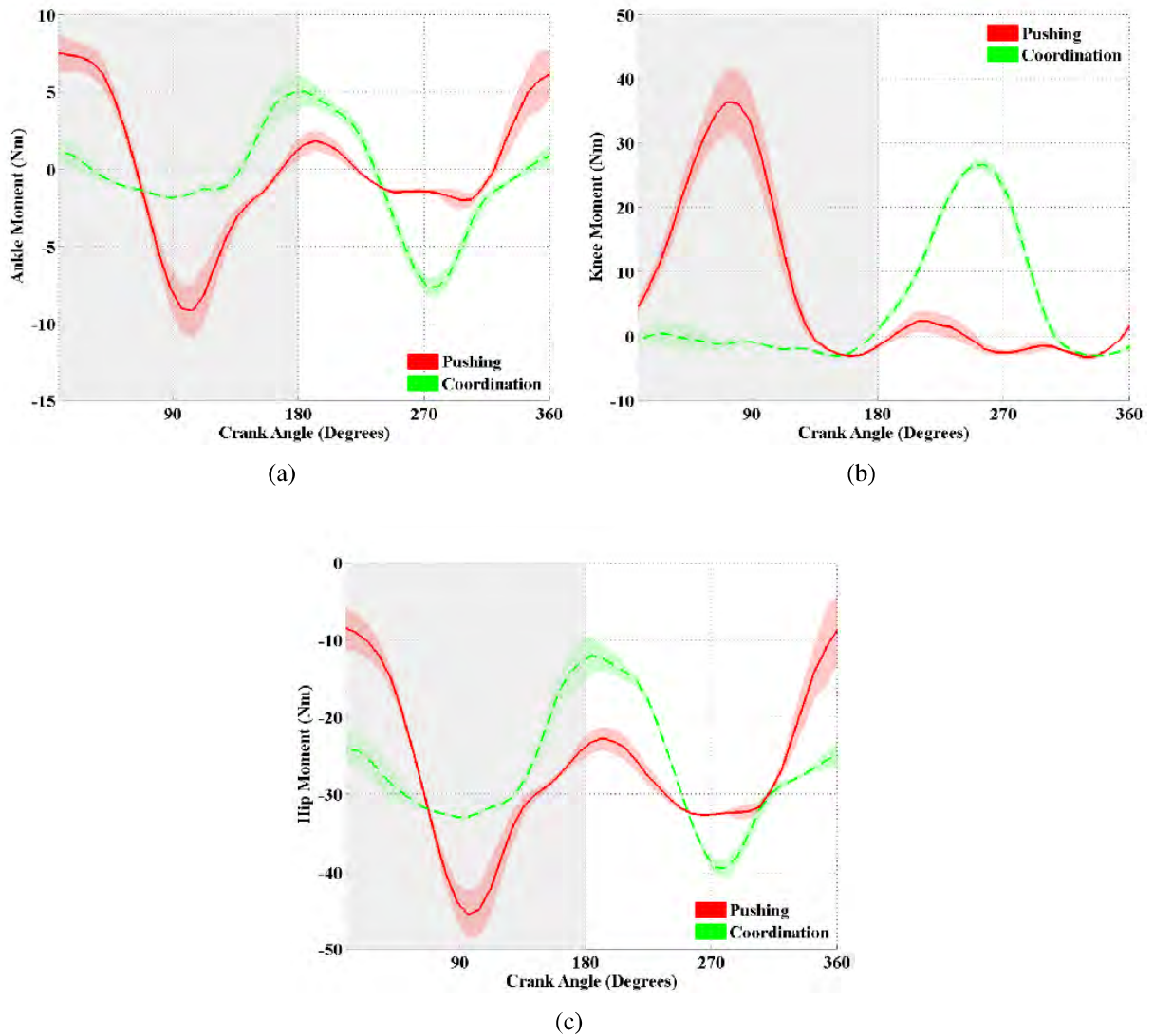


Figure 4.16: Mean values of the (a) ankle, (b) knee and (c) hip moments, for the pushing (solid red line) and coordination (dashed green line) limbs, at 50 rpm and 15 Nm, of the subject 4.

(“coordination” limb), the last is normally the limb with which the user kicks a ball. Consequently, in an applied force pattern, a limb will present higher applied force values. The analysis of the positive and negative mechanical work (W^+ and W^- , respectively) performed by each limb, based on the Mimmi *et al.*'s [90] classification, has shown a higher contribution (higher W^+ – Figure 4.14 (a) and (b)) and a higher resistance (higher absolute W^- – Figure 4.14 (c) and (d)) of the pushing limb, when compared to the coordination limb, which is consistent with the Mimmi *et al.*'s [90] observations. This difference between the force applied by each limb is observed in the force patterns, as shown in Figure 4.15. According to the authors, the difference between the force applied by each limb increases with the cadence increasing, which is consistent with data observed in Figure 4.14 (b) and in Figure 4.15. The user's position, in relation to the chair, may also influence the force applied in the pedals, since, if the user is not in a centered position, more force will be applied on the side for which the user is deviated. Regarding the pedal angle magnitude ($\Delta\beta$), as the effect of the factor limb was not statistical significant, the distinct function of the lower limbs may not influence the range of (β).

The different lower limbs' function is also observed throughout the lower limbs joints' moments, as

shown in Figure 4.16. The shape of the ankle and hip moments is similar, whereas the knee moment follows the behavior of the force applied on the pedals (Figure 4.15 (b)). As the workload increases the moments follow the same behavior with higher amplitudes. The change of the joints' moments with the cadence increase is not as significant as with the increase of the workload. The effects of the workload and cadence on the joints' moments are similar to the ones observed in the effective force pattern.

The studies that analyzed the influence of the workload and cadence were, generally, performed in standard cycling devices, different from the cycling device used in this study (semi-recumbent). The inconsistency of some observed results with the observed in the literature may be related with the cycling device's different configuration.

The subjects reported a higher difficulty to maintain a constant cadence for 40 rpm, since the device operation induced some propulsive power, even when the users were pedaling actively, overcoming the users' action, who sometimes had to brake the motor to maintain the targeted cadence. These aspects may result in abnormal changes in the force output. The high variability of the results between subjects and in different conditions may result on different pedaling strategies adopted by each subject to overcome different workloads and maintain a constant cadence.

The system developed to measure the force applied in the pedals presents some limitations that may influence the analysis of the cycling strategy. This system only measures the normal component of the applied force, and does not measure the force which may be applied in the upward direction during the upstroke phase, since the feet of the subject are fixed to the pedals by Velcro strips. In addition, due to the mechanical system and force sensors configuration, a portion of the applied force may not be detected by the force sensors.

4.9 Conclusions

The lower limbs muscles' function during cycling include the production of external power during extension, aiding in the limb recovery during flexion, assisting in the transition between extension and flexion, and assisting in the transition between flexion and extension. Muscle abnormalities, such as inappropriate muscle contraction between the agonists and antagonists, muscle spasticity, limited ranges of motion (ROM), and abnormal synergistic muscle activity patterns, are generally observed in stroke patients, and cause an asymmetrical limbs function. The muscle activity level and activation timing may be induced by numerous factors, such as workload, pedaling rate, body position, shoe-pedal interface and fatigue.

Rectus femoris is one of the major power muscles and is responsible for the maintenance of the crank progression during phase transitions. It activates, during forward pedaling, at the end of the upstroke and at the start of the downstroke phases. The *tibialis anterior* muscle transfers energy from the limbs at the end of the upstroke phase and during the transition between upstroke and downstroke phases, whereas the *gastrocnemius medialis* is activated, at the end of downstroke phase and in the transition between downstroke and upstroke phases.

During cycling, as the workload and cadence increased, the amplitude of the pedal angle increased. The variation is higher as the cadence rises, which may be due to the faster transition between cycling phases. In general, a higher workload resulted in a higher positive force output, in order to overcome the higher crank resistance. Some subjects also reduced the resistive force, during the upstroke phase, in order to achieve a higher force effectiveness. The influence of cadence in the force output resulted in

different variations than those reported in literature, which may be related to the cycling device's configuration being different. Each lower limb has a different function (pushing or coordination function), which influence the force applied by each limb (the pushing limb applies more force), and results in an asymmetrical force pattern, even in healthy subjects. This difference is higher as the cadence rises. The analysis of the joints' moments allows to obtain more information of the lower limbs muscles' action. The assessment of training parameters, such as angles, applied forces and joints' moments, may provide relevant data for diagnosing lower limbs' motor impairments and in the definition of the rehabilitation strategy more adequate to the problem.

The analysis performed in this chapter allowed the selection of the muscles that will be addressed in this studied (*rectus femoris*, *tibialis anterior* and *gastrocnemius medialis*), based on their importance during walking and cycling and since they are related with disturbances typically observed in stroke patients. The identification of the factors that could influence the EMG pattern may contribute in the protocol design and in the results analysis.

The behaviors observed in the tests performed on the healthy subjects allowed the identification of the cadence and workload as factors that may be explored in the rehabilitation. As the increase of the cadence results in a higher pedal angle (β) magnitude, it may be used in the rehabilitation of the dorsiflexion and plantarflexion movements, which are related with the *tibialis anterior* and *gastrocnemius medialis*, and are, generally, impaired in stroke patients. A higher workload may be explored as a training to increase the muscle strength of the paretic limb, since it involves a higher applied force.

As the healthy subjects present an asymmetrical cycling, due to the different function of each limb, they could participate in the testing of the force biofeedback system, which will be developed in this study in order to increase the cycling symmetry and rehabilitate the paretic limb of stroke patients.

Force and EMG Biofeedback

5.1 Introduction

The independent application of cycling and biofeedback, as detailed in Chapter 2, has already shown positive results in the rehabilitation of stroke patients. There is a lack for more studies that combine both therapies. Cycling combined with force biofeedback was studied in [18, 19], whereas cycling together with EMG biofeedback was studied in [8, 17].

The effect of providing different types of biofeedback (force and EMG biofeedback) together with cycling exercise on the exercise variables and on the user's pedaling strategy will be explored in this chapter. The experimental setups used to provide the two biofeedback types, as well as, a detailed description of the biofeedback systems, exercise conditions and assessment metrics will be described in the following sections. The two biofeedback systems and a set of training conditions will be studied in healthy subjects, to explore the most appropriate conditions to apply force and EMG biofeedback combined with cycling exercise in the rehabilitation of stroke patients.

The sensors instrumented on the *THERA-live* device and the *Matlab* software will be used to compute visual biofeedback of the force applied on each pedal, which will be provided to the user, in order to improve his cycling symmetry. The *YSY EST EVOLUTION* will be used to provide EMG biofeedback of the muscle's activation pattern, and its effect on the exercise variables will be analyzed. Further details of these systems, as well as, the results of the application of the systems to healthy subjects, are detailed in this chapter.

5.2 Force Biofeedback

One general consequence of stroke is the asymmetrical movements between lower limbs, which affects the performance of activities, such as walking and cycling [25]. The paretic limb's force pattern of patients with post-stroke hemiparesis was studied by Brown and Kautz [26, 28, 30], who observed the paretic limb performs less propulsive force and more resistive force than the healthy limb. The authors also observed the healthy limb performs the major contribution to the movement.

The analysis of the force pattern in stroke patients allows the assessment of the degree of asymmetry and may be used as biofeedback to inform the patient about some possible asymmetries in the force applied by the limbs. Providing visual information about the contribution of each limb to the movement, together with a reasonable objective, may assist the patients to perform more positive mechanical work

with the unhealthy limb. According to Ambrosini *et al.* [5], training toward a symmetrical cycling pattern may induce motor changes and may reduce muscle weakness and gait asymmetry. Force biofeedback's mechanisms may be used as a rehabilitation tool, in order to recover motor impairments.

Regarding cycling and force biofeedback training, there is a need to explore the best way to provide information about the symmetry of the force applied on the pedals during cycling exercise. The biofeedback should be simple and intuitive, so the user easily knows what needs to be done to achieve the objective pattern. The need for a target value or range that provides a reference for the user attempt to obtain a symmetrical pattern should also be explored. In general, it should be explored if the provision of force biofeedback changes the users' pedaling strategy.

The use of cycling and force biofeedback as a stroke rehabilitation therapy will be supported if it increases the participation of the paretic limb in the exercise and if training with a more symmetrical pattern results in specific motor improvements in the paretic limb and preferably in a general level, for instance, improvements on gait.

5.2.1 Force Biofeedback Experimental Setup

The experimental setup that provides the force biofeedback to the user, which was based on the work of Ferrante *et al.* [18], is comprised of five components: the subject, the cycling device equipped with the sensors, the acquisition board, the *Data PC* and the *Data PC display*. A loop is formed by these six components, as shown in Figure 5.1.

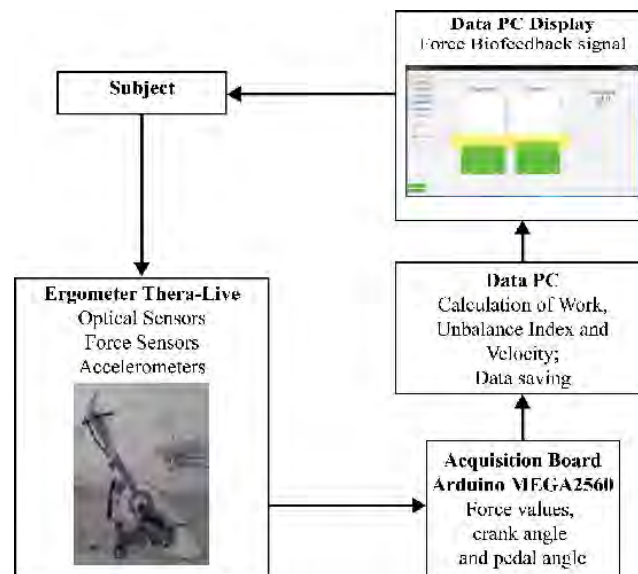


Figure 5.1: Experimental setup used for the Force Biofeedback intervention.

The subject performs the exercise on the cycling device (*THERA-Live*), which is instrumented with optical sensors, force sensors and accelerometers (described in Chapter 3). The data of the sensors is acquired by the acquisition board (*Arduino MEGA 2560*), which sends the force values (F_p), as well as, the crank and pedal angles (ϕ and β , respectively) to the *Data PC*. This device proceeds to the data saving and to the computation of metrics, such as the net mechanical work (W – equation (3.6)), Unbalance Index (equation (2.3)) and cadence values. Finally, the values of the work performed by each limb and the cadence values are displayed back to the subject by the *Data PC*, using an interface developed in the *Matlab* software (The MathWorks Inc., USA).

Visual information of the work applied in the pedals, by each limb, is presented in the form of two bars. When the work performed by each limb stays in a specific interval (target band – yellow band in Figure 5.2), the two bars turn green (Figure 5.2 (a)); whereas, when the work applied by either lower limb deviates from the target band, the two bars turn red (Figure 5.2 (b)). This system provides a simple and intuitive way to inform the user about the symmetry of his force pattern, as well as, visual instructions about the way to correct the pattern, when it is asymmetrical.

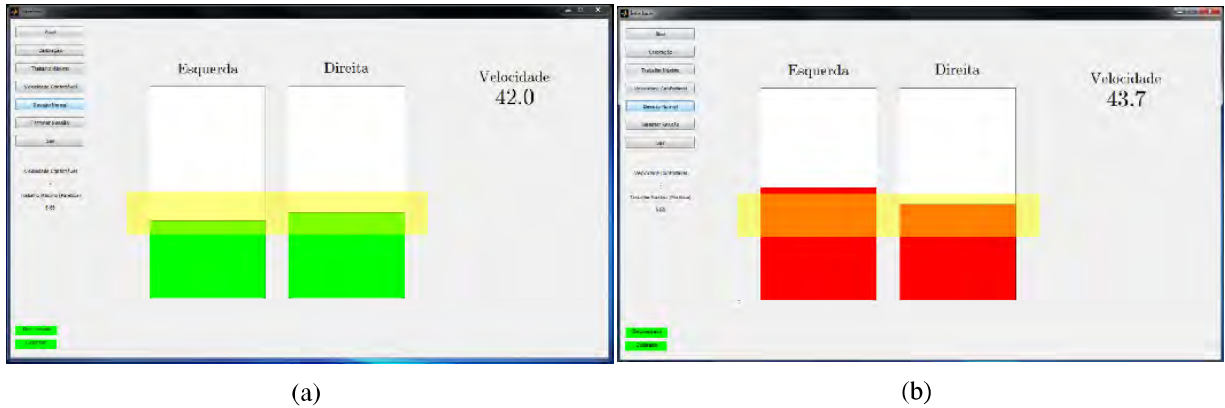


Figure 5.2: Force biofeedback system: (a) green bars represent a symmetrical force pattern and (b) red bars represent an asymmetrical force pattern.

In the work of Ferrante *et al.* [18], the bars were updated whenever a revolution was completed. An identical system was implemented in a preliminary test. However, the subjects reported difficulty to achieve the target band due to the high sensibility of the force measurement system and the low biofeedback frequency. As in this system the values of the bars are updated at the end of each revolution, they only provide the value of net mechanical work (W) of the complete revolution, which results from the difference between the propulsive and resistive forces applied during the revolution. Therefore, the user has difficulty to identify on which cycling phase (downstroke or upstroke) he should change his pedaling strategy to achieve a symmetrical cycling pattern. By receiving biofeedback with a higher frequency, the user may have a faster perception about the effectiveness of his pedaling strategy, for instance, whether he is applying an excess or a shortage of force on the downstroke phase, or if he is applying an excess of resistive force during the upstroke phase. As described in Chapter 2, the biofeedback frequency has already been identified as a probable cause of the reduced effectiveness of a biofeedback therapy in the stroke patients. In addition to the low biofeedback frequency, the high sensibility of the force measurement system increased the difficulty to identify the ideal action to achieve a symmetrical pattern, since the change in the applied force resulted in a considerable change in the bar length, and the subject did not receive instantaneous visual information of the implemented action. Consequently, due to the high sensibility of the force measurement system and the low biofeedback frequency, the W performed by each lower limb during a revolution, might not be the most appropriate condition to define the value of the bars of the force biofeedback system developed in this study. Therefore, new conditions to define the bars values were developed and explored.

To increase the biofeedback frequency, a system that updates the value of the applied work on each 8, 16, 32 or 64 degrees was implemented. During cycling, whenever the defined step value (8, 16, 32 or 64) is achieved, the value of the work performed during that step is added to the bar value, whereas the value of the oldest step is subtracted. The value of the bars is approximately equal to the value of the work applied on the last 360 degrees. All these biofeedback frequency values were tested, nevertheless,

the 8 and 16 values were excluded, since the updating frequency was too high, as the system did not provide enough time for the user to know what to do to achieve a symmetrical pattern.

A second system, which only considers the work performed by each limb during the downstroke phase (half a revolution), was implemented. This system compares the work performed by the lower limb after it ends the downstroke phase, with the work performed by the other limb during its downstroke phase. By using this system the user will receive information about propulsive force applied on the pedals. This system updates the bars on each 180 degrees.

The target band defines the interval of values to define a revolution as symmetrical and successful. The target band includes a superior and an inferior value, which correspond to $\pm 25\%$ of a target value. In the work of Ferrante *et al.* [18], the target value was defined by the maximal work performed by the paretic limb in a 30 seconds trial of active cycling, during which patients were asked to pedal with maximal effort. However, as the force measurement systems are different, the condition to define the target band was slightly changed. Herein, the target value is defined as 75% of the maximal work performed by the non-preferred limb (pushing limb), during 10 revolutions.

A set of tests were conducted in healthy subjects, to assess the effectiveness of force biofeedback in the symmetry during cycling, as described in the following.

5.2.2 Procedure

Six healthy subjects were recruited to test the developed force biofeedback system. The characteristics of the subjects are presented in Table 5.1.

Table 5.1: Mean and standard deviation values of the demographic and anatomical characteristics of the subjects

Age (years)	24.33 (1.61)
Sex (Male / Female)	4 / 2
Height (m)	1.77 (0.06)
Weight (Kg)	71.50 (11.00)
Preferred Foot (Left / Right)	2 / 4
Thigh Length (cm) – trochanter to tibiale	52.17 (2.87)
Shank Length (cm) – tibiale to sphyrion	43.67 (3.66)
Foot Length – heel to tip longest toe	26.50 (0.80)
Distance of the chair to the crank axis (cm)	51.83 (2.87)

All subjects were asked to perform four trials of 2 minutes each, with different biofeedback conditions, in a random order. The workload of the cycling device for all trials was 8 Nm. The subjects were instructed to pedal at the cadence that seemed more indicated to them to achieve the target band, in order to prevent the information overlapping problem, addressed in Chapter 2, since the inexistence of a target cadence avoided the needing of providing two simultaneous feedback types (force and cadence), which might reduce the effectiveness of force biofeedback. The target band was defined in an initial trial of 10 revolutions at 40 rpm. In all trials, where force biofeedback was provided, the subjects were instructed to attempt to keep the two bars on the target band. A rest period of 2 minutes was respected between each trial. The four performed trials were the following:

1. No Biofeedback (NF);

The subjects perform cycling without visual biofeedback of the work applied by each leg.

2. Visual Force Biofeedback Updated on each 32 degrees (F32);

In the second training type, visual force biofeedback, updated on each 32 degrees, is provided to the subjects.

3. Visual Force Biofeedback Updated on each 64 degrees (F64);

This exercise condition is similar to the second, but the biofeedback frequency is lower (updated on each 64 degrees).

4. Visual Force Biofeedback of Half a Revolution (FHR).

In this trial, the subjects perform cycling with biofeedback of the force applied by each limb only during the downstroke phase.

The height of the chair, the position of the subjects, the zero degree of the crank arm and the calibration process, were equal to the study presented in Chapter 4. In addition to the sensors data (effective force (F) and angles values (ϕ and β)), the modified Unbalance Index (U), the number of revolutions of which absolute value of modified Unbalance Index less than or equal to 25%, and the number of revolutions that fulfill the target band, as well as, the cadence data were also analyzed. In this work, given the high sensibility of the force measurement system, a revolution will be considered symmetrical if the absolute value of the Unbalance Index ($|U|$) is less than or equal to 25%. The $|U|$ of a revolution that fulfill the target band condition is always less than or equal to 25%. Therefore, the success of the target band will be determined by the number of symmetrical revolutions ($|U|$ less than or equal to 25%) that achieved the target band. The data of 20 revolutions (21th to 50th), was analyzed for each trial and subject. The first 20 revolutions were not considered in order to ensure a lower deviation on the results.

The Unbalance Index formula, presented in Chapter 2 (equation (2.3)), was changed to provide information about the lower limb that performed more net mechanical work. The value of the modified Unbalance Index (U) is given by (5.1):

$$U = \frac{W_R - W_L}{|W_R| + |W_L|} \times 100 \quad (5.1)$$

where W_L and W_R are the work (equation (3.6)) done by the left and right limb, respectively. The U could range from -100 (the left limb performs all work) to 100 (the right limb performs all work). The U is zero, when the net mechanical work performed by both limbs is equal. A lower $|U|$ corresponds to a higher cycling symmetry.

The modified Unbalance Index (U) underwent descriptive analysis to determine if it was normally distributed and its variances homogeneous. The results show the variable was skewed and thus the cube root transformation of the $|U|$ was used in the analysis. A two-way ANOVA with replication was used to identify the differences of the $|U|$, for the factors trial and subject, and the interaction between the two factors.

The number of revolutions of which absolute value of $|U|$ was less than or equal to 25%, and the number of revolutions that fulfill the target band, in each biofeedback type, were analyzed through a cross tabulation table, in order to assess associations between the biofeedback type and the success of failure of the test conditions.

A Chi-Square test was performed to assess if the type of force biofeedback (factor Trial) and the number of revolutions in which $|U|$ was less than or equal to 25% are associated and if the type of force biofeedback (factor Trial) and the number of revolutions that fulfill the target band condition are associated as well. The effects of the factors and interactions were considered statistically significant when the p-value was < 0.05 .

5.2.3 Results

The mean of the cube root of the absolute values of the Unbalance Index $|U|$, of all healthy subjects, for each type of force biofeedback, are represented in Figure 5.3.

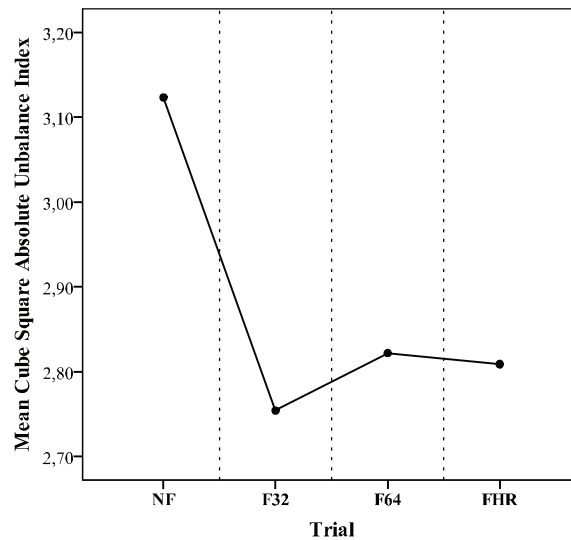


Figure 5.3: Mean of the cube root of the $|U|$, of all healthy subjects, for each type of force biofeedback.

The mean of the cube root of the $|U|$, for each healthy subject and for each type of force biofeedback, are represented in Figure 5.4.

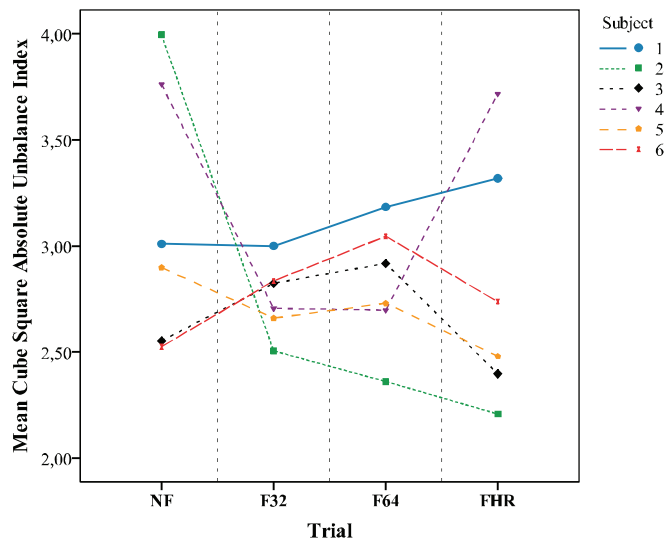


Figure 5.4: Mean of the cube root of the $|U|$ for each healthy subject and for each type of force biofeedback.

The results of a two-way ANOVA with replication of the factors trial and subject, and the interaction between these two factors, on the cube root of the $|U|$, are represented in Table 5.2.

The effect of the two factors and the interaction between the two, on the $|U|$ values, was statistically significant.

Table 5.3 present the cross tabulation of the number of revolutions in which $|U|$ was less than or equal to 25% and that fulfill the target band condition, for each biofeedback trial. In this table are present, for each biofeedback trial (NF, Force Biofeedback Updated on each 32 degrees (F32), Force Biofeedback Updated on each 64 degrees (F64) and Force Biofeedback of Half a Revolution (FHR)), the

Table 5.2: The F ratio values, degrees of freedom (df) and the significance-values (p -value) resulted from a two-way ANOVA with replication of the factor trial and subject, and the interaction between these two factors, on the cube root of the $|U|$

Factor	F	df	p -value
Trial	7.64	3	<0.01
Subject	10.18	5	<0.01
Trial \times Subject	9.50	15	<0.01

observed frequencies (Count), the relative frequencies (% within Trial) and the standardized residuals (Std. Residual).

Table 5.3: Cross tabulation table of the number of revolutions in which $|U|$ less than or equal to 25% and that fulfill the target band condition, for each biofeedback trial

		$ U \leq 25\%$		Total	Within Target Band		Total	
		No	Yes		No	Yes		
Trial	NF	Count	106	74	180	170	10	180
		% within Trial	58.9%	41.1%	100.0%	94.4%	5.6%	100.0%
	F32	Count	78	102	180	142	38	180
		% within Trial	43.3%	56.7%	100.0%	78.9%	21.1%	100.0%
	F64	Count	78	102	180	152	28	180
		% within Trial	43.3%	56.7%	100.0%	84.4%	15.6%	100.0%
	FHR	Count	78	102	180	137	43	180
		% within Trial	43.3%	56.7%	100.0%	76.1%	23.9%	100.0%
	Total	Count	340	380	720	601	119	720
		% within Trial	47.2%	52.8%	100.0%	83.5%	16.5%	100.0%

Based on the values of the standardized residuals, it can be inferred that the trial without force biofeedback (NF) is more associated with the failing of the tested conditions (higher standardized residual in the **No** column). In addition, the FHR is the trial more associated with the fulfillment of the target band (higher standardized residual in the **Yes** column).

The results of the Pearson Chi-Square test for each tested condition ($|U|$ less than or equal to 25% and within the target band condition) are represented in Table 5.4.

Table 5.4: Results of the Pearson Chi-Square test for each for the tested conditions ($|U|$ less than or equal to 25% and within the target band condition)

Pearson Chi-Square			
Condition	Value	df	p -value
$ U \leq 25\%$	13.10	3	<0.01
Within Target Band	25.64	3	<0.01

Based on Pearson Chi-Square tests, it is possible to conclude that there was an association between the type of force biofeedback (Trial) and the number of revolutions in which $|U|$ was less than or equal to 25%, as well as, between the type of force biofeedback (Trial) and the number of revolutions that fulfill the target band condition.

The number of revolutions in which $|U|$ was less than or equal to 25% and that fulfill the target band condition, for each type of force biofeedback, are presented in Figure 5.5 (a) and (b), respectively. The white bars represent the number of revolutions in which the condition was not achieved, and black ones represent the number of revolutions where the condition was met.

The plots of Figure 5.6 display the mean values of the effective force for the pushing and coordination limbs (solid red and dashed green lines, respectively), for cycling without biofeedback NF (Figure 5.6 (a))

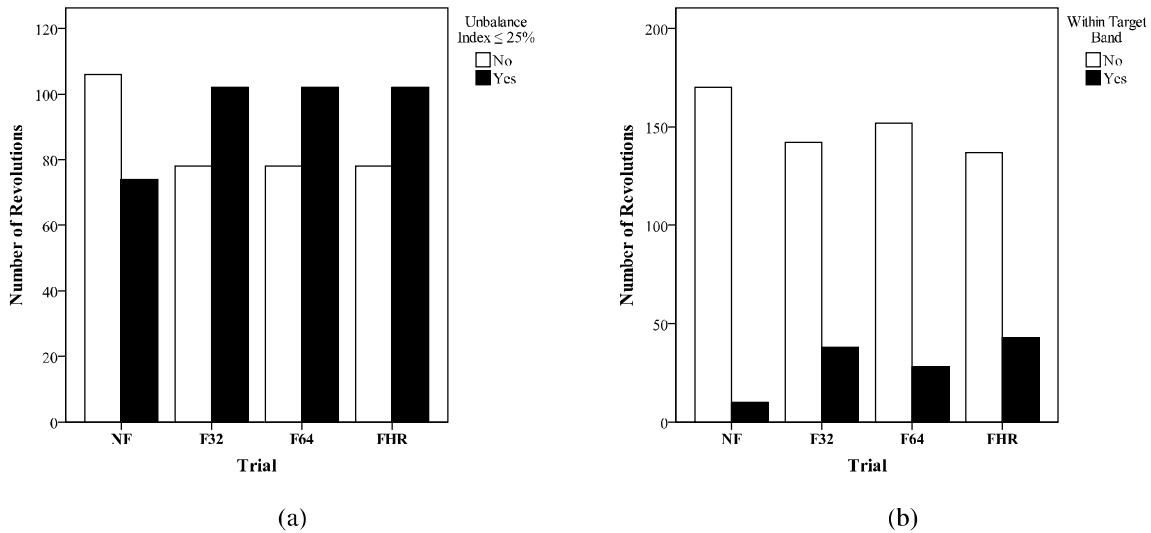


Figure 5.5: Number of revolutions where, for each trial of force biofeedback, (a) the $|U|$ was less than or equal to 25%; and (b) the target band condition was fulfilled. The white bars represent the number of revolutions in which the conditions were not achieved, and black ones represent the number of revolutions where the conditions were met.

and with force biofeedback F32, F64 and FHR (Figure 5.6 (b), (c) and (d), respectively), of the subject 5, with respect to crank angle. The grey area represents the upstroke phase of the pushing limb and the shaded area along the curves represents the standard deviation values. Although data was recorded for six subjects, to better describe the observed results, detailed analysis of the force applied by subject 5 is presented. The force patterns of the others subjects were similar to this subject.

5.2.4 Discussion

The provision of force biofeedback resulted in a higher cycling symmetry (lower absolute Unbalance Index), as shown in Figure 5.3. The biofeedback type affects significantly the $|U|$, as shown in Table 5.2. Visual force biofeedback updated on each 32 degrees (F32) was the training type where higher symmetry was achieved. The success of force biofeedback of half a revolution (FHR) and of force biofeedback updated on each 64 degrees (F64) was similar, as shown in Figure 5.3.

The subjects' response to each force biofeedback trial was different, as shown in Figure 5.4. Two subjects (1 and 6) presented the lowest $|U|$ value in the NF trial, meaning these subjects did not adapt to the force biofeedback's training conditions, since the provision of force biofeedback resulted in higher asymmetry. This higher asymmetry may be caused, for instance, by the fact that the target band is not the most appropriate. Thus, the pedaling strategy adopted by these subjects, in order to attempt to achieve the target band, resulted in a higher asymmetry, contrarily to the desired. The other subjects presented a lower $|U|$ in, at least, one biofeedback type, which suggests that biofeedback of the force applied by each limb can improve the cycling symmetry.

Table 5.3 shows that cycling without force biofeedback (NF) tends to be more associated with the failure of the tested conditions ($|U|$ value less than or equal to 25% and bars within the target band). The number of revolutions where the $|U|$ was less than or equal to 25% were the same for the three types of force biofeedback. However, the $|U|$ values of the remaining revolutions were lower in the F32, when compared to the F64 and FHR trials, which suggests F32 is the most effective biofeedback type to achieve a symmetrical cycling. The Table 5.3 and Figure 5.5 (black bars) show FHR is the trial most

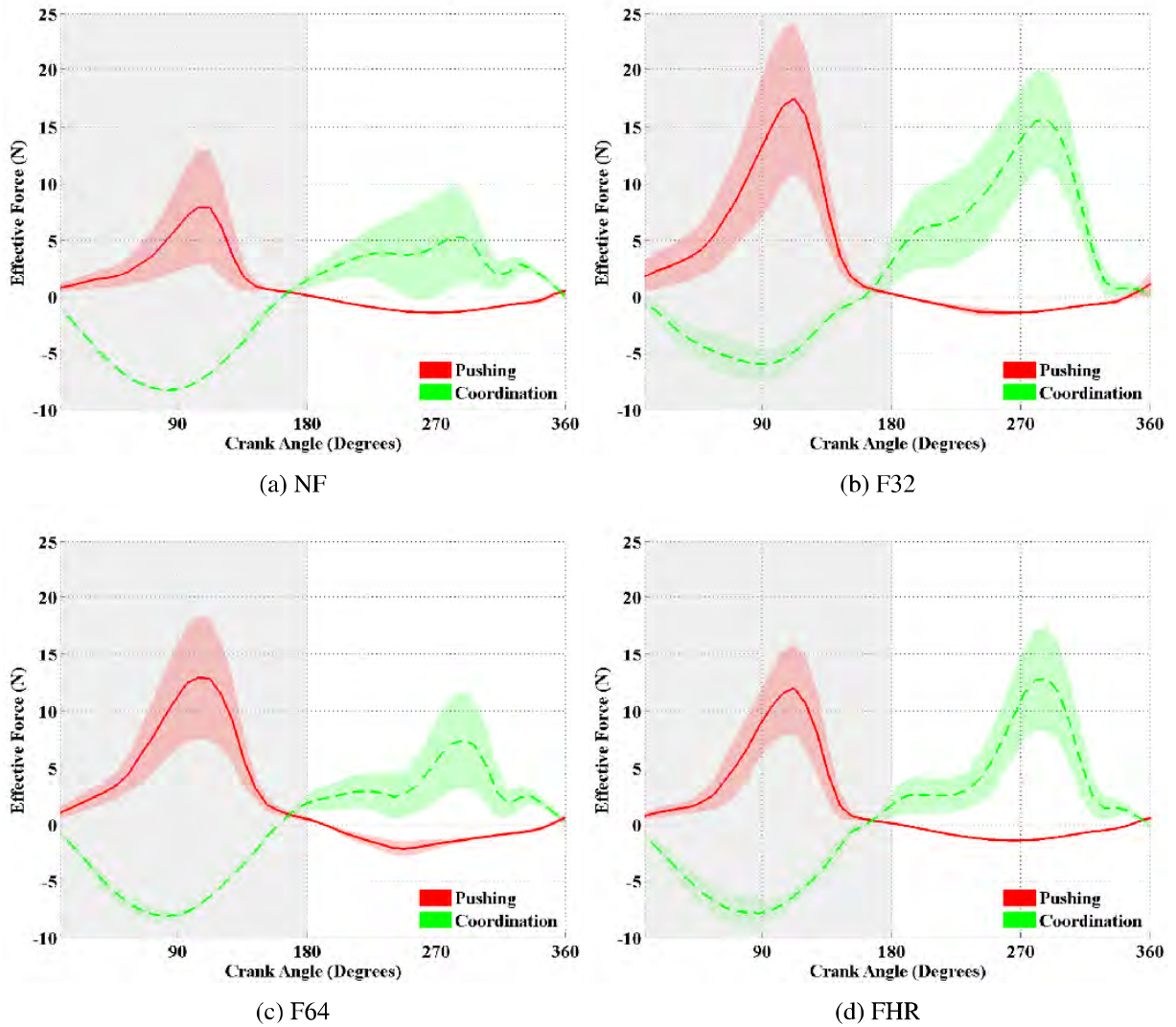


Figure 5.6: Mean values of the effective force for the pushing and coordination limbs (solid red and dashed green lines, respectively), for cycling (a) without force biofeedback (NF); and with force biofeedback (b) updated on each 32 degrees (F32); (c) updated on each 64 degrees (F64); and (d) of half a revolution (FHR), at 8 Nm, for thirty revolutions (21th to 50th revolution) of the subject 5. The grey area represents the upstroke phase of the pushing limb and the shaded area along the curves represents the standard deviation values.

associated to the achievement of the target band. The easier achievement of the target band in the FHR trial maybe due to the value of the bars being defined solely by the amount of force applied, during the downstroke phase.

By comparing the number of revolutions where $|U|$ is less than or equal to 25% with the number of revolutions where the target band is achieved (black bars – Figure 5.5 (a) and (b), respectively), it is clear that only a small number of symmetrical revolutions ($|U|$ less than or equal to 25%) achieved the target band. This suggests the condition to define the target band may not have been the most appropriate for healthy subjects. Instead of using 75% of the pushing leg’s work as reference, the use of the work performed by the limb with the coordination function might be more appropriate. A new target band was defined for each type of force biofeedback, which may influence the obtained results, since the target band differed between trials, for the same subject.

Figure 5.6 shows the effective force pattern of both lower limbs of subject 5, in the four trials (NF, F32, F64 and FHR). The effective force pattern of the trials NF and F64 ((Figure 5.6 (a) and (c), re-

spectively) present a similar behavior. In these two trials, the pushing limb performed more propulsive force than the coordination limb, during their downstroke phases. The higher force of the pushing limb, during its downstroke phase, may be related with the higher resistive force applied by the coordination limb, during its upstroke phase. The F64 had the higher $|U|$ of the three force biofeedback types. The lower success of this trial may be related to its biofeedback frequency, which may not be high enough to induce changes in the user's pedaling strategy. In addition to the lowest values of $|U|$, the effective force pattern of the F32 trial (Figure 5.6 (b)) is also the most symmetrical of the four biofeedback types, which suggests that this type as the most effective in the increasing of the cycling symmetry. The propulsive and resistive forces applied by each lower limb were similar, moreover, the amount of resistive force was the lowest of the four biofeedback types. The higher success of this biofeedback type may be due to the higher biofeedback frequency, since the bars are updated 11 times on each revolution, whereas the bars of the F64 and the FHR are updated only 5 and 2 times, respectively. In the FHR (Figure 5.6 (d)), the amount of propulsive force applied by each limb is similar, which was the objective of this biofeedback type. However, the effective force pattern in this biofeedback type was not symmetrical, since the coordination limb performed quite more resistive force than the pushing limb. This asymmetry is not reflected in the $|U|$ values because, in this trial, only the work applied during the downstroke phase is used to compute the index.

FHR, despite having the best results on the achievement of the target band, only enhances the amount of the force applied by each limb during the downstroke phase. This may improve the muscle strength of the weaker limb, by equating the work performed by each limb. However, this solution does not improve the coordination of both limbs during the different phases of cycling, as opposed to the F32 or F64 biofeedback types. In these types, the value of the bars is defined by the net mechanical work (W) performed during the two phases of cycling. Therefore, they promote an increase of the propulsive force applied by the weaker limb, during the downstroke phase, as well as, a reduction of the resistive force, during the upstroke phase. However, in these training types, a revolution may be wrongly considered symmetrical, since a limb that applies much propulsive force during the downstroke phase, but also applies much resistive force in the following phase, could have the same net mechanical work (W) as a limb that performs a normal propulsive force and little resistive force.

The results show that the provision of force biofeedback resulted in a higher cycling symmetry, more revolutions with $|U|$ less than or equal to 25% and more revolutions that achieved the target band. Therefore, this system and some of these conditions will be tested in stroke patients, to study the same parameters, and the effects of force biofeedback and cycling in the walking capacity.

5.3 EMG Biofeedback

As previously indicated, inappropriate muscle contraction between the agonist and antagonist, muscle spasticity with limited ranges of motion (ROM), and abnormal synergistic muscle activity patterns are some of the causes of the asymmetrical limbs function. Several studies have identified EMG pattern abnormalities in stroke patients with motor impairments [26,28,30,30,48]. The specificity of information about muscle activation and the speed at which the information is provided to the patients are, according to Wolf *et al.* [65], the unique attributes of EMG biofeedback. Some reviews about the application of EMG biofeedback in stroke patients [4, 65, 105, 106] reported improvements in specific parameters of impairment, such as muscle strength, ROM and reduction of muscle tone, but reported a failure of EMG

biofeedback therapies on the generalization to functional improvements.

A review of Van Peppen *et al.* [105] reported that patients benefit from exercise programs in which functional tasks (ADLs) are intensively trained, whereas impairment-focused programs, such as muscle strengthening, biofeedback and neuromuscular or transcutaneous nerve stimulation, generally, only improve the addressed impairment, failing to transpose these improvements in the ADLs. The combination of an impairment-focused therapy, EMG biofeedback, with a task-oriented exercise, cycling, may enhance the recovery of functional tasks' abilities. Therefore, it is hypothesized that providing biofeedback related with the activity of the muscles that have a major role in gait and in cycling exercise, together with a predefined target pattern that the patient should follow, may help the rehabilitation process, by stimulating the muscles that are related with the motor impairments, while performing a functional task.

There are issues that need to be explored before the recommendation of cycling and EMG biofeedback as a stroke rehabilitation therapy. The first step is the selection of the muscles that will be addressed, which should be based on their importance on the ADLs, as well as, their impact and contribution on the general motor impairments. In this study, as specified in Chapter 4, the addressed muscles are the *rectus femoris*, *tibialis anterior* and *gastrocnemius medialis*. The second step is to study the influence of the EMG biofeedback in the pedaling strategy and training variables, which include the training workload and cadence, the force applied in the pedals, the angle of the pedals, the net contribution of each limb to the movement, the symmetry of the force pattern and the muscle activation. This will allow, for instance, to analyze whether the forces applied by the paretic and healthy limbs respond to the EMG biofeedback and influences the cycling symmetry. And lastly, explore the existence of functional improvements, such as the locomotor abilities, as a result of cycling with EMG biofeedback training.

5.3.1 EMG Biofeedback Experimental Setup

Electromyography biofeedback was studied using the *YSY EST EVOLUTION* device (Chapter 3). The EMG biofeedback system is comprised of 6 components: the subject, the cycling device equipped with the sensors, the acquisition board, the *Data PC*, the *YSY EST EVOLUTION* device, and the EMG biofeedback *Display*. The experimental setup of this system is illustrated in Figure 5.7.

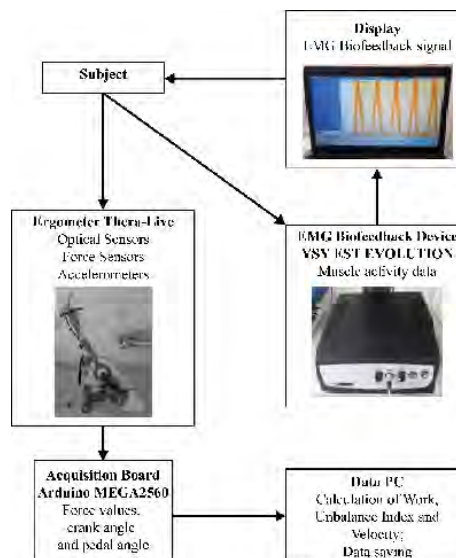


Figure 5.7: Experimental setup used for the EMG Biofeedback intervention.

The functions performed by the sensors instrumented on the cycling device, by the acquisition board and by the *Data PC* are the same as the functions described in the force biofeedback experimental setup. Nevertheless, the *Data PC* only proceeds to the computation of the variables and to the data saving. The *YSY EST EVOLUTION* device reads the electrical activation pattern of the selected muscle through three surface electrodes placed on the user. The EMG biofeedback signal, as well as, the target signal are provided to the user through the *Display* (Figure 3.14). The user has to attempt to make the muscle's activation pattern to follow the target signal.

Although, according to the user's manual and as described in Chapter 3, the minimum time required for the signal to travel from the beginning to the end of the display (complete passage) in the faster mode is 1 second. However, the minimum time of the available device was approximately 5 seconds. As the muscle's activation patterns of the studied muscles, presented in Chapter 4, follow approximately a triangular shape, two target signals were considered, as shown in Figure 5.8.

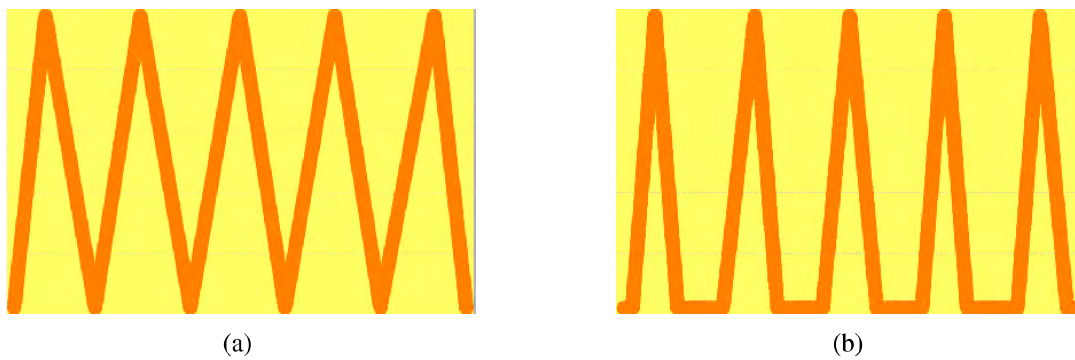


Figure 5.8: Designed target signals: **(a)** triangular wave and **(b)** triangular 50% duty cycle wave.

Due to the minimum time limitation of the *YSY EST EVOLUTION* device, one complete passage will correspond to five revolutions in the cycling device, as shown in Figure 5.8 (five signal peaks). The target signal with five peaks was the one that represented the best relation between the signal velocity and the display size. These two target signals were tested by healthy subjects on the selected muscles. The triangular 50% duty cycle (Figure 5.8 (b)) wave was the one that was best followed by the healthy subjects. Therefore, this wave was selected as the target signal of the EMG biofeedback system, since it was the one that best represented the muscles' activation patterns.

The user should maintain a constant cadence to synchronize the cycling and the signal of the muscle's activation pattern with the target signal. Therefore, due to the target signal (five signal peaks) and the time limitations (signal velocity) of the device, the available cadences for the EMG biofeedback training are presented in Table 5.5. To each signal velocity (complete passage time – time for the signal to travel from the beginning to the end of the display) will correspond a training cadence that the users will have to attempt to keep constant.

Table 5.5: EMG biofeedback training cadences (rpm) for each complete passage time (s)

Complete Passage Time (s)	Cadence (rpm)
5	60
6	50
7	42.86
8	37.50
9	33.33
10	30

To synchronize the cycling and the signal of the muscle's activation pattern with the target signal, the

use of auditory feedback of the speed was studied. However, this idea was dropped due to the possible overloading of information. Therefore, the user will have to synchronize, visually, the moment of higher muscle activation with the peaks of the target signal. By doing it, the cadence will be kept approximately constant.

This system was tested in healthy subjects to analyze the interaction of the subjects with the EMG biofeedback and the behavior of some variables in different muscles and conditions.

5.3.2 Procedure

Five healthy subjects (Table 5.6) were recruited to test the developed system.

Table 5.6: Mean and standard deviation values of the demographic and anatomical characteristics of the subjects

Age (years)	23.00 (1.55)
Sex (Male / Female)	3 / 2
Height (m)	1.74 (0.05)
Weight (Kg)	70.80 (12.42)
Preferred Foot (Left / Right)	1 / 4
Thigh Length (cm) – trochanter to tibiale	57.40 (1.85)
Shank Length (cm) – tibiale to sphyrion	42.60 (3.44)
Foot Length – heel to tip longest toe	26.80 (1.33)
Distance of the chair to the crank axis (cm)	49.00 (5.14)

All subjects were asked to perform 9 trials of 2 minutes with EMG biofeedback (EMG Biofeedback (EMGF)) of the *rectus femoris*, *tibialis anterior* and *gastrocnemius medialis*, of the subjects' pushing limb. For each muscle, the subjects performed a trial with different workloads (0, 4 and 8 Nm). The subjects were instructed to pedal at approximately 43 rpm (passage time of 7 seconds), while attempting to make the muscle's activation pattern follow the target signal. A rest period of 2 minutes was respected between the each trial. In addition, the subjects performed a trial without EMG biofeedback (NF) at 43 rpm and 8 Nm, in which the muscle activation pattern was recorded during 2 minutes.

The electrodes used in this trials were the *Dura-Stick Plus 2in Square*. The electrodes position and the recommendations for the EMG signal acquisition (Surface Electromyography for the Non-Invasive Assessment of Muscles (SENIAM)'s recommendations [107]), are presented in Appendix C.

The height of the chair, the position of the subjects, the zero degree of the crank arm and the calibration process, were equal to the previous studies.

In addition to the sensors data (force F_p and angles values (ϕ and β)), the values of the net mechanical work (W – equation (3.6)) applied by each limb were analyzed. Regarding EMG biofeedback, the sensibility and the average activation values, provided by the *YSY EST EVOLUTION* device, were used to compute one metric, which was defined in this work, to compare the results within conditions and subjects. The Muscle Activation Rate (MAR) is defined by the ratio between the average activation value and the sensibility value. The data of 30 revolutions (31th to 60th) was analyzed for each trial and subject. The data of first 30 revolutions was not considered in order to ensure a lower deviation on the results.

The MAR and the W performed by the pushing and coordination limbs, for each muscle, underwent descriptive analysis to determine if they were normally distributed and its variances homogeneous. Two-way ANOVAs were used to analyze the effects of the factors (workload and subject), on each variable (MAR, W pushing limb and W coordination limb) and for each of the three muscles. The effects of the factors and interactions were considered statistically significant when the p-value was < 0.05 .

5.3.3 Results

Although data was recorded for five subjects, to better describe the observed results, a detailed analysis of the variables of subject 5 is presented. The variables' variation for the others subjects was largely similar to subject 5.

The mean muscle's activation patterns, of the *rectus femoris*, *gastrocnemius medialis* and *tibialis anterior*, of subject 5, with and without EMG biofeedback (EMGF and NF, respectively), are presented in Figure 5.9, Figure 5.10 and Figure 5.11, respectively.

The results of two-way analyses of variance (ANOVAs) of the effects of workload and subject, on the MAR and on the W performed by the pushing and coordination limbs, for each muscle, are represented in Table 5.7.

Table 5.7: The F ratio values, degrees of freedom (df), the significance-values (p -value) resulted from two-away ANOVAs of the effects of the workload and subject, on the MAR and on the W performed by the pushing and coordination limbs variables, for each muscle

Muscle	Factor	Variable	F	df	p -value
Rectus Femoris (RF)	Workload	MAR	5.97	2	0.026
		W - Pushing Limb	3.08	2	0.102
		W - Coordination Limb	2.32	2	0.160
	Subject	MAR	3.70	4	0.055
		W - Pushing Limb	1.02	4	0.450
		W - Coordination Limb	3.97	4	0.046
Gastrocnemius Medialis (GM)	Workload	MAR	1.60	2	0.261
		W - Pushing Limb	12.19	2	<0.01
		W - Coordination Limb	1.53	2	0.274
	Subject	MAR	3.15	4	0.078
		W - Pushing Limb	9.62	4	<0.01
		W - Coordination Limb	0.61	4	0.665
Tibialis Anterior (TA)	Workload	MAR	1.98	2	0.201
		W - Pushing Limb	1.94	2	0.206
		W - Coordination Limb	2.69	2	0.128
	Subject	MAR	4.49	4	0.034
		W - Pushing Limb	0.72	4	0.600
		W - Coordination Limb	2.95	4	0.090

The effect of the workload was statistically significant only on the MAR of the *rectus femoris* (RF). Regarding the subject factor, its effect was statistically significant on the MAR and W performed by the coordination limb of the RF; on the W performed by the pushing limb of the *gastrocnemius medialis* (GM); and on the MAR of the *tibialis anterior* (TA).

The mean values of the MAR of all healthy subjects, for the three workload values and for the three analyzed muscles, are presented in Figure 5.12. The *rectus femoris* (RF), *gastrocnemius medialis* (GM) and *tibialis anterior* (TA) curves are represented the solid red, dotted green and dashed blue lines, respectively.

The mean values of the net mechanical work (W) for the pushing and coordination limbs (solid red and dashed green lines, respectively), of all healthy subjects, for the three workload values and the three analyzed muscles (*rectus femoris* RF, *gastrocnemius medialis* GM and *tibialis anterior* TA), are presented in Figure 5.13.

The mean values of the effective force for the pushing and coordination limbs (solid red and dashed green lines, respectively), for the *rectus femoris*, *gastrocnemius medialis* and *tibialis anterior*, of the subject 5, are presented in Figure 5.14. The grey area represents the upstroke phase of the pushing limb and the shaded area along the curves represents the standard deviation values.

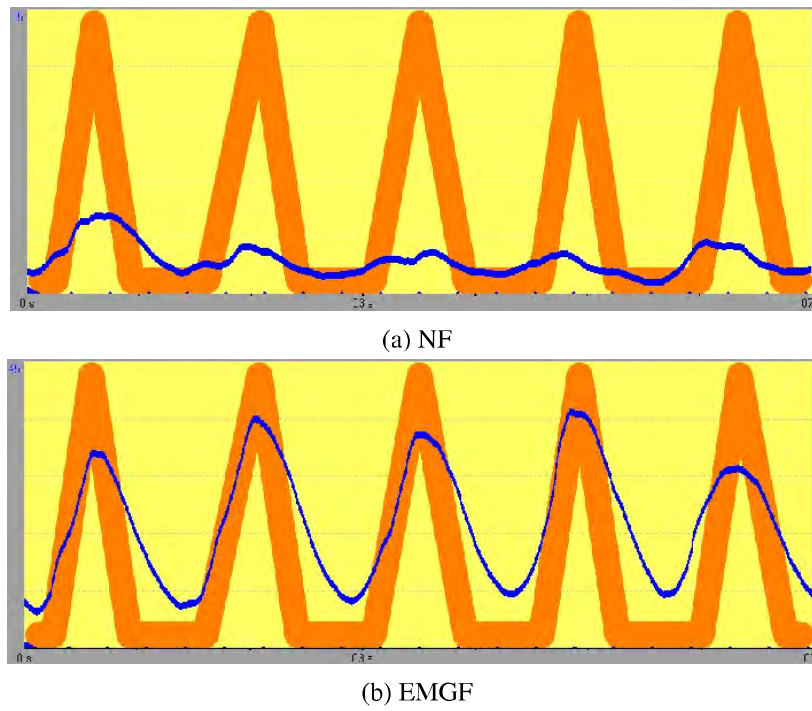


Figure 5.9: *Rectus femoris*' mean activation pattern (a) without EMG biofeedback and (b) with EMG biofeedback, at 43 rpm and 4 Nm, for subject 5.

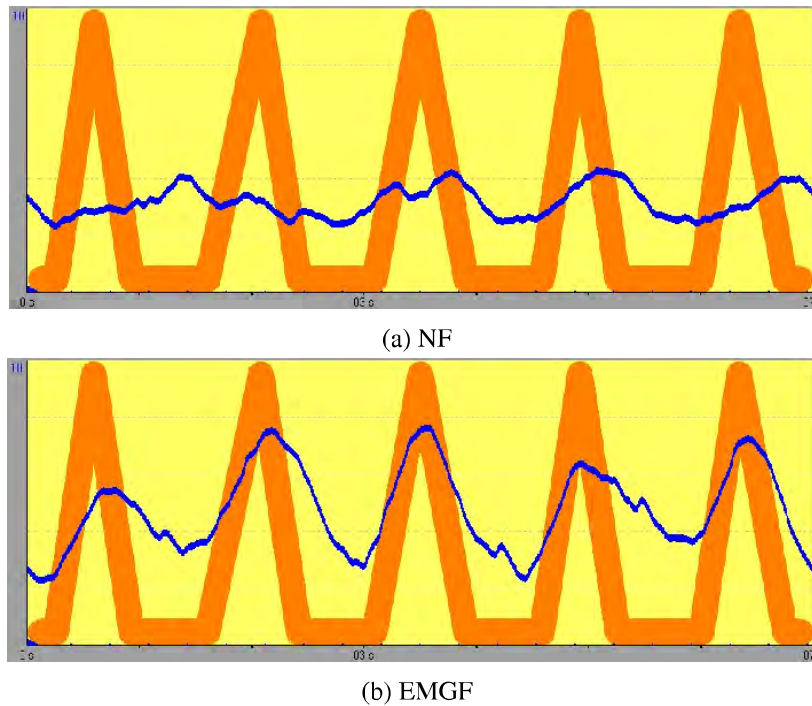


Figure 5.10: *Gastrocnemius medialis*' mean activation pattern (a) without EMG biofeedback and (b) with EMG biofeedback, at 43 rpm and 4 Nm, for subject 5.

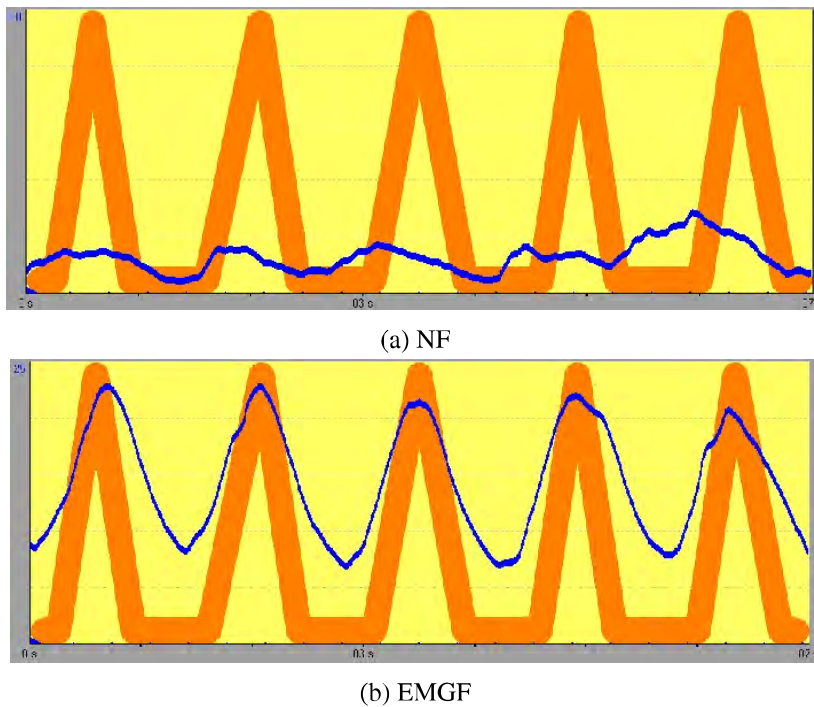


Figure 5.11: *Tibialis anterior*' mean activation pattern (a) without EMG biofeedback and (b) with EMG biofeedback, at 43 rpm and 4 Nm, for subject 5.

5.3.4 Discussion

The subjects were capable of controlling the activation of the three studied muscles (*rectus femoris*, *gastrocnemius medialis* and *tibialis anterior* – RF, GM and TA, respectively), while cycling with the provision of EMG biofeedback. The angles of activation were similar to the patterns of activation reported in the literature, as shown in Figure 4.4. Due to *YSY EST EVOLUTION* restrictions, the activation moments cannot be shown. However, it was visually observed the RF was activated on the second half of the upstroke phase and in transition between the upstroke and downstroke phases. The TA was activated mainly in the first half of the of the upstroke, slightly early than the observed in the standard bicycle, since due to the semi-recumbent devices' training configuration, the foot starts the dorsiflexion in the beginning of the upstroke phase. The activation moment of the GM was similar to the pattern observed in the literature. However, as during training in a semi-recumbent device the foot plantarflexion is reduced, the activation of GM was the one which promoted the most unnatural movements.

The plots of Figure 5.9, Figure 5.10 and Figure 5.11 present the muscle activation of the RF, GM and TA, respectively, without and with the provision of EMG biofeedback (NF and EMGF, respectively). With EMGF, the subject increased the muscle activation value and was able to follow the target signal. The off regions of the target signal were not perfectly followed, the subject was not able to fully relax the muscle, which may be due to the high training speed. The sensibility values for the RF and TA had to be reduced, in the NF trial, in order to adjust the signal scale to the measured muscle activation, since it was lower than the one achieved during the EMGF trials. These results suggest EMG biofeedback increases muscle activity and allows the synchronization of the training cadence with the device operation timings.

The Muscle Activation Rate (MAR – Figure 5.12) and the work (W) applied by the “pushing” and “coordination” limbs (Figure 5.13) increased with the increase of the workload. As observed in Chapter 4, the application of more propulsive force (more net mechanical work W) is required to maintain a con-

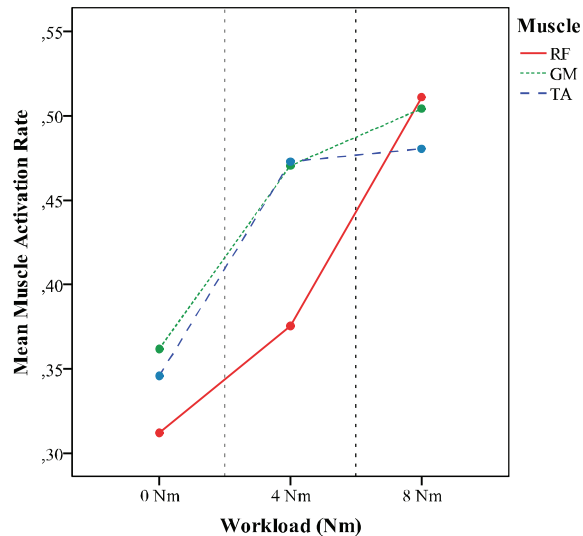


Figure 5.12: Mean values of the MAR of all healthy subjects, for the three workload values (0, 4 and 8 Nm) and for the three analyzed muscles (*rectus femoris*, *gastrocnemius medialis* and *tibialis anterior*). The *rectus femoris* (RF), *gastrocnemius medialis* (GM) and *tibialis anterior* (TA) curves are represented the solid red, dotted green and dashed blue lines, respectively.

stant cadence in a higher workload. Higher MAR is observed for a higher workload, which is consistent with Hug *et al.* [92], who reported an increased EMG activity level as the workload increased. However, the increase of MAR with the workload increase was only statistically significant for the RF (Table 5.7). Regarding the work performed by the pushing limb, only the increase in the GM was statistically significant, with the workload increase, as shown in Table 5.7.

The difference on the net mechanical work (W) applied by each limb is greater in GM, as shown in Figure 5.13. In this muscle, the analyzed limb (pushing limb) performed more W than the other limb, whereas in the RF and TA, the coordination limb performed more work. As the GM activation occurs during the downstroke phase, the users might have applied more force with the analyzed limb to increase the muscle activation and follow the target signal, which increased the difference of the force applied by each limb, as shown in Figure 5.14 (b). On the other hand, as the activation of the RF and the TA occurs, mainly during the upstroke phase, the users might have applied more upward force with the pushing leg, which cannot be measured with the installed sensors. Therefore, in these two muscles the limb that applied more positive effective force was not the analyzed limb, as shown in Figure 5.14 (a) and Figure 5.14 (c).

The learning period for EMG biofeedback is longer than for the force biofeedback, since the user has to understand how, when and where the trained muscle is activated. By attempting to activate the target muscle, the movement performed to increase the muscle activation produces involuntarily higher downward or upward force, which increases the training cadence. Then, due to the higher speed, the muscle activation peak will not match with the respective target signal's peak. This issue complicates the synchronization of the training cadence with the *YSY EST EVOLUTION* operation timings and the target signal. The transition of one passage to the next (on each 5 revolutions) may confuse the subjects, resulting in a desynchronization of the muscle activation with the target signal. The electrodes condition might have also influenced the obtained muscle activation signal. In addition, in the male subjects, the area where the electrodes were placed was not shaved, which may have also influenced the acquired signal.

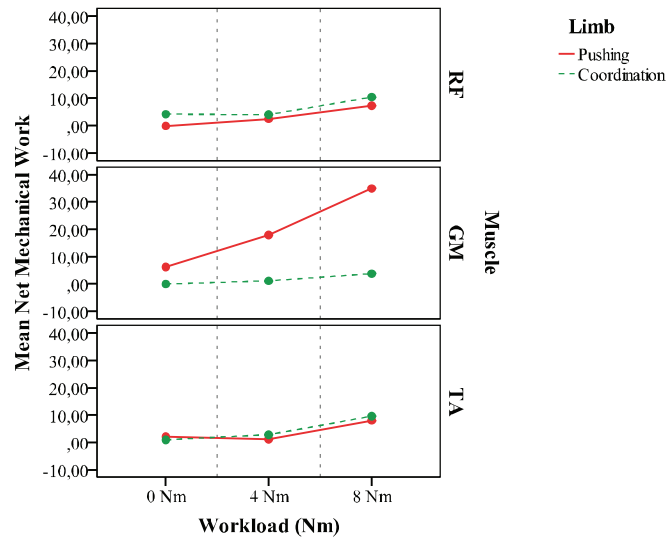


Figure 5.13: Mean values of the net mechanical work, for the pushing and coordination limbs (solid red and dashed green lines, respectively), of all healthy subjects, for the three workload values (0, 4 and 8 Nm) and for the three analyzed muscles (*rectus femoris* (RF), *gastrocnemius medialis* (GM) and *tibialis anterior* (TA)).

The results show that the provision of EMG biofeedback resulted a higher muscle activity and allowed the synchronization of the training cadence and the muscle activation pattern with the target signal. The muscle activation pattern and the work performed by each limb were higher with the increase of the workload. The force pattern of the analyzing limb changed with the region activation of the analyzed muscle. Therefore, this system and some of these conditions will be tested in stroke patients, to study the effects of EMG biofeedback together with cycling in the training variables and in the walking capacity.

5.4 Conclusions

The effects of providing force and EMG biofeedback together with cycling exercise on the exercise variables were explored in this chapter.

In force biofeedback, the net mechanical work (W) performed by each limb was provided to the users in the form of two bars. The users had to attempt to keep the two bars on a target band. Healthy subjects tested this system in four different biofeedback conditions: (1) no biofeedback (NF); (2) force biofeedback updated on each 32 degrees (F32); (3) force biofeedback updated on each 64 degrees (F64); and (4) force biofeedback of the downstroke phase, exclusively (FHR). Providing force biofeedback, resulted in a higher cycling symmetry (lower $|U|$). The force biofeedback updated on each 32 degrees, had the lowest $|U|$ values and the most symmetrical effective force pattern.

The results suggest that the force biofeedback system provides a simple and intuitive way to inform the user about his cycling symmetry, since the healthy subjects were able to reduce the asymmetry of the force applied by each limb, during cycling exercise. Although the condition to define the target band may not have been the most appropriate, the provision of an objective allows the users to have a visual reference to achieve the training objective (a more symmetrical cycling). Therefore, the target band should continue to be used. In addition, the users changed their pedaling strategy when force biofeedback was provided, especially in the F32 and FHR. The biofeedback in the F32 trial appears to be the most appropriate, whereas the target band was achieved more times in the FHR trial. Therefore, these two biofeedback types should be further explored in stroke patients, in order to compare whether a

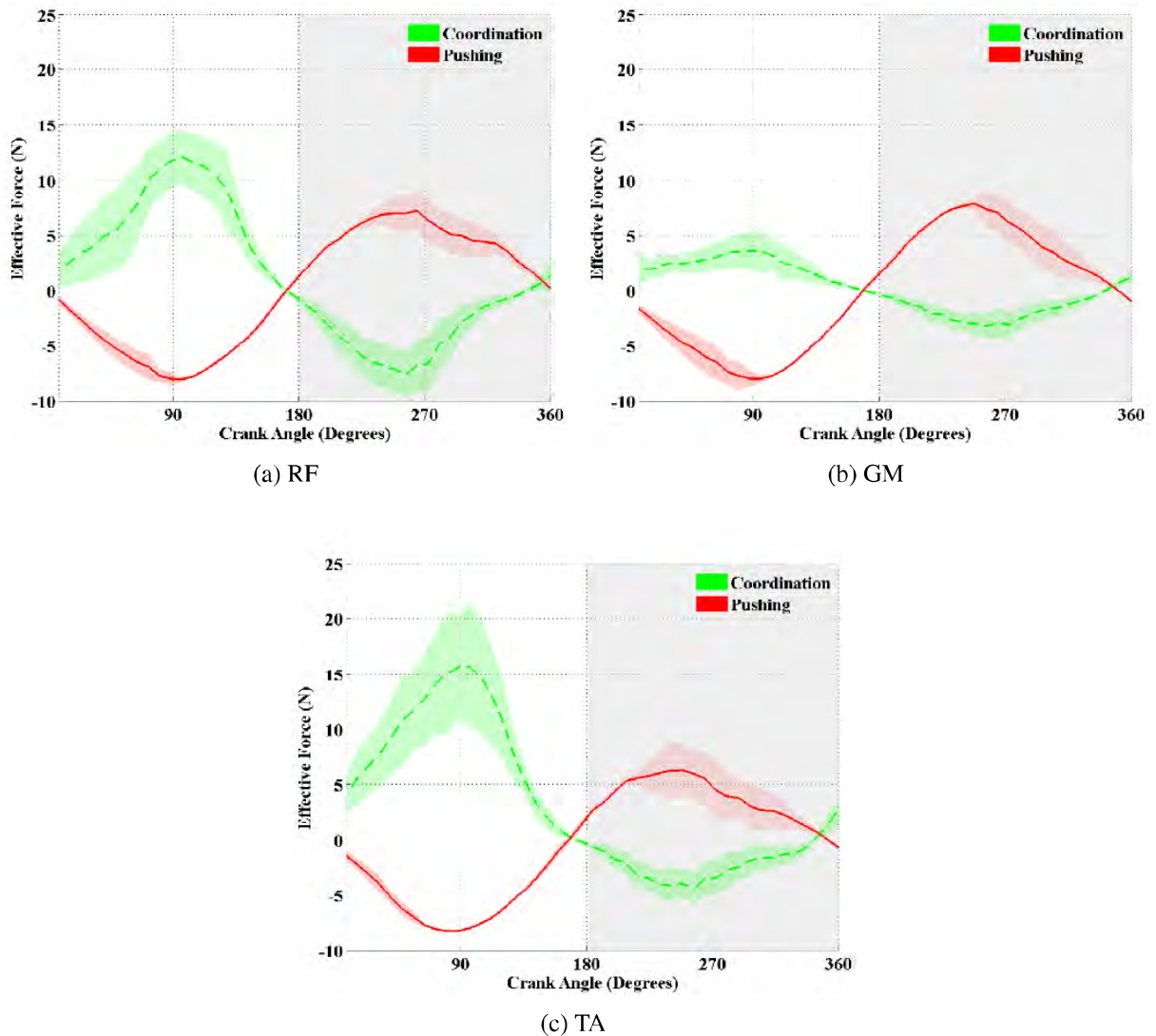


Figure 5.14: Mean values of the effective for the pushing and coordination limbs (solid red and dashed green lines, respectively), for the (a) *rectus femoris*, (b) *gastrocnemius medialis* and (c) *tibialis anterior*, at 43 rpm and 4 Nm, for thirty revolutions (31st to 60th revolution) of the subject 5. The grey area represents the upstroke phase of the pushing limb and the shaded area along the curves represents the standard deviation values.

trial that implies the coordination of both limbs (F32), but that may be more complex, results in higher improvements than a trial that only promotes the increase of the amount of applied force (FHR). These results provide evidence that the test should be performed on stroke patients and a positive answer to #RQ4 is to be expected, since force biofeedback changed the user's pedaling strategy and improved the cycling performance.

Regarding EMG biofeedback, the effects of providing the muscle's activation pattern, of the *rectus femoris*, *gastrocnemius medialis* and *tibialis anterior*, to healthy subjects, were studied. The *YSY EST EVOLUTION* device was used to provide biofeedback of the EMG signal. The users had to attempt to follow a predefined target signal, while training in the cycling device at a pre-defined cadence. The provision of EMG biofeedback resulted in a higher muscle activation and in a synchronization between the training cadence and the muscle activation pattern with the target signal. The angles of muscle activation were similar to the angles reported in the literature. The use of EMG biofeedback influenced the W applied by each limb. The analyzed limb (pushing limb) performed statistically significant more

W than the other one for the GM, suggesting the users performed more force to increase the muscle activation. In RF and TA the analyzed limb performed less W than the other limb. However, although the difference was not statistically significant, it may be due to the activation phase occurring during the upstroke phase.

The results of providing EMG biofeedback suggest that the selected muscles contribute to the cycling movement. However, the provision of the muscle activation pattern of the GM, during cycling in a semi-recumbent device, might promote unnatural movements. The users were able to synchronize the muscle activation pattern with the target signal, thus it should also be used in the stroke patients. The training variables were influenced by the biofeedback and the training conditions (workload), which suggest that the user's pedaling strategy is changed when EMG biofeedback is provided. Providing EMG biofeedback to stroke patients will allow to explore the influence of this biofeedback type on the participation of paretic limb in the movement and, more important, the effects of use this therapy on the rehabilitation of the motor function of stroke patients. As EMG biofeedback also changed the user's pedaling strategy and improved the cycling performance, the test should also be performed on stroke patients and a positive answer to #RQ4 is to be expected.

Both types of biofeedback promoted an improvement of the training variables, by increasing the cycling symmetry or the muscles activation. The next step includes to test whether these improvements are also observed in stroke patients and assess if an intervention of force or EMG biofeedback together with cycling is reflected in improvements in the locomotor abilities of stroke patients.

Study Design and Case Studies

6.1 Introduction

To assess the effectiveness of a therapy in the rehabilitation of an impairment, is crucial to perform studies with patients of the target disorder. Therefore, in this chapter will be presented the key aspects of the study design that will be implemented in stroke patients.

The objectives of this study are the assessment of whether the application of force or EMG biofeedback has influence on the users' pedaling strategy, on the training variables and, the most important, if either one of the therapies results in improvements on the stroke patients' locomotor abilities. An intervention with both therapies will be implemented to stroke patients. The effects of each therapy on the cycling performance will be assessed by comparing the training variables, such as, the applied effective force (F), the pedal angles (β , Unbalance Index (U) and muscle activation, during cycling without and with each type of biofeedback. This assessment will allow to clarify if the provision of biofeedback promotes changes in the patients' pedaling strategy. In addition, the effects of the intervention on the patient's motor function will be assessed by performing assessment tests at the beginning and at the end of the intervention, such as the FMA and the 10MWT. The cycling assessment test will allow to evaluate improvements on the motor function during the performance of cycling exercise, whereas the walking assessment test will be used to check if the intervention improved the patients' walking capacity. Through these analyzes will be possible to assess the effectiveness of cycling with force or EMG biofeedback as a stroke rehabilitation therapy. This study will also allow the evaluation of the appropriateness of the system developed to provide force biofeedback, as well as, of the *YSY EST EVOLUTION* device, to provide EMG biofeedback to stroke patients. Some problems and possible improvements to these systems may be identified through their application in stroke patients.

Specifically, in this chapter is presented the proposed protocol for the application in stroke patients. The inclusion and exclusion criteria, the organization of the patients in the experimental and control groups and the determination of the sample size, will be presented in this chapter. All phases of the protocol, the assessment tests, including a walking and a cycling assessment, and the intervention planning are also presented, as well as, a set of conditions in which the subjects will perform the therapies and the assessment metrics.

The effects of force and EMG biofeedback on cycling performance and in patients' pedaling strategy were tested during a single session. Two stroke patients (Patient 1 and Patient 3) performed a single session of force biofeedback, whereas Patient 1 performed a single session of EMG biofeedback. In

addition, part of the proposed study (5 sessions during 2 weeks) was implemented in two stroke patients (Patient 2 and Patient 3) to assess the effects of an intervention of EMG biofeedback in the patients' motor function. The results of the tests are presented in this chapter.

6.2 Patient Selection – Inclusion and Exclusion Criteria

The inclusion and exclusion criteria were chosen based on the opinion of a medical team, formed by three physiatrists and one neurologist, and on the number of possible subjects, which could fulfill these criteria on the area of influence of the Hospital de Braga. The study criteria are presented in Table 6.1.

Table 6.1: Inclusion and exclusion criteria of the designed study

Inclusion Criteria	First-time stroke
	Ischemic stroke;
	Only motor deficits on the date of the assessment by the neurologist;
	Time since stroke of more than 3 months and less than 2 years;
	Walking ability (with or without walking aid);
	Spasticity level less or equal to 2 in the MAS (lower limbs);
	Preserved ROMs of hip, knee and ankle;
	Not doing physiotherapy, by the time of the study;
	Age superior than 18 years;
	Informed consent;
Exclusion Criteria	Other neurological disease (Central or Peripheral Nervous System) associated (dementia, extrapyramidal, inflammatory or neuromuscular);
	Orthopedic disease (lower limbs orthopedic surgeries, for instance, knee and hip prosthesis);
	Need for lower limbs orthosis (AFO (Ankle-Foot Orthosis) or Foot-up);
	Severe cardiovascular disease;

The post-stroke time is a relevant criterion of the studies, since both acute and sub-acute stroke patients have the issue of isolating the effects from spontaneous recovery or ongoing CNS plasticity [22, 65]. On the other hand, although some interventions with chronic stroke patients (more than 6 months post-stroke) have observed positive results, some authors suggest no functional recovery can be expected after 6 months since stroke [108]. As patients of the selected time range are, generally, no longer hospitalized, the rehabilitation process is performed in a clinical facility near the patient's home. Thus, the patients would perform the study and receive conventional therapy. However, as the rehabilitation training and approach could change in the different rehabilitation clinics, the patients would not receive the same treatment. Therefore, the criterion of not doing physiotherapy, by the time of the study, was included.

The inclusion and the exclusion criteria will be checked by a neurologist and a physiatrist. The study will be performed in the Clinical Academic Center – Hospital de Braga. All participants provided a written informed consent and the study was approved by the Ethics Subcommittee for Life and Health Sciences of University of Minho and by the Health Ethics Committee of Hospital de Braga.

6.3 Sample Size

In this study, the effectiveness of cycling with force and EMG biofeedback as stroke rehabilitation therapies will be assessed through two groups: the Experimental Group 1 (EG1) and the Experimental Group 2 (EG2). The EG1 will receive EMG biofeedback and the EG2 will be provided with force biofeedback. Wolf and colleagues [65] suggested that in controlled clinical biofeedback studies on stroke patients, the experimental groups, who will be provided with biofeedback training, should be compared with (1) a control group who will receive no treatment; (2) a group of patients who will receive a specific

exercise program; (3) a group who will be given the same biofeedback training as supplement to specific exercises; or (4) patients who will receive false feedback. In this study, the Control Group (CTG) will receive no treatment. The subjects will be randomly divided by the three groups. All groups will be assessed at the beginning and at the end of the study, to verify whether occurred motor recoveries, during the study period. The CTG will only perform the assessment tests.

Determine the adequate sample size is crucial in the design of clinical studies. The sample should represent the population from which it is selected, thus true inferences about the target population can be made from the results obtained [109].

The adequate sample size can be calculated, through prevalence value, as given by (6.1):

$$n = \frac{Z^2 P(1 - P)}{d^2} \quad (6.1)$$

where n is the sample size, Z is the Z statistic for a level of confidence, P is the expected prevalence or proportion and d is the precision [110].

The prevalence is an estimate of the number of people which have a disease at a given point or period in time [1]. A study by Gonçalves *et al.* [111] determined a stroke prevalence of 8% for the Coimbra population (data from 1992). This value was used in the calculation of the sample size needed for our study. The conventional Confidence Interval (CI) used in the studies is 95%, while the recommended value of precision (d), for prevalence values below 10%, is half of the prevalence value [109]. The recommended sample size for these values is 177 subjects per group. However, as this study is a preliminary study and due to resources limitation (time and availability of subjects) a larger d value was used (10%). In this case, the sample size that is recommended for a 95% CI and a precision of 10% is 28.27 subjects (29 subjects for each study group – 87 subjects total).

6.4 Protocol

The following sections present the major characteristics of the designed study, including the description of the three study groups in which the subjects will be divided, the assessment tests that will be performed (walking and cycling assessment tests), as well as, the intervention schedule and characteristics. The schematic of the designed study, which presents the different phases of the study, is represented in Figure A.9.

6.4.1 Patients Assessment

Demographic data (age, sex, weight and height) and medical characteristics (time after stroke, clinical/etiologic classification of the stroke, muscle tone of the lower limbs and the start and duration of the physiatric treatment performed) of all subjects will be analyzed to assess each group.

Patients' motor function will be assessed through the Fugl-Meyer Assessment (FMA) scale [112]. This functional scale is a stroke-specific impairment index designed for assessing the recovery in post-stroke hemiparetic patients. It is divided into 5 domains: motor function (lower and upper limbs), sensory function, balance, joint range of motion and joint pain. The lower extremities' domain (maximum of 40 points) and the balance domain (maximum of 14 points) will be assessed in the beginning and at the end of the study. Further details of each test, as well as, the scoring criteria are described in the Appendix D.

The ROM (hip, knee and ankle) and the spasticity (modified Ashworth Scale [113] – MAS) of the

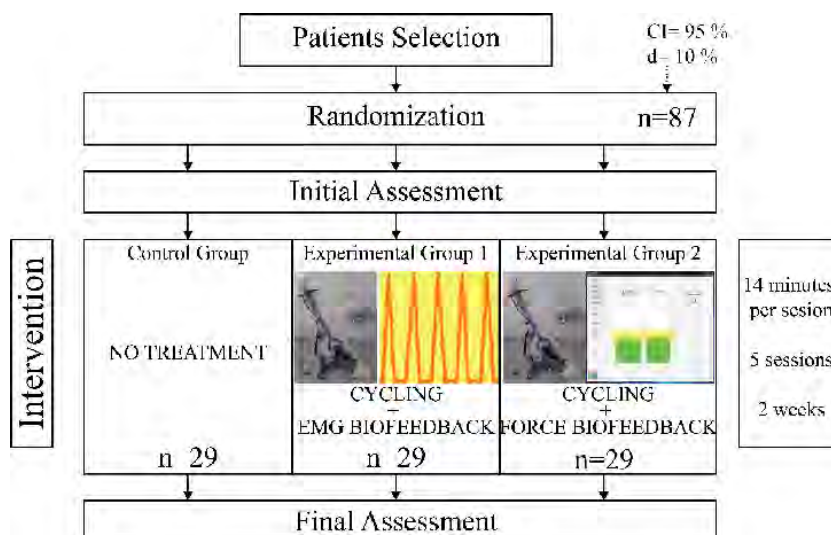


Figure 6.1: Schematic representation of the designed study.

lower limbs will be assessed to check if there were improvements in the lower limbs function. The single foot support time, for each limb, will also be assessed. These assessment tests will be performed in all subjects, by a physiatrist, at the beginning and at the end of the intervention.

The patients' assessment also include a walking and a cycling test. As the restoration of the walking ability is the major goal of post-stroke lower limbs rehabilitation, the walking assessment test will be performed in order to explore the effects of the intervention on the patient's walking ability (functional changes). The cycling assessment test will also be performed, at the beginning and at the end of the intervention, in order to analyze its effects on cycling performance (through training variables).

A 30 minutes rest between the initial assessment and the first session and between the last session and final assessment will be respected, in order to prevent muscle fatigue. An interval of 15 minutes between the walking and cycling assessments will also be respected.

6.4.1.1 Gait Assessment Test

In the walking assessment test, the patients will perform the 10 meters walking test (10MWT). In both tests, measurements will be performed at subjects' comfortable speed.

The 10MWT is used to measure and compute several parameters, such as the course time, number of steps, step length, and average speed [2]. The subjects will walk 10 meters at self-selected comfortable speed. They will walk in plastic course, using heelstraps and sponges with paint to mark the foot in the plastic. This will allow the assessment of the step and strike length, the distance between feet and the foot angle, as shown in Figure 6.2.

6.4.1.2 Cycling Assessment Test

The pedaling assessment test comprises 30 seconds of passive cycling exercise followed by 1 trial of 1 minute of active cycling. During the active period, the work produced by each limb is computed, to assess the asymmetry between the lower limbs. As in the tests in healthy subjects (Chapter 5), the formula of the Unbalance Index, presented in Chapter 2 (equation (2.3)), was changed again, in order to provide information about the lower limb (paretic or healthy) that performed more net mechanical work (W – equation (3.6)). The modified formula (U) is given by (6.2):

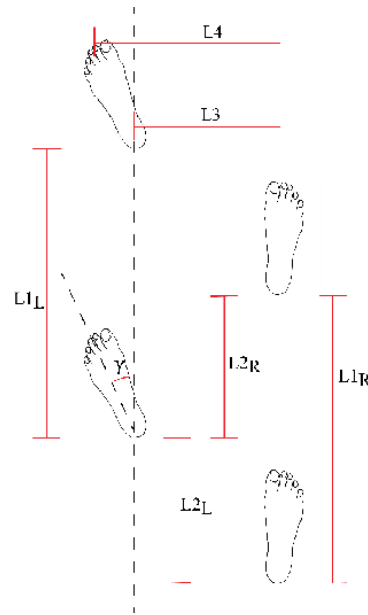


Figure 6.2: Gait parameters: left stride length ($L1_L$), right stride length ($L1_R$), left step length ($L2_L$), right step length ($L2_R$), distance between heels ($L3$), distance between toes ($L4$), and paretic limb foot angle (γ).

$$U = \frac{W_H - W_P}{|W_H| + |W_P|} \times 100 \quad (6.2)$$

where W_{HL} and W_{PL} are the net mechanical work done by the healthy and paretic limb, respectively. The U value could range from -100 (the paretic limb performs all work) to 100 (the healthy limb performs all work). U is zero, when the net mechanical work performed by both limbs is equal. The mean cadence and cadence variability will also be evaluated during this test, as well as, the MAR. The workload of the cycling assessment test will be defined by a test that will be performed before the cycling assessment test, which will be described on the next section.

6.4.2 Procedure

The subjects will perform the intervention on a chair or on a wheelchair, based on the ambulatory capacity of the patient. To standardize the condition under which the cycling protocol is conducted, the distance from the seat edge to the crank axis will be adjusted similarly to Fujiwara *et al.* in [41] so that the knee extension angle is 10 degrees less from full extension when the subjects extend their knees maximally.

As previously described, due to the EMG biofeedback device's timing limitation, the training velocities are limited to the values presented in Table 5.5 (Chapter 5). The training cadence will be defined by a trial where the subjects are instructed to pedal at their comfortable cadence. Then, the subject will be instructed to pedal at the tabulated cadence that is closer to their comfortable cadence. The displaying of visual information of the cadence in the force biofeedback interface (Figure 5.2 – Chapter 5), and the synchronization between the signal velocity and the target signal in the EMG biofeedback training, help the subjects to maintain a constant speed during training. The intervention workload will be determined through a comfortable workload test, as implemented in [2, 8, 19, 29, 43, 114]. The subject starts pedaling at 0 Nm at the selected cadence and the workload is increased 1 Nm, each minute, until the patient achieves the Stage 13 of Borg rate of Perceived Exertion [115] or cannot maintain the cadence for more

than 30 seconds.

To reduce the influence of the weight and inertial forces on the effective force results, one constant value for each pedal, computed through 10 revolutions of passive exercise (initial calibration), at the comfortable cadence and workload values defined in the current session, will be subtracted from the force values.

The target band of the force biofeedback interface will be limited by a superior and an inferior value, which correspond to $\pm 25\%$ of a target value. The target value will be defined, before each trial, as 75% of the work performed by the paretic limb during 20 revolutions of active cycling, which is performed with the comfortable workload and cadence values defined in the current session. The target will visually limit the work performed by the healthy limb, so that it does not override the action of the paretic limb.

The electrodes used in this trials will be the Dura-Stick Plus 2" Square. The electrodes position and the recommendations for the EMG signal acquisition (SENIAM's recommendations [107]), are presented in Appendix C.

The data of the sensors (force (F_p) and angles values (ϕ and β)) will be collected and analyzed, as well as, the computed values (net mechanical work of the healthy and paretic limbs – W_{HL} and W_{PL} , respectively), modified Unbalance Index (U) and cadence) and the joint moments. Regarding EMG biofeedback, the minimum, average, and maximum values, provided by the *YSY EST EVOLUTION* will be collected to compute the MAR.

6.4.3 Intervention

The experimental groups (EG1 and EG2) will perform 5 sessions of cycling exercise, during 2 weeks. In each session, the subjects will perform a protocol of different cycling tasks in a total of 14 minutes, as represented in Table 6.2.

Table 6.2: Cycling tasks performed during a session of the study

Order	Exercise	Duration (minutes)
1st	Passive Cycling	1
2nd	Active Cycling	2
3rd	Active Cycling with Biofeedback	8
4th	Passive Cycling	1
5th	Active Cycling	2

In the 8 minutes trial, the EG1 will perform cycling together with EMG biofeedback of the *rectus femoris* muscle, and will attempt to follow the EMG target signal (Figure 5.8 (b) – Chapter 5), whereas the EG2 will perform cycling with force biofeedback updated on each 32 degrees (F32), as described in Chapter 5.

6.5 Case Studies

Due to the lack of patients, which fulfilled the inclusion and exclusion criteria on the area of influence of our clinical partner (Hospital de Braga) and due to time limitations, the study could not be fully implemented.

The application of an intervention of cycling with force or EMG biofeedback will be supported if the therapies promote changes in the pedaling strategy and in the training variables, such as, the applied effective force (F), the pedal angles (β), the (U) and the muscle activation. This analysis will allow to answer to the #RQ4. Therefore, the behavior of the training variables without and with biofeedback,

in stroke patients, should be compared before the implementation of the study, in order to assess if biofeedback promotes changes in the pedaling strategy. If so, the therapy may result in improvements on the patient’s motor function, since the patient will perform several sessions that promote changes in his pedaling strategy. The effects of cycling with force and EMG biofeedback on the training variables and on the pedaling strategy were assessed in a stroke patient (Patient 1), during a single session. Moreover, Patient 3 also performed a single session of force biofeedback with the same purposes as in Patient 1.

The designed study was implemented in two stroke patients (Patient 2 and Patient 3), who performed an intervention (5 sessions during 2 weeks) of cycling with EMG biofeedback. The objective of these two case studies was to assess the effect of an intervention of cycling with EMG biofeedback on the patients’ motor function, during cycling and walking, in order to answer to the #RQ2 and #RQ3, in addition to the assessment of therapy effects on the pedaling strategy and training variables (#RQ4). The proposed protocol (trials and training conditions) was adapted for each patient’s characteristics, medical conditions and rehabilitation degree.

The demographic, anatomical and medical characteristics of the three stroke patients are presented in Table 6.3.

Table 6.3: Demographic, anatomical and medical characteristics of the studied patients

Characteristics	Patient 1	Patient 2	Patient 3
Age (years)	28	49	67
Sex	Male	Female	Male
Weight (Kg)	67	74	69
Height (m)	1.81	1.72	1.71
Body Mass Index (BMI)	20.45	32.03	23.60
Thigh Length (cm) – trochanter to tibiale	47	38	57
Shank Length (cm) – tibiale to sphyrion	38	39	45
Foot Length (cm) – heel to tip longest toe	25	25	27
Time after stroke (months)	11.3 (chronic)	1.6 (sub-acute)	1.1 (sub-acute)
Ischemic / Hemorrhage Stroke	Hemorrhage	Ischemic	Hemorrhage
Clinical/Etiologic stroke classification	Right middle cerebral artery (MCA) Aneurysm – right fronto-temporal hematoma	Stenosis and Irregularities in the intracranial arteries	Hypertensive Hemorrhage
Motor deficit	Left Hemiparesis	Right Hemiparesis	Right Hemiparesis
Lower limb’ muscle tone (MAS)	Grade 1+ on knee extensors Grade 2 on triceps surae	Normal	Grade 1+
Walking aid	No (uses Ankle-Foot Orthosis – AFO)	No ambulatory capacity	No ambulatory capacity
Physiatric treatment performed (start and duration)	Regular since stroke	Ongoing (Start: 9 days since stroke)	Ongoing (Start: 21 days since stroke)
Distance of the chair to the crank axis (cm)	53	25	35

The results observed in these three patients will be presented in the following sections.

6.5.1 Patient 1

Patient 1 was recruited to perform a single session of cycling with force and with EMG biofeedback, in order to assess the behavior of the training variables without and with biofeedback. This single session will allow to assess if biofeedback promotes changes in the patient’s pedaling strategy. This patient was a chronic stroke patient (11.3 months since stroke), which presented left hemiparesis and used an Ankle-Foot Orthosis. Patient 1 suffered a hemorrhage stroke, has some limitations on the ROM and was doing

regular physiotherapy, by the time of the study, which do not fulfill the inclusion criteria. In addition, one exclusion criterion is not verified, since Patient 1 uses an Ankle-Foot Orthosis.

Patient 1 performed the initial assessment tests, before performing a session of force and EMG biofeedback. The training workload was defined, by the comfortable workload test, as 0 Nm. During the force biofeedback tests, 3 trials of 2 minutes each (no force biofeedback, force biofeedback updated on each 32 degrees and force biofeedback of half a revolution – NF, F32 and FHR, respectively), were performed by the patient. The target band was defined in an initial trial of 10 revolutions at the selected comfortable workload and cadence. In the force biofeedback trials, the patient was instructed to pedal at the comfortable cadence that appeared more adequate to him, to achieve the target band. Then, the patient performed 2 trials of 3 minutes, one without biofeedback and other with EMG Biofeedback (NF and EMGF, respectively). A rest period of 3 minutes was respected between each trial. In addition to the referred metrics, the mean values of the negative (paretic limb performed more work) and positive (healthy limb performed more work) Unbalance Index (U^- and U^+ , respectively), as well as, the number of revolutions whose U was negative, of 60 revolutions (36th to 95th), were analyzed for each trial. The first 35 revolutions were not considered in order to ensure a lower deviation on the results.

Regarding EMG biofeedback, the cadence of 43 rpm (passage time of 7 seconds) was selected as the comfortable cadence for the patient. The data of 60 revolutions (51st to 110h) was analyzed for each biofeedback condition. The first 50 revolutions were not considered in order to ensure a lower deviation on the results.

6.5.1.1 Assessment

The FMA score, the single foot support time, the range of motion ROM of the paretic limb and the results of the 10MWT, of Patient 1, are presented in Table 6.4.

Table 6.4: Patient 1 assessment tests’ results. The metrics measured in the 10MWT are presented as mean (Standard Deviation (SD)) values

	Tests	Values
FMA	Lower Limbs (maximum 40)	24
	Balance (maximum 14)	12
Single foot support time	Paretic Limb (s)	2
	Healthy Limb (s)	> 20
ROM	Hip	Preserved (active and passive)
	Knee	Active 0-100°
		Passive Complete
	Ankle	Passive – 5° Dorsiflexion
10MWT	Time (s)	29.82
	Steps number	31
	Speed (m/s)	0.34
	Left Stride length – $L1_L$ (m)	0.86 (0.07)
	Right Stride length – $L1_R$ (m)	0.85 (0.09)
	Left Step length – $L2_L$ (m)	0.57 (0.03)
	Right Step length – $L2_R$ (m)	0.52 (0.03)
	Distance between heels – $L3$ (m)	0.21 (0.03)
	Distance between toes – $L4$ (m)	0.29 (0.02)
	Paretic limb foot angle – γ (degrees)	24.06 (3.28)

The difference between the single foot support times for each limb is notorious (2 and >20 seconds for the paretic and healthy limbs, respectively) and highlights the impairment motor function of the paretic limb. The ROM of this patient in the knee and ankle of the paretic limb presents some limitations. During walking, the patient presented a lateral rotation of the left limb (hip abduction and rotation). The values of the stride and step lengths for each side are approximately equal. The difference in the step

length (slightly larger on the left side – paretic side) may be due to a higher ability of the healthy limb to support the body weight, which may allow a longer step with the paretic one.

The training parameters measured on the initial cycling assessment test are presented in Table 6.5. As this study was performed in a single session the final assessment tests were not performed.

Table 6.5: Mean (SD) values of the training parameters of the initial cycling assessment test of Patient 1

Tests		Begin
Mean Net Mechanical Work	Paretic Limb (W_{PL})	1.02 (1.34)
	Healthy Limb (W_{HL})	2.15 (0.74)
Mean Unbalance Index (U)		45.22 (43.33)
Mean Absolute Unbalance Index ($ U $)		54.08 (31.36)
$U < 0$ (number of revolutions)		11
$ U \leq 25\%$ (number of revolutions)		14
Mean Cadence (rpm)		55.58 (1.66)
Muscle Activation Rate (MAR)		0.32

The assessment cycling test shows a lower mean contribution of the paretic limb to the movement (W_{PL}) less than (W_{HL}). The mean U reports an asymmetrical force pattern, but in 14 revolutions the $|U|$ was less than or equal to 25%. As the mean $|U|$ is superior to the mean U , the paretic limb performed a higher contribution to the movement than the healthy limb (in 11 revolutions).

6.5.1.2 Results and Discussion

Force Biofeedback

Patient 1 performed all force biofeedback trials with success. The mean cadence, mean absolute, negative and positive Unbalance Index values ($|U|$, U^- and U^+ , respectively), as well as, the number of revolutions where the paretic limb performed more work, in which the $|U|$ was less than or equal to 25% and that fulfill the target band, for each type of force biofeedback, are presented in Table 6.6.

Table 6.6: Mean (SD) values of cadence, absolute, negative and positive Unbalance Index values and number of revolutions that fulfill the conditions, in the different trials of the force biofeedback of Patient 1

Tests	NF	F32	FHR
Mean Cadence (rpm)	51.50 (1.04)	42.55 (8.24)	45.07 (1.23)
Mean Absolute Unbalance Index ($ U $)	30.33 (27.46)	80.96 (30.43)	80.76 (31.81)
Mean Negative Unbalance Index (U^-)	-37.47 (32.38)	-66.80 (32.15)	-90.78 (23.51)
Mean Positive Unbalance Index (U^+)	24.87 (21.97)	87.03 (27.90)	57.38 (36.76)
Unbalance Index < 0 (number of revolutions)	26	18	42
Absolute Unbalance Value $\leq 25\%$ (number of revolutions)	33	6	4
Within objective band (number of revolutions)	12	4	1

The mean value of the cadence with force biofeedback (F32 and FHR) was lower than without biofeedback (NF). This suggests a change in the pedaling strategy to achieve the objective of the training. The higher standard deviation of the cadence in the F32 trial, may be due to the higher feedback frequency of this biofeedback type. The bars updated 11 times during each revolution, which suggests the patient, in order to achieve the target band, applied more or less force in the pedals during training, increasing or decreasing the cadence.

The symmetry during training without biofeedback (NF) was higher than in the trials where force biofeedback was provided (lower ($|U|$, U^- and U^+ – Table 6.6). The number of revolutions where the $|U|$ was less than or equal to 25% and that fulfill the objective band were also higher in the NF trial. Force biofeedback (F32 and FHR) promoted a higher net mechanical work performed by the paretic limb (higher U^-), but fail in the achievement of a higher cycling symmetry (lower number of revolutions with

$|U|$ less than or equal to 25%). The force biofeedback conditions might be inadequate for the patient characteristics. The parameter to define the target band (75% of the maximal work performed by the paretic limb) might have been inadequate for this patient, since the number of revolutions that fulfill the target band is less than the number in which the $|U|$ was less than or equal to 25%. The provision of FHR resulted in increasing the number of revolutions where the paretic limb performed more net mechanical work than the healthy limb. In this type of biofeedback the paretic limb performed a higher contribution to the movement in more revolutions than the healthy limb.

During the three analyzed trials, the pedal angle ranged from 25 to 55 degrees, the pattern between both limbs was more similar with FHR, and the standard deviation was higher in the F32. This higher variation may be due the higher feedback frequency, since in the FHR the bars are only updated 2 times on each revolution.

The effective force patterns of the paretic (solid red line) and healthy limb (dashed green line), for each biofeedback trial, with respect of the crank angle are represented in Figure 6.3. The grey area represents the upstroke phase of the paretic limb and the shaded area along the curves represents the SD values.

The plots of the effective force show that the lower $|U|$, U^- and U^+ values of the NF trial do not correspond to a higher symmetrical force pattern since, as shown in Figure 6.3 (a), the paretic limb (solid red line) performed more propulsive force (positive effective force) than the healthy limb (dashed green line), but the amount of resistive force (negative effective force) was also superior (between 0 and -3 for the healthy and; 0 and -10 for the paretic limb). The propulsive force is the applied force that contributes to the movement of the cycling device (positive force), whereas the resistive force is the force that counteracts the movement of the cycling device (negative force). The force pattern in F32 is approximately similar with the one without biofeedback. However, the standard deviation was higher, which suggests a changing in the pedaling strategy in order to achieve the objective, when this biofeedback type was provided. As a new target band, as indicated in Chapter 5, is defined for each trial, the value obtained for the FHR trial was 3 times inferior than the values obtained in the others two trials. Therefore, the force values, measured in this trial, are considerably lower than in the others. The definition of a new target value on every trial may have influenced the results and the interpretation of the appropriateness of providing force biofeedback to this patient, since the conditions under which the trials were performed are different. The condition and the way that the target band is defined, in stroke patients, should be reviewed.

The issue of the force biofeedback system reported in Chapter 5, in which the cycling exercise might be incorrectly classified as symmetrical if the force pattern of a limb that apply more propulsive force, during the downstroke phase, but also apply more resistive force during the upstroke, is compared with the force pattern of a limb that performed less propulsive and less resistive force. The overall contribution to the movement of both limbs is the same, being classified as symmetrical, but the force patterns behavior is different. This issue was also observed in this case study, as shown in Table 6.6 and Figure 6.3 (a). The force pattern of the paretic limb of this patient is characterized by a normal positive effective force, as shown in Figure 6.3. However, during the upstroke phase, the paretic limb performed a great amount of negative force, which performs resistance to the movement. Therefore, this patient may benefit more from a trial that promotes the coordination, such as the F32, than a trial that promotes only the amount of force produced during the downstroke phase, such as the FHR. Due to the characteristics of this patient, the condition to define the target band may not be the most appropriated, since it considers

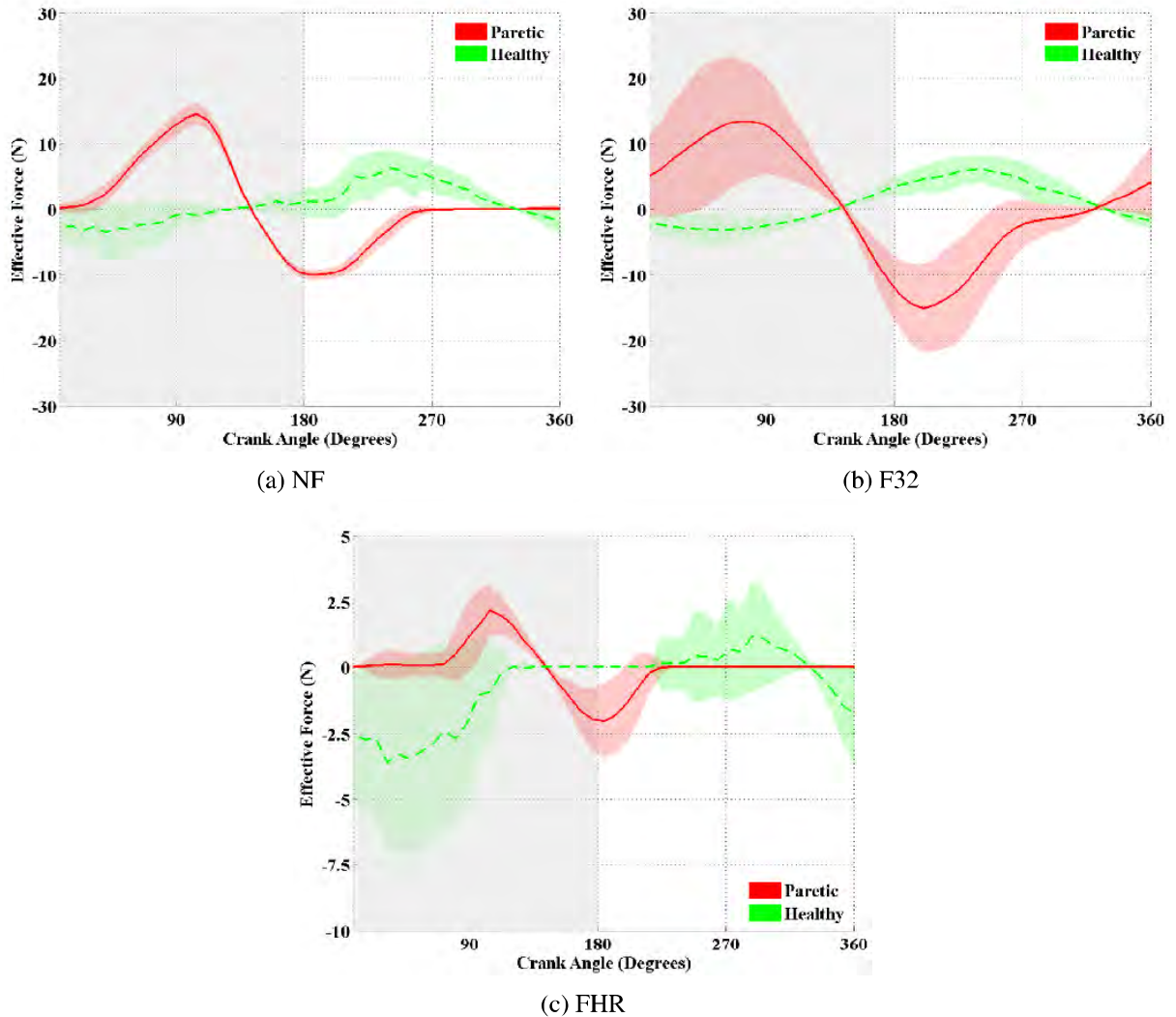


Figure 6.3: Mean values of the effective force for both lower limbs, for cycling with (a) no biofeedback (NF); (b) force biofeedback updated on each 32 degrees (F32); and (c) force biofeedback of half a revolution (FHR), for sixty revolutions (36th to 95th revolution) of Patient 1. The grey area represents the upstroke phase of the parietic limb and the shaded area along the curves represents the SD values.

that the parietic limb will perform less force than the healthy limb. In this case, a condition or a system that promotes a reduction of the resistive force may be more appropriate.

The pedaling strategy of Patient 1 may have changed when F32 was provided, which is supported through an increase of the standard deviation in the force pattern. This might suggest a patient's attempt to reduce the resistive force applied by the parietic limb, during the upstroke phase.

EMG Biofeedback

A target cadence of 43 rpm (passage of 7 seconds) was defined as the comfortable and cadence. The average cadence for the NF trial was 45.98 (1.64), while in the EMGF trial the average cadence was 54.61 (2.60). The higher cadence achieved during the EMGF trial may be due to the patient's attempt to synchronize the muscle activation peak with the target signal.

The MAR and the work performed by each limb (parietic and healthy – W_{PL} and W_{HL} , respectively), for the two trials (without and with EMG Biofeedback – NF and EMGF, respectively) are presented in

Table 6.7.

Table 6.7: MAR and work (mean (SD) values) performed by each limb, of Patient 1, during cycling without and with EMG biofeedback

Tests	NF	EMGF
MAR	0,325	0,575
W_{PL}	-0,36 (0,41)	4,08 (2,27)
W_{HL}	1,32 (0,92)	2,47 (1,27)

Providing EMG biofeedback resulted in a higher muscle activation (higher MAR and higher work performed by both limbs. The paretic limb performed more net mechanical work (W_{PL}) when EMG biofeedback of the RF was provided to Patient 1. This limb improved from the limb that performed mostly resistive movement, to the one that contributed more to the movement. As the *rectus femoris*' activation occurs during upstroke phase, in order to increase the muscle activation signal, the patient may have performed more upward force in the pedal, reducing the amount of resistive force. The W_{HL} also increased, probably to follow the movement of the other limb. Providing EMG biofeedback of the RF changed the patient's pedaling strategy and seems to have reduced the problem of the resistive force applied by paretic limb, observed in the force biofeedback trials.

The mean muscle activation patterns of the *rectus femoris* of Patient 1, for the NF and EMGF trials, are presented in Figure 6.4 (a) and (b), respectively.

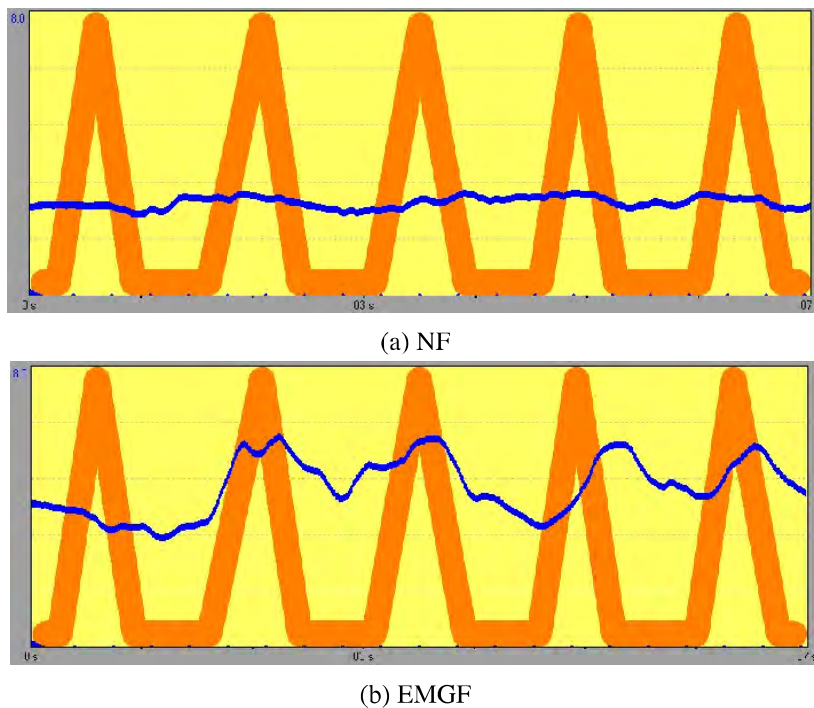


Figure 6.4: *Rectus femoris*' mean activation pattern of Patient 1 with (a) no biofeedback; and (b) EMG biofeedback.

The curves of the muscle activation correspond to the average of the muscle activation pattern achieved during all passages. Considering the time of each passage (7 seconds) and the duration of trials, the presented RF' activation patterns correspond to the average of 27 passages. Therefore, the initial passages may have a negative influence on the final muscle activation pattern, since at beginning of the trials the patient has to synchronize the training cadence and the muscle activation pattern with the target signal. The mean muscle activation patterns confirm the increasing of the MAR with the provision

of EMG biofeedback. A higher mean activation value and a pattern that better follows the target signal was achieved with EMG biofeedback. However, although some muscle peaks are observed in the EMGF trial, they are slightly desynchronized with the target signal, suggesting a difficulty to synchronize the training cadence and the muscle activation pattern with the target signal.

The mean values of the pedal angle for the paretic (solid red line) and healthy (dashed green line) limbs of Patient 1, without (a) and with EMG (b) biofeedback, are presented in Figure 6.5, respectively.

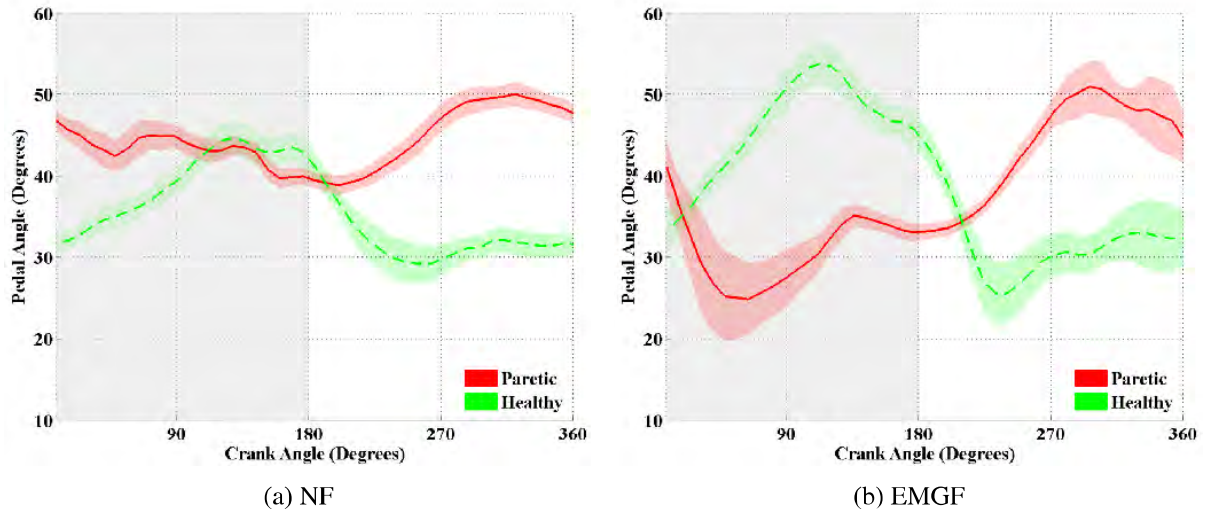


Figure 6.5: Mean values of the pedal angle (β) for the paretic (solid red line) and healthy (dashed green line) limbs of Patient 1 with (a) no biofeedback; and (b) EMG biofeedback, of Patient 1.

During cycling the NF trial the behavior and the values of β of both limbs were different. However, the magnitude and the behavior of the pedal angles of both limbs increased and was similar, when EMG biofeedback was provided to the patient. The paretic limb changed from a range between 40 and 50 degrees to a range between 20 and 50 degrees, promoting the foot movement, which may have a positive effect in the rehabilitation of the plantarflexion and dorsiflexion movements.

The mean values of the effective force for both lower limbs of Patient 1, without (a) and with EMG (b) biofeedback, are presented in Figure 6.6, respectively.

In NF trial, the contribution of the paretic limb to the crank movement was minimal, being the healthy limb (dashed green line) the one that performed the major contribution to the movement. When EMG biofeedback was provided, the force applied by the healthy limb was slightly higher to the force applied during the NF trial. However, in the EMGF trial, the paretic limb applied more positive effective force than the healthy one and became the limb that performed the major contribution to the movement. As also shown in Table 6.7, the provision of EMG biofeedback increased the participation of the paretic limb in the training. The resistive force performed by the paretic limb was similar to the one applied by the healthy limb, and was significantly lower than the resistive force applied during the force biofeedback trials. These results suggest the effectiveness of EMG biofeedback of the RF in reducing the resistive force applied by the paretic limb of Patient 1, during the upstroke phase.

The mean values of the ankle (top), knee (middle) and hip (bottom) moments for the the paretic (solid red line) and healthy limb (dashed green line), without (left) and with (right) EMG biofeedback, of Patient 1, with respect to crank angle, are presented in Figure 6.7, respectively. These values were computed through the model for biomechanical analysis of the lower limbs during cycling, presented in Chapter 4.

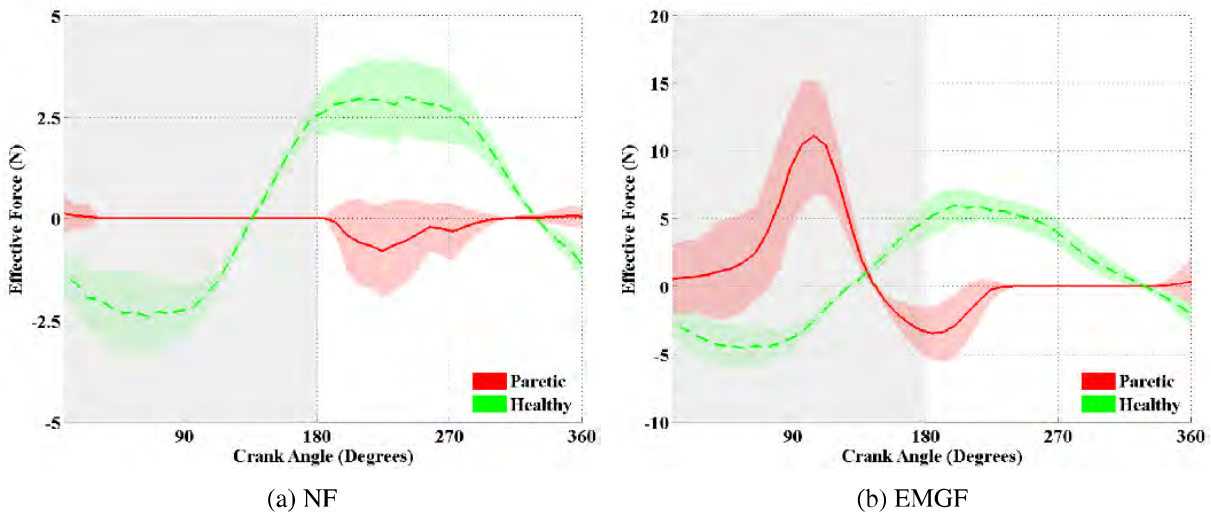


Figure 6.6: Mean values of the effective force for both lower limbs, for cycling with (a) no biofeedback; and (b) EMG biofeedback, of Patient 1.

The difference between the joints' moments in the trial without biofeedback (left) is lower, which may be due to the low values of the applied forces. As the values of the applied forces in the EMG biofeedback trial are higher, the joints' moments of the lower limbs are slightly different, in particular, the knee and ankle's moments. The angle of the higher positive effective force is easily identified in the knee and ankle moments pattern. As opposed to Mimmi *et al.* [90], the hip moment does not enhance difference between the force applied by each lower limb, which may be due to the different cycling device configuration, since the Mimmi *et al.*'s cycling device was a standard cycling device, while the one used in this study is a semi-recumbent device. During training in a standard cycling device the hip is directly above of the pedal, which may influence the hip moment.

The accessory "Leg Support" (Appendix A.6) is normally used, attached to the cycling device's pedals, in patients with weak limbs to help the unhealthy limb to mimic the natural motion of the ankle joint. However, the available cycling device did not include this accessory. Therefore, this patient had to pedal without the Leg Supports, which resulted in a misalignment of the paretic limb joints with the pedal, due to hip abduction, hip rotation and foot inversion. These muscles' movements, generally observed in the paretic limb of stroke patients, prevent a correct contact of the foot with the pedal, reducing the amount of the applied and effective forces. The use of the Leg Supports can stabilize the sagittal plane of the paretic lower limb, preventing the hip abduction, the hip rotation and the foot inversion. Not using this accessory may have influenced and limited the effectiveness of these therapies.

The overall results presented in this section show that Patient 1 was able to increase the muscle activation and the work performed by the paretic limb, as well as, to follow the target signal. In addition, providing EMG biofeedback also resulted in an increasing of the propulsive force (positive) applied by the paretic limb, during the downstroke phase and, more important, a reduction of the amount of resistive force (negative). The range of the pedal angles (β) of the paretic limb increased and the β 's behavior of both limbs became similar. In summary, the provision of EMG increased the contribution of the paretic limb to the movement and solved the excess of resistive force applied by this limb, during the upstroke phase.

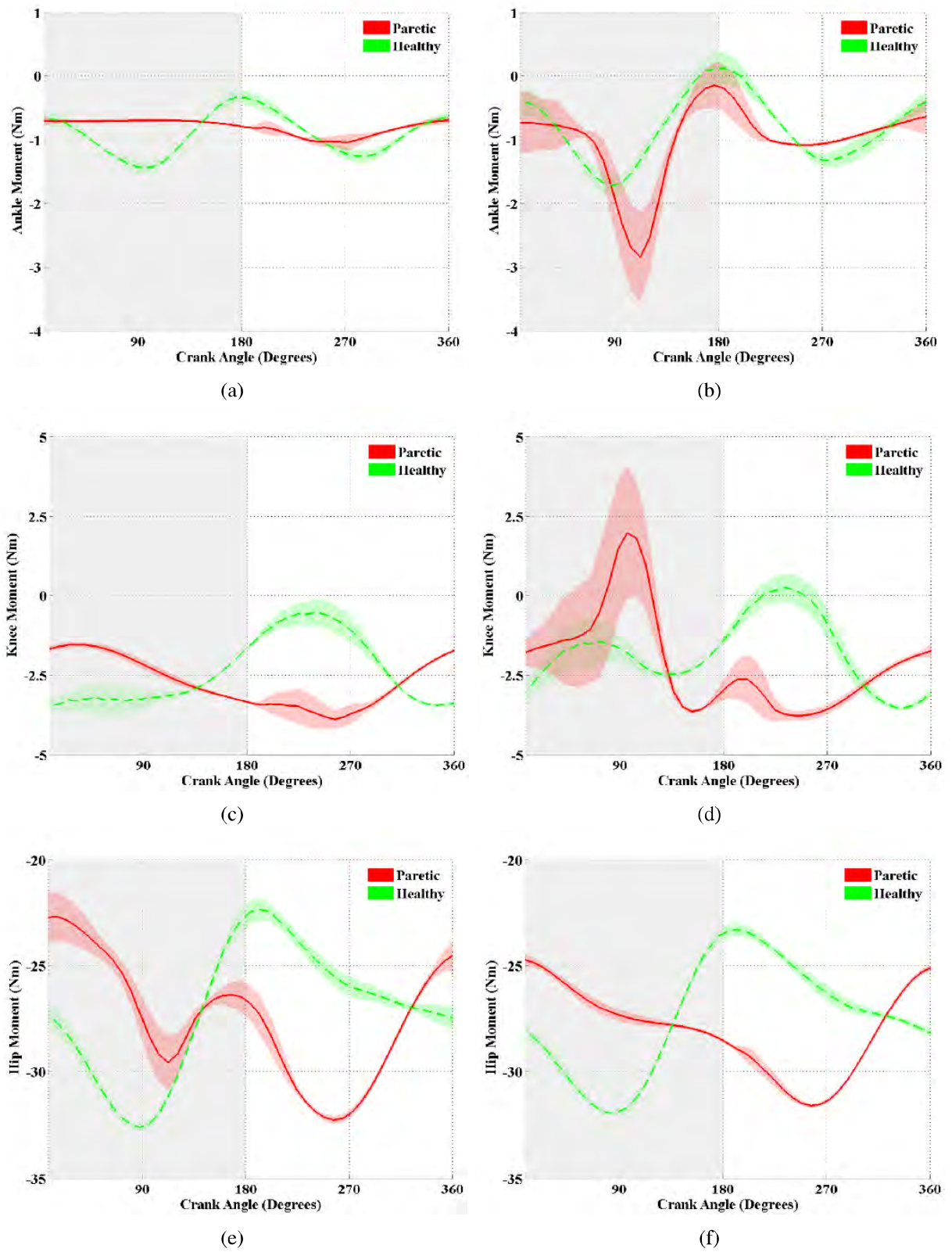


Figure 6.7: Mean values of the ankle (top), knee (middle) and hip (bottom) moments with (a) (c) (e) no biofeedback; and (b) (d) (f) EMG biofeedback, for both lower limbs of Patient 1.

6.5.2 Patient 2

Patient 2 was one of the two patients selected to study the effects of the EMG biofeedback therapy on the motor function and on the walking ability, in addition to the assessment of its effects on the pedaling strategy and training variables. This patient was a sub-acute stroke patient (1.6 months since stroke), which presented right hemiparesis and no ambulatory capacity (unable to walk or stand without assistance). During the intervention period, the patient also performed one hour and a half of conventional physiotherapy and 30 minutes of occupational therapy, every weekday, in the Hospital de Braga. The time since stroke, the ongoing physiotherapy and the no ambulatory capacity do not fulfill the inclusion criteria.

As this patient was not able to walk or stand without assistance, the Single foot support time test and the 10MWT could not be performed. The assessment tests were performed before performing the first session of EMG biofeedback, as planned in the proposed protocol. This patient performed 5 sessions, during 2 weeks, in which EMG biofeedback was provided, as proposed in Section 6.4.4 (2 minutes in the NF trials, and 8 minutes for the EMGF trial). A rest period of 3 minutes was respected between each trial.

The training workload and cadence were defined through the comfortable tests. The data of 60 revolutions (11th to 70th for the NF trials, and 141st to 200th for the EMGF trials) was analyzed for each biofeedback condition. The initial revolutions were not considered in order to ensure a lower deviation on the results. Patient 2 performed the intervention on a wheelchair with 46 centimeters of height. The remaining parameters were similar to the previous studies.

6.5.2.1 Assessment

The FMA score, and the ROM of the paretic limb's joints of Patient 2, assessed by a physiatrist, are presented in Table 6.8. For reasons unrelated to this work, the same assessment at the end of the intervention was not possible to perform.

Table 6.8: Patient 2 assessment tests' scores

	Tests	Begin
FMA	Lower Limbs (maximum 40)	15
	Balance (maximum 14)	7
ROM	Hip	Preserved
	Knee	Preserved
	Ankle	Preserved

The FMA scores for Patient 2 are lower than those of Patient 1, but the first has no limitations in the ROMs of the paretic limb.

The training parameters measured on the initial and final cycling assessment tests are presented in Table 6.9.

in a smaller difference between the W performed by each limb. Therefore, a more balanced cycling was achieved after the intervention, since the difference between the contribution of each lower limb to the movement decreased. The U slightly increased in the final assessment. The MAR value was also smaller in the final assessment. In summary, apparently there were no improvements in the training variables, at the end of the intervention, with the exception of the W performed by the healthy and paretic limbs. This evolution was also observed in the study of Ferrante *et al.* [18], in which, although the work performed by the paretic limb of a patient reduced, the difference between both limbs became lower,

Table 6.9: Mean (SD) values of the training parameters of the initial and final cycling assessment tests of Patient 2

Tests		Begin	End
Mean Net Mechanical Work	Paretic Limb (W_{PL})	-0.25 (1.01)	-0.76 (1.04)
	Healthy Limb (W_{HL})	5.55 (3.72)	3.71 (1.60)
Mean Unbalance Index (U)		86.76 (28.22)	93.84 (15.94)
Mean Absolute Unbalance Index ($ U $)		90.10 (14.04)	93.84 (15.95)
$U < 0$ (number of revolutions)		1	0
$ U \leq 25\%$ (number of revolutions)		0	1
Mean Cadence (rpm)		38.56 (5.15)	37.18 (1.61)
Muscle Activation Rate (MAR)		0.4	0.31

since the work performed by the healthy limb also lowered.

6.5.2.2 Results and Discussion

All sessions were successfully performed, with the exception of the first and third sessions, which had to be finished earlier (first session: 6 minutes of EMGF, instead 8; third session: stopped after the EMGF trial), due to patient fatigue and knee pain, respectively. The mean workload and cadence values of each trial (without and with EMG biofeedback – NF and EMGF, respectively) for each session are presented in Table 6.10. The results regarding the NF trial are from the first trial without biofeedback of the protocol (Section 6.4.3).

Table 6.10: Used workload and target cadence values; and mean (SD) cadence measure in the NF and EMGF trials, for each session, of Patient 2

Trial		Workload (Nm)	Target Cadence (rpm)	Mean Cadence (rpm)
1st Session	NF	0	30.00	38.57 (5.15)
	EMGF			40.56 (5.05)
2nd Session	NF	0	37.50	47.76 (2.84)
	EMGF			39.44 (3.24)
3rd Session	NF	3	37.50	45.02 (2.05)
	EMGF			38.83 (1.08)
4th Session	NF	4	37.50	40.28 (1.58)
	EMGF			40.93 (1.06)
5th Session	NF	4	37.50	33.78 (2.17)
	EMGF			32.78 (1.09)

During the intervention, Patient 2 was able to increase the training workload, which may be related with an increase of the patient's endurance or with the learning of how to more effectively interact with the cycling device and biofeedback (learning period). In the first session, the target cadence was defined as the lowest value, in order to prevent fatigue. However, the patient pedaled at a higher cadence, as shown in Table 6.10. Therefore, in the following sessions the target cadence was increased (37.5 rpm – passage of 8 seconds), in order to adapt the target cadence to the patient comfortable speed. The mean cadence values, in the different sessions, were close to the target cadence, wherein the differences may be due to the patient's attempt to synchronize the muscle activation pattern with the target signal.

The values of the MAR of the *rectus femoris* of Patient 2, for all sessions without and with EMG biofeedback (NF and EMGF – solid red and dashed green lines, respectively), are presented in Figure 6.8.

Figure 6.8 shows that higher MAR was achieved in the NF trial. The MAR values for the EMGF trial, throughout the intervention, present an increasing trend. The trend of the variable in the NF trials is inconclusive. The lower MAR values measured when EMG biofeedback was provided may have resulted from a change in the patient's pedaling strategy. During the NF trial, as the patient does not receive information about his muscle activation pattern, its value will not be limited due to any intentional action of the patient. However, when EMG biofeedback is provided, the patient starts to attempt to change his

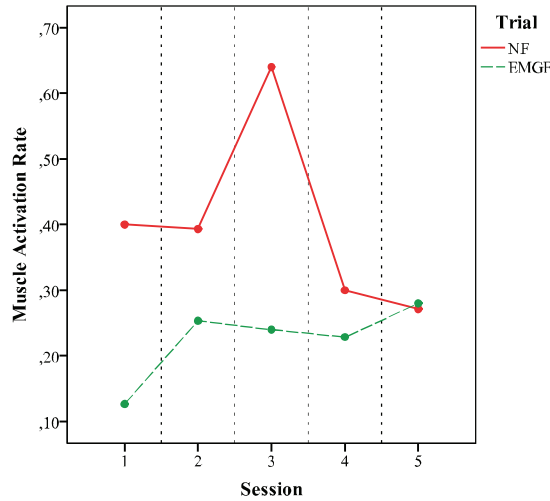


Figure 6.8: Values of the MAR of the *rectus femoris* muscle of Patient 2, for the 5 sessions, without and with EMG biofeedback (NF and EMGF, respectively).

muscle activation pattern, in order to follow the target signal, which may influence the muscle activation pattern and limit its value. Therefore, the muscle activation may be greater in the NF than in the EMGF trial, resulting in a higher MAR.

The mean values of the net mechanical work (W) performed by each lower limb of Patient 2, without and with EMG biofeedback, for all five sessions, are presented in Figure 6.9. The W_{PL} and W_{HL} in the NF trial are represented by the solid red and dotted green lines, respectively, whereas the W_{PL} and W_{HL} in the EMGF trial are represented by the dash-dot blue and dashed black lines.

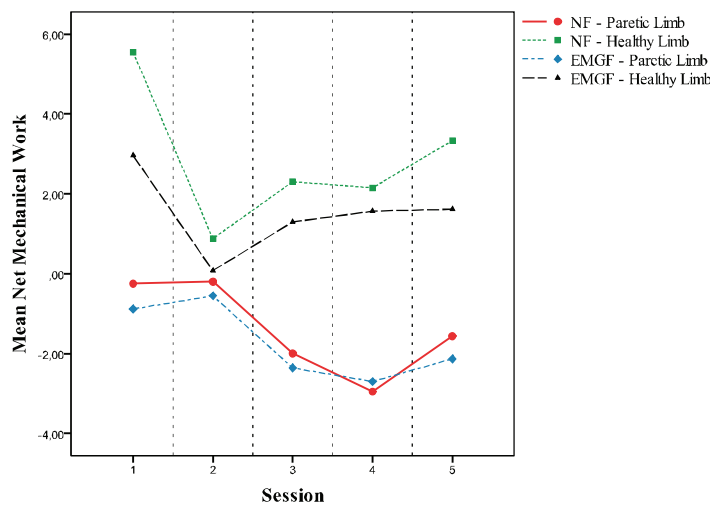


Figure 6.9: Mean values of the net mechanical work performed by the paretic and healthy limbs in the NF trial (solid red and dotted green lines, respectively) and in the EMGF trial (dash-dot blue and dashed black lines, respectively), of Patient 2.

The net contribution of the paretic limb (W_{PL}) was negative in all sessions without and with EMG biofeedback. Therefore, the paretic limb performed more resistive (negative) force than propulsive (positive) force. However, when EMG biofeedback was provided the difference between the net mechanical work applied by each lower limb decreased. The contribution of each lower limb to the movement was more balanced, when EMG biofeedback was provided.

The mean muscle activation patterns of the *rectus femoris* of Patient 2, in session 4, without and with

EMG biofeedback, are displayed in Figure 6.10 (a) and (b), respectively.

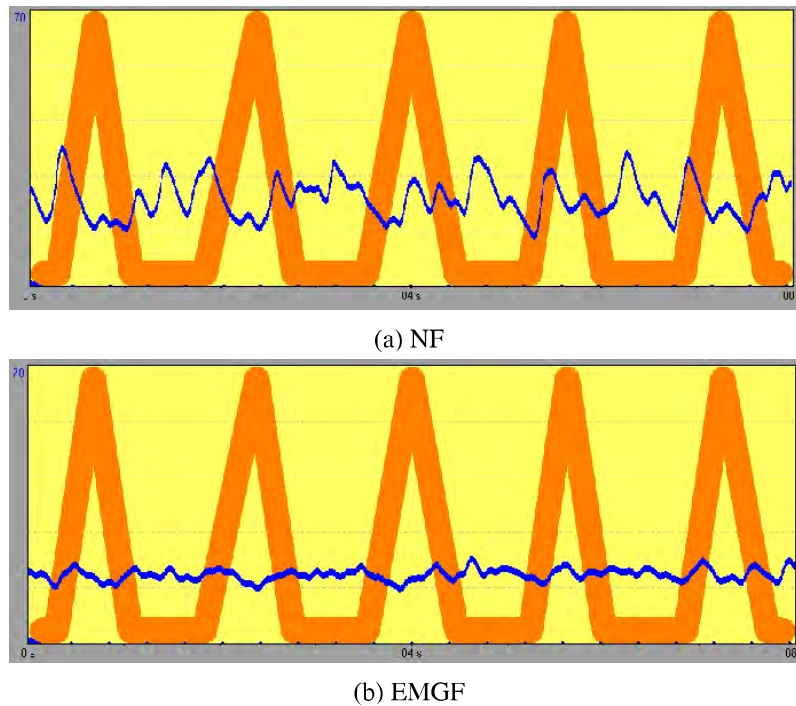


Figure 6.10: *Rectus femoris*' mean activation pattern in the session 4 of Patient 2 with (a) no biofeedback; and (b) EMG biofeedback.

The variation of mean muscle activation pattern without EMG biofeedback is higher than for the EMGF trial. Regarding the EMGF trial, the mean muscle activation pattern does not follow the target signal, as shown in Figure 6.10 (b). Although the patient was able to activate the *rectus femoris* and follow the target signal, during the EMGF trial, in some passages, the muscle activation was out of phase with the target signal, which may be due to the difficulty of synchronizing the training cadence and the muscle activation pattern with the target signal. As this signal results from the average of all passages (60 for the EMG trial), a passage in which the patient fails to synchronize (passages with a shifted muscle activation pattern) or to activate the muscle as expected, due to fatigue or distraction, will influence the final result. The transition from one passage to the next confused the patient and also caused desynchronization of the signals, since it implied a fast patient's reaction to resynchronize both signals. Therefore, the final muscle activation pattern does not follow the target signal. The sensibility value defined in the calibration of the *YSY EST EVOLUTION* device might also be inadequate to the patient performance during the trials. Its value was quite higher ($70 \mu\text{V}$) than the one used in Patient 1 ($8 \mu\text{V}$).

Regarding the pedal angles (β), their behavior did not change significantly when EMG biofeedback was provided. The pedal angle ranged from 5 to 50 degrees, with smaller ranges in some sessions. The difference between the paretic and the lower limb was in the maximum 10 degrees. The pedal angle pattern of both limbs also followed the normal phase shift of 180 degrees.

The mean values of the effective force of both lower limbs of Patient 2, in sessions 4 (top) and 5 (bottom), without (left) and with (right) EMG biofeedback, are presented in Figure 6.11. The grey area represents the upstroke phase of the paretic limb and the shaded area along the curves represents the SD values.

Almost all resistive (negative) force was performed by the paretic limb during its upstroke phase, in

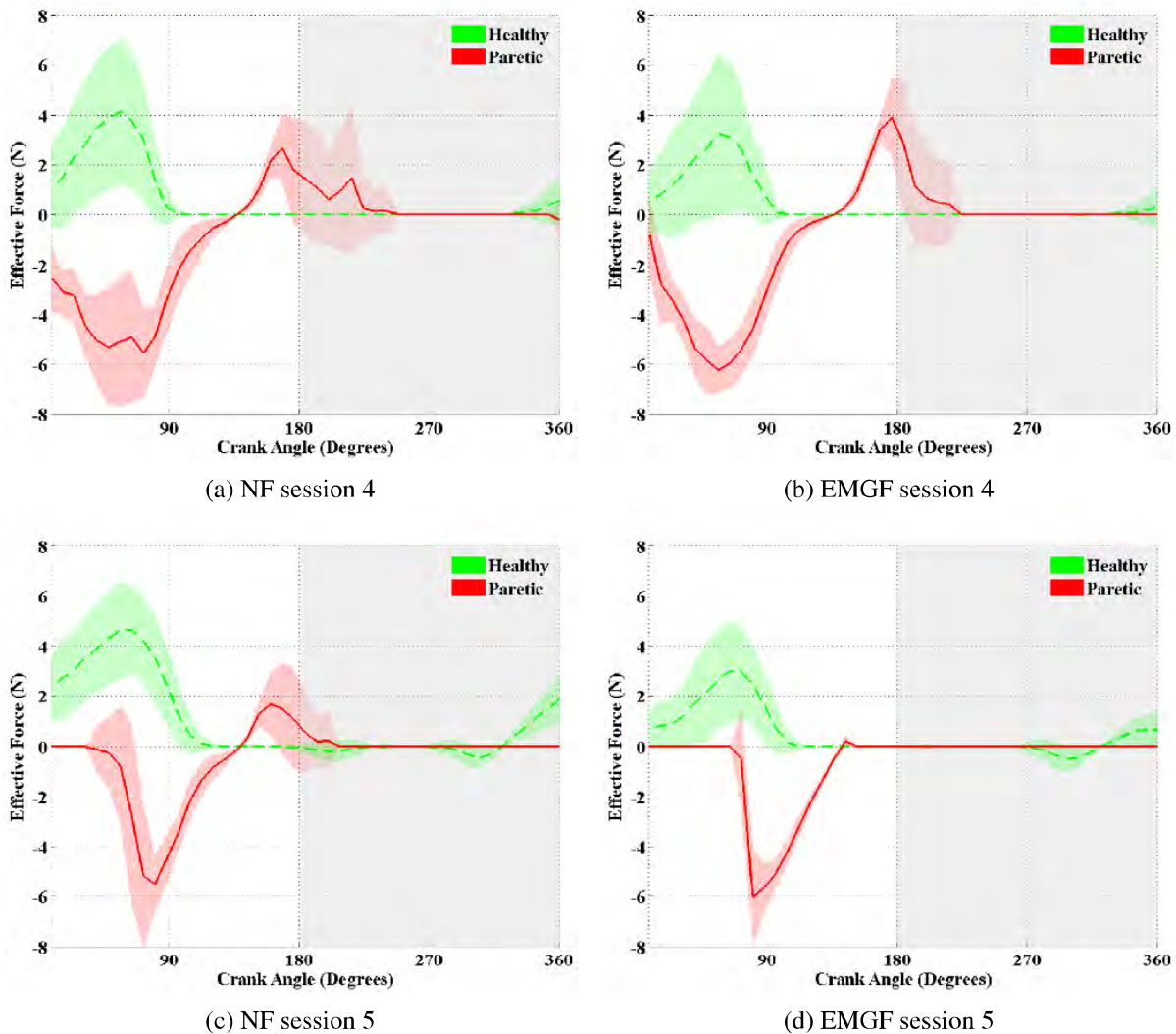


Figure 6.11: Mean values of the effective force for the paretic (solid red line) and healthy (dashed green line) lower limbs, for cycling in session 4 (top) and in session 5 (bottom) with (a) (c) no biofeedback; (b) (d) EMG biofeedback; for sixty revolutions (11th to 70th and 141st to 200th in the NF and EMGF trials, respectively) of Patient 2. The grey area represents the upstroke phase of the paretic limb and the shaded area along the curves represents the SD values.

the sessions 4 and 5, as shown in Figure 6.11. The provision of EMG biofeedback had different results on the effective force pattern, in the two sessions. In the fourth, when EMG biofeedback was provided to the patient, the positive effective force performed by the paretic limb was slightly higher, but the crank angles range, where the propulsive force was applied, was lower. In the fifth session, although the positive effective force performed by the paretic limb reduced to practically zero, when compared to the NF trial, when EMG biofeedback was provided, the range of crank angles in which the paretic limb performed resistive (negative) force was lower. These results show that, in this patient, EMG biofeedback may induce positive changes in the effective force pattern of the paretic limb, by an increase of the applied positive effective force, or by a reduction of the crank angles range in which the paretic limb perform resistive force. These changes resulted in a higher participation of the paretic limb to the movement of the cycling device.

The mean values of the ankle (top), knee (middle) and hip (bottom) moments for paretic (solid red line) and healthy (dashed green line) limbs, without (left) and with (right) EMG biofeedback, of Patient

2, with respect to crank angle, are presented in Figure 6.12, respectively.

The joints' moments, without and with EMG biofeedback, were quite similar, with the exception of the ankle moment, where the moment of the paretic limb in the NF and EMGF is different, since it is possible to identify the absence of positive effective force applied by the paretic limb, observed in the EMGF trial (Figure 6.11 (d)). The ankle moment of the paretic limb also allows the identification of the intervals where the paretic limb performed more resistive force (45 to 135 degrees, approximately), as observed in the effective force patterns (Figure 6.11 (c) and (d)). However, this interval is more evident in the plots of the effective force. Regarding the joints' moments of each lower limb, the behavior of the ankle and knee moments of the paretic and healthy limbs is different, whereas the hip moments are slightly similar.

Performing cycling at a constant cadence and attempt to synchronize the muscle activation pattern with the target signal, may be too complex for a sub-acute stroke patient, which has yet several motor impairments. The duration of the EMGF trial (8 minutes) may be too long and may have resulted in fatigue, which may reduce the effectiveness of providing EMG biofeedback. In addition, if the patient pays more attention to the target signal than to the moment of appropriate muscle activation, unnatural movements may be promoted by the patient.

The absence of the accessory "Leg Support" (Appendix A.6) also did not prevent the hip abduction, hip rotation and the foot inversion in this patient. However, the use of a wheelchair during the intervention allowed a limitation of these unnatural movements in Patient 2.

A reduction of the difference of the net contribution of each lower limb to the movement was observed throughout the sessions, when EMG biofeedback was provided. Therefore, a more balanced cycling was achieved during the EMGF trials. This improvement also was transferred to normal cycling, since it was also observed in the final cycling assessment test, performed at the end of the intervention. Additionally, the patient was able to increase the training workload throughout the intervention, which suggests a learning of how to more effectively exercise on the cycling device and/or an increase of the endurance capacity. Two different positive changes were observed in the force pattern when EMG biofeedback was provided to the patient: an increase in the positive effective force and a reduction of the crank angles range in which resistive force was applied. This results in a higher contribution of the paretic limb to the movement of the cycling device.

6.5.3 Patient 3

Both therapies (force and EMG biofeedback) were tested in Patient 3 with two different purposes. A single session of cycling with force biofeedback was performed by this patient, in order to assess the effects of this therapy on the training variables and on the patient's pedaling strategy. This single session was performed before the implementation of an intervention of EMG biofeedback, in order to study the effects of this therapy on the motor function and on the walking ability, in addition to the assessment of its effects on the pedaling strategy and training variables. The initial assessment tests were performed after the force biofeedback session, in order to isolate any possible effects of the force biofeedback therapy on the patient's motor function from the effects of the EMG biofeedback therapy.

Patient 3 was a sub-acute stroke patient (1.1 months since stroke), which presented right hemiparesis and no ambulatory capacity (unable to walk or stand without assistance). During the intervention period, the patient also performed one hour and a half of conventional physiotherapy and 30 minutes of occupational therapy, every weekday, in the Hospital de Braga. The time since stroke, the hemorrhage stroke,

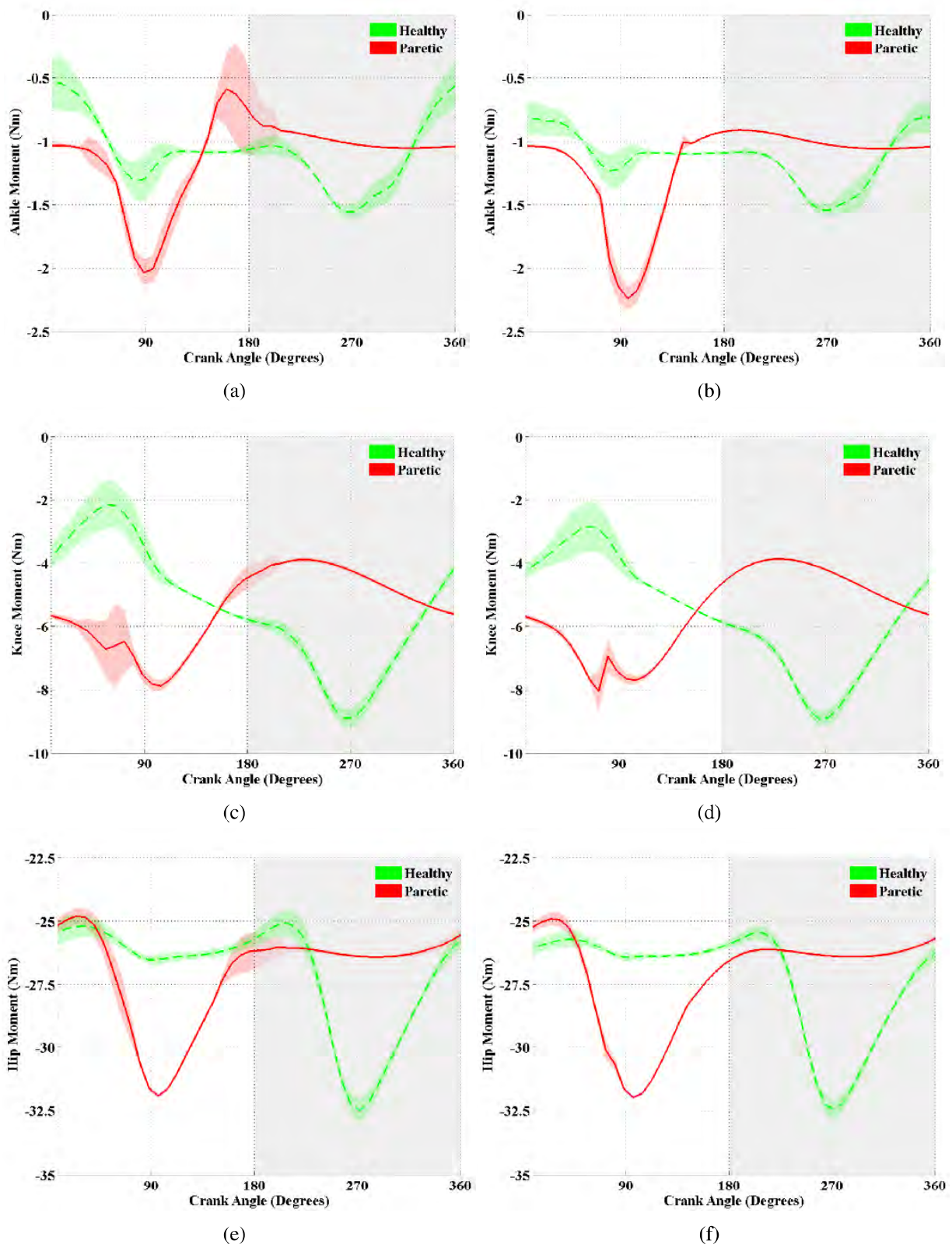


Figure 6.12: Mean values of the ankle (top), knee (middle) and hip (bottom) moments with (a) (c) (e) no biofeedback; and (b) (d) (f) EMG biofeedback, for both lower limbs of Patient 2.

the ongoing physiotherapy and the no ambulatory capacity do not fulfill the inclusion criteria. Similarly to Patient 2, this patient was not able to walk or stand without assistance. Therefore, the Single foot support time test and the 10MWT could not be performed. The assessment tests were performed before performing the first session and after the fifth session of the EMG biofeedback intervention.

A single session of force biofeedback was performed and included three cycling trials: (1) 2 minutes of cycling without force biofeedback (NF); (2) 4 minutes of cycling with force biofeedback updated on each 32 degrees (F32); and (3) 4 minutes of cycling with force biofeedback of half a revolution (FHR). A rest period of 3 minutes was respected between each trial. The training workload was defined, by the comfortable workload test, as 0 Nm. The target band was defined in an initial trial of 10 revolutions at the selected comfortable workload and cadence. In the force biofeedback trials, the patient was instructed to pedal at the comfortable cadence that appeared more adequate to him, to achieve the target band. In addition to the referred metrics, the mean values of the negative (paretic limb performed more work) and positive (healthy limb performed more work) Unbalance Index (U^- and U^+ , respectively), as well as, the number of revolutions whose U was negative, of 60 revolutions (21st to 80th), were analyzed for each trial. The initial revolutions were not considered in order to ensure a lower deviation on the results.

Regarding the EMG biofeedback intervention, this patient performed 5 sessions, during 2 weeks, in which EMG biofeedback was provided. However, the EMGF trial time was reduced from 8 to 4 minutes, in order to prevent the fatigue observed in Patient 2. The training workload and cadence were defined through the comfortable tests, before the beginning of each session. A rest period of 3 minutes was respected between each trial. The data of 60 revolutions (16th to 75th for the trials without biofeedback, and 101st to 160th for the EMG biofeedback trials) was analyzed for each biofeedback condition. The initial revolutions were not considered in order to ensure a lower deviation on the results.

Patient 3 also performed the intervention on a wheelchair with 46 centimeters of height. The remaining parameters were similar to the previous studies.

6.5.3.1 Assessment

The FMA score and the ROM of the paretic limb's joints of Patient 3, assessed by a physiatrist, at the beginning and at the end of the intervention, are presented in Table 6.11.

Table 6.11: Patient 3 assessment tests' scores

Tests		Begin	End
FMA	Lower Limbs (maximum 40)	14	20
	Balance (maximum 14)	5	7
ROM	Hip	Preserved	Preserved
	Knee	Preserved	Preserved
	Ankle	Preserved	Preserved

The FMA' scores in Patient 3 were lower than the other two patients. After the intervention the score of this patient increased in both domains (lower limbs and balance). However, this improvement may not be attributed entirely to the EMG intervention, once the patient was performing daily physiotherapy and occupational therapy, in addition to the intervention. As this patient is a sub-acute stroke patient, this improvement may also be due to spontaneous recovery.

The training parameters measured on the initial and final cycling assessment tests are presented in Table 6.12.

The training parameters of the initial and final cycling assessment tests are quite similar. However, as in Patient 2 and in Ferrante *et al.* [18], although net mechanical work performed by the paretic limb was

Table 6.12: Mean (SD) values of the training parameters of the initial and final cycling assessment tests of Patient 3

Tests		Begin	End
Mean Net Mechanical Work	Paretic Limb (W_{PL})	-0.53 (0.48)	-2.70 (0.54)
	Healthy Limb (W_{HL})	6.10 (3.62)	1.17 (0.65)
Mean Unbalance Index (U)		98.26 (6.14)	99.86 (0.80)
Mean Absolute Unbalance Index ($ U $)		98.26 (6.14)	99.86 (0.80)
$U < 0$ (number of revolutions)		0	0
$ U \leq 25\%$ (number of revolutions)		0	0
Mean Cadence (rpm)		41.98 (1.62)	42.94 (0.97)
Muscle Activation Rate (MAR)		0.42	0.4

lower (more resistive work), the difference between the net mechanical work performed by each limb was smaller in the final assessment test, due to a reduction of the net mechanical work performed by the healthy limb (W_{HL}). Therefore, this intervention also resulted in a more balanced cycling exercise, since the contribution of both limbs to the moment became more identical.

6.5.3.2 Results and Discussion

Force Biofeedback

Patient 3 performed all force biofeedback trials with success. The mean cadence, mean absolute, negative and positive Unbalance Index values ($|U|$, U^- and U^+ , respectively), as well as, the number of revolutions where the paretic limb performed more work, in which the $|U|$ was less than or equal to 25% and that fulfill the target band, for each type of force biofeedback, are presented in Table 6.13.

Table 6.13: Mean (SD) values of cadence, absolute, negative and positive Unbalance Index values and number of revolutions that fulfill the conditions, in the different trials of the force biofeedback of Patient 3

Tests	NF	F32	FHR
Mean Cadence (rpm)	42.67 (0.97)	21.59 (8.34)	39.68 (1.42)
Mean Absolute Unbalance Index ($ U $)	68.37 (36.40)	32.73 (21.16)	50.17 (35.45)
Mean Negative Unbalance Index (U^-)	-62.67 (37.26)	-31.70 (30.82)	-54.22 (37.51)
Mean Positive Unbalance Index (U^+)	71.44 (36.04)	32.96 (18.77)	40.76 (28.87)
Unbalance Index < 0 (number of revolutions)	21	11	42
Absolute Unbalance Value $\leq 25\%$ (number of revolutions)	10	25	19
Within objective band (number of revolutions)	0	4	5

The cadence was similar in all trials, with the exception of the F32 trial. The lower cadence of this trial may be a pedaling strategy, adopted by Patient 3, in order to achieve a higher symmetry, since the patient was instructed to pedal at the comfortable cadence that appeared more adequate to him, to achieve the target band. At lower cadence the patient may have a higher control on the force applied by each lower limb.

The trials where force biofeedback was provided to Patient 3 (F32 and FHR) present the higher symmetry (lower $|U|$, U^- and U^+ values), which suggests force biofeedback was effective on promoting the cycling symmetry. During the NF trial, the paretic limb performed a higher contribution than the healthy one in 21 of 60 revolutions, being this trial the one with a higher U^- . The F32 trial was the most effective in the adoption of a symmetrical cycling (lower $|U|$, U^- and U^+ values and higher number of revolutions with $|U|$ less than or equal to 25% (25 of 60 revolutions), which may be due to the higher feedback frequency, since the bars are updated 11 times against the 2 times of the FHR training. The number of revolutions in which the paretic limb performed more work than the healthy one, was higher in the FHR trial (21 in the NF; 11 in the F32 and 42 in the FHR of 60 revolutions). Nevertheless, FHR had a lower U^- than the NF, meaning that higher symmetry was achieved, during these 42 revolutions

of the FHR trial. The number of revolutions in which the bars fulfill the target band was, once again, significantly lower than the number of revolutions with $|U|$ less than or equal to 25%. Therefore, as the $|U|$ of a revolution that fulfil the target band is less than or equal to 25%, this great difference suggests the condition that defines the target band values is not the most adequate.

The mean values of the pedal angle (β) of the paretic (solid red line) and healthy (dashed green line) limbs, for each biofeedback trial (NF (a), F32 (b) and FHR (c)), with respect of the crank angle are represented in Figure 6.13. The grey area represents the upstroke phase of the paretic limb and the shaded area along the curves represents the SD values.

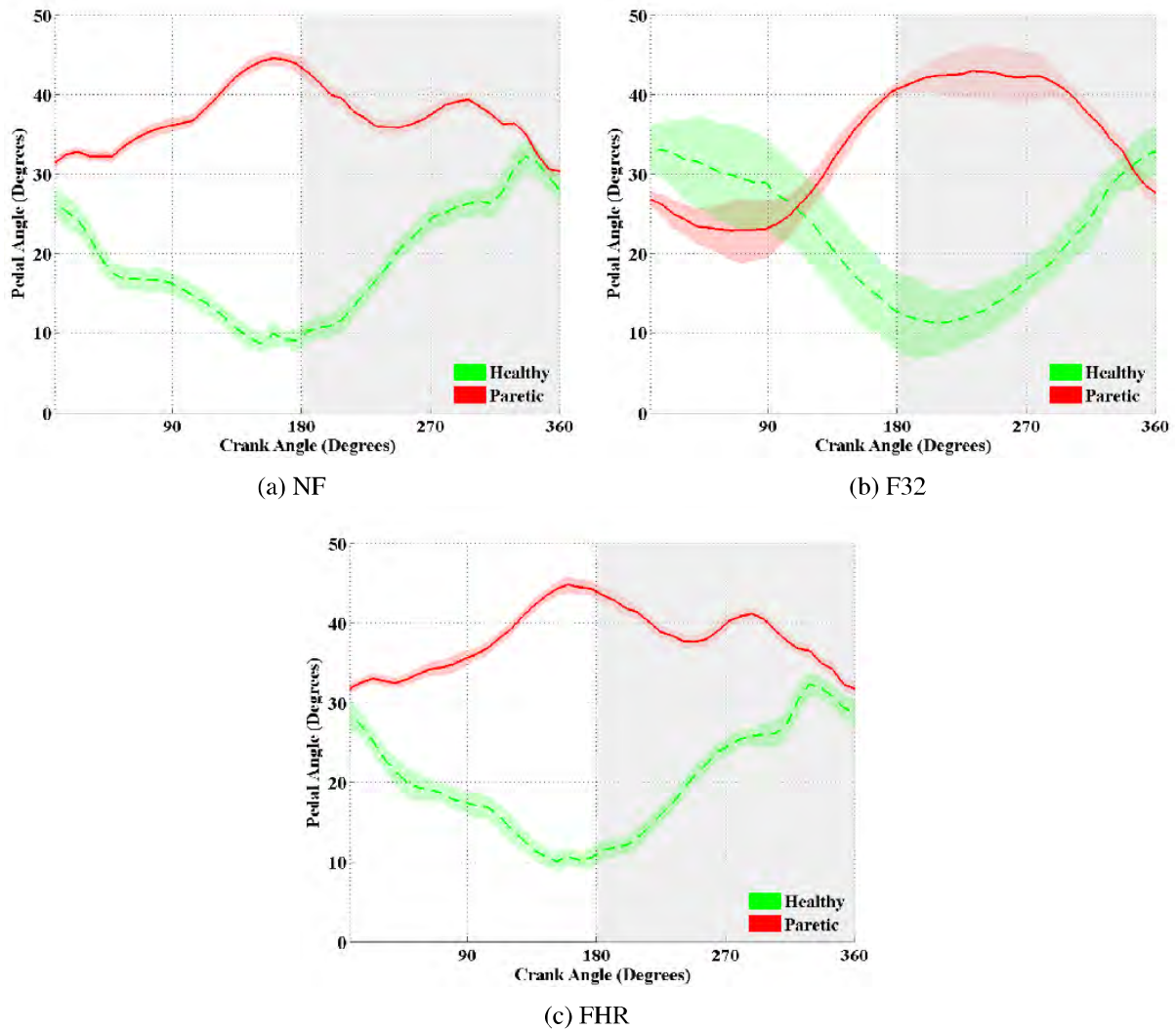


Figure 6.13: Mean values of the pedal angle for both lower limbs, for cycling with (a) no biofeedback (NF); (b) force biofeedback updated on each 32 degrees (F32); and (c) force biofeedback of half a revolution (FHR), for sixty revolutions (21st to 80th) of Patient 3. The grey area represents the upstroke phase of the paretic limb and the shaded area along the curves represents the SD values.

The pedal angle pattern was similar in the NF trial and in the FHR trial. Although the behavior of each lower limb is the same (increase of the angle during upstroke phase and reduction during the downstroke phase), the range of the angle values is different. The β of the healthy limb ranged from 10 to 30 degrees, whereas in the paretic limb it ranged from 30 to 45 degrees, approximately. These different ranges may be due to a lower control of the paretic limb's foot. A different pattern is observed in the F32 trial, where β follows approximately a sinusoidal behavior, which may be due to the higher

biofeedback frequency, and suggests the patient adopted a different pedaling strategy in order to fulfill the force biofeedback objective.

The mean values of the effective force applied by the paretic (solid red line) and healthy (dashed green line) limb, for each biofeedback trial (NF (a), F32 (b) and FHR (c)), with respect of the crank angle are represented in Figure 6.14.

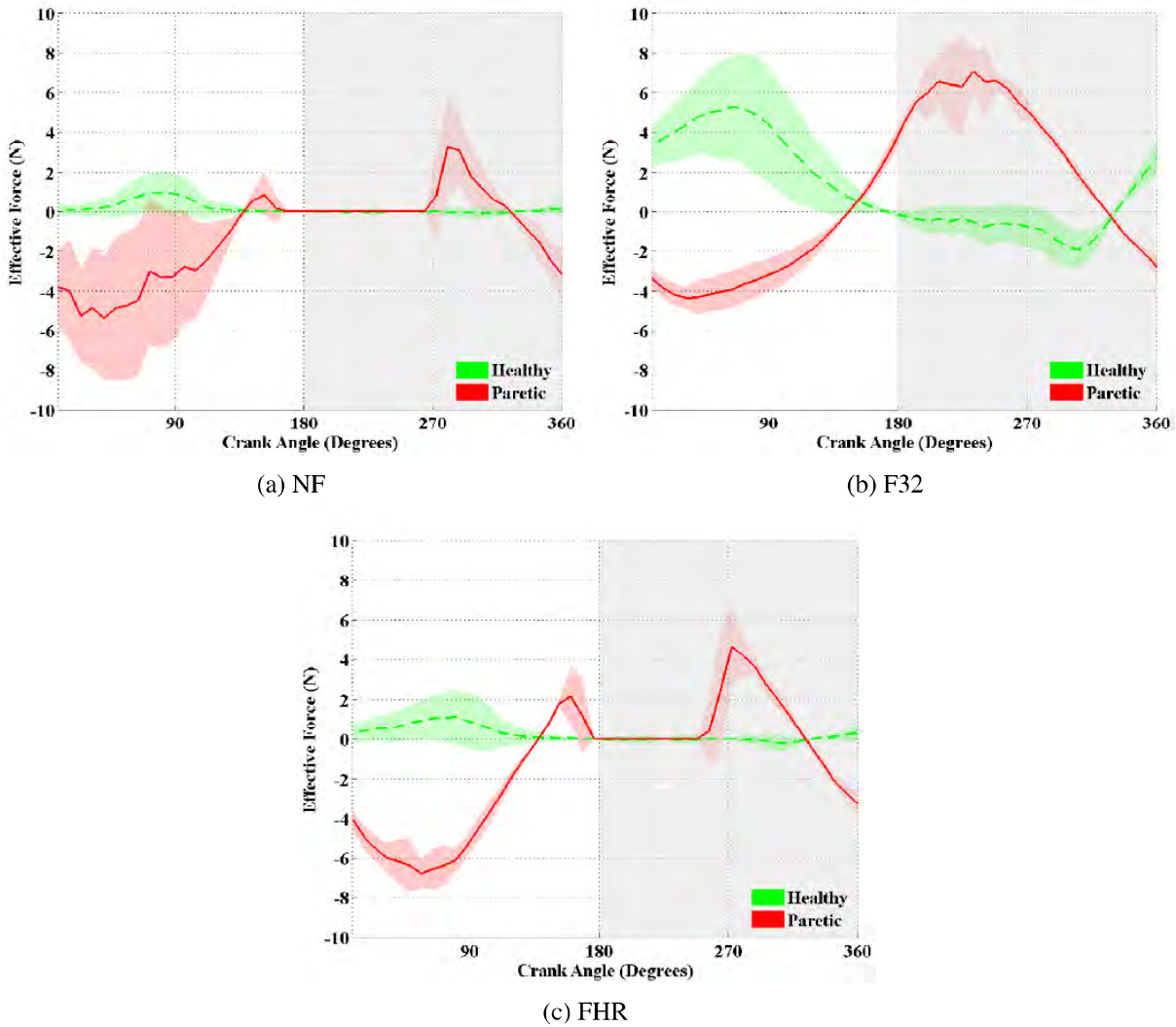


Figure 6.14: Mean values of the effective force for both lower limbs, for cycling with (a) no biofeedback (NF); (b) force biofeedback updated on each 32 degrees (F32; and (c) force biofeedback of half a revolution (FHR), of Patient 3.

In the trial without biofeedback (NF) and in the FHR trial (Figure 6.14 (a) and (c)), the paretic limb performed more propulsive force (positive effective work) than the healthy one. However, the amount of the resistive force performed by the paretic limb, when comparing with the healthy limb, was higher. In these two trials, the patient was not able to apply force when the paretic limb was extending in relation to the body position, since propulsive force was not produced by the paretic limb, during the first half of the downstroke phase (180 to 270 degrees, approximately). The amount of positive effective force performed by the paretic limb, during the second half of the downstroke phase (270 to 360 degrees, approximately), was higher in the FHR trial than in the NF trial. As the FHR training type only considers the amount of force applied during the downstroke, the reduction of the resistive force during the upstroke phase is not promoted. The force pattern of each lower limb, during the F32 trial, is similar. The paretic

limb applied more resistive force (negative effective force), but the force pattern behavior and ranges are similar, which suggests the success of this type of feedback in increasing the force pattern symmetry.

The provision force biofeedback resulted in an increased cycling symmetry. Force biofeedback updated on each 32 degrees (F32) resulted in the highest symmetry, and was the one where the lower U is the result of a similar force pattern behavior. The adoption of a different pedaling strategy, in this type of force biofeedback, is also observed through the pedal angle (similar behavior and ranges for both lower limbs). The provision of FHR increased symmetry between the force applied during the downstroke phase, but had no positive effect in the resistive force applied during the upstroke phase, since, in this biofeedback type, it is not considered in the generation of the force biofeedback. Therefore, the F32 training will promote the coordination, since it requires a balance between the propulsive and resistive force, whereas the FHR training will promote only the amount of applied produced during the upstroke phase, which may increase the muscle strength, but has no effects on the coordination.

EMG Biofeedback

All sessions of the EMG biofeedback intervention were successfully performed by Patient 3. The mean workload and cadence values of each trial (without and with EMG biofeedback – NF and EMGF, respectively) for each session are presented in Table 6.14. The results regarding the NF trial are from the first trial without biofeedback of the protocol (Section 6.4.3).

Table 6.14: Used workload and target cadence values; and mean (SD) cadence measure in the NF and EMGF trials, for each session, of Patient 3

Trial	Workload (Nm)	Target Cadence (rpm)	Mean Cadence (rpm)
1st Session	NF	3	41.98 (1.62)
	EMGF		44.90 (1.11)
2nd Session	NF	2	48.59 (0.58)
	EMGF		42.94 (1.25)
3rd Session	NF	3	39.22 (1.52)
	EMGF		43.59 (1.95)
4th Session	NF	3	40.37 (2.88)
	EMGF		42.29 (1.95)
5th Session	NF	3	42.92 (0.97)
	EMGF		45.59 (1.30)

The workload values defined through the comfortable workload tests were the same (3 Nm) in all trials, with the exception of the second session (2Nm). This patient was able to start the intervention at a higher workload than Patient 2. Regarding cadence, the measured values, in the different sessions, were close to the target cadence, which suggests it was appropriate to the patient ability.

The values of the MAR of the *rectus femoris* of Patient 3, for all sessions without and with EMG biofeedback (NF and EMGF – solid red and dashed green lines, respectively), are presented in Figure 6.15.

The MAR values were lower in the trial without biofeedback, in the two first and in the last sessions, whereas higher MAR values were measured in the third and fourth sessions. The initial higher values, for the EMGF trial, may be due to the learning period. In the beginning, as the patient was not experienced with the cycling device, providing biofeedback of the muscle activation pattern may help the patient to better understand the moment and the movement of activation of the studied muscle. Then, the action adopted by the patient to follow the target signal, during the EMGF trial, might limit the MAR value. As in the final sessions, the patient had already knowledge of the movement and moment to activate the target muscle, and as during the NF the muscle activation is not limited by the intentional action of the

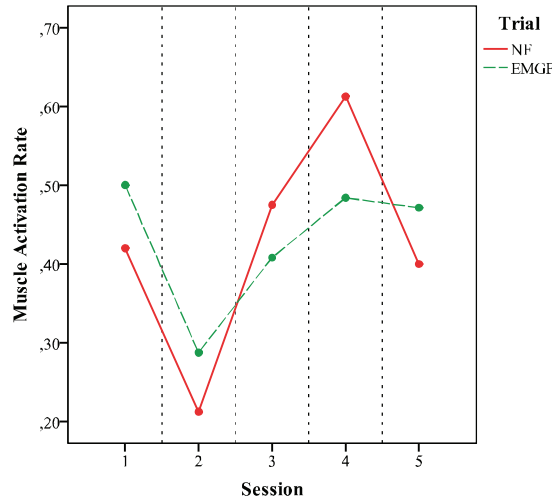


Figure 6.15: Values of the MAR of the *rectus femoris* muscle of Patient 3, for the 5 sessions, without and with EMG biofeedback (NF and EMGF, respectively).

patient, higher MAR values were achieved in trial without EMG biofeedback.

The mean values of the net mechanical work (W) performed by each lower limb of Patient 2, without and with EMG biofeedback, for all five sessions, are presented in Figure 6.16. The W_{PL} and W_{HL} in the NF trial are represented by the solid red and dotted green lines, respectively, whereas the W_{PL} and W_{HL} in the EMGF trial are represented by the dash-dot blue and dashed black lines.

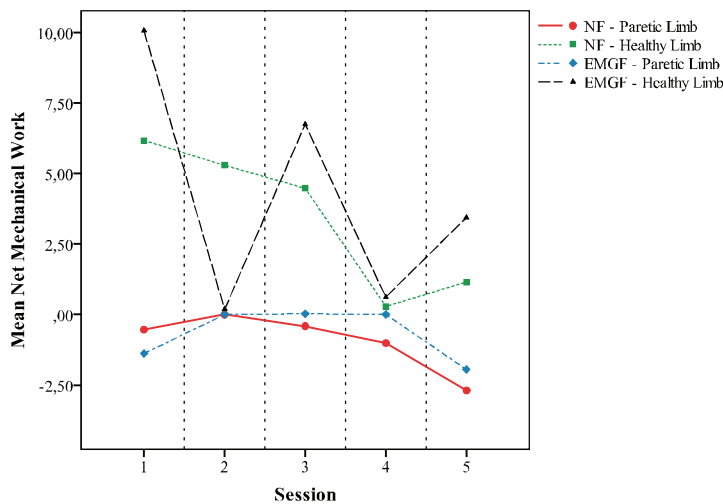


Figure 6.16: Mean values of the net mechanical work performed by the paretic and healthy limbs in the NF trial (solid red and dotted green lines, respectively) and in the EMGF trial (dash-dot blue and dashed black lines, respectively), of Patient 3.

As in Patient 2, the net contribution of the paretic limb (W_{PL}) of Patient 3, without and with EMG biofeedback, was similar and always negative or zero. However, unlike Patient 2, during the trials with EMG biofeedback, the healthy limb performed more net mechanical work than in the trials without biofeedback, with the exception of the second and fourth sessions, where the net contribution of both limbs was quite low. The effect of providing of EMG biofeedback on the net mechanical work was inconclusive. The mean muscle activation patterns of the *rectus femoris* of Patient 3, in session 3 without biofeedback (top) and with EMG biofeedback in session 3 (middle) and session 4 (bottom), are presented in Figure 6.17.

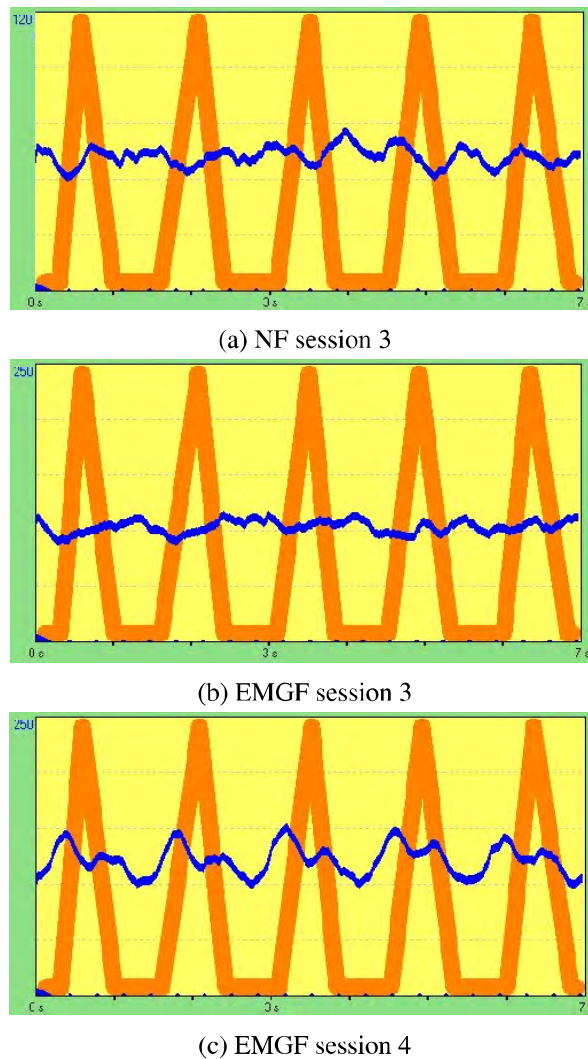


Figure 6.17: *Rectus femoris*' mean activation pattern of Patient 3: (a) session 3 without biofeedback; (b) session 3 with EMG biofeedback; and (c) session 4 with EMG biofeedback.

The provision of EMGF biofeedback resulted in a higher RF activation, since the value of sensibility increased from 120 to 250 μV , as shown in Figure 6.17 (a) and (b). The patient was able to better follow the target signal, in the fourth session than in the third session, when EMG biofeedback was provided. The patient may have had more success in synchronize the muscle activation pattern and the target signal in session 4. In this last session, although Patient 3 was able to follow the target signal, the difference between the signal peaks and the signal minimums is lower. The lower amplitude may be due to the influence of passages in which the muscle activation pattern did not follow the target signal (desynchronization), since the signals presented in Figure 6.17 result from the average of 17 and 34 passages, for the NF and EMGF trials, respectively. The transition from one passage to the next implied a fast patient's reaction, in order to resynchronize the muscle activation pattern with the target signal, which, sometimes, confused the patient and caused desynchronization of the signals, influencing negatively the average of muscle activation pattern. Once again, these results suggest this intervention may be too complex for the characteristics of the patient, since he had to control the cycling exercise while simultaneously receiving and interpreting the EMG biofeedback, which may have influenced the results obtained.

The mean values of the pedal angle (β) evolution for the paretic (solid red line) and healthy (dashed green line) limbs of Patient 3, in session 3 without biofeedback (a) and with EMG biofeedback in session

3 (b) and session 4 (c), are presented in Figure 6.18, respectively. The grey area represents the upstroke phase of the paretic limb and the shaded area along the curves represents the SD values.

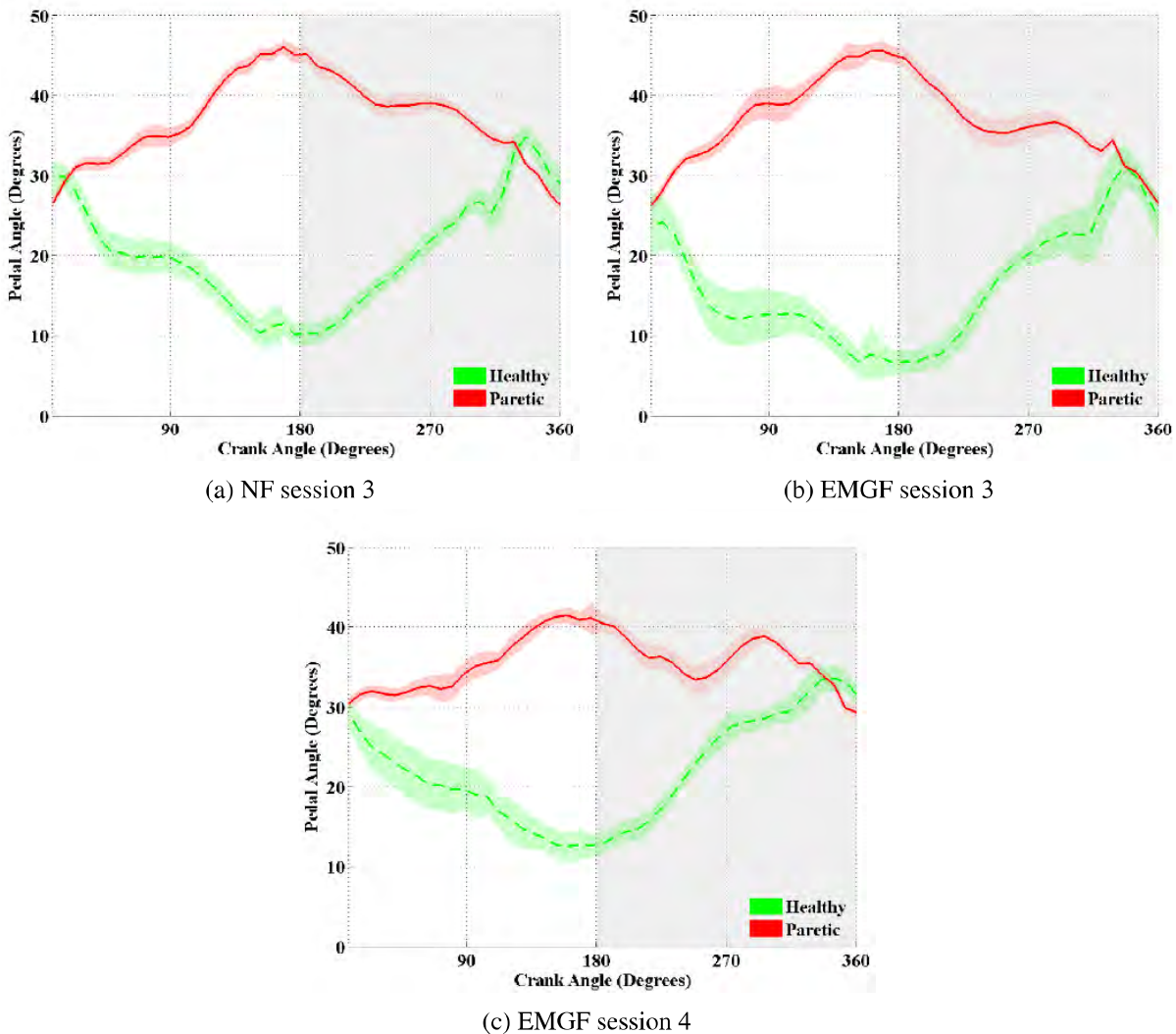


Figure 6.18: Mean values of the pedal angle for both lower limbs, for cycling (a) without biofeedback (session 3); (b) with EMG biofeedback (session 3); and (c) with EMG biofeedback (session 4), for sixty revolutions (16th to 75th in the no biofeedback trial, and 101st to 160th for the EMG biofeedback trials) of Patient 3. The grey area represents the upstroke phase of the paretic limb and the shaded area along the curves represents the SD values.

The pedal angle pattern was similar in the NF trial and in the EMGF trials. This pattern was also similar to the one observed in some force biofeedback trials. The behavior of β was the same for both lower limbs, but the angle ranges of each limb were different. The healthy limb (dashed green line) ranged from 5 to 35 degrees, whereas the paretic limb (solid red line) ranged from 25 to 45 degrees. These different ranges may be due to a lower control of the paretic limb's foot. The provision of EMG biofeedback did not result in a change of the patient's pedaling strategy regarding the pedals angles, as opposed to the force biofeedback (F32).

The mean values of the effective force for the paretic (solid red line) and healthy (dashed green line) limbs, in session 3 without biofeedback (a) and with EMG biofeedback in session 3 (b) and session 4 (c), are presented in Figure 6.19.

In session 3, the contribution of the paretic limb (solid red line) decreased, when EMG biofeedback was provided. Although the resistive force applied by the paretic limb decreased, the positive effective

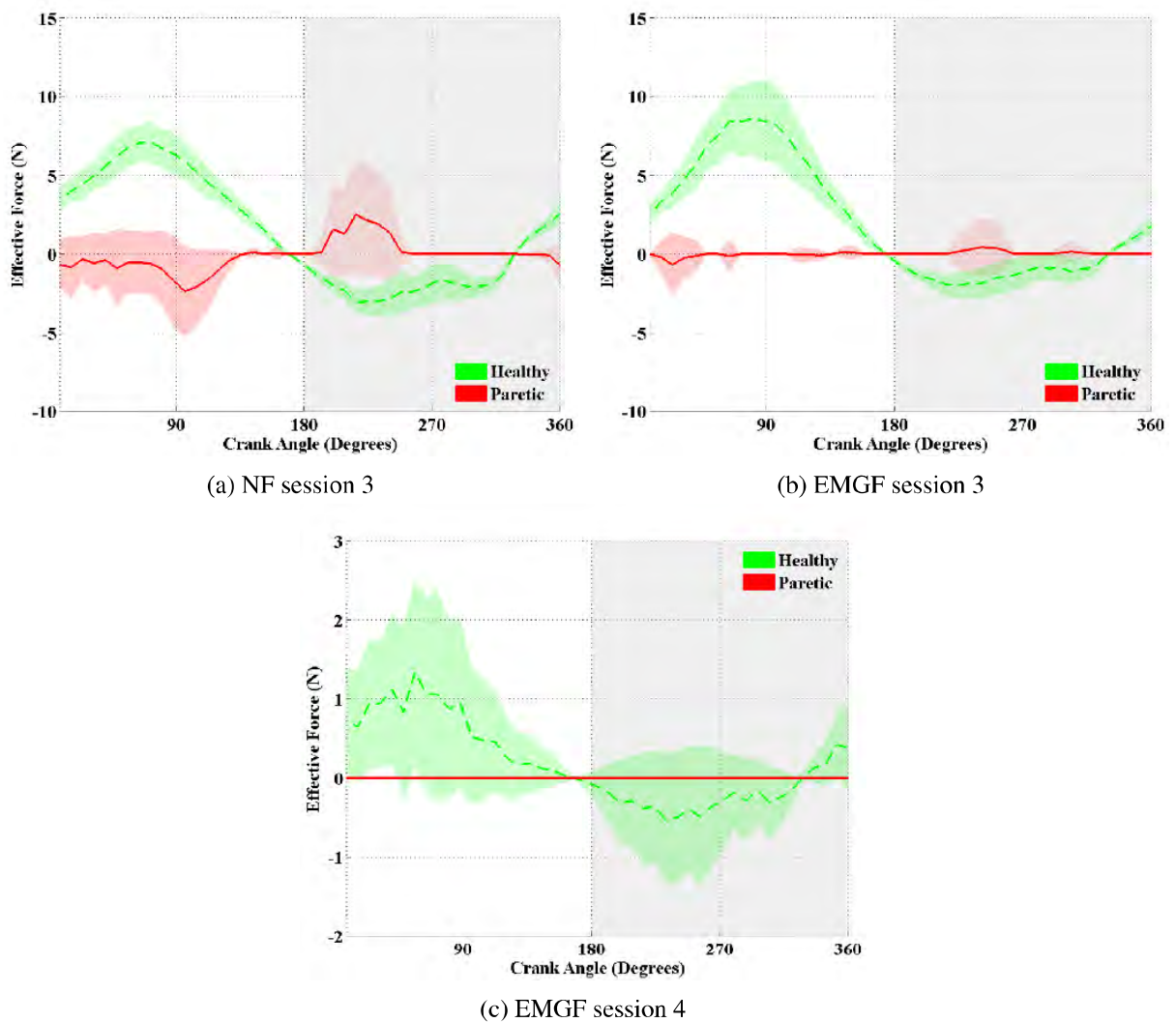


Figure 6.19: Mean values of the effective force for both lower limbs, for cycling (a) without biofeedback (session 3); (b) with EMG biofeedback (session 3); and (c) with EMG biofeedback (session 4), of Patient 3.

force also decreased to a value closer to zero. Regarding the fourth session, the contribution of the healthy limb (dashed green line) was lower, when comparing to the anterior session, and there was no contribution of the paretic limb. However, in this session, the mean muscle activation pattern, when EMG biofeedback was provided (Figure 6.17 (c)), was the one that better followed the target signal, even without the participation of the paretic limb in the movement. This patient might have used only the healthy limb to propel the cycling device and keep it in a constant cadence, while the paretic limb only performed the movement of activation (during the upstroke phase). Due to the phase of activation of the RF upward force, which is not measured in this study, might have been applied by the patient, in order to increase the RF's activation. This situation, as previously observed, may be due to the complexity of this intervention to a sub-acute patient. A solution may be the use of a cycling device with an isokinetic mode, where the cadence is always maintained constant, regardless the applied force (the training workload is automatically adjusted). Therefore, the patient could focus exclusively in the muscle activation, instead of to attempt to keep a constant cadence, in order to synchronize the muscle activation pattern with the target signal.

Although a reduction of the difference of the net contribution of each lower limb to the movement

was observed in the final assessment, the EMG intervention did not result in clear improvements on the training variables. Providing EMG biofeedback had no positive effect on the contribution of the paretic limb to the movement, since there was no contribution of the paretic limb, in the session in which the mean muscle activation pattern better followed the target signal. The FMA score increased from the beginning to the end of the study. However, this improvement may be due to the spontaneous recovery, to the conventional physiotherapy and occupational therapy or to the intervention.

The absence of the accessory “Leg Support” affected the performance of Patient 3 since, hip abduction, hip rotation and the foot inversion were observed during the intervention. In this case, the wheelchair did not prevent these unnatural movements.

The effective force values may have been influenced by the initial calibration (Section 6.4.2). As this calibration is performed in the passive mode (average of the force applied during 10 revolutions, for each lower limb), if the patient does not follow the movement of the pedals and performs resistance to the movement, for instance, with the paretic limb, the computed constants may have a higher value, which is not representative of the limbs’ weight and inertia. Consequently, the value of the force measured during the trials will be low, due to this calibration. Therefore, the way to reduce the effect of the limbs’ weight and inertia should be reviewed.

6.6 Conclusions

A study was designed, in order to assess whether the application of force or EMG biofeedback influence the users’ pedaling strategy, the training variables and, the most important, if either of the therapies results in improvements on the stroke patients’ motor function, specially the locomotor abilities.

The adequate sample size was determined as 87 subjects, which would be divided in three groups. The first group (CTG) received no treatment; the EG1 performed an intervention of cycling with EMG biofeedback and; the last group (EG2), performed cycling with force biofeedback. All subjects of all groups performed an initial and final assessment, where the subjects’ motor function and cycling performance were assessed.

The intervention included 5 sessions of 14 minutes, during 2 weeks, where 5 trials were performed: (1) 1 minute of passive cycling; (2) 2 minutes of active cycling; (3) 8 minutes of active cycling with biofeedback (EMG (*rectus femoris*) or force biofeedback); (4) 1 minute of passive cycling; and (5) 2 minutes of active cycling. Due to lack of stroke patients that fulfilled the inclusion and exclusion criteria and due to time limitations, the planed protocol could not be implemented. However, different components and conditions of the designed study were implemented in three stroke patients. Single sessions of the studied therapies were conducted, in order to assess theirs effects on the pedaling strategy and on the training variables. Patient 1 performed a single session of force and EMG biofeedback, while Patient 3 performed a single session of force biofeedback. The planed intervention (5 sessions during 2 weeks) of cycling with EMG biofeedback was applied in two patients (Patient 2 and Patient 3), in order was to assess the effects of this therapy on the patients’ motor function, during cycling and walking, in addition to the assessment of therapy effects on the pedaling strategy and training variables.

Patient 1 is a hemorrhage chronic stroke patient with left hemiparesis. His FMA score was 24 for the lower limbs and 12 for balance. The single foot support time was 2 seconds for the paretic and more than 20 seconds for the healthy one. The initial cycling assessment showed that the paretic limb performed a positive W , but contributed less to the movement than the healthy one. Patient 1 performed a single

session of force and EMG biofeedback. Regarding force biofeedback, this patient performed 3 trials of 2 minutes of NF, F32 and FHR. Although the provision of force biofeedback resulted in a higher negative, positive and absolute Unbalance Index (U^- , U^+ and $|U|$, respectively), the contribution of the paretic limb to the movement increased. The force pattern showed that the paretic limb applied more positive effective force than the healthy one, but the amount of resistive force, during the upstroke phase, was also higher, resulting in a lower W . The lower U , achieved in the NF trial, did not correspond to a symmetrical force pattern. Although the force pattern of the NF and F32 trials was similar, the standard deviation of the F32 trial was higher, suggesting a changing in the user's pedaling strategy. Patient 1 also performed 2 trials of 3 minutes of cycling with EMG biofeedback (NF, EMGF). In the NF trial, the W of the paretic limb was negative and lower than the W of the healthy one. When EMG biofeedback was provided, the W of the paretic limb became positive and higher than the healthy limb. The force pattern of the paretic limb changed from a limb with a minimal contribution to the movement (higher effective force, but also higher resistive force), to a limb that performed more effective force and with an amount of resistive force similar to the healthy limb. In addition, the pedal angle (β) patterns became similar, by increasing the pedal angle range of the paretic limb. The paretic limb increased its range of movement in the pedal and followed the same pattern that the healthy limb, which had not occurred in the NF trial.

Patient 2 is an ischemic sub-acute stroke patient with right hemiparesis, and with no ambulatory capacity. The designed intervention of EMG biofeedback (5 sessions during 2 weeks) was implemented in this patient. The patient was able to increase the training workload throughout the intervention, which suggests a learning of how to more effectively exercise on the cycling device and/or an increase of the endurance capacity. Although the W performed by the paretic limb was always negative (performed more resistance to the movement than contribution), with EMG biofeedback the difference between the W of both lower limbs was slightly lower. Therefore, after the EMG intervention the contribution to the movement of both lower limbs was more similar. Two different changes were observed in the force pattern of the paretic limb when EMG biofeedback was provided: an increase of the positive effective force or a reduction of the crank angles (ϕ) where resistive force was applied. The paretic limb increased its contribution to the movement, by increasing the propulsive force or by reducing the resistance to movement. These results suggest providing EMG biofeedback will result in a change in the user's pedaling strategy. Regarding the FMA scores, they were 15 and 7 for the lower limbs and balance, respectively. The difference between the contribution of each limb reduced between the initial and the final cycling assessment, due to a reduction of the W performed by the healthy limb.

Patient 3 is a hemorrhage sub-acute stroke patient with right hemiparesis, and with no ambulatory capacity. The designed intervention of EMG biofeedback was also implemented in this patient, but the training time of the trial with biofeedback was reduced to 4 minutes. Apparently, no effects on the cycling performance and on the training variables resulted from providing EMG biofeedback. For instance, there was no contribution of the paretic limb in the trial where the mean muscle activation pattern better followed the target signal. However, the FMA score of this patient improved between the beginning and the end of the EMG intervention. The lower limbs score improved from 14 to 20, while the balance score improved from 5 to 7. This motor function improvement may have resulted from the EMG intervention, conventional physiotherapy and occupational therapy, and from spontaneous recovery. Regarding the cycling performance at the end of the intervention, the difference between the W performed by each lower limb was lower, due to a reduction of the W performed by the healthy limb, similarly to Patient 2. The EMG intervention resulted in a more balance contribution of each lower limb to the movement.

In addition to the EMG biofeedback intervention, this patient performed a single session of cycling with force biofeedback (2 minutes of NF and 4 minutes of F32 and FHR). The F32 trial was the most effective in increasing the symmetry of cycling, since lower U values, similar pedal angles ranges and similar force patterns were achieved. In the NF and FHR trials, the paretic limb performed more work than the heathy one, but the amount of resistive force was quite higher. These results suggest that F32 promotes the changing of the user's pedaling strategy and improves the cycling symmetry.

7. Conclusions and Future Work

7.1 Conclusions

The intent of this study was to assess the application of cycling leg exercise together with force or EMG biofeedback in the rehabilitation of stroke patients. Several Research Questions were raised at the Introduction and have been answered throughout the document. In this chapter, these answers are collected and surveyed, as follows.

Three key aspects had to be analyzed in different periods of the application of these therapies, in order to clarify the relevance and the effects of cycling with force or EMG biofeedback, before recommend the application of these therapies in the stroke rehabilitation (#RQ1).

The first aspect is to assess the effects of providing each therapy on the patient's pedaling strategy and on the cycling performance (#RQ4). This was assessed by comparing the training variables, such as the applied effective force (F), the pedal angles (β), Unbalance Index (U) and muscle activation (MAR), during cycling without and with each type of biofeedback.

Then, is required to evaluate the effects of providing the therapy during several sessions, by analyzing whether the cycling performance (through training variables) improve, over the course of the sessions (#RQ3). This aspect was assessed by analyzing the evolution of the variables throughout the sessions.

The last aspect is to assess if the application of the therapies over a period of time results in improvements on the patient's motor function (#RQ2). The initial and final walking and cycling assessment tests, as well as, the FMA and ROM were used to assess the occurrence of improvements on the patient's motor function, after the an intervention of cycling with biofeedback.

The systems used to provide force and EMG biofeedback were tested in healthy subjects (Chapter 5). The trials regarding healthy subjects were performed in order to test and optimize the systems used to provide force and EMG biofeedback. The relevance of providing a target band and a target signal, in the force and EMG biofeedback's systems, was analyzed, as well as, the most appropriate feedback frequency. In addition, these tests were also used to perform an initial analysis of #RQ4, since, whether changes on the users' pedaling strategy and cycling performance are observed in healthy subjects, they are also likely to be observed in stroke patients.

Regarding force biofeedback, the healthy subjects were able to reduce the asymmetry of the force applied by each limb and changed their pedaling strategy when force biofeedback was provided. The provision of a target band allowed to have a visual reference to achieve the training objective. The results also showed that the F32 trial was the most effective in the achievement of the cycling symmetry,

followed by the FHR. The F32 trial promoted a coordinate action of both limbs during both phases of cycling, whereas the FHR trial promoted the propulsive force applied by each limb (downstroke phase). The tests of EMG biofeedback in the healthy subjects, showed that the region of activation of the selected muscle (*rectus femoris*) is the same as in a standard cycling device. In addition, it also showed that the users were able to increase their muscle activation pattern and to synchronize the muscle activation pattern with the target signal, when EMG biofeedback was provided.

A study, presented in Chapter 6, was designed to assess the three identified aspects (#RQ2, #RQ3 and #RQ4), in stroke patients, but was not fully implemented. Two different approaches were implemented in order to analyze the relevance of cycling with force or EMG biofeedback in the stroke rehabilitation.

Single sessions of cycling with force biofeedback or EMG biofeedback were performed, in order to analyze whether these therapies induced changes in the patient's pedaling strategy (#RQ4), which would allow to support the application of these therapies during several sessions. Therefore, Patient 1 performed a single session in which different trials of force and EMG biofeedback were tested, whereas Patient 3 performed a single session of force biofeedback trials.

The effects of an intervention of cycling with EMG biofeedback on the cycling performance and on the patient's motor function were assessed in two stroke patients (Patient 2 and Patient 3), which performed the suggested protocol (5 sessions, during 2 weeks). These interventions also allowed to assess the effects of providing EMG biofeedback on the cycling performance and on the patients' pedaling strategy. The results observed in the three stroke patients are presented in Chapter 6.

The provision of force biofeedback to Patient 1 (single session), resulted in an increase of the contribution of the paretic limb to movement, but it also increased the U values. The force patterns with and without force biofeedback show a change on the pedaling strategy of Patient 1, when force biofeedback was provided, by increasing the standard deviation of effective force. Regarding Patient 3 (single session), the provision of force biofeedback (especially F32) had notorious improvements, since it resulted in a higher cycling symmetry (lower U values), similar pedal angles ranges and similar force patterns of the lower limbs. These results allow to respond positively to the #RQ4, since the provision of cycling with force biofeedback resulted in changes on the patients' pedaling strategy (Patient 1 and Patient 3), increased the contribution of the paretic limb (Patient 1 and Patient 3), and led to a more symmetrical cycling exercise (Patient 3), as had been hypothesized.

Patient 1 showed noticeable improvements regarding the provision of EMG biofeedback of the *rectus femoris*, since the abnormal amount of resistive force applied by the paretic limb, observed during cycling without biofeedback, reduced to normal levels, similar to the healthy limb. As in force biofeedback, the results of providing EMG biofeedback also allow to corroborate the positive answer to the #RQ4, since the defined hypotheses were also verified.

The single sessions allowed to conclude that both therapies can change the patients' pedaling strategy and improve the cycling performance.

The intervention of 5 sessions (during 2 weeks) of cycling with EMG biofeedback allow to infer about three research questions (#RQ2, #RQ3 and #RQ4). Providing EMG biofeedback had different results on two stroke patients (Patient 2 and Patient 3), when compared with cycling without biofeedback. Concerning Patient 3, apparently no effects on the cycling performance resulted from providing EMG biofeedback. However, the difference between the net mechanical work W of both lower limbs of Patient 2 was slightly lower, during cycling with EMG biofeedback, meaning that the contribution of each limb to the movement was more balanced. In addition, two positive changes were observed in the force pattern

of the paretic limb: an increase of the positive effective force and a reduction of the crank angles where resistive force was applied, which result in a higher participation of the paretic limb to the movement of the cycling device. Although no positive changes were observed in Patient 3, the results observed in Patient 2, when EMG biofeedback was provided, are consistent with the results observed in Patient 1 and corroborate the positive answer to the #RQ4.

The implementation of the EMG biofeedback intervention resulted in improvements in some of the training variables throughout the sessions, which corroborate the hypothesis presented in #RQ3. The difference between the contribution of each limb reduced between the initial and the final cycling assessment, due to a reduction of the W performed by the healthy limb, in both Patient 2 and Patient 3. Therefore, the contribution of both lower limbs become more balance between the beginning and the end of the intervention. In addition, Patient 2 was able to increase the training workload throughout the intervention, which suggests a learning of how to more effectively exercise on the cycling device and/or an increase the endurance capacity.

Regarding the improvement of the patient's motor function after the intervention (#RQ2), the FMA score of Patient 3 improved between the beginning and the end of the intervention. However, this improvement on the patient's motor function cannot be attributed exclusively to the intervention, since it may also have resulted from spontaneous recovery, since Patient 3 was a sub-acute stroke patient, or from the conventional physiotherapy and occupational therapy that the patient was doing. An improvement of the patient motor ability was hypothesized in #RQ2, which was observed in Patient 3, who performed the initial and the final assessment tests. The motor function of Patient 2 was not assessed at the end of the study. These results are insufficient to infer about the effects of cycling with EMG biofeedback in the stroke patients' motor ability, since the motor function of only one patient was assessed, and the observed improvements cannot be attributed exclusively to the intervention. This therapy should be applied in more stroke patients in order to clarify the #RQ2.

In overall, the tests performed in this preliminary study allowed to conclude that force and EMG biofeedback change the patients' pedaling strategy and improve the cycling performance, which support the hypotheses defined in the #RQ4. As both therapies had positive results in at least one patient, it is not possible to conclude which one may produce better results in stroke rehabilitation, or even to differentiate among the positive results. The intervention of EMG biofeedback resulted in an improvement of the cycling performance throughout the intervention, which also supports the considerations defined in the #RQ3. Regarding the motor function (#RQ2), the patient whose motor function was assessed at the beginning and end of the intervention (Patient 3), showed improvements. However, the number of patients to whom the intervention was implemented is insufficient to recommend or not cycling leg exercise together with force or EMG biofeedback as a stroke rehabilitation therapy (#RQ1). Therefore, the designed study should be implemented in more patients, in order to provide more information that allows to clarify the #RQ1 and the #RQ2.

7.2 Future Work

In the future, the designed protocol should be implemented to a large number of stroke patients, who fulfill the inclusion and exclusion criteria, in order to clarify the research questions and check whether the hypotheses are verified in more stroke patients.

Different components of this study may be improved in order to increase their effectiveness on the

training and patient assessment, as well as, in the achievement of the rehabilitation's objectives. Some of these improvements are described below.

The system to measure the force applied in the pedals ought to be improved, in order to measure the anterior-posterior and medio-lateral force components, in addition to the normal force. The system should also be changed to allow the measurement of the force applied in the upward direction, during the upstroke phase. These two modifications will provide more information about the pedaling strategy of the healthy subjects and, more important, of the stroke patients. A better way to control the position of the subject regarding the cycling device ought to be found, in order to reduce the influence of an incorrect position on the force pattern.

Regarding force biofeedback, alternative solutions to the system's limitations ought to be explored, such as more appropriate conditions to define the target band. In addition, the force biofeedback system should be adapted to patients like Patient 1, whose paretic limb applies a normal amount of propulsive force during the downstroke phase, but also applies an excess of resistive force, during the upstroke phase. One rehabilitation issue that can be further explored is to study which of the two force biofeedback types (F32 and FHR) results in more improvements in the gait ability, by performing trials in more stroke patients. This will allow to verify whether a therapy that promotes coordination (F32) has greater effects than an exercise that promotes the force applied by each limb (FHR). In addition, alternative ways to provide information about the symmetry of the force pattern applied by each limb during cycling exercise should be further explored, instead of the used bars' system. An alternative solution may be to provide a plot of the force applied by each limb, with a target pattern that represents an effective force pattern (high propulsive force and low resistive force), similar to the EMG biofeedback setup. In this case, the force plot would be updated with a fast rate, such as on each 8 degrees. This system might be a solution for the problem observed in the bars' system, since the last is based on the difference between the propulsive and resistive force. In the bars' system, an effective force pattern with much propulsive force, but also with an abnormal amount of resistive force, when compared with a force pattern with a normal amount of propulsive and resistive force, could be considered symmetrical. As in the proposed system the patient receives biofeedback of his effective force pattern, the problem described does not occur.

Providing EMG biofeedback while the user performs cycling in a device with isokinetic mode (same cadence regardless the applied force) will allow the users to just focus on muscle activation. This training would be interesting to assess if the difficulty to synchronize the training cadence and the muscle activation pattern with the target signal negatively influences the effectiveness of this intervention, both in the exercise performance, as in recovering the motor capacity. An additional test to further analyze the interaction of stroke patients with EMG biofeedback could be to study the effects, on the paretic limb activity, of providing the muscle activation pattern of the healthy and paretic limbs, simultaneously. However, this might be too complex for the subjects. If possible, in future tests, new electrodes should be used in every new session, in order to eliminate the influence that their condition may cause in the signal quality of the muscle activation pattern. The Leg Supports should be used, during the future trials, or alternative solutions that allow a reduction of the hip abduction and rotation and foot inversion should be sought.

The use of the biomechanical model to obtain information about the internal muscular actions and the moments acting on the lower limbs' joints ought to be further explored. The used model should first be optimized to a semi-recumbent configuration, since it was developed for a standard cycling device, which may have influenced the success of the application of this model. Biomechanical models may, in

the future, be used as complementary diagnostic tools, and as a tool to assess the motor recovery after a rehabilitation intervention. Further, it should be verified how the body segments parameters should be acquired.

New functions may be developed and installed in the new models of the cycling devices, such as a mechanism that analyzes whether the position of the foot on the pedal is correct, as well as, the position of the leg. This mechanism might be used to assess the lower limbs condition, and during training, to alert the patient and/or the therapist when the position of the limb or foot is not correct. Assessing the pedaling strategy and the training variables with different pedal's configurations may also be explored. Developing a system of pedals that allows to change the position of the pedals in the coronal and in the sagittal planes, as well as, which allows to fix a specific pedal angle. This would allow to study new interactions between the user and the cycling device. As stroke patients have limbs with different motor functions, a system that allows having different workloads in each limb may enable a reduction of the contribution of the healthy limb to the movement and an increase of the paretic limb's contribution.

Bibliography

- [1] Alan S Go, Dariush Mozaffarian, Veronique L Roger, Emelia J Benjamin, et al. Heart disease and stroke statistics–2014 update: a report from the american heart association. *Circulation*, 129(3):e28, 2014.
- [2] A Kamps and K Schüle. Cyclic movement training of the lower limb in stroke rehabilitation. *Neurol Rehabil*, 11(5):S1–S12, 2005.
- [3] Stefano Masiero, Patrizia Poli, Giulio Rosati, Damiano Zanotto, Marco Iosa, Sefano Paolucci, and Giovanni Morone. The value of robotic systems in stroke rehabilitation. *Expert review of medical devices*, 11(2):187–198, 2014.
- [4] Ruth Dickstein. Rehabilitation of gait speed after stroke: a critical review of intervention approaches. *Neurorehabilitation and Neural Repair*, 2008.
- [5] Emilia Ambrosini, Simona Ferrante, Giancarlo Ferrigno, Franco Molteni, and Alessandra Pedrocchi. Cycling induced by electrical stimulation improves muscle activation and symmetry during pedaling in hemiparetic patients. *Neural Systems and Rehabilitation Engineering, IEEE Transactions on*, 20(3):320–330, 2012.
- [6] David A Brown, Sabina Nagpal, and Sam Chi. Limb-loaded cycling program for locomotor intervention following stroke. *Physical therapy*, 85(2):159–168, 2005.
- [7] Christine C Raasch and Felix E Zajac. Locomotor strategy for pedaling: muscle groups and biomechanical functions. *Journal of Neurophysiology*, 82(2):515–525, 1999.
- [8] Kathryn M Sibley, Ada Tang, Dina Brooks, David A Brown, and William E McIlroy. Feasibility of adapted aerobic cycle ergometry tasks to encourage paretic limb use after stroke: a case series. *Journal of Neurologic Physical Therapy*, 32(2):80–87, 2008.
- [9] S Ferrante, A Pedrocchi, G Ferrigno, and F Molteni. Cycling induced by functional electrical stimulation improves the muscular strength and the motor control of individuals with post-acute stroke. *European journal of physical and rehabilitation medicine*, 44(2):159–67, 2008.
- [10] J Szecsi, C Krewer, F Müller, and A Straube. Functional electrical stimulation assisted cycling of patients with subacute stroke: kinetic and kinematic analysis. *Clinical Biomechanics*, 23(8):1086–1094, 2008.

- [11] Thomas W Janssen, J Marijke Beltman, Peter Elich, Peter A Koppe, Hermanna Konijnenbelt, Arnold de Haan, and Karin H Gerrits. Effects of electric stimulation- assisted cycling training in people with chronic stroke. *Archives of physical medicine and rehabilitation*, 89(3):463–469, 2008.
- [12] So Young Lee, Sa-Yoon Kang, Sang Hee Im, Bo Ryun Kim, Sun Mi Kim, Ho Min Yoon, and Eun Young Han. The effects of assisted ergometer training with a functional electrical stimulation on exercise capacity and functional ability in subacute stroke patients. *Annals of rehabilitation medicine*, 37(5):619–627, 2013.
- [13] Emilia Ambrosini, Simona Ferrante, Alessandra Pedrocchi, Giancarlo Ferrigno, and Franco Molteni. Cycling induced by electrical stimulation improves motor recovery in postacute hemiparetic patients a randomized controlled trial. *Stroke*, 42(4):1068–1073, 2011.
- [14] Hsin-chang Lo, Yung-Chun Hsu, Ya-Hsin Hsueh, and Chun-Yu Yeh. Cycling exercise with functional electrical stimulation improves postural control in stroke patients. *Gait & posture*, 35(3):506–510, 2012.
- [15] Sang-I Lin, Chao-Chen Lo, Pei-Yi Lin, and Jia-Jin J Chen. Biomechanical assessments of the effect of visual feedback on cycling for patients with stroke. *Journal of Electromyography and Kinesiology*, 22(4):582–588, 2012.
- [16] Pei-Yi Lin, Jia-Jin Jason Chen, and Sang-I Lin. The cortical control of cycling exercise in stroke patients: An fnirs study. *Human brain mapping*, 34(10):2381–2390, 2013.
- [17] David A Brown and Gary A DeBacher. Bicycle ergometer and electromyographic feedback for treatment of muscle imbalance in patients with spastic hemiparesis suggestion from the field. *Physical therapy*, 67(11):1715–1719, 1987.
- [18] Simona Ferrante, Emilia Ambrosini, Paola Ravelli, Eleonora Guanziroli, Franco Molteni, Giancarlo Ferrigno, and Alessandra Pedrocchi. A biofeedback cycling training to improve locomotion: a case series study based on gait pattern classification of 153 chronic stroke patients. *Journal of neuroengineering and rehabilitation*, 8(1):47, 2011.
- [19] Huei-Ching Yang, Chia-Ling Lee, Roxane Lin, Miao-Ju Hsu, Chia-Hsin Chen, Jau-Hong Lin, and Sing Kai Lo. Effect of biofeedback cycling training on functional recovery and walking ability of lower extremity in patients with stroke. *The Kaohsiung journal of medical sciences*, 30(1):35–42, 2014.
- [20] Paulette M Van Vliet and Gabriele Wulf. Extrinsic feedback for motor learning after stroke: what is the evidence? *Disability & Rehabilitation*, 28(13-14):831–840, 2006.
- [21] Gerard J Tortora and Bryan H Derrickson. *Principles of anatomy and physiology*. John Wiley & Sons, 2008.
- [22] Susan B O’Sullivan, Thomas J Schmitz, and George Fulk. *Physical rehabilitation*. FA Davis, 2013.
- [23] D Evans, J Price, and W Barron. Profiles of general demographic characteristics. 2000 census of population and housing. *Washington, DC: US Department of Commerce*, 2001.

-
- [24] European Registers of Stroke (EROS) Investigators et al. Incidence of stroke in europe at the beginning of the 21st century. *Stroke*, 40(5):1557–1563, 2009.
- [25] Hsin-Yung Chen, Shih-Ching Chen, Jia-Jin Jason Chen, Li-Lan Fu, and Yu Lin Wang. Kinesiological and kinematical analysis for stroke subjects with asymmetrical cycling movement patterns. *Journal of Electromyography and Kinesiology*, 15(6):587–595, 2005.
- [26] David A Brown and Steven A Kautz. Speed-dependent reductions of force output in people with poststroke hemiparesis. *Physical therapy*, 79(10):919–930, 1999.
- [27] Riccardo Mazzocchio, Sabine Meunier, Simona Ferrante, Franco Molteni, and Leonardo G Cohen. Cycling, a tool for locomotor recovery after motor lesions? *NeuroRehabilitation*, 23(1):67–80, 2008.
- [28] DA Brown and SA Kautz. Increased workload enhances force output during pedaling exercise in persons with poststroke hemiplegia. *Stroke*, 29(3):598–606, 1998.
- [29] Kathleen Potempa, Martita Lopez, Lynne T Braun, J Peter Szidon, Louis Fogg, and Tyler Tincknell. Physiological outcomes of aerobic exercise training in hemiparetic stroke patients. *Stroke*, 26(1):101–105, 1995.
- [30] SA Kautz and DA Brown. Relationships between timing of muscle excitation and impaired motor performance during cyclical lower extremity movement in post-stroke hemiplegia. *Brain*, 121(3):515–526, 1998.
- [31] J Rösche, C Paulus, U Maisch, A Kaspar, E Mauch, and HH Kornhuber. The effects of therapy on spasticity utilizing a motorized exercise-cycle. *Spinal cord*, 35(3):176–178, 1997.
- [32] Angela L Ridgel, Jerrold L Vitek, and Jay L Alberts. Forced, not voluntary, exercise improves motor function in parkinson’s disease patients. *Neurorehabilitation and Neural Repair*, 2009.
- [33] M Laupheimer, S Härtel, S Schmidt, and K Börs. Forced exercise-effects of motomed® therapy on typical motor dysfunction in parkinson’s disease. *Neurol Rehabil*, 17(5/6):239–246, 2011.
- [34] Angela L Ridgel, Hassan Mohammadi Abdar, Jay L Alberts, Fred M Discenzo, and Kenneth A Loparo. Variability in cadence during forced cycling predicts motor improvement in individuals with parkinson’s disease. *Neural Systems and Rehabilitation Engineering, IEEE Transactions on*, 21(3):481–489, 2013.
- [35] Angela L Ridgel, Chul-Ho Kim, Emily J Fickes, Matthew D Muller, and Jay L Alberts. Changes in executive function after acute bouts of passive cycling in parkinson’s disease. *J Aging Phys Act*, 19(2):87–98, 2011.
- [36] Angela L Ridgel, Corey A Peacock, Emily J Fickes, and Chul-Ho Kim. Active-assisted cycling improves tremor and bradykinesia in parkinson’s disease. *Archives of physical medicine and rehabilitation*, 93(11):2049–2054, 2012.
- [37] W Diehl, K Schüle, and T Kaiser. Use of an assistive movement training apparatus in the rehabilitation of geriatric patients. *NeuroGeriatric*, 5:3–12, 2008.
-

- [38] John Branten, C Leijgraaff, and P Huijbregts. Strength training: The use of the theravital bicycle trainer for the treatment of gait dysfunction in extended care patients. *ORTHOPAEDIC DIVISION REVIEW*, (B):27, 2006.
- [39] Michal Katz-Leurer, Iris Sender, Ofer Keren, and Zeevi Dvir. The influence of early cycling training on balance in stroke patients at the subacute stage. results of a preliminary trial. *Clinical rehabilitation*, 20(5):398–405, 2006.
- [40] Kazunori Seki, Motohiko Sato, and Yasunobu Handa. Increase of muscle activities in hemiplegic lower extremity during driving a cycling wheelchair. *The Tohoku journal of experimental medicine*, 219(2):129–138, 2009.
- [41] Toshiyuki Fujiwara, Meigen Liu, and Naoichi Chino. Effect of pedaling exercise on the hemiplegic lower limb. *American journal of physical medicine & rehabilitation*, 82(5):357–363, 2003.
- [42] Ada Tang, Kathryn M Sibley, Scott G Thomas, Mark T Bayley, Denyse Richardson, William E McIlroy, and Dina Brooks. Effects of an aerobic exercise program on aerobic capacity, spatiotemporal gait parameters, and functional capacity in subacute stroke. *Neurorehabilitation and neural repair*, 23(4):398–406, 2009.
- [43] Rachel Holt, Catherine Kendrick, Kate McGlashan, Stephen Kirker, and Jumbo Jenner. Static bicycle training for functional mobility in chronic stroke: case report. *Physiotherapy*, 87(5):257–260, 2001.
- [44] Barbara M Quaney, Lara A Boyd, Joan M McDowd, Laura H Zahner, Jianguhua He, Matthew S Mayo, and Richard F Macko. Aerobic exercise improves cognition and motor function poststroke. *Neurorehabilitation and Neural Repair*, 2009.
- [45] Olive Lennon, Aisling Carey, Niamh Gaffney, Julia Stephenson, and Catherine Blake. A pilot randomized controlled trial to evaluate the benefit of the cardiac rehabilitation paradigm for the non-acute ischaemic stroke population. *Clinical Rehabilitation*, 22(2):125–133, 2008.
- [46] Michal Katz-Leurer, Eli Carmeli, and Mara Shochina. The effect of early aerobic training on independence six months post stroke. *Clinical rehabilitation*, 17(7):735–741, 2003.
- [47] Mi-Joung Lee, Sharon L Kilbreath, Maria Fiatarone Singh, Brian Zeman, Stephen R Lord, Jacqueline Raymond, and Glen M Davis. Comparison of effect of aerobic cycle training and progressive resistance training on walking ability after stroke: a randomized sham exercise–controlled study. *Journal of the American Geriatrics Society*, 56(6):976–985, 2008.
- [48] John C Rosecrance and Carol A Giuliani. Kinematic analysis of lower-limb movement during ergometer pedaling in hemiplegic and nonhemiplegic subjects. *Physical therapy*, 71(4):334–343, 1991.
- [49] DA Brown, SA Kautz, and CA Dairaghi. Muscle activity adapts to anti-gravity posture during pedalling in persons with post-stroke hemiplegia. *Brain*, 120(5):825–837, 1997.
- [50] E. Mayo and Carron Gordon Johanne Higgins Sara Mcewen Nancy Salbach Nancy Sharon Wood-Dauphinee, Sara Ahmed. Disablement following stroke. *Disability & Rehabilitation*, 21(5-6):258–268, 1999.

- [51] Joanna O Kelly, Sharon L Kilbreath, Glen M Davis, Brian Zeman, and Jacqui Raymond. Cardiorespiratory fitness and walking ability in subacute stroke patients. *Archives of physical medicine and rehabilitation*, 84(12):1780–1785, 2003.
- [52] Katherine J Sullivan, Tara Klassen, Sara Mulroy, et al. Combined task-specific training and strengthening effects on locomotor recovery post-stroke: a case study. *Journal of Neurologic Physical Therapy*, 30(3):130–141, 2006.
- [53] Lynne R Sheffler and John Chae. Neuromuscular electrical stimulation in neurorehabilitation. *Muscle & nerve*, 35(5):562–590, 2007.
- [54] Sandeep K Subramanian, Crystal L Massie, Matthew P Malcolm, and Mindy F Levin. Does provision of extrinsic feedback result in improved motor learning in the upper limb poststroke? a systematic review of the evidence. *Neurorehabilitation and Neural Repair*, 24(2):113–124, 2010.
- [55] Robert Riener, Lars Lünenburger, and Gery Colombo. Human-centered robotics applied to gait training and assessment. *Journal of rehabilitation research and development*, 43(5):679–694, 2005.
- [56] CM Cirstea, A Ptito, and MF Levin. Feedback and cognition in arm motor skill reacquisition after stroke. *Stroke*, 37(5):1237–1242, 2006.
- [57] Katherine Durham, Paulette M Van Vliet, Frances Badger, and Catherine Sackley. Use of information feedback and attentional focus of feedback in treating the person with a hemiplegic arm. *Physiotherapy Research International*, 14(2):77–90, 2009.
- [58] Heidi Sveistrup. Motor rehabilitation using virtual reality. *Journal of neuroengineering and rehabilitation*, 1:10, 2004.
- [59] Isabelle V Bonan, Florence M Colle, Jean P Guichard, Eric Vicaud, Martine Eisenfisz, P Tran Ba Huy, and Alain P Yelnik. Reliance on visual information after stroke. part i: Balance on dynamic posturography. *Archives of physical medicine and rehabilitation*, 85(2):268–273, 2004.
- [60] Mariusz Drużbicki, Andrzej Kwolek, Agnieszka Depa, and Grzegorz Przysada. The use of a treadmill with biofeedback function in assessment of relearning walking skills in post-stroke hemiplegic patients—a preliminary report. *Neurologia i neurochirurgia polska*, 44(6):567–573, 2010.
- [61] Gabriele Wulf, Nancy McNevin, and Charles H Shea. The automaticity of complex motor skill learning as a function of attentional focus. *The Quarterly Journal of Experimental Psychology: Section A*, 54(4):1143–1154, 2001.
- [62] Nancy H McNevin, Charles H Shea, and Gabriele Wulf. Increasing the distance of an external focus of attention enhances learning. *Psychological research*, 67(1):22–29, 2003.
- [63] He Huang, Steven L Wolf, and Jiping He. Recent developments in biofeedback for neuromotor rehabilitation. *Journal of neuroengineering and rehabilitation*, 3:11, 2006.
- [64] R Barclay-Goddard, T Stevenson, William Poluha, ME Moffatt, and Shayne P Taback. Force platform feedback for standing balance training after stroke. *Cochrane Database Syst Rev*, 4, 2004.

- [65] Steven L Wolf. Electromyographic biofeedback applications to stroke patients a critical review. *Physical therapy*, 63(9):1448–1459, 1983.
- [66] Deborah E Thorpe and Joanne Valvano. The effects of knowledge of performance and cognitive strategies on motor skill learning in children with cerebral palsy. *Pediatric Physical Therapy*, 14(1):2–15, 2002.
- [67] Thomas Platz, Thomas Winter, Nicole Müller, Cosima Pinkowski, Christel Eickhof, and Karl-Heinz Mauritz. Arm ability training for stroke and traumatic brain injury patients with mild arm paresis: a single-blind, randomized, controlled trial. *Archives of Physical Medicine and Rehabilitation*, 82(7):961–968, 2001.
- [68] Carolee J Winstein, Alma S Merians, and Katherine J Sullivan. Motor learning after unilateral brain damage. *Neuropsychologia*, 37(8):975–987, 1999.
- [69] Meg E Morris, Timothy M Bach, and Patricia A Goldie. Electrogoniometric feedback: its effect on genu recurvatum in stroke. *Arch Phys Med Rehabil*, 73(12):1, 1992.
- [70] Timothy J Brindle, Arthur J Nitz, Tim L Uhl, Edward Kifer, and Robert Shapiro. Kinematic and emg characteristics of simple shoulder movements with proprioception and visual feedback. *Journal of Electromyography and Kinesiology*, 16(3):236–249, 2006.
- [71] Onur Armagan, Funda Tascioglu, and Cengiz Oner. Electromyographic biofeedback in the treatment of the hemiplegic hand: a placebo-controlled study. *American Journal of Physical Medicine & Rehabilitation*, 82(11):856–861, 2003.
- [72] Steven L Wolf and Stuart A Binder-Macleod. Electromyographic biofeedback applications to the hemiplegic patient changes in upper extremity neuromuscular and functional status. *Physical therapy*, 63(9):1393–1403, 1983.
- [73] Steven L Wolf and Stuart A Binder-Macleod. Electromyographic biofeedback applications to the hemiplegic patient changes in lower extremity neuromuscular and functional status. *Physical Therapy*, 63(9):1404–1413, 1983.
- [74] Jovana Kojović, Nadica Miljković, Milica M Janković, and Dejan B Popović. Recovery of motor function after stroke: A polymyography-based analysis. *Journal of neuroscience methods*, 194(2):321–328, 2011.
- [75] Catherine M Sackley and Nadina B Lincoln. Single blind randomized controlled trial of visual feedback after stroke: effects on stance symmetry and function. *Disability & Rehabilitation*, 19(12):536–546, 1997.
- [76] Ulla Talvitie. Socio-affective characteristics and properties of extrinsic feedback in physiotherapy. *Physiotherapy Research International*, 5(3):173–189, 2000.
- [77] Cristiano De Marchis, Maurizio Schmid, Daniele Bibbo, Anna Margherita Castronovo, Tommaso D’Alessio, and Silvia Conforto. Feedback of mechanical effectiveness induces adaptations in motor modules during cycling. *Frontiers in computational neuroscience*, 7, 2013.

-
- [78] Chul Gyu Song, Jong Yun Kim, and Nam Gyun Kim. A new postural balance control system for rehabilitation training based on virtual cycling. *Information Technology in Biomedicine, IEEE Transactions on*, 8(2):200–207, 2004.
- [79] Therapeutic Alliances Inc. The ergys 2 rehabilitation system for home and clinics, March 2014.
- [80] Tzora Active System LTD. Active passive digital trainer i-motion, March 2014.
- [81] medica Medizintechnik GmbH. *Thera-trainer Tigo - User manual.*, 2013.
- [82] RECK-Technik GmbH & Co. KG. *Instruction manual - MOTOMed viva2.*, 2017.
- [83] RECK-Technik GmbH & Co. KG. *Instruction manual - MOTOMed letto2.*, 2007.
- [84] Lorenzo Comolli, Simona Ferrante, Alessandra Pedrocchi, Marco Bocciolone, Giancarlo Ferrigno, and Franco Molteni. Metrological characterization of a cycle-ergometer to optimize the cycling induced by functional electrical stimulation on patients with stroke. *Medical engineering & physics*, 32(4):339–348, 2010.
- [85] D Bibbo, S Conforto, I Bernabucci, M Schmid, and T D'Alessio. A wireless integrated system to evaluate efficiency indexes in real time during cycling. In *4th European Conference of the International Federation for Medical and Biological Engineering*, pages 89–92. Springer, 2009.
- [86] Jeff Newmiller, ML Hull, and FE Zajac. A mechanically decoupled two force component bicycle pedal dynamometer. *Journal of Biomechanics*, 21(5):375–386, 1988.
- [87] M Grohler, Thomas Angeli, Thomas Eberharter, Peter Lugner, Winfried Mayr, and Christian Hofer. Test bed with force-measuring crank for static and dynamic investigations on cycling by means of functional electrical stimulation. *Neural Systems and Rehabilitation Engineering, IEEE Transactions on*, 9(2):169–180, 2001.
- [88] STMicroelectronics. Application note - Tilt measurement using a low-g3-axis accelerometer. Technical Report April, 2010.
- [89] Rodrigo R Bini, Patria Anne Hume, James Croft, and Andrew Edward Kilding. Pedal force effectiveness in cycling: a review of constraints and training effects. *Journal of Science and Cycling*, 2(1):11–24, 2013.
- [90] Giovanni Mimmi, Paolo Pennacchi, and Lucia Frosini. Biomechanical analysis of pedalling for rehabilitation purposes: experimental results on two pathological subjects and comparison with non-pathological findings. *Computer methods in biomechanics and biomedical engineering*, 7(6):339–345, 2004.
- [91] YSY MEDICAL. YSY EST EVOLUTION - User Manual. Technical report, Gualargues Le Montueux, France, 2010.
- [92] François Hug and Sylvain Dorel. Electromyographic analysis of pedaling: a review. *Journal of Electromyography and Kinesiology*, 19(2):182–198, 2009.
-

- [93] David J Sanderson, Ewald M Hennig, and Alec H Black. The influence of cadence and power output on force application and in-shoe pressure distribution during cycling by competitive and recreational cyclists. *Journal of sports sciences*, 18(3):173–181, 2000.
- [94] SA Kautz and ML Hull. A theoretical basis for interpreting the force applied to the pedal in cycling. *Journal of biomechanics*, 26(2):155–165, 1993.
- [95] Keith L Moore, Arthur F Dalley, and Anne MR Agur. *Clinically oriented anatomy*. Lippincott Williams & Wilkins, 2013.
- [96] Christine C Raasch, Felix E Zajac, Baoming Ma, and William S Levine. Muscle coordination of maximum-speed pedaling. *Journal of biomechanics*, 30(6):595–602, 1997.
- [97] François Hug, Nicolas A Turpin, Arnaud Guével, and Sylvain Dorel. Is interindividual variability of emg patterns in trained cyclists related to different muscle synergies? *Journal of Applied Physiology*, 108(6):1727–1736, 2010.
- [98] François Hug, Nicolas A Turpin, Antoine Couturier, and Sylvain Dorel. Consistency of muscle synergies during pedaling across different mechanical constraints. *Journal of neurophysiology*, 106(1):91–103, 2011.
- [99] D Intiso, V Santilli, MG Grasso, R Rossi, and I Caruso. Rehabilitation of walking with electromyographic biofeedback in foot-drop after stroke. *Stroke*, 25(6):1189–1192, 1994.
- [100] Signe Brunnström. *Movement therapy in hemiplegia: a neurophysiological approach*. Facts and Comparisons, 1970.
- [101] ML Hull and M Jorge. A method for biomechanical analysis of bicycle pedalling. *Journal of biomechanics*, 18(9):631–644, 1985.
- [102] G. Mimmi, P. Pennacchi, and L. Frosini. System for the biomechanical analysis of pedalling. In *Proceedings of 5th Symposium on Computer Methods in Biomechanics and Biomedical Engineering*, 2001.
- [103] Charles E Clauser, John T McConville, and John W Young. Weight, volume, and center of mass of segments of the human body. Technical report, DTIC Document, 1969.
- [104] Giovanni Mimmi, Carlo Rottenbacher, and Giovanni Bonandrini. Pedalling strength analysis in pathological and non-pathological subjects on cycle-ergometer instrumented with three-components pedals. 2007.
- [105] R PS Van Peppen, Gert Kwakkel, Sharon Wood-Dauphinee, H JM Hendriks, Ph J Van der Wees, and Joost Dekker. The impact of physical therapy on functional outcomes after stroke: what’s the evidence? *Clinical rehabilitation*, 18(8):833–862, 2004.
- [106] H Woodford and C Price. Emg biofeedback for the recovery of motor function after stroke. *Cochrane Database Syst Rev*, 2, 2007.
- [107] Hermie J Hermens, Bart Freriks, Roberto Merletti, Dick Stegeman, Joleen Blok, Günter Rau, Cathy Disselhorst-Klug, and Göran Hägg. European recommendations for surface electromyography. *Roessingh Research and Development, Enschede*, 1999.

- [108] Kauko Pitkänen, Juhani Sivenius, Ina M Tarkka, et al. How much exercise does the enhanced gait-oriented physiotherapy provide for chronic stroke patients? *Journal of neurology*, 251(4):449–453, 2004.
- [109] L Naing, T Winn, and BN Rusli. Practical issues in calculating the sample size for prevalence studies. *Archives of Orofacial Sciences*, 1(1):9–14, 2006.
- [110] Wayne W Daniel. *Biostatistics: a foundation for analysis in the health sciences*. New York, USA, 1995.
- [111] A FREIRE Gonçalves and S Massano Cardoso. Prevalência dos acidentes vasculares cerebrais em coimbra. *Acta medica portuguesa*, 10(8-9):543–50, 1997.
- [112] Axel R Fugl-Meyer, L Jääskö, Ingegerd Leyman, Sigyn Olsson, and Solveig Steglind. The post-stroke hemiplegic patient. 1. a method for evaluation of physical performance. *Scandinavian journal of rehabilitation medicine*, 7(1):13–31, 1974.
- [113] Richard W Bohannon and Melissa B Smith. Interrater reliability of a modified ashworth scale of muscle spasticity. *Physical therapy*, 67(2):206–207, 1987.
- [114] Neil F Gordon, Meg Gulanick, Fernando Costa, Gerald Fletcher, Barry A Franklin, Elliot J Roth, and Tim Shephard. Physical activity and exercise recommendations for stroke survivors an american heart association scientific statement from the council on clinical cardiology, subcommittee on exercise, cardiac rehabilitation, and prevention; the council on cardiovascular nursing; the council on nutrition, physical activity, and metabolism; and the stroke council. *Stroke*, 35(5):1230–1240, 2004.
- [115] Gunnar A Borg. Psychophysical bases of perceived exertion. *Med sci sports exerc*, 14(5):377–381, 1982.
- [116] Gordon Robertson, Graham Caldwell, Joseph Hamill, Gary Kamen, and Saunders Whittlesey. *Research Methods in Biomechanics, 2E*. Human Kinetics, 2013.

Appendices

Appendix A

A.1 *THERA-Live* Technical Data

	THERA-live 230 V	THERA-live 115 V
Length	54 cm / 21.3"	
Width	46 cm / 18.1"	
Height	46 cm / 18.1"	
Basic exerciser	100-115 cm / 39.4-45.3"	
with upper body exerciser	101 cm / 39.8"	
with handles		
Weight	25 kg / 55.2 lbs	
Basic exerciser	32 kg / 70.6 lbs	
with upper body exerciser	28.5 kg / 62.2 lbs	
with handles		
Crank length	75 mm / 110 mm / 2.92"/4.31"	
fixed	65-115 mm / 2.59-4.53"	
variable		
Speed range	0-60 rpm	
Torque range	ca. 0-12 Nm / 0-8.85 ft lbs	
Power supply	230 V~, 50/60 Hz	115 V~, 50/60 Hz
Power consumption	130 VA	
Fuse rating	2 × 1.0 A idle	2 × 1.6 A idle
Materials used	Steel, polystyrene, polyurethane and others	
Safety class	I	
Safety grade	Type B ⚡	
Safety rating	I PXO	
Noise emission level	Lpa ≤ 70 dB (A)	
Noise emission rating	To DIN 45635-19-01-KL2	
Ambient conditions for operation	10 °C to 35 °C 0 to 90 % Rh 970 to 1030 hPa	50 °F to 95 °F 0 to 90 % Rh 970 to 1030 hPa
Ambient conditions for transport/ storage	-30 °C to 65 °C 0 to 90 % Rh 970 to 1030 hPa	-22 °F to 149 °F 0 to 90 % Rh 970 to 1030 hPa

Figure A.1: Technical data of the *THERA-Live* cycling device.

A.2 OPB763T Optical Sensor

A.2.1 OPB763T Properties

Absolute Maximum Ratings ($T_A=25^\circ\text{C}$ unless otherwise noted)

Supply Voltage, V_{CC} (not to exceed 3 seconds)	10 V
Storage Temperature Range	-40°C to $+85^\circ\text{C}$
Operating Temperature Range	-40°C to $+70^\circ\text{C}$
Lead Soldering Temperature (1/16" inch (1.6 mm) from case for 5 seconds with soldering iron) ⁽¹⁾	260° C
Input Diode Power Dissipation ⁽²⁾	100 mW
Output Photologic® Power Dissipation ⁽³⁾	200 mW
Total Device Power Dissipation ⁽⁴⁾	300 mW
Voltage at Output Lead (Open Collector Output)	35 V
Diode Forward DC Current	40 mA
Diode Reverse DC Voltage	3 V

Figure A.2: Absolute maximum ratings of the optical sensor *OPB763T*.

Electrical Characteristics ($T_A = 25^\circ\text{C}$ unless otherwise noted)

SYMBOL	PARAMETER	MIN	TYP	MAX	UNITS	TEST CONDITIONS
Input Diode						
V_F	Forward Voltage	-	-	1.8	V	$I_F = 40\text{ mA}$, $T_A = 25^\circ\text{C}$
I_R	Reverse Current	-	-	100	μA	$V_R = 2.0\text{ V}$, $T_A = 25^\circ\text{C}$
Output Photologic® Sensor						
V_{CC}	Operating DC Supply Voltage	4.75	-	5.25	V	
I_{CCL}	Low Level Supply Current: Buffered Totem-Pole Output ⁽⁵⁾⁽⁶⁾ Buffered Open-Collector Output ⁽⁵⁾⁽⁶⁾	-	-	10	mA	$V_{CC} = 5.25\text{ V}$, $I_F = 0\text{ mA}$ (output open)
	Inverted Totem-Pole Output ⁽⁵⁾ Inverted Open-Collector Output ⁽⁵⁾	-	-	10	mA	$V_{CC} = 5.25\text{ V}$, $I_F = 0\text{ mA}$ (output open)
I_{CCH}	High Level Supply Current: Buffered Totem-Pole Output ⁽⁵⁾⁽⁶⁾ Buffered Open-Collector Output ⁽⁵⁾	-	-	10	mA	$V_{CC} = 5.25\text{ V}$, $I_F = 25\text{ mA}$ (output open)
	Inverted Totem-Pole Output ⁽⁵⁾⁽⁶⁾ Inverted Open-Collector Output ⁽⁵⁾⁽⁶⁾	-	-	10	mA	$V_{CC} = 5.25\text{ V}$, $I_F = 0\text{ mA}$ (output open)
I_{OH}	High Level Output Voltage: Buffered Open-Collector Output	-	-	100	μA	$V_{CC} = 4.5\text{ V}$, $I_F = 25\text{ mA}$, $V_{OH} = 30\text{ V}$, $T_A = 25^\circ\text{C}$
	Inverted Open-Collector Output	-	-	100	μA	$V_{CC} = 4.5\text{ V}$, $I_F = 0\text{ mA}$, $V_{OH} = 30\text{ V}$, $T_A = 25^\circ\text{C}$

Electrical Characteristics ($T_A = 25^\circ\text{C}$ unless otherwise noted)

SYMBOL	PARAMETER	MIN	TYP	MAX	UNITS	TEST CONDITIONS
Output Photologic® Sensor (continued)						
$I_{F(+)}$	LED Positive-Going Threshold Current ⁽²⁾	-	-	25	mA	$V_{CC} = 5\text{ V}$, $T_A = 25^\circ\text{C}$
$I_{F(-)}/I_{F(+)}$	Hysteresis ⁽²⁾	1.1	-	2.0	-	$V_{CC} = 5\text{ V}$
I_{OS}	Short Circuit Output Current: Buffered Totem-Pole Output ⁽¹⁾	-15	-	-100	mA	$I_F = 25\text{ mA}$, $V_{CC} = 5.25\text{ V}$, Output = GRD
	Inverted Totem-Pole Output ⁽¹⁾	-15	-	-100	mA	$I_F = 0\text{ mA}$, $V_{CC} = 5.25\text{ V}$, Output = GRD
V_{OL}	Low Level Output Voltage: Buffered Totem-Pole Output ⁽¹⁾⁽⁴⁾ Buffered Open-Collector Output ⁽¹⁾⁽⁴⁾	-	-	0.4	V	$V_{CC} = 4.5\text{ V}$, $I_{OH} = 12.8\text{ mA}$, $I_F = 0\text{ mA}$ or $I_F = 30\text{ mA}$
	Inverted Totem-Pole Output Inverted Open-Collector Output ⁽¹⁾⁽⁴⁾	-	-	0.4	V	$V_{CC} = 4.5\text{ V}$, $I_{OH} = 12.8\text{ mA}$, $I_F = 25\text{ mA}$
V_{OH}	High Level Output Voltage: Buffered Totem-Pole Output ⁽¹⁾	2.4	-	-	V	$V_{CC} = 4.5\text{ V}$, $I_{OH} = -800\text{ }\mu\text{A}$, $I_F = 25\text{ mA}$
	Inverted Totem-Pole Output ⁽¹⁾⁽⁴⁾	2.4	-	-	V	$V_{CC} = 4.5\text{ V}$, $I_{OH} = -800\text{ }\mu\text{A}$, $I_F = 0\text{ mA}$
	Inverted Totem-Pole Output ⁽²⁾	2.4	-	-	V	$V_{CC} = 4.5\text{ V}$, $I_{OH} = -800\text{ }\mu\text{A}$, $I_F = 30\text{ mA}$
	Inverted Open-Collector Output ⁽²⁾	2.4	-	-	V	$V_{CC} = 4.5\text{ V}$, $I_{OH} = -800\text{ }\mu\text{A}$, $I_F = 30\text{ mA}$

Figure A.3: Electrical characteristics of the optical sensor *OPB763T*.

A.2.2 Optical Sensors' Electronic Board

In Figure A.4 is presented the circuit developed to connect the optical sensors to the sensors' acquisition board (Section A.3), in order to power the internal optical sensor and to obtain the signal from the two optical sensors. The output of the external sensor (*C*) is connected to the control board, whereas the output of the internal sensor (*D*) is connected to another electronic circuit, which contains the components for the processing and acquisition of the sensors' signals.

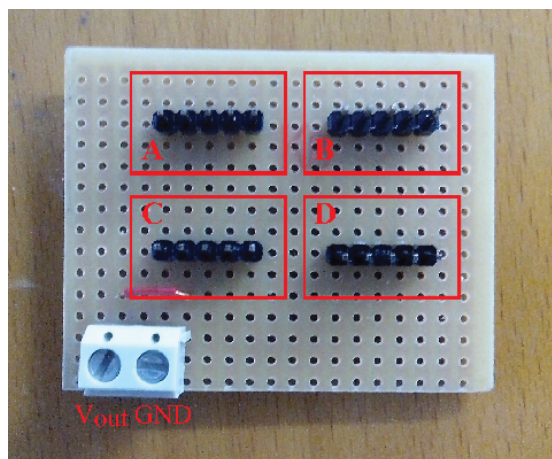


Figure A.4: Veroboard for the connection of the external (*A*) and the internal (*B*) optical sensors with the electronic control board (*C*) and the sensors' acquisition board (*D*), respectively. The ground (*GND*) and the external optical sensor output (V_{out}) are connected to the sensors' acquisition board through the white Printed Circuit Board (PCB) connector.

A.3 Sensors' Acquisition Board

The sensors' acquisition board, which is presented in Figure A.5, contains the electronic components to power the sensors, connect them to the microcontroller board, and components essential to the acquisition of the sensors' signals. This board includes the circuit (Figure A.5 – Area C) that allows the operation of optical sensor, which is placed on the internal encoder's disk. The external optical sensor is connected to the microcontroller through Area B (Figure A.5). The Serial Clock Line (SCL) and the Serial Data Line (SDA) lines (I²C protocol) of the two accelerometers are connected in the Area D (Figure A.5). The Area E (Figure A.5) contains the components of the four voltage dividers to measure the applied force on the *Flexiforce* sensors.

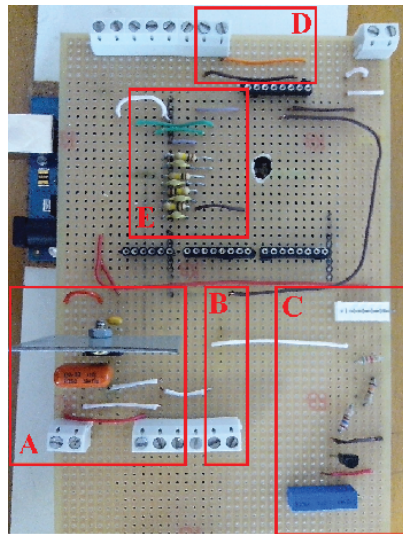


Figure A.5: Sensors' acquisition board. A – Voltage regulator circuit. B – External optical sensor connector. C – Internal optical sensor control circuit. D – I²C protocol lines connector (accelerometers). E – Voltage divider circuits (*Flexiforce* sensors).

In order to transform the 12 V of the battery, which is used to power the sensors, in the recommend supply voltage of the sensors (5 V), a voltage regulator circuit (Figure A.5 – Area A) was installed. This circuit, as shown in Figure A.6, uses an Integrated Circuit 7805 and two capacitors.

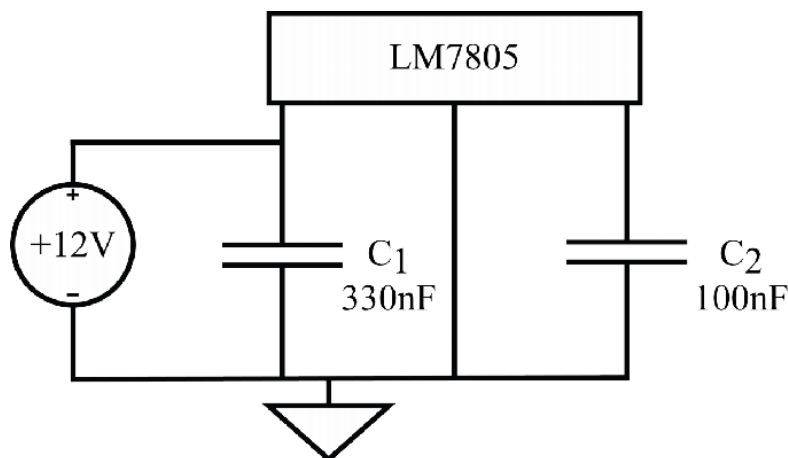


Figure A.6: Voltage divider circuit.

A.4 GY-521 – MPU6050 Accelerometer

A.4.1 MPU6050 Accelerometer Features

- Digital-output triple-axis accelerometer with a programmable full scale range of $\pm 2g$, $\pm 4g$, $\pm 8g$ and $\pm 16g$;
- Integrated 16-bit ADCs enable simultaneous sampling of accelerometers while requiring no external multiplexer;
- Accelerometer normal operating current: $500 \mu A$;
- Low power accelerometer mode current: $10 \mu A$ at 1.25 Hz, $20 \mu A$ at 5 Hz, $60 \mu A$ at 20 Hz, $110 \mu A$ at 40 Hz;
- Orientation detection and signaling;
- Tap detection;
- User-programmable interrupts;
- High-G interrupt;
- User self-test;

A.4.2 MPU6050 Accelerometer Specifications

VDD = 2.375V-3.46V, V_{LOGIC} (MPU-6050 only) = 1.8V \pm 5% or VDD, T_A = 25°C

PARAMETER	CONDITIONS	MIN	TYP	MAX	UNITS	NOTES
ACCELEROMETER SENSITIVITY						
Full-Scale Range	AFS_SEL=0 AFS_SEL=1 AFS_SEL=2 AFS_SEL=3		± 2 ± 4 ± 8 ± 16		<i>g</i> <i>g</i> <i>g</i> <i>g</i>	
ADC Word Length	Output in two's complement format		16		bits	
Sensitivity Scale Factor	AFS_SEL=0 AFS_SEL=1 AFS_SEL=2 AFS_SEL=3		16,384 8,192 4,096 2,048		LSB/ <i>g</i> LSB/ <i>g</i> LSB/ <i>g</i> LSB/ <i>g</i>	
Initial Calibration Tolerance			± 3		%	
Sensitivity Change vs. Temperature	AFS_SEL=0, -40°C to +85°C		± 0.02		%/°C	
Nonlinearity	Best Fit Straight Line		0.5		%	
Cross-Axis Sensitivity			± 2		%	
ZERO-G OUTPUT						
Initial Calibration Tolerance	X and Y axes Z axis		± 50 ± 80		mg mg	1
Zero-G Level Change vs. Temperature	X and Y axes, 0°C to +70°C Z axis, 0°C to +70°C		± 35 ± 60		mg mg	
SELF TEST RESPONSE						
Relative	Change from factory trim	-14		14	%	2
NOISE PERFORMANCE						
Power Spectral Density	@10Hz, AFS_SEL=0 & ODR=1kHz		400		$\mu g/\sqrt{Hz}$	
LOW PASS FILTER RESPONSE						
	Programmable Range	5		260	Hz	
OUTPUT DATA RATE						
	Programmable Range	4		1,000	Hz	
INTELLIGENCE FUNCTION INCREMENT			32		mg/LSB	

Figure A.7: Specifications of the MPU6050 accelerometer.

A.5 Flexiforce Sensor

A.5.1 Flexiforce Properties

Table A.1: Physical properties and Typical performance of *Flexiforce* Sensor

Physical Properties	
Thickness	0.008 in (0.208 mm)
Length	7.75 in (197 mm)
	6 in (152 mm)
	4 in (102 mm)
	2 in (51mm)
Width	0.55 in (14 mm)
Sensing Area	0.375 in (9.53 mm) diameter
Connector	3-pin Male Square Pin (center pin is inactive)
Substrate	Polyester
Typical Performance	
Standard Force Ranges	0 - 1 lb (4.4 N)
	0 - 25 lb (110 N)
	0 - 100 lb (440 N)
Linearity (Error)	$< \pm 3\%$
Repeatability	$< \pm 2.5\%$ of full scale (Conditioned sensor, 80% of full force applied)
Hysteresis	$< 4.5\%$ of full scale (Conditioned sensor, 80% of full force applied)
Drift	$< 5\%$ per logarithmic time scale (Constant load of 25 lb (111 N))
Response Time	$< 5 \mu\text{sec}$
Operating Temperature Range	15 °F – 140 °F (-9 °C – 60 °C)
Output Change per Degree of Temperature Change	$\pm 0.2 \text{ \%}^\circ\text{F}$ (0.36% °C)

A.5.2 Sensors Calibration

Different weights were used to calibrate the force sensors. The values of the weights and the respective sensor electrical tension are presented in Table A.2. The voltage value for each pedal results from the sum of the voltages from the sensors of the pedal.

Table A.2: Voltage readings (V) for different conditions of weight, in the left and right pedals

Weight (Kg)	Left Pedal (V)	Right Pedal (V)
0	0.00	0.00
2	0.15	0.30
4	0.58	0.78
5	0.80	1.12
7	1.24	1.50
9	1.55	1.93
10	1.98	2.09
12	2.30	2.44
14	2.65	2.62
20	3.18	3.41

The plot of the voltage readings in function of the applied force (N), for each pedal, is represented in Figure A.8.

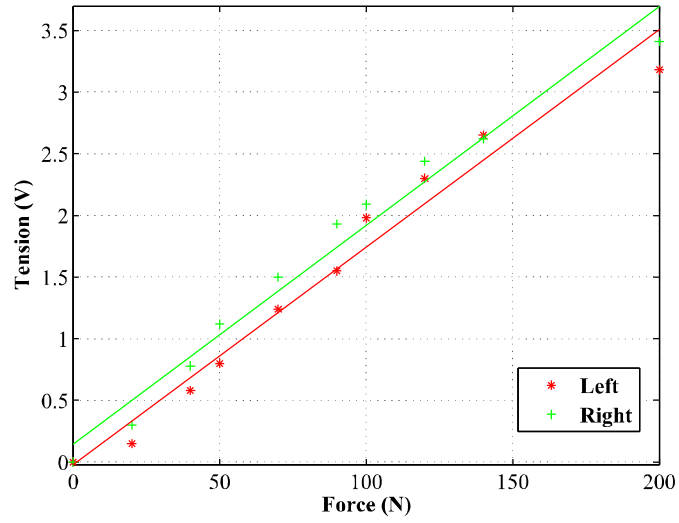


Figure A.8: Electrical tension (V) values as function of the applied force (N), for the left pedal (red) and right (green) pedals.

The coefficients values (a and b) of the polynomial function, which were obtained from the voltage readings through a polynomial curve fitting, are presented in Table A.3.

Table A.3: Coefficients values of the polynomial function, obtained through a polynomial curve fitting of the voltage readings

	Left Pedal	Right Pedal
a	0.0177	0.0177
b	-0.0226	0.1460

A.6 Leg Supports



Figure A.9: Accessory Leg Supports. [81]

B.1 Biomechanical Analysis of Lower Limbs during Cycling

The biomechanical model, represented in Figure 4.5, is based on the following hypothesis:

- The mass of each link-segment is concentrated in its center of mass;
- The position of the each center of mass is fixed;
- The joints are modeled as rotational joints;
- The inertia moment of each link-segment referred to its center of mass is constant during the motion;
- The geometric dimensions of the link-segments are constant.

The lengths of the thigh, shank and foot (l_1 , l_2 and l_3 , respectively), as well as, the crank arm length (L_2) and the horizontal and vertical seat distance (L_3 and L_4 , respectively) have to be measured, in order to calculate the angular displacements, velocities and accelerations.

The foot angle (ε_2) was approximated to a sine wave through the fitting of the foot angle data (β) to a Fourier series. The angular velocity ($\dot{\varepsilon}_2$) and acceleration ($\ddot{\varepsilon}_2$) were obtained through the first and second derivatives of the fitted data, respectively. The crank rotation angle (ε_3) is obtained through the crank angle (ϕ), measured by the optical encoders. The crank angular velocity ($\dot{\varepsilon}_3$) is assumed constant, thus, the crank arm angular acceleration is equal to zero. The angle ε_4 is fixed and equal to 180 degrees.

In order to compute the angles of the moving links (crank arm, foot, shank and thigh), the loop equation can be written as shown in equation (B.1):

$$l_1 e^{i\theta} + l_2 e^{i\varepsilon_1} + l_3 e^{i\varepsilon_2} - L_2 e^{i\varepsilon_3} + L_3 e^{i\frac{3\pi}{2}} + L_4 e^{i\pi} = 0 \quad (\text{B.1})$$

By distinguishing the real part from the imaginary part, the following equations are obtained:

$$\begin{cases} l_1 \cos \theta + l_2 \cos \varepsilon_1 + l_3 \cos \varepsilon_2 - L_2 \cos \varepsilon_3 - L_4 = 0 \\ l_1 \sin \theta + l_2 \sin \varepsilon_1 + l_3 \sin \varepsilon_2 - L_2 \sin \varepsilon_3 - L_3 = 0 \end{cases} \quad (\text{B.2})$$

Finally, the angle of the thigh (θ) and knee (ε_1) can be calculated as given by (B.3) and (B.4).

$$\theta = 2 \tan^{-1} \left[\frac{2G \pm [(2G)^2 - 4(E+F)(E-F)]^{\frac{1}{2}}}{2(E+F)} \right] \quad (\text{B.3})$$

$$\varepsilon_1 = \tan^{-1} \left[\frac{(C-D) - l_1 \sin \theta}{(A-B) - l_1 \cos \theta} \right] \quad (\text{B.4})$$

where

$$\begin{aligned}
A &= L_4 + L_2 \cos \epsilon_3 \\
B &= l_3 \cos \epsilon_2 \\
C &= L_3 + L_2 \sin \epsilon_3 \\
D &= l_3 \sin \epsilon_2 \\
E &= (A - B)^2 + (C - D)^2 + l_1^2 - l_2^2 \\
F &= 2(A - B)l_1 \\
G &= 2(C - D)l_1
\end{aligned}$$

Based on the first derivate with respect to time of the loop equation (B.1), the angular velocities of the thigh ($\dot{\theta}$) and knee ($\dot{\epsilon}_1$) are calculated as given by equations (B.5) and (B.6), respectively.

$$\dot{\theta} = \frac{Q_1(-l_2 \cos \epsilon_1) - Q_2(-l_2 \sin \epsilon_1)}{-l_1 \sin \theta (-l_2 \cos \epsilon_1) - (l_1 \cos \theta)(-l_2 \sin \epsilon_1)} \quad (\text{B.5})$$

$$\dot{\epsilon}_1 = \frac{Q_2(-l_1 \sin \theta) - Q_1(-l_1 \cos \theta)}{-l_1 \sin \theta (-l_2 \cos \epsilon_1) - (l_1 \cos \theta)(-l_2 \sin \epsilon_1)} \quad (\text{B.6})$$

where

$$\begin{aligned}
Q_1 &= -L_2 \dot{\epsilon}_3 \sin \epsilon_3 + l_3 \dot{\epsilon}_2 \sin \epsilon_2 \\
Q_2 &= -L_2 \dot{\epsilon}_3 \cos \epsilon_3 - l_3 \dot{\epsilon}_2 \cos \epsilon_2
\end{aligned}$$

Similarly, through the second derivate, the angular accelerations of the thigh ($\ddot{\theta}$) and knee ($\ddot{\epsilon}_1$) can be computed as given by (B.7) and (B.8).

$$l_1(\sin \theta)\ddot{\theta} - l_2(\sin \epsilon_1)\ddot{\epsilon}_1 = Q_3 \quad (\text{B.7})$$

$$l_1(\cos \theta)\ddot{\theta} + l_2(\cos \epsilon_1)\ddot{\epsilon}_1 = Q_4 \quad (\text{B.8})$$

where

$$\begin{aligned}
Q_3 &= -L_2 \ddot{\epsilon}_3 \cos \epsilon_3 - l_3 \ddot{\epsilon}_2 \cos \epsilon_2 + l_3 \ddot{\epsilon}_2 \sin \epsilon_2 + l_1 \dot{\theta}^2 \cos \theta + l_2 \dot{\epsilon}_1^2 \cos \epsilon_1 \\
Q_4 &= -L_2 \ddot{\epsilon}_3 \sin \epsilon_3 + l_3 \dot{\epsilon}_2^2 \sin \epsilon_3 - l_3 \ddot{\epsilon}_2 \cos \epsilon_2 + l_1 \dot{\theta}^2 \sin \theta + l_2 \dot{\epsilon}_1^2 \sin \epsilon_1
\end{aligned}$$

The linear accelerations of the segments' CGs of the thigh, shank and foot, obtained through the second derivative of the location equations, are given by equations (B.9), (B.10) and (B.11), respectively.

$$a_t = d_1(-\dot{\theta}^2 + \ddot{\theta})e^{i\theta} \quad (\text{B.9})$$

$$a_s = -l_1 \dot{\theta}^2 e^{i\theta} + l_1 \ddot{\theta} e^{i\theta} - d_2 \dot{\epsilon}_1^2 e^{i\epsilon_1} + id_2 \ddot{\epsilon}_1 e^{i\epsilon_1} \quad (\text{B.10})$$

$$a_f = -l_1 \dot{\theta}^2 e^{i\theta} + l_1 \ddot{\theta} e^{i\theta} - l_2 \dot{\epsilon}_1^2 e^{i\epsilon_1} + il_2 \ddot{\epsilon}_1 e^{i\epsilon_1} - d_3 \dot{\epsilon}_2^2 e^{i\epsilon_2} + id_3 \ddot{\epsilon}_2 e^{i\epsilon_2} \quad (\text{B.11})$$

where d_1 , d_2 and d_3 are the distances from the proximal joint to the CGs of the thigh and shank and from the ankle to the foot's CG, respectively. The components x and y of the linear accelerations were obtained from the vertical (real) and horizontal (imaginary) components of each acceleration, respectively.

Knowing the angular accelerations of the segments, the pedal forces, the CGs accelerations and the free-body diagram (Figure B.1), the internal actions and the moments acting on each joint can be determined (equations (4.1) to (4.7)).

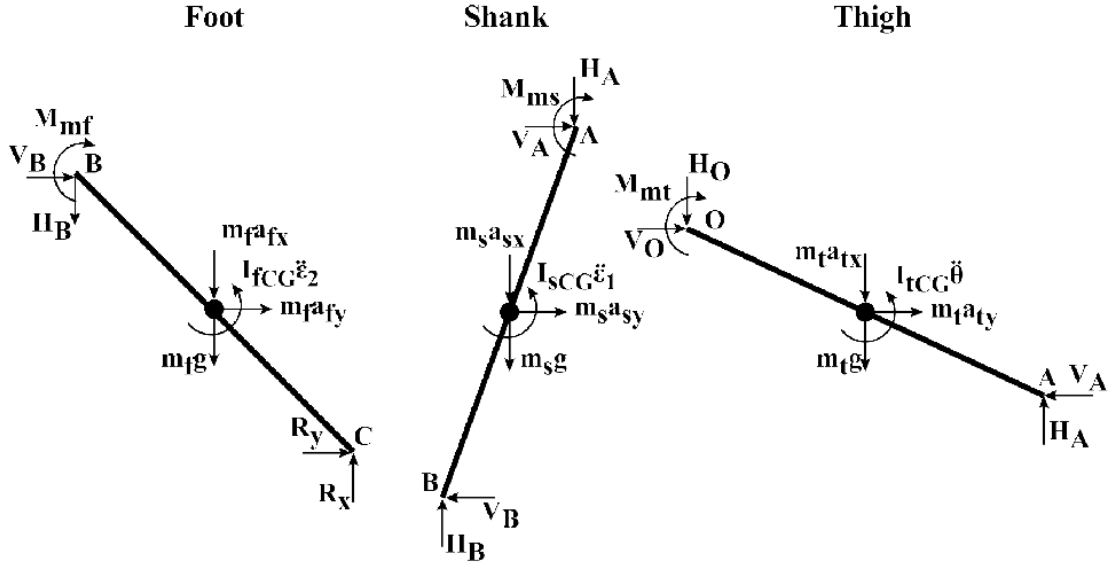


Figure B.1: Free-body diagram.

The variables m_f , m_s and m_t are the masses of the segments (foot, shank and thigh, respectively) and I_{fCG} , I_{sCG} and I_{tCG} are the moments of inertia of the segments (foot, shank and thigh, respectively) about their CG.

The force components (R_x and R_y) were obtained through the effective force (F) and the crank angle (ϕ), as shown by (B.12) and (B.13).

$$R_x = F \times \sin \phi \quad (\text{B.12})$$

$$R_y = F \times \cos \phi \quad (\text{B.13})$$

B.2 Body Segment Parameters

The mass of the segment i is calculated as given by equation (B.14):

$$m_i = P_i \times m_{totalbody} \quad (\text{B.14})$$

where P is the mass proportion of the segment i , n is the number of body segments (equation (B.15)) and $m_{totalbody}$ (equation (B.16)) is the mass of the body [116].

$$\sum_{i=1}^n P_i = 1.0 \quad (\text{B.15})$$

$$m_{totalbody} = \sum_{i=1}^n m_i \quad (\text{B.16})$$

The distance between the proximal end to a segment's CG as proportion of the segment's length, is given by the parameter $R_{proximal}$ [116]. The distance from the center of gravity to the proximal end of a segment ($r_{proximal}$) is given by (B.17):

$$r_{proximal} = R_{proximal} \times length \quad (\text{B.17})$$

The moment of inertia of a segment about its center of gravity (I_{CG}), is computed as shown in equation (B.18):

$$I_{CG} = m(K_{CG} \times length)^2 \quad (\text{B.18})$$

where K_{CG} is the length of the radius of gyration of a segment about its center of gravity as a proportion of the segment's length [116].

The values of the previously mentioned parameters (P , $R_{proximal}$, K_{CG}) for the lower limbs segments, estimated by Clauser *et al.* [103], are represented in Table B.1. The length of each segment was measured manually, for each subject, considering the distance between the segment's endpoints.

Table B.1: Body segments parameters estimated by Clauser *et al.* [103]

Segments	Endpoints	P	$R_{proximal}$	K_{CG}
Foot	Heel to tip longest toe	0.0147	0.4485	0.4265
Leg	<i>Tibiale</i> to <i>sphyrion</i>	0.0435	0.3705	0.3567
Thigh	<i>Trochanter</i> to <i>tibiale</i>	0.1027	0.3719	0.3475

C.1 Procedures for Recording Muscle Activity

C.1.1 Recommendations for Electrodes Placement

Many research groups follow the SENIAM's (Surface Electromyography for the Non-Invasive Assessment of Muscles [107]) recommendations for the acquisition of muscle activity and, most of which were followed in this study.

The recommendations include guidelines about the electrodes shape, size, inter electrode distance and electrode material. The SENIAM's recommendations about these features are:

- No clear and objective criteria for electrode shape;
- The size of the electrodes in the direction of the muscle fibers should be 10 mm at maximum;
- Inter electrodes distance of 20 mm;
- Pre-gelled Ag/AgCl electrodes;
- User self-test;

The *YSY EST EVOLUTION* device is used with *Dura-Stick Plus 2 in Square* electrodes, as shown in Figure C.1.

The area where the electrodes will be placed should be shaved, and the skin cleaned with alcohol. The alcohol should vaporize before placing the electrodes, which must be placed in the location where it is possible to obtain a good and stable EMG recording. An elastic band or double side taped should be used for fixation of the electrodes and cables, to prevent movement perturbation and so that the cables do not pull the electrodes. In this work, the skin of the male subjects was not shaved, and due to the experimental setup characteristics, the electrodes were not fixed with an elastic band.

C.1.2 Electrodes Position

The determination of the correct position for the electrodes placement, on each muscle (Figure C.1), starts with the subjects in a specific posture to measure relative distances between anatomical landmarks. The correct position for the electrodes, according to the recommendations of SENIAM [107], on the studied muscles, is detailed in Table C.1.

Table C.1: Recommendations for the electrodes location of the *rectus femoris*, *gastrocnemius medialis* and *tibialis anterior*, according to SENIAM [107]

Muscle	Electrodes Location
<i>Rectus Femoris</i> (RF)	At the middle line between anterior superior iliac spine and the patella
<i>Gastrocnemius Medialis</i> (GM)	On the most, prominent bulge of the muscle
<i>Tibialis Anterior</i> (TA)	At 1/3 of the, line between the tip of the fibula and the tip of medial malleolus



(a)



(b)



(c)



(d)

Figure C.1: Electrodes location in the three studied muscles: (a) *rectus femoris*, (b) *gastrocnemius medialis* (c) *tibialis anterior*, and (d) Reference electrode, which is placed on the wrist.

D.1 Fugl-Meyer Assessment of Physical Performance

D.1.1 Balance

Maximum Possible Score – 14 points

Table D.1: Procedure and scoring criteria for assessment of the balance (maximum possible score: 14 points) [112]

Test	Scoring Criteria
Sit without support	0 – Cannot maintain sitting without support; 1 – Can sit unsupported less than 5 minutes; 2 – Can sit longer than 5 minutes;
Parachute reaction, non-affected side	0 – Does not abduct shoulder or extend elbow; 1 – Impaired reaction; 2 – Normal reaction;
Parachute reaction, affected side	0 – Does not abduct shoulder or extend elbow; 1 – Impaired reaction; 2 – Normal reaction;
Stand with support	0 – Cannot stand; 1 – Stands with maximum support; 2 – Stands with minimum support for 1 minute;
Stand without support	0 – Cannot stand without support; 1 – Stands less than 1 minute or sways; 2 – Stands with good balance more than 1 minute;
Stand on unaffected side	0 – Cannot be maintained longer than 1 to 2 seconds; 1 – Stands balanced for 4 to 9 seconds; 2 – Stands balanced for more than 10 seconds;
Stand on affected side	0 – Cannot be maintained longer than 1 to 2 seconds; 1 – Stands balanced for 4 to 9 seconds; 2 – Stands balanced for more than 10 seconds;

D.1.2 Lower Extremities

Maximum Possible Score – 40 points

Table D.2: Procedure and scoring criteria for assessment of the lower limbs (maximum possible score: 40 points) [112]

Position	Test	Scoring Criteria	
Supine	Reflex Activity	- Achilles - Patella - Hip flexion	0 – No reflex activity; 2 – Reflex activity; 0 – Cannot be performed;
	Flexor Synergy	- Knee flexion - Ankle dorsiflexion - Hip extension	1 – Partial motion; 2 – Full motion;
	Extensor Synergy (motion is resisted)	- Adduction - Knee extension - Ankle plantarflexion	0 – No motion; 1 – Weak motion; 2 – Almost full strength compared to normal;
Sitting (knees free of chair)	Movement Combining Synergies	- Knee flexion beyond 90°	0 – No active motion; 1 – From slightly extended position knee can be flexed but not beyond 90°; 2 – Knee flexion beyond 90°;
		- Ankle dorsiflexion	0 – No active flexion; 1 – Incomplete active flexion; 2 – Normal dorsiflexion;
Standing	Movement Out of Synergy Hip at 0°	- Knee flexion	0 – Knee cannot flex without hip flexion; 1 – Knee begins flexion without hip flexion, but does not get to 90°, or hip flexes during motion; 2 – Full motion as described;
		- Ankle dorsiflexion	0 – No active motion; 1 – Partial motion; 2 – Full motion;
Sitting	Normal Reflexes	- Knee flexors - Patellar - Achillies	0 – 2 of the 3 are markedly hyperactive; 1 – One reflex is hyperactive or 2 reflexes are lively; 2 – No more than 1 reflex lively;
Supine	Coordination/Speed Heel to opposite knee (5 repetitions in rapid succession)	- Tremor	0 – Marked tremor; 1 – Slight tremor; 2 – No tremor;
		- Dysmetria	0 – Pronounced or unsystematic; 1 – Slight or systematic; 2 – No dysmetria;
		- Speed	0 – 6 seconds slower than unaffected side; 1 – 2 to 5 seconds slower; 2 – Less than 2 seconds difference;